The role of *AIMP3*, a putative tumour suppressor gene, as a predictive biomarker of response to chemo/radiotherapy *in vitro* and in patients with muscle-invasive bladder cancer.

Pratik Man Singh Gurung

A thesis submitted for the degree of Doctor of Philosophy

University College London

Research Department of Urology

Division of Surgery & Interventional Science

University College London

Declaration

I, Pratik MS Gurung, confirm that the work presented in this thesis is my own. Where information has been derived from other sources, I confirm that this has been indicated in the thesis. Where help and materials have been obtained, I have acknowledged as appropriate.

Dedication

This thesis is dedicated to my wife, Kamana, for her loving support and understanding. I also dedicate this work to my parents, Chhatra and Kamala, for their continual love, guidance and encouragement. This work is also dedicated to my supervisors, mentors and teachers who have patiently taught, guided and supported me.

Acknowledgements

I would like to acknowledge, with gratitude, the supervision and/or collaborative support of the following:

Translational Uro-oncology Group, Research Department of Urology, Division of Surgery & Interventional Science, UCL

- Professor John D Kelly

This body of work would not have been possible without the support, supervision and mentorship of Prof Kelly. He has been enthusiastic and instrumental in formulating my PhD studentship and in guiding me expertly and patiently throughout the process. I would not have been able to secure the grants and funding without his help.

Prostate Cancer Research Centre, Division of Surgery & Interventional Science, UCL

- Professor John RW Masters
- Dr Magali Williamson
- Dr Aamir Ahmed

I would like to thank Prof Masters for allowing me to complete the bulk of my lab-work in his lab, for providing all the cell lines used and for regularly providing critical appraisal of my work throughout the three years.

I am hugely indebted to Dr Williamson and Dr Ahmed for teaching me most of the lab-based techniques and for patiently answering my endless questions.

Advanced Diagnostics Unit, Department of Histopathology, UCL

- Dr Alexander Freeman
- Dr Philippa Munson

I am thankful to Dr Freeman for reviewing the immunostaining and for providing urothelial and other control tissues used in the tissue microarrays. I am grateful to Dr Munson for overseeing the immunostaining and tissue-microarray methodologies within her department.

Radiation Biology Group, University of Leeds

- Professor Susan C Short

I am grateful to Prof Short for supervising the radiobiological aspects of my cell-line work and for allowing me access to the Irradiation Department facilities at the UCL Cancer Institute.

Cancer Research UK & UCL Clinical Trials Centre

- Dr Nicholas Counsell

I am grateful to Dr Counsell for teaching me Survival Analyses on SPSS and for reviewing my results.

School of Cancer & Enabling Sciences, University of Manchester

- Professor Catharine West

I am indebted to Prof West for kindly allowing me to interrogate the BCON trial TMA set.

Mount Vernon Cancer Centre, Northwood, Middlesex, London

- Professor Peter Hoskins

I thank Prof Hoskins for approving the use of the BCON set and for reviewing the results.

Department of Oncology, University of Southampton

- Dr Simon Crabb
- Mr James Douglas

I am grateful to Dr Crabb and Mr Douglas for allowing access to the Radical Cystectomy TMA set.

Department of Oncology, St. Bartholomew's Hospital, London

- Dr Thomas Powles

I am grateful to Dr Powles for providing the LaMB trial TMA set.

Department of Pathology, The Royal London Hospital, Whitechapel, London

- Professor Suhail Baithun
- Dr Louis Beltran
- Mr Stephen Jones

I am grateful to Prof Baithun and Mr Jones for approving the collation of bladder cancer tissues into the Neoadjuvant TMA set. I thank Dr Beltran for reviewing the immunostaining on the TMAs.

Abstract

Bladder cancer is the second most common urological cancer after prostate cancer and is one of the leading causes of cancer mortality in most western countries. For organ-confined, muscle-invasive disease, the standard of care, in terms of definitive cure, remains radical surgery (cystectomy) with lymphadenectomy. However, survival rates remain poor following supposedly curative treatment. Radical radiotherapy and more recently, multimodality treatment incorporating chemo-radiotherapy, are alternatives which allow bladder preservation in those choosing not to undergo or are unsuitable for radical surgery. However, survival rates following radiotherapy are generally lower relative to radical cystectomy and multimodality treatments can only be offered to select cases in few institutions. Biomarkers which can accurately predict tumour response to radiotherapy or chemotherapy can aid the selection of patients who are likely to respond well to treatment options incorporating radiotherapy and/or chemotherapy, as alternatives to radical cystectomy, in the management of bladder cancer. Such a strategy would allow personalised cancer care with patients likely to benefit from treatments that they are likely to respond well to and concomitantly avoid complications arising from other treatments less likely to benefit them.

This thesis investigated the novel tumour suppressor gene, *AIMP3* which is involved in the DNA damage response (DDR) pathway following exposure to genotoxic insults such as irradiation and chemotherapy. The expression and cellular localisation of AIMP3 protein was characterised in a panel of bladder cancer cell

lines. Expression of AIMP3 was altered by gene knockdown with siRNA transfection and survival outcomes assessed following irradiation and chemotherapy.

The predictive value of AIMP3 expression in determining survival outcome of patients with muscle-invasive bladder cancer who had undergone radical radiotherapy, with or without carbogen supplementation, in the BCON trial, was assessed. Prognostic significance was evaluated by interrogating a control cohort of patients who had undergone radical cystectomy and had not had exposure to radiotherapy or either neoadjuvant or adjuvant chemotherapy. Reportedly important DDR proteins, including Mre11, p53 and ERCC1, were also interrogated in the BCON, Radical Cystectomy, Neodjuvant and LaMB trial TMA datasets.

Clonogenic survival outcomes following AIMP3 knockdown were also investigated in cisplatin-sensitive (RT112) and cisplatin-resistant (RT112CP) cell lines following cisplatin exposure. Survival outcome, stratified for AIMP3 as well as ERCC1, Mre11 and p53 status, were interrogated in the Neoadjuvant set, which incorporated a cohort of patients who had undergone cisplatin-based neoadjuvant chemotherapy prior to radical treatment. This was validated in a second cohort of patients who had undergone cisplatin-based chemotherapy as part of the LaMB trial.

Table of contents

List of figures

List of tables

List of abbreviations

AIMP	amino acyl tRNA synthetase (ARS) – interacting protein
ANOVA	analysis of variance
ARS	amino acyl tRNA synthetase
ATLD	ataxia-telangiectasia-like disorder
ATM	ataxia telangiectasia mutated
ATPase	adenosine triphosphatase
ATR	ATM-and-RAD3-related
ATRIP	ATR interacting protein
AURKA	aurora kinase A
BCG	bacille calmette-guerin
BER	base excision repair
B-ERC	biobank ethics research committee
BRCA	breast carcinoma associated protein
BRCT	BRCA1 C-terminal
BSA	bovine serum albumin
CDDP	cis-diamminedichloroplatinum
CDK	cyclin dependent kinase
CGH	comparative genomic hybridisation
Chk	checkpoint protein kinase
CR	complete response
CtIP	C terminal binding protein interacting protein

DAPI	4', 6-diamidino-2-phenylindole
DDR	DNA damage response
DNA	deoxyribonucleic acid
DNAPKcs	DNA dependent protein kinase catalytic subunit
DSB	double strand break
dsDNA	double-stranded DNA
EDTA	Ethylenediaminetetraacetic acid
eEF	eukaryotic elongation factor
EEF1E1	eukaryotic elongation factor 1 epsilon 1
EF-1	elongation factor 1
ER	endoplasmic reticulum
ERCC1	excision repair cross complementation 1
eRF	eukaryotic release factor
FACS	fluorescence-activated cell sorting
FANCD2	Fanconi Anaemia Complementation Group D2
FBP	FUSE binding protein
FCS	fetal calf serum
FFPE	formalin-fixed paraffin-embedded
FITC	fluorescein isothiocyante
FUSE	far upstream element
GAPDH	Glyceraldehyde 3-phosphate dehydrogenase
GO	gene ontology
Gp96	96kDa glycoprotein

GST	glutathione *S* transferase
HNPCC	hereditary non-polyposis colorectal cancer
HR	homologous recombination
HRP	horseradish peroxidase
hSMG1	human suppressor of morphogenesis in genitalia-1
H2AX	histone 2A variant X
H&E	Hematoxylin and eosin
ICL	inter-strand cross-link
IHC	immunohistochemistry
IMS	industrial methylated spirit
ISUP	International Society of Urological Pathology
KAP1	KRAB (Kruppel associated box domain)-associated-protein-1
kDa	kilodaltons
MDC1	mediator of DNA damage checkpoint protein 1
MDM2	murine double minute 2
MIBC	muscle invasive bladder cancer
MMEJ	microhomology-mediated endjoining
MMT	multimodal treatment
MRN	Mre11/Rad50/Nbs1
MSP	methylation specific PCR
mTOR	mammalian target of rapamycin
NBS	Nijmegen breakage syndrome
NER	nucleotide excision repair

NHEJ	non-homologous end-joining
NMD	nonsense-mediated mRNA decay
NMIBC	non muscle invasive bladder cancer
OMS	oncomethylome sciences
OS	overall survival
PARP	Poly (ADP ribose) polymerase
PBS	phosphate buffered saline
PCR	polymerase chain reaction
PFS	progression-free survival
PI3K	phospho-inositide 3-kinase
PIKK	PI3K-related protein kinases
PVDF	Polyvinylidene fluoride
RC	radical cystectomy
RCT	randomised controlled trial
RFS	recurrence-free survival
RIPA	radio-immunoprecipitation assay
RNA	ribonucleic acid
RPA	replication protein A
RT	radiotherapy
RTOG	Radiation Therapy Oncology Group
RTPCR	reverse transcribed PCR
SD	standard deviation
SDS PAGE	sodium dodecyl sulphate polyacrylamide gel electrophoresis

SE	standard error
siRNA	small-interfering RNA
SMC1	structural maintenance of chromosomes 1
SPSS	statistical package for social sciences
ssDNA	single-stranded DNA
STR	short tandem repeat
TGFβ	transforming growth factor β
TMA	tissue microarray
TNFα	tumour necrosis factor α
TRAF2	tumour necrosis factor receptor associated factor 2
TRITC	tetramethyl rhodamine iso-thiocyanate
TSG	tumour suppressor gene
TURBT	transurethral resection of bladder tumour
UCL	University College London
UCLH	University College London Hospital
VRS	valyl-tRNA synthetase
WHO	World Health Organisation
XPA	xeroderma pigmentosum A
XRCC1	X-ray repair cross complement group 1
5FU	5-fluorouracil
53BP1	p53 binding protein 1

Chapter 1

Introduction

1.1 Cancer

Cancer can be regarded as a large spectrum of diseases characterised by unregulated, neoplastic cellular proliferation and transformation, which is distinct from the tightly controlled morphology and physiology of normal cells in the tissues from where they arise. Such malignant neoplasms may grow to disrupt the normal functions of the affected organ. In the course of malignant growth, which is a multi-step process called tumour pathogenesis, some cancer cells may acquire the ability to penetrate and infiltrate adjacent normal tissues – a process often called "local invasion". In some cases, cancer cells proceed to penetrate blood or lymphatic vessels, becoming circulating tumour cells, and can metastasise to more distant organs of the body. During this process of transformation and evolution, from normal cells to metastatic cancer cells, the cells acquire a multitude of distinct capabilities, sometimes referred to as "hallmarks of cancer" or "hallmark capabilities", which enable them to become tumorigenic and ultimately, metastatic (Hanahan and Weinberg, 2011). These capabilities include the ability to: sustain proliferative signalling; evade growth suppressors; resist cell death; enable replicative immortality; induce angiogenesis; and, activate invasion and metastasis.

Cancer is increasingly becoming a prominent disease globally with rising prevalence and associated economic burden. Worldwide, approximately 12.7 million cancer cases and 7.6 million cancer deaths are estimated to have occurred in 2008 (Jemal A *et al*, 2011). In terms of causation, environmental and lifestyle factors (e.g. tobacco smoking, diet, physical activity, infections, radiation, environmental pollutants, etc.)

are thought to account for 90-95% of cases, while a small percentage, of around 5-10% of cancers, are attributed to inherited genetic defects (Anand P *et al*, 2008).

In the genetic context, the multi-step process of tumour pathogenesis involves the accumulation of multiple genetic aberrations. These commonly involve the activation of oncogenes, inactivation of tumour-suppressor genes (TSGs) and alteration of microRNA genes (Croce CM, 2008). These genetic aberrations can often arise as a result of the aforementioned environmental factors. Except in the scenario of hereditary or familial cancers, aberrations in a single gene are rarely sufficient for the development of a malignant tumour.

1.1.1 Molecular basis of cancer: oncogenes and tumour suppressor genes

1.1.1.1 Oncogenes

Oncogenes were originally identified in cancer-causing viruses. A viral transforming gene, v-*src*, in the Rous sarcoma virus which causes sarcoma in chickens, was noted to be derived from normal cellular gene (Stehelin D, 1976). Normal cellular genes, from which viral oncogenes (v-*onc*) were derived, were then referred to as proto-oncogenes (c-*onc*). Subsequently, many of the viral oncogenes have been identified independently in tumours that arise spontaneously without viral transformation. In spontaneously arising non-viral tumours, proto-oncogenes, rather than being activated by viral transduction, are activated by other means such as mutations, chromosomal translocation and amplifications, and become tumour-inducing oncogenes. The implication of this is that, in every cell in the human body, there are genes with the potential to be activated or altered with the consequent risk

of contributing to the rise of malignancy. The products of oncogenes can be categorised as: chromatin remodelers, growth factors, growth factor receptors, transcription factors, signal transducers and apoptosis regulators (Croce CM, 2008).

One of the most common oncogenes in human cancers is the *Ras* set of genes (including HRas, KRas and NRas). *Ras* encodes for small GTPases involved in cellular signal transduction and its mutation leads to permanently activated protein products which, in turn, lead to continuous cell proliferation and growth (Godsell DS, 1999). Another common oncogene in human cancers is the *Myc* gene, which is a transcription factor capable of regulating cell growth and proliferation (Oster SK *et al*, 2002). There are numerous oncogenes, in addition to the ones briefly mentioned above, which are involved in cancer initiation and progression.

1.1.1.2 *Tumour suppressor genes*

In contrast to oncogenes, tumour suppressor genes (TSGs), as their name suggests, represent genes that tend to exert a negative regulatory role in controlling cell growth and help inhibit tumour development. Whereas activated oncogenes act in a dominant manner and an activating event is usually required, TSGs act in a recessive manner where genetic alterations result in gene inactivation. As such inactivating mutations may be inherited (through germline transmission in all cells), TSGs are commonly implicated in the development of familial cancers owing to loss of the second functional allele (somatic mutation) in a "two-hit" manner as hypothesised by Knudson for retinoblastoma (Knudson AG, 1971). Mutations in TSGs also occur frequently in sporadic (non-inherited) tumours and, in accordance with the "two hit" hypothesis, both somatic mutations need to occur in the same cell.

Tumour suppressor genes were initially identified through somatic cell fusion (hybrid) experiments where fusion of a normal cell to a malignant one resulted in the hybrids having their malignant phenotype suppressed to a normal phenotype (reviewed by Harris H, 1988). These studies lent support to the statistical analysis provided by Knudson in his "two-hit" hypothesis in retinoblastoma cases. When the retinoblastoma gene (*RB1*) was subsequently cloned and was demonstrated to be altered in retinoblastoma, the "two-hit" hypothesis was established as a model and also provided proof that TSGs could be identified by studying chromosomal deletions and by analysing genetic linkage in familial cancers (Friend SH *et al*, 1986). Subsequently, such strategies proved helpful in identifying other important TSGs such as p53, BRCA1, APC and BRCA2 (Baker SJ *et al*, 1989; Smith SA *et al*, 1992; Levy DB *et al*, 1994; Gudmundsson J *et al*, 1995).

Besides retinoblastoma, inherited *RB1* mutations are found in a broad range of tumours (Burkhart and Sage, 2008). Cells with deficient functional RB1 protein (pRB) demonstrate altered: (a) regulation of gene expression in proliferating cells through transcription factors; (b) differentiation through cell cycle stops and exit (leading to senescence); (c) maintenance of genomic stability through response to DNA damaging genotoxic stressors; and, (d) cell survival through regulation of apoptosis (reviewed in: Gordon and Du, 2011).

As with RB1, p53, which is encoded by the *TP53* gene, is an important TSG and is the most frequently inactivated gene in human cancers (Olivier M *et al*, 2002). The loss of wild-type p53 expression in tumour cells confers a selective survival

advantage. Due to this and its central role in many signaling pathways regulating cell fate, p53 is regarded as the "guardian of the genome" and much research has been dedicated to elucidating its roles in many cancers. P53 was initially identified in cells transformed by simian virus 40 (SV40) (Linzer and Levine, 1979; Melero JA *et al*, 1979). As p53 formed stable complexes in these SV40 transformed cells, it was assumed to be an oncogene; however, the demonstration that these were in fact mutant forms of p53 led to the suggestion of a tumour suppressor role (Finlay CA *et al*, 1989). Heterozygosity of p53 in the germline of patients with Li-Fraumeni syndrome, a rare syndrome characterised by early-onset occurrence of a variety of tumours, and subsequent somatic loss of the remaining wild-type p53 allele, confirmed p53 as a tumour suppressor (Malkin D *et al*, 1990). The increased incidence of tumours in p53-null mice and their increased sensitivity to radiation- and chemical-induced tumorigenesis also indicated an important tumour supressing role (Donehower LA *et al*, 1992).

There are many well-studied TSGs such as *APC*, *BRCA1*, *BRCA2* and *PTEN*. It is beyond the scope of this thesis to expand in detail about them and the aforementioned summaries on the salient points relating to *RB* and *p53* serve simply to illustrate the important principles of TSGs – *AIMP3*, which is the focus of this research, is a reported TSG.

1.2 ARS (Aminoacyl-tRNA synthetase) – interacting multifunctional protein (AIMP)

1.2.1 Introduction to the AIMP family

Protein biosynthesis is a complex process requiring numerous factors to ensure that the genetic code is translated with fidelity. Aminoacyl-tRNA synthetases (ARSs) are essential enzymes which are evolutionarily highly conserved and play a critical role in protein synthesis by catalysing the attachment of specific amino acids to their cognate tRNAs (Schimmel and Soll, 1979) (Ko YG *et al*, 2002; Park SG *et al*, 2010). In this group of enzymes, there is conservation in their catalytic functions across different species; however, there are certain characteristics that distinguish higher eukaryotic ARSs from their prokaryotic counterparts. Among these, one of the key distinguishing features is the presence, in eukaryotes, of a macromolecular protein complex called AIMP (ARS-Interacting Multifunctional Protein).

AIMP comprises eight different ARSs including bifunctional glutamyl-prolyl-tRNA synthetase (EPRS), isoleucyl-tRNA synthetase (IRS), leucyl-tRNA synthetase (LRS), methionyl-tRNA synthetase (MRS), glutaminyl-tRNA synthetase (QRS), lysyl-tRNA synthetase (KRS), arginyl-tRNA synthetase (RRS), and aspartyl-tRNA synthetase (DRS) and three non-enzymatic factors. The three non-enzymatic factors are designated AIMP1 (p43), AIMP2 (p38) and AIMP3 (p18) depending on their sizes where AIMP1 is 43kDa, AIMP2 is 38kDa and AIMP3 is 18kDa, respectively.

The entire structure and the full range of functional interactions of this macromolecular complex are not yet completely understood; however, there is cumulating evidence to suggest that this complex may work as a molecular hub with a central role in coordinating protein biosynthesis, through its catalytic ARS domains, as well as by playing an important role in the regulation of diverse signalling pathways through its non-enzymatic, AIMP co-factors (Park SG *et al*, 2010; Kim KJ *et al*, 2008). These non-enzymatic pathways, which are separate from the canonical pathway of protein synthesis, have been investigated recently and have been implicated in human pathophysiology including cancer, infection, inflammation and metabolic abnormalities.

1.2.2 Structural design of the multiprotein complex

The currently accepted model of the architecture of the multiprotein complex consists of three domains (**Figure 1.1*A***) (Norcum and Warrington, 1998). In this model, domain 1 harbours MRS (Methionyl-tRNA synthetase), QRS (Glutaminyl-tRNA synthetase) and DRS (Aspartyl-tRNA synthetase); domain 2 harbours KRS (Lysyl-tRNA synthetase) and RRS (Arginyl-tRNA synthetase); domain 3 harbours EPRS (Glutaminyl-prolyl-tRNA synthetase), IRS (Isoleucyl-tRNA synthetase) and LRS (Leucyl-tRNA synthetase). Systematic depletion studies, by specific depletion of each component with its siRNA (small-interfering RNA), have demonstrated that the cellular stability of the components depend upon their interdependence (Han JM *et al*, 2006). In this model, the three subdomains are thought to be linked by the three AIMPs. In particular, AIMP2 appears to play a central role by acting as the scaffolding protein for the complex assembly and the components can be grouped into two subdomains based on their associations with AIMP2. So, RRS, QRS, and

AIMP1 form one subdomain by interacting with the N-terminal region of AIMP2; the C-terminal domain of AIMP2 links the remainder of the components (Kim J Y *et al*, 2002) (**Figure 1.1*B***).

Figure 1.1*A*

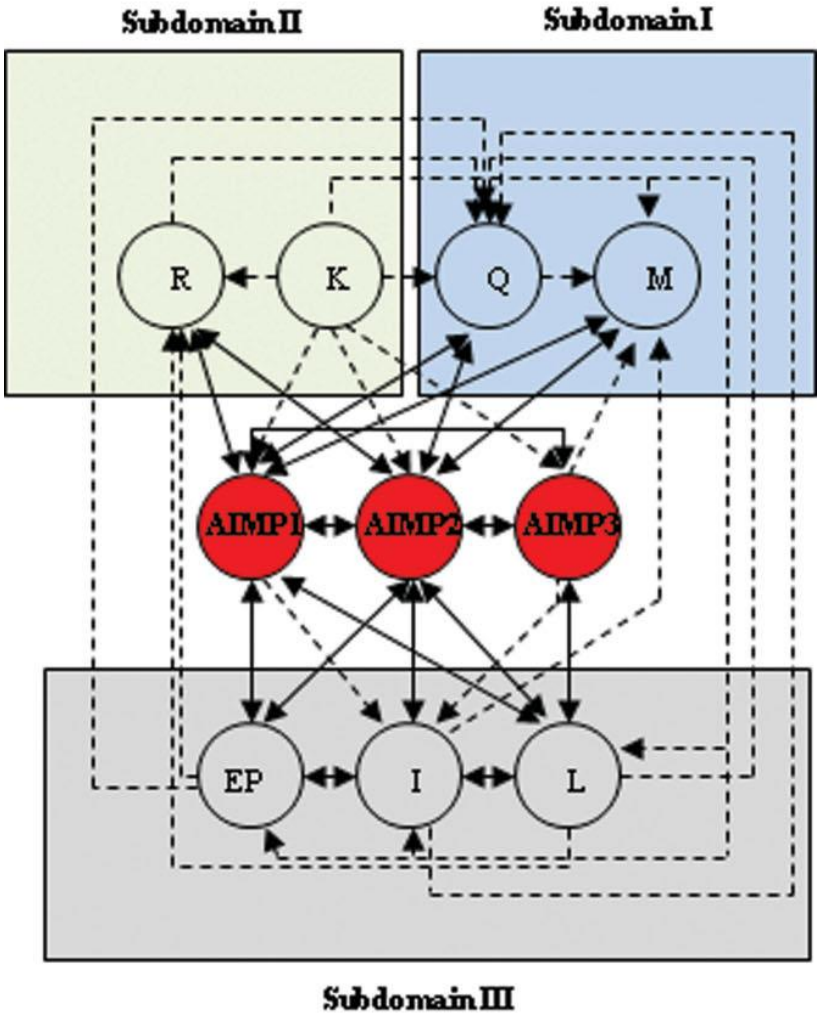

Figure 1.1*B*

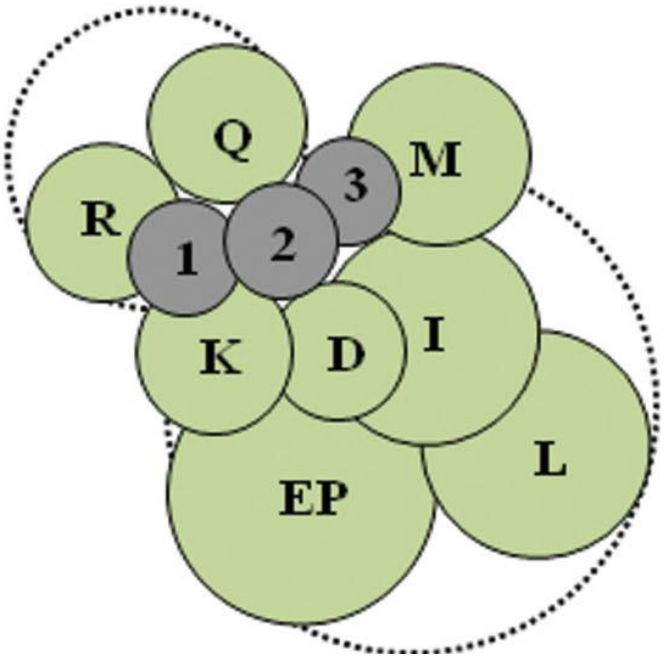

Figure 1.1: Interaction network and molecular arrangement of ARSs and AIMPs in the multiprotein complex (taken from: Park S G *et al*, 2010).

A: The interaction network between the components is indicated by arrows. The pairs of proteins whose stability are mutually dependent are marked by double-headed arrows (e.g. EPRS and IRS; IRS and LRS). If the stability of one component depends on the other partner, it is linked by single arrow dotted line (e.g. KRS and RRS; KRS and QRS). The three AIMPs are multiply linked to most of the enzyme components.

B: The components of the multi-tRNA synthetase complex can be also grouped into two subdomains based on their affiliation to AIMP2. RRS (R), QRS (Q), and AIMP1 form one subdomain through the interactions with the N-domain (not shown in diagram) of AIMP2. The rest of the components of the complex MRS (M), IRS (I), DRS (D), KRS (K), EPRS (EP), and LRS (L) are clustered with the C-domain (not shown in diagram) of AIMP2.

1.2.3 The role of AIMPs in the structure and stability of the multiprotein complex

Although the three AIMPs are relatively small in the context of the whole complex, they appear to be integral to the assembly and stability of the complex. AIMP2 appears to interact with the majority of the tRNA synthetase enzymes (Robinson JC *et al*, 2000; Kim JY *et al*, 2002). Each AIMP appears to have their preferential enzymes but they also appear to interact with other enzymes less tightly (Quevillon S *et al*, 1999; Robinson JC *et al*, 2000; Quevillon and Mirande, 1996). All three AIMPs appear to be tightly linked to each other and their cellular stabilities also appear to be interdependent (Han J M *et al*, 2006). On electron microscopy, after specific immunogold antibody labeling, AIMP1 appears to be near the centre of the multiprotein complex (Norcum and Warrington, 2000). In turn, AIMP1, along with RRS and QRS, interacts with the N terminus domain of AIMP2, which in turn interacts with the other tRNA synthetases via its C terminus domain (Kim J Y *et al*, 2002).

1.2.4 AIMP1/p43

AIMP1 is the largest of the auxiliary, non-catalytic proteins, being 43kDa in size. It has been reported to perform a number of diverse roles in both the intracellular and extracellular compartments (Lee SW *et al*, 2008). In the cytosol, it is involved in protein synthesis through its interaction with RRS within the multiprotein complex (Park SG *et al*, 1999). It is also found to locate in the endoplasmic reticulum (ER) and binds to gp96 (96 kDa glycoprotein) whilst suppressing autoimmune responses (Han JM *et al*, 2007). Gp96-based immunotherapy is being evaluated in phase III clinical trials for many cancers (Wood CG *et al*, 2009). AIMP1 also binds to Smurf2 in the nucleus whilst downregulating TGFβ (transforming growth factor β)

signalling (Lee YS *et al*, 2008). Regulation of TGFβ signalling plays an important role in the progression of many human cancers (Samanta D *et al*, 2012).

AIMP1 is also involved extracellularly through its secretion as a cytokine (Lee SW *et al*, 2008). It has diverse effects in different cells including immune response (Kim E *et al*, 2006), angiogenesis (Park SG *et al*, 2002) and wound healing (Park SG *et al*, 2005). Interestingly, on the basis of its involvement in immune response and angiogenesis, systemic injections of purified recombinant human AIMP1 were performed in mouse xenograft models which demonstrated significant anti-tumour activity (Lee YS *et al*, 2006). Secreted AIMP1 has also been shown to act like a hormone, in a glucagon-like manner, through its pancreatic involvement in the regulation of glucose metabolism (Park SG *et al*, 2006). In this study by Park SG *et al*, compared to wild-type mice, AIMP1-deficient mice were shown to have reduced plasma glucose levels, increased liver glycogen accumulation and reduced glucose tolerance.

1.2.5 AIMP2/p38

In addition to its intricate structural relationship with other components of the multi-ARS complex, AIMP2/p38 appears to also have an important role in determining cell fate by behaving as a tumour suppressor gene. It has been shown to mediate TGFβ signaling for c-myc downregulation by translocating into the nucleus and binding to FUSE (far upstream element)-binding protein (FBP) upon TGFβ stimulation (Kim M J *et al*, 2003). FBP is the transcriptional activator of the proto-

oncogene c-myc (Avigan MI *et al*, 1990). Therefore, there is transcriptional suppression of c-myc through AIMP2 activation of TGFβ.

AIMP2 can also exert pro-apoptotic activity in response to DNA damage via interaction with p53 (Han J M *et al*, 2008). DNA damage activates AIMP2 and causes it to translocate to the nucleus to bind to p53 and this binding is thought to prevent p53 from MDM2 (murine double minute 2)-mediated destruction. MDM2 is a negative regulator of p53 as it mediates the degradation of p53 (Haupt Y *et al*, 1997).

AIMP2 also modulates cell fate via the TNFα signalling pathway (Ko HS *et al*, 2005). This interaction was demonstrated to occur through TRAF2 (tumour necrosis factor receptor associated factor 2) which is targeted for ubiquitylation by AIMP2 (Choi JW *et al*, 2009). TNFα signaling is pro-apoptotic and, therefore, downregulation of TRAF2 via AIMP2 promotes apoptosis. In addition to these tumour suppressor roles of AIMP2 through regulation of cell proliferation and apoptotic pathways, knockdown studies in mice have demonstrated that AIMP2 heterozygosity (AIMP2 +/-) predisposes to susceptibility to various tumours (Choi J W *et al*, 2009).

1.2.6 AIMP3/p18

1.2.6.1 Introduction to AIMP3

AIMP3/p18 is the smallest molecule in the multi-ARS complex. It was shown to demonstrate sequence homology with β and γ subunits of elongation factor-1 (EF-1)

over a decade ago (Quevillon and Mirande, 1996). The implication of this was that AIMP3 had a potential role in linking the aminoacylation of tRNA and protein synthesis in the ribosome because EF-1 (elongation factor-1) is a multi-protein complex that is involved in elongating the amino acid sequence during protein synthesis. EF-1 is comprised of α, β, γ and δ subunits, which work together to ensure the delivery of aminoacyl-tRNAs to the ribosome, thereby elongating mRNA. Elongation is one of three critical sequences of steps occurring during protein synthesis; the sequence is: (i) initiation, conducted by eukaryotic initiation factor (eIF), (ii) elongation, conducted by eukaryotic elongation factor (eEF), and (iii) termination, conducted by eukaryotic release factor (eRF). AIMP3, through its role in elongation, is also referred to as EEF-1 ε1 (eukaryotic translation elongation factor 1 epsilon-1). It is a 174 amino acid protein and shares sequence similarity with the amino-terminal ends of the β and γ subunits of EF-1 (Quevillon and Mirande, 1996).

1.2.6.2 *Overall structure of AIMP3*

The three-dimensional structure of human AIMP3 has been determined by X-ray crystallography (Kim KJ *et al*, 2008). AIMP3 consists of seven α-helices and three β-strands and is divided into two structural domains (**Figure 1.2**). The 56 amino-acid N-terminal domain (AIMP3-N) spanning residues from M1 to N56, contains two α helices (α1 and α2) and three anti-parallel β strands. The 111 amino-acid C-terminal domain contains a bundle of five helices (T64-Y152) followed by coiled region (P153-L169).

Figure 1.2 *A*

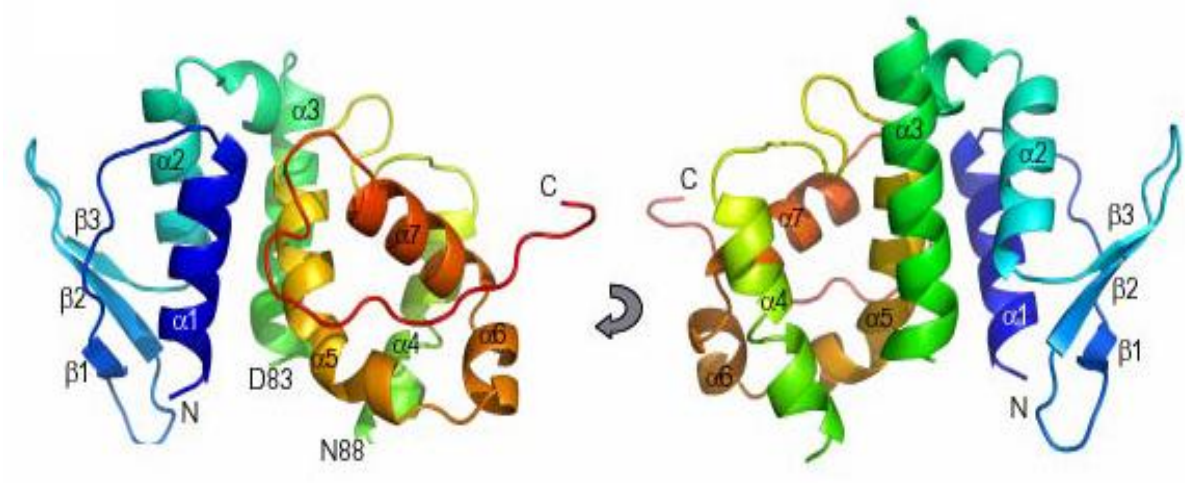

Figure 1.2 *B*

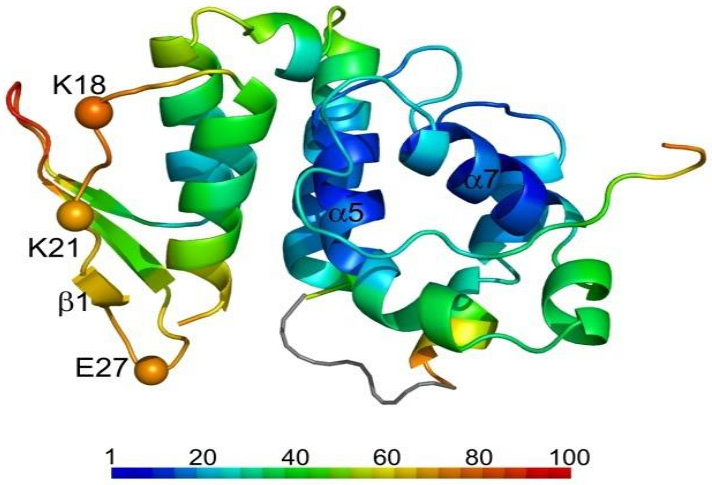

Figure 1.2: Structural characteristics of human AIMP3. (taken from: Kim KJ *et al*, 2008)

A Ribbon diagrams of AIMP3 representing the N-terminal and C-terminal domains. The N-terminal domain consists of a three-stranded anti-parallel β-sheets (β1, β2 and β3) and two α helices (α1 and α2). The C-terminal domain contains five α helices (α3 to α7) with a long coiled structure at the C-terminus. Residues 84-88 are missing (residues D83 and N88 are used as references in the diagram). The left image is rotated by 180^{o} in the y-axis.

B B-factor representation by colours. The β-sheet at the N-terminal domain has higher B-factor (orange colour) and helices α5 and α7 form a stable core (blue colour) at the C-terminal domain. Missing loop region connecting helices α3 and α4 are lined in grey colour. Three residues (K18, K21 and E27) with undefined side chains are shown as spheres. [B-factor is also known as the "temperature factor" or the "Debye-Waller" factor. The higher the B factor, the less stable the configuration of the atoms in the crystal structure of the protein. This leads to more scatter of X rays (due to more dispersed electrons in the dispersed atoms) and a higher B factor value].

1.2.6.3 Important functional interactions of AIMP3

GST (glutathione *S* transferase) homology domains are found in the N-terminal regions of two ARSs (MRS and EPRS) and two AIMPs (AIMP2 and AIMP3) (Lee SW, 2004). The N-terminal appendix of MRS, which contains a GST homology domain, interacts with AIMP3; AIMP3 is required for the cellular stability of MRS but does not need MRS for its own stability (Han J M *et al*, 2006). Since these GST domains are only detected in these complex-forming ARSs and AIMPs, and the N-terminal appendix of VRS (valyl-tRNA synthetase) that also forms a complex with elongation factor, they are thought to be critical for the assembly of protein complexes (Negrutskii BS *et al*, 1999).

Park BJ *et al* have produced several lines of evidence from animal models and cancer tissue material which strongly suggest a tumour suppressor role for AIMP3 (Park BJ *et al*, 2005). Park BJ *et al* investigated the effects of AIMP3/p18 knock-down (p18 -/- and p18+/-) in mice. Firstly, p18 null mice (p18 -/-) were unable to survive *in utero* indicating that AIMP3 plays a critical role in embryogenesis. In the case of AIMP3 heterozygosity (p18 +/-), the mice were born alive with normal anatomical and morphological shape, but they showed higher susceptibility to spontaneous tumour development when compared to their wild-type (p18 +/+)

littermates. A broad range of common tumours (breast, lung, hepatocellular) were observed and the incidence of spontaneous tumour development was found to be significantly elevated as the mice got older (after 15 months). It was suggested that this may have been due to the reduced activity of AIMP3, owing to reduced levels in the heterozygote state, leading to reduced function in the response against DNA damaging insults. Indeed, generally reduced levels of AIMP3 were found in the tissues of most organs of these mice when compared to the corresponding tissues in the wild-type; however, the level of reduction was found to be variable between different tissues.

Park BJ *et al* also demonstrated that AIMP3 regulates cell cycle and apoptosis indicating a tumour suppressor role for AIMP3 *in vitro.* When comparing cell proliferation, by tritium-labelled thymidine incorporation, cell-counting and in situ fluorescence staining with Ki-67, in splenocytes and thymocytes from p18+/+ and p18+/- littermates, enhanced proliferation was observed in p18+/- cells compared to the wild type. When cell cycle progression was measured by flow cytometry, p18+/- splenocytes showed a faster cell cycle progression than the wild-type. When observing the expression of p18 during the different stages of the cell cycle, by firstly synchronizing the cells by serum starvation and then re-feeding the cells with cultured media, both Western analysis and FACS (fluorescence-activated cell sorting) demonstrated that p18 is significantly induced during the DNA synthesis phase (S phase).

In addition, Park BJ *et al* also demonstrated that AIMP3 localises to the nucleus from a cytoplasmic location during S phase of the cell cycle. Furthermore, AIMP3

is also found to translocate to the nucleus in response to DNA damage and oncogenic stresses (Park BJ *et al*, 2005; Park BJ *et al*, 2006). In the nucleus, AIMP3 is shown to interact with ATM (ataxia telangiectasia mutated) and ATR (ATM-and-RAD3-related), the upstream kinases of p53. Thus, AIMP3 appears to work against DNA damage via p53 in cooperation with AIMP2, although its working mechanism is suggested to be distinct from AIMP2 (Han J M *et al*, 2008).

AIMP3 (+/-) heterozygous cells are more susceptible to cell transformation induced by oncogenic stimulation such as Ras or Myc when compared with AIMP3 wild-type cells. These transformed AIMP3 +/- cells demonstrate abnormalities in cell division and nuclear structure and instability in their chromosomal structure (Park B J *et al*, 2006). These findings lend further support to the notion that AIMP3 is a tumour suppressor whose absence or reduction can make cells more susceptible to oncogenic transformation. As with AIMP2, AIMP3 is regarded as a haplo-insufficient tumour suppressor. Both are harboured within the multi-ARS translational machinery to perform their roles in the canonical enzymatic pathway but are also involved in the regulation of cell fate by acting as tumour suppressors.

1.3 DNA damage response (DDR) pathway

1.3.1 Introduction to the DDR pathway

DNA damage can occur with varying severity and the most deleterious form of DNA damage is when double strand breaks (DSBs) occur. DSBs can occur by exposure to extracellular agents (e.g., ionising radiation, reactive chemicals such as chemotherapeutic agents) or due to intracellular by-products of metabolism (e.g., reactive oxygen species) (Michel B *et al*, 1997; Sun H *et al*, 1989; Ward JF *et al*,

1988). DSBs, if left unrepaired, can lead to either cell death or cell survival with mutations leading ultimately to cancer (Khanna and Jackson, 2001). Therefore, when DSBs occur, there needs to be a mechanism in place, within the cell machinery, to detect these and enable DNA damage repair whilst coordinating the repair process with cell-cycle progression. To enable this mechanism, the cell cycle is slowed to allow damage repair to occur. This ensures that an accurate copy of the genome is passed on to the next generation of cells when DNA damage is repairable and, when not repairable, by triggering apoptosis, inaccurate copies are not transmitted to the offspring (Su TT *et al*, 2006). The DDR pathway is the sequence of events within the cell that takes place to ensure this. Therefore, this DDR machinery is highly conserved in eukaryotes. Defective DDR machinery can lead to DNA damage sensitivity and genomic instability with consequent increase in mutations that, in turn, increases cancer susceptibility in humans. This is observed in people with genetic instability conditions, such as Lynch or Li-Fraumeni syndromes, which are caused by defective DDR genes and which result in a significantly increased cancer incidence (Srivastava S *et al*, 1990; Malkin D *et al*, 1990; Lynch and de la Chapelle, 1999).

The DDR pathway involves a multitude of serine/threonine phosphorylation events which encompass three major groups of proteins: (1) sensors, which detect DNA damage directly or indirectly, (2) transducers, which involve proximal and distal kinases that relay and amplify the damage signal, and (3) effector proteins, that control cell cycle progression, chromatin restructuring, DNA repair and apoptosis (Kurz and Lees-Miller, 2004). The main mechanisms of repair of DSBs include homologous recombination (HR) of sister chromatids, microhomology-mediated

endjoining (MMEJ) or non-homologous end-joining (NHEJ) of the broken ends of the DNA strands (Khanna and Jackson, 2001; van Gent DC *et al*, 2001; Lieber M, 2010). NHEJ, which repairs DNA breaks without using a template, is the predominant, but error-prone, repair mechanism throughout the cell cycle and is particularly important during the G1 phase of the cell cycle (Rothkamm K *et al*, 2003; Chen BP *et al*, 2005). HR is a more accurate repair mechanism and is mainly involved in repairing stalled replication forks but can also repair DSBs during the S and G2 phases when an undamaged sister chromatid is available to act as a template for repair (Arnaudeau C *et al*, 2001; Beucher A *et al*, 2009). Whereas NHEJ, also referred to as "classical end joining", requires the presence of proteins such as DNA-PK, Ku70-Ku80, and DNA ligase IV-XRCC4 heterodimers, MMEJ is also referred to as the "alternative end joining" mechanism because it is independent of the DNA-PK pathway and characteristically utilizes microhomologous sequences of approximately 5-25 nucleotides as templates for repair (reviewed in: McVey and Lee, 2008).

The major sensor of DNA damage is believed to be the Mre11/Rad50/Nbs1 (MRN) complex as it is located early at sites of DSBs and has been shown to be required for the ataxia telangiectasia mutated (ATM) signaling pathway and is placed upstream of ATM (Stracker *et al*, 2002; Berkovich *et al*, 2007, Shirata *et al*, 2005). In addition to its role as a sensor of DNA damage, MRN is also implicated in triggering downstream signal transduction and coordinating the repair process.

The major proximal kinases include (ATM) and ATM-and-RAD3-related (ATR). ATM and ATR belong to the phosphoinositide 3-kinase (PI3K)-related protein

kinases (PIKKs) family, which also includes DNAPKcs (DNA dependent protein kinase catalytic subunit), mTOR (mammalian target of rapamycin), and hSMG1 (human suppressor of morphogenesis in genitalia-1) (reviewed in: Lovejoy and Cortez, 2009). DNAPK is closely involved in NHEJ repair of DSBs (Smith and Jackson, 1999). If cells lack DNAPK, they are more sensitive to DNA damage by ionising radiation and chemotherapeutic agents (Jeggo PA, 1998). Conversely, increased DNA damage resistance can result in cancers through overactivation of DNAPK (Muller C *et al*, 1998). mTOR plays a central role in the signaling pathway that regulates cell growth and proliferation (Wullschlegger S, 2006). Inappropriate amplification of the mTOR signalling pathway is implicated in a variety of cancers (Shaw and Cantley, 2006). hSMG1 is involved in the surveillance of DNA integrity and, in particular, it is critical in the nonsense-mediated mRNA decay (NMD) pathway which degrades premature termination codon (PTC)-containing transcripts (Yamashita A *et al*, 2001; Brumbaugh KM *et al*, 2004). PIKK family members have similar structural domains (**Figure 1.3**) and get activated by associating with protein complexes (Lovejoy and Cortez, 2009).

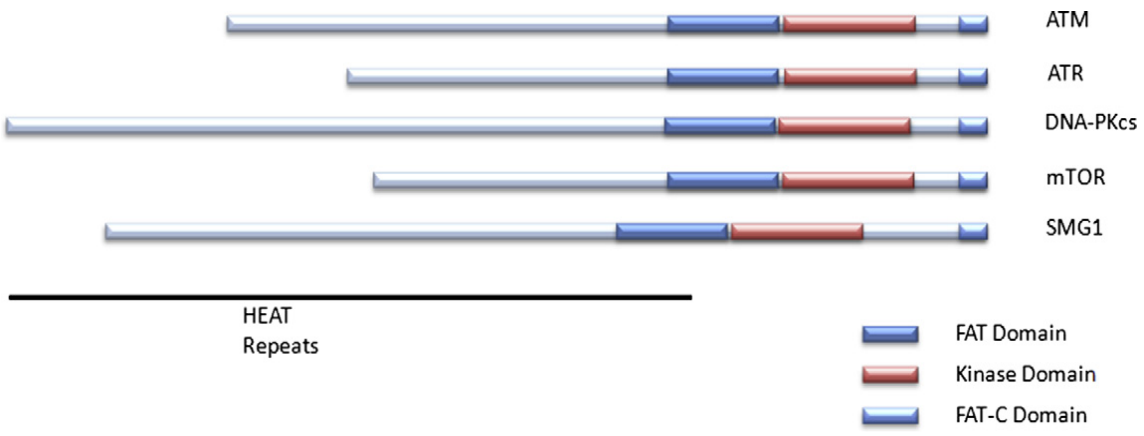

Figure 1.3: PIKK family members. The PIKK family members have a C-terminal protein kinase domain flanked on either side by an N-terminal FAT (FRAP, ATM, TRRAP) domain and FAT-C (C-terminal of FAT) domain. The N-termini are largely composed of HEAT (*h*untingtin, *e*longation factor 3, *A* subunit of protein phosphatase 2A and *T*OR1) repeats. (taken from: Derheimer and Kastan, 2010).

According to one of the currently accepted models of ATM and ATR activation, ATM is activated directly by DSBs and relays/amplifies the damage signal by phosphorylating checkpoint protein kinase 2 (Chk2 kinase) and many other DDR proteins (Shiloh Y, 2006). In contrast, ATR responds primarily to stalled replication forks on single-stranded DNA (ssDNA) during S phase and relays/amplifies the signal by phosphorylating Chk1 kinase and a large subset of ATM substrates (Cimprich and Cortez, 2008). However, there are many similarities between ATM and ATR including a functional overlap in the downstream proteins which are phosphorylated to effect cell cycle arrest and DNA repair.

Whereas Chk2 and Chk1 are distal kinases, which relay the signal of proximal kinases such as ATM and ATR to cause cell-cycle arrest and allow DNA repair, other effectors such as p53 and structural maintenance of chromosomes 1 (SMC1) enforce cell cycle arrest directly. Others such as p53 binding protein 1 (53BP1) affect the cell cycle by amplifying the damage signal. Furthermore, there are proteins, such as histone H2AX and KAP-1 (KRAB (Kruppel associated box domain)-associated-protein-1)), which are thought to facilitate DNA repair, in response to DNA breaks, by inducing chromatin changes that allow repair proteins access to sites of damage (Ziv *et al*, 2006; Pandita and Richardson, 2009).

1.3.2 Mre11/Rad50/Nbs1 (MRN) complex

The MRN complex can be considered as a heterohexameric hub made up of a "head", "coils", a "hook" and a "flexible adapter" unit comprising of Mre11, Rad50 and Nbs1 proteins (**Figure 1.4**) (reviewed in: Williams GJ, *et al* 2010).

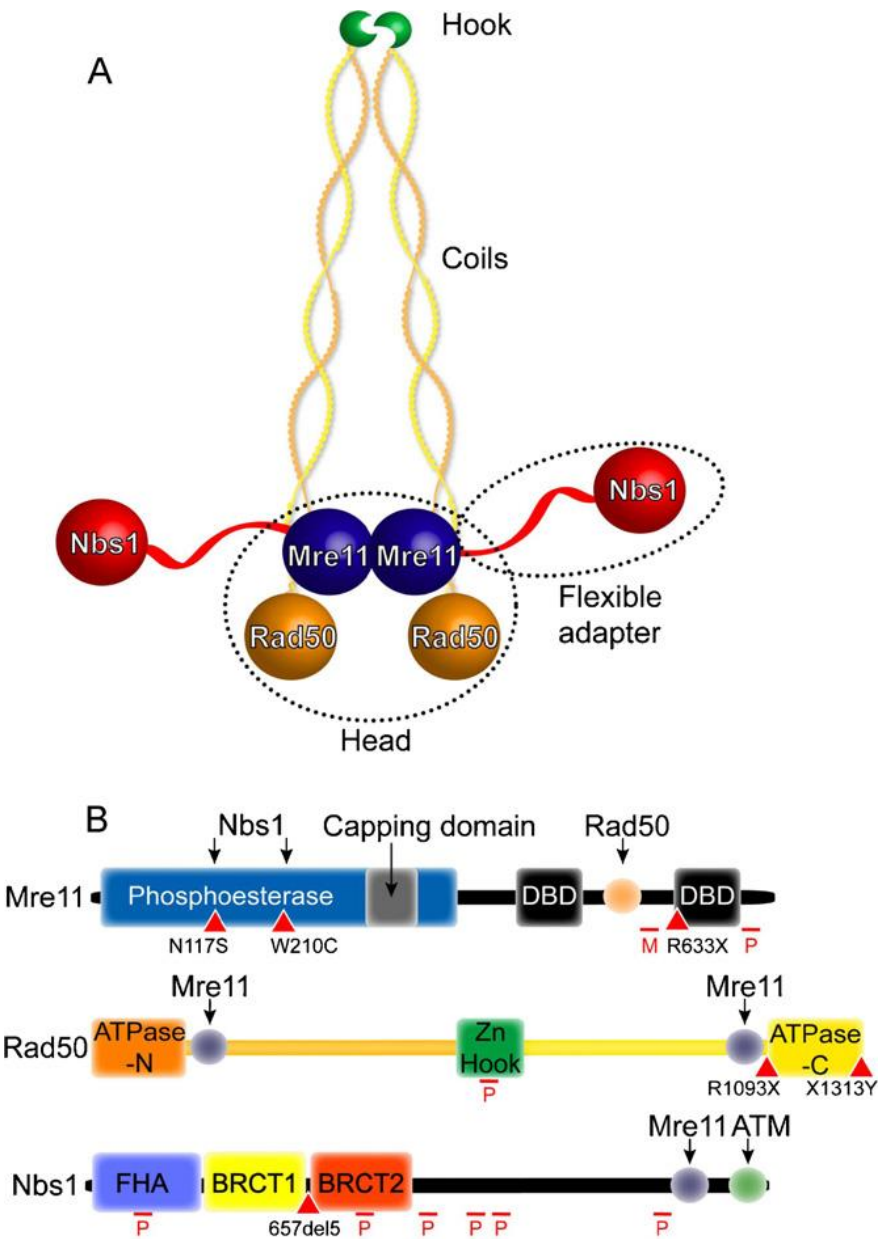

Figure 1.4: Overall MRN assembly and key domains. (***A***) MRN can assemble as a heterohexamer and consists of 4 key regions: the processing "head", formed by the Mre11 dimer and two Rad50 ABC ATPase domains (indicated by dotted line), the "coils" and "hook" encoded by the region of Rad50 separating the N- and C-terminal ABC ATPase halves, and the Nbs1 "flexible adapter" (indicated by dotted line) that provides the key link to signaling functions. (***B***) Schematic representations of the MRN subunits Mre11, Rad50 and Nbs1 showing key domains, coloured as in other figures. The approximate locations of reported methylation sites are indicated by M and DNA damage inducible phosphorylation sites by P (see text for details). The major sites corresponding to inherited human disorders associated with each gene are indicated by a red triangle, with amino acid substitutions labelled for Mre11 and Rad50 (X is a stop codon) and 657del5 representing the major Nbs1 mutation responsible for >90% of NBS cases. (taken from: Williams GJ *et al*, 2010)

The "head" region consists of a DNA-binding Rad50-Mre11 complex formed from two Rad50 units combined with two Mre11units (**Figure 1.4*A***). Mre11 can bind DNA and has ssDNA endonuclease and 3'-5' dsDNA exonuclease activities (Hopfner *et al*, 2001). Rad50 can also bind DNA and has adenylate kinase and ATPase activities (Bhaskara V *et al*, 2007; Paull TT *et al*, 1999). The Rad50-Mre11 complex is evolutionarily highly conserved which indicates its importance (de Jager M *et al*, 2004).

The "coil" region is a long, anti-parallel coil, formed by the coding of the intervening region between the ATPase domains of Rad50 (**Figure 1.4**). The coil extends from the Rad50-Mre11 complex to form the Zinc "hook" region (**Figure 1.4**). Nbs1 forms the "flexible adaptor" region of the MRN complex and has several important roles including the nuclear localisation of the MRN complex in response to DNA damage and activation of ATM and ATR in response to DSBs and replication fork stalling, respectively.

Mre11, in its functional state when bound to DNA, is dimeric in structure (Williams RS *et al*, 2008). Rad50 has a unique architecture with a long anti-parallel coil separating an ATPase domain at one end and a Zn-hook domain at another (**Figure 1.4**). The MRN head contains the Mre11 dimer combined with two Rad50 ATPase domains and undergoes conformational changes depending upon the status of binding or hydrolysis of ATP (Hopfner KP *et al*, 2000). Mutations that disrupt Rad50 ATPase activity can render cells sensitive to DSB causing agents (Chen L *et al*, 2005). Nbs1 consists of an FHA (fork head associated) domain and a tandem repeat BRCT ((Breast carcinoma associated protein 1 (BRCA1) C-terminal)) domain (**Figure 1.4**); these domains on Nbs1 can interact with the Mre11-Rad50 complex through a host of other proteins such as CtIP (C terminal binding protein interacting protein), MDC1 (mediator of DNA damage checkpoint protein 1), and ATR (reviewed in: Williams GJ *et al*, 2010). CtIP is important in homologous recombination (HR) repair by initiating end resection of DSBs in S and G2 phases (Sartori AA *et al*, 2007). CtIP has also been shown to promote MMEJ repair in G1 phase (Yun and Hiom, 2009). CtIP, along with a host of proteins such as MDC1 and 53BP1 (p53 binding protein 1), are among the earliest proteins found to assemble at foci of DNA damage (reviewed in: van den Bosch *et al*, 2003).

The importance of the MRN complex is underscored by the fact that it is evolutionarily highly conserved and human disorders arise if there is misregulation or inherited mutation in any of the components. Nijmegen breakage syndrome (NBS) occurs in patients with mutations in Nbs1 (Carney JP *et al*, 1998). Mutations

in Mre11 cause ataxia-telangiectasia-like disorder (ATLD) (Stewart GS *et al*, 1999) and NBS-like disorder results from a mutation in Rad50 (Waltes R *et al*, 2009).

1.3.3 ATM

Ataxia–telangiectasia (A–T) is a rare, autosomal-recessive, inherited disorder which occurs due to mutations in the ATM (A-T mutated) gene (Savitsky K *et al*, 1995). ATM patients show features including neural degeneration in the cerebellum, immunodeficiency, growth retardation, premature aging, cancer predisposition, and severe sensitivity to ionizing radiation (Shiloh Y, 2003). ATM-deficient mice display many of these phenotypes (Xu and Baltimore, 1996; Xu Y *et al*, 1996). Cells taken from A-T patients exhibit defects in checkpoint activation in the DDR pathway, radiation hypersensitivity and an increased frequency of chromosome breakage (Shiloh Y, 1997; Petrini JH, 2000).

In common with other members of the PIKK family such as DNAPKcs, mTOR, hSMG1 and ATR, the ATM protein is a serine/threonine protein kinase. ATM exists as an inactive dimer under normal conditions but undergoes monomerisation when activated by autophosphorylation on Ser1981 following DNA damage (Bakkenist and Kastan, 2003). When DNA damage is detected by the MRN complex, MRN interacts directly with ATM and stimulates an increase in the kinase activity of the substrates of monomeric ATM such as p53 and Chk2 (Lee and Paull, 2005). The requirement of ATM for the efficient induction of p53 following irradiation had been demonstrated previously (Kastan MB *et al*, 1992). One of the important roles of p53 is to effect a G1 to S phase entry checkpoint in cells exposed

to irradiation (Kastan MB *et al*, 1991). P53 induces p21, a cyclin dependent kinase (CDK), which inhibits Cyclin-E/CDK2 resulting in cell cycle arrest between G1 and S phase. Thus, ATM plays a critical role in cell cycle progression through its activation of p53.

However, one of the characteristic features of cells lacking ATM is that they demonstrate "radioresistant DNA synthesis (RDS)" by undergoing reduced inhibition of DNA synthesis during S phase following ionising radiation (Painter and Young, 1980). As p53 is involved in the G1/S checkpoint, and not in an intra-S arrest, other effectors have been implicated amongst which is the Nbs1 protein, part of the MRN complex (Lim DS *et al*, 2000). BRCA1 is also implicated in effecting an intra-S arrest in response to irradiation through phosphorylation at serine 1387 by ATM (Xu B *et al*, 2002). Furthermore, phosphorylation of BRCA1 at serine 1423 by ATM was demonstrated to cause G2/M arrest following irradiation (Xu B *et al*, 2001).

In addition to a role in cell cycle progression, ATM also appears to be important for DNA damage repair. The histone variant H2AX is phosphorylated to γH2AX in response to irradiation and is present at foci surrounding DSBs (Rogakou EP *et al*, 1998). The subsequent disappearance of γH2AX from these sites is an indirect indicator of DNA damage repair (Lobrich M *et al*, 2010). In the absence of ATM, γH2AX is persistent at foci of DSBs following irradiation suggesting that ATM has an important role in the repair process itself (Riballo E *et al*, 2004). Furthermore, it has been demonstrated that, following irradiation, ATM can contribute to the

phosphorylation of H2AX to γH2AX (Burma S *et al*, 2001). γH2AX then binds MDC1, which contains BRCT domains, which in turn gets phosphorylated by ATM (Lukas C *et al*, 2004). It is thought that this binding and activation of γH2AX and MDC1 by ATM along with components of the MRN complex creates a multi-molecular docking complex for other components of the DDR pathway to localise at sites of DSBs (**Figure 1.5**). For instance, RING-finger ubiquitin ligases, RNF8 and RNF168, are recruited into the complex by the phosphorylation of MDC1 and, in turn, RNF8 phosphorylates γH2AX and helps to recruit 53BP1 and BRCA1 (Mailand N *et al*, 2007; Doil C *et al*, 2009). RNF168 helps to maintain γH2AX in the ubiquitinated state thereby stabilising 53BP1 and BRCA1 in the complex. ATM phosphorylates both 53BP1 and BRCA1 (Lavin MF, 2008). Thus ATM plays a central role in the DDR pathway by influencing cell cycle progression and DNA repair mechanisms.

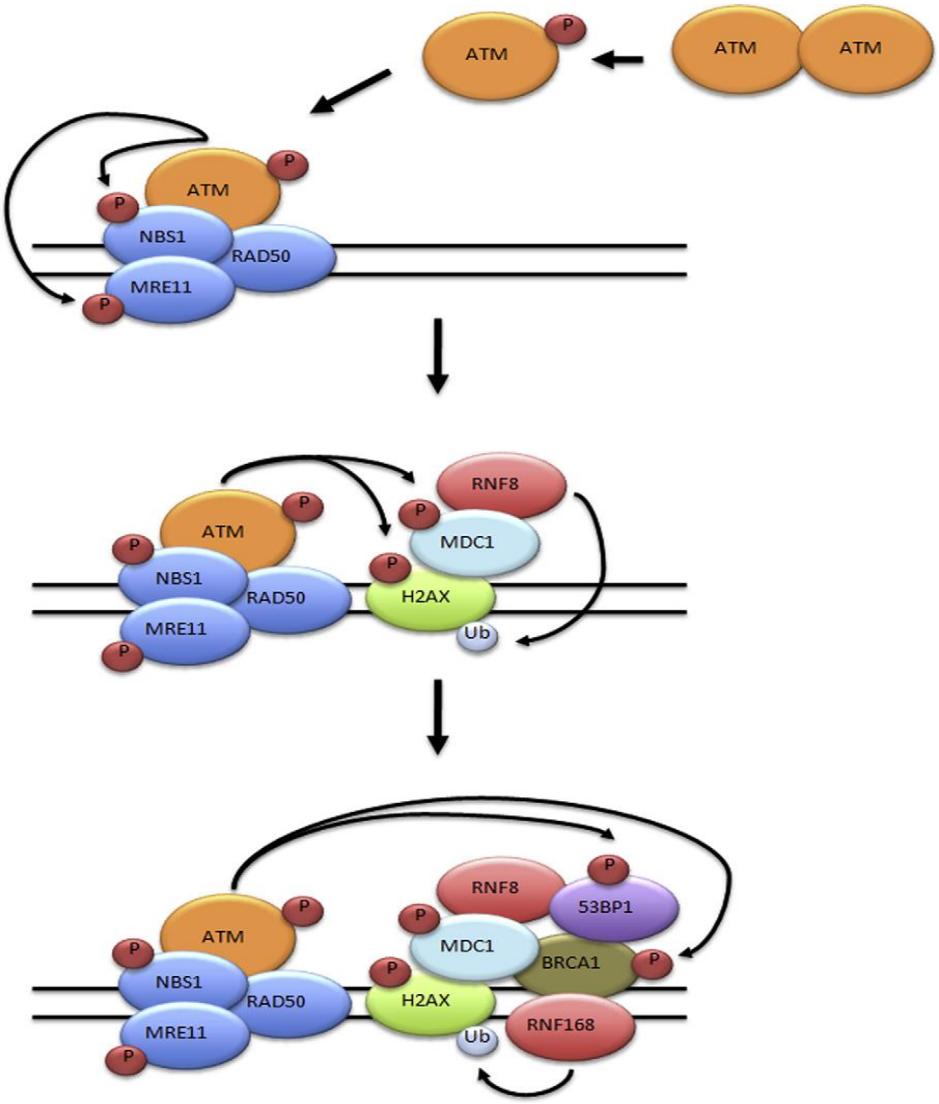

Figure 1.5: Recruitment of DNA damage response proteins to a DNA double-strand break. Prior to DNA damage ATM exists as an inactive dimer. Following the induction of a DNA double-strand break, ATM undergoes auto-phosphorylation producing active ATM monomers. ATM and MRN are rapidly recruited to the site of the DNA double-strand break. Upon recruitment, ATM phosphorylates MRE11, NBS1, and H2AX. The phosphorylation of H2AX leads to the recruitment of MDC1. MDC1 is phosphorylated by ATM and phosphorylated MDC1 serves as a docking site recruiting the RING-finger ubiquitin ligase RNF8. RNF8 mono-ubiquitinates cH2AX resulting in the recruitment of 53BP1, BRCA1, and RNF168. The RING-finger ubiquitin ligase RNF168 maintains the ubiquitinated status of cH2AX, aiding in the stabilization 53BP1 and BRCA1 at the break site. (taken from: Derheimer and Kastan, 2010)

1.3.4 ATR

ATR is so named because of its sequence homology with ATM and Rad3 (A-T and Rad 3-related) and, due to this homology, has many overlapping functions with ATM. ATR phosphorylates Chk1 preferentially whilst ATM phosphorylates Chk2 but there is some crosstalk in the network (Kastan and Bartek, 2004). The functional differences of ATM and ATR have been demonstrated by studies of ATM and ATR null mice. ATM null mice are viable and demonstrate infertility and growth retardation (Barlow C *et al*, 1996; Elson A *et al*, 1996). In contrast, knock-out of ATR results in early embryonic lethality and the mice demonstrate a phenotype which resembles "mitotic catastrophe" (Brown EJ, 2000; de Klein A, 2000). ATR may be essential for life due to its additional role in monitoring DNA replication in mitosis during cell division (Kimprich and Cortez, 2008). In humans, mutations in ATR predispose to Seckel's syndrome which is characterized by dwarfism, microcephaly and mental retardation (O'Driscoll M *et al*, 2003). Although increased incidence of tumours have not been demonstrated in humans due to lack of ATR, haploinsufficiency of ATR in mice has been demonstrated to cause enhanced tumorigenesis (Elson A, 1996; Kastan and Bartek, 2004).

Although a variety of DDR signals including DSBs can stimulate ATR activation, it is thought that single-stranded DNA (ssDNA), formed during DNA replication and DNA repair, is the major activator of ATR (Zou and Elledge, 2003). Replication protein A (RPA) coats ssDNA arising from DNA damage and localizes ATR to those sites by interacting with ATRIP (ATR interacting protein) (Cotez D *et al*, 2001; Ball HL *et al*, 2007). Although RPA-coated ssDNA is essential for localizing the ATR-ATRIP complex to DNA damage sites, the activation of ATR is dependent

upon the co-localization of Rad9-Rad1-Hus1 (9-1-1) complex, a ring-shaped heterotrimeric molecule that recognizes DNA ends adjacent to RPA-coated ssDNA (Parrilla-Castellar ER *et al*, 2004; Kanoh Y *et al*, 2006). 9-1-1 recruits TOPBP1, which contains BRCT domains, and which strongly activates ATR (Kumagai A, 2006; Lee J *et al*, 2007). However, the mechanism of activation of ATR is not as well defined as the activation of ATM. Indeed, although RPA-ssDNA mediated interaction with ATR-ATRIP and 9-1-1, is believed to be the main activation pathway of ATR, other RPA-independent pathways have been described, including that involving AIMP3 (Park BJ *et al*, 2005; Roche KC *et al*, 2007; Sivasubramaniam S *et al*, 2008).

As with ATM, ATR is also involved in cell cycle regulation (mainly through activation of Chk1 – described below) and DNA repair at sites of stalled replication forks. ATR has been shown to phosphorylate a number of proteins involved in DNA repair including BRCA1, WRN (Werner), FANCD2 (Fanconi Anaemia Complementation Group D2) and XPA (Xeroderma pigmentosum A) (Tibbetts RS *et al*, 2000; Pichierrie P *et al*, 2003; Andreassen PR *et al*, 2004; Wu X *et al*, 2007). WRN phosphorylation, either by ATM or ATR leads to its activation at sites of replication blocks during the S phase of the cell cycle. FANCD2 phosphorylation by ATR leads to its monoubiquitination and localization to DNA damage foci. XPA is a nucleotide excision repair protein, and its phosphorylation by ATR is important for its intracellular localization, which indicates that ATR is involved in other types of DNA damage in addition to ssDNA exposed at replication forks.

1.3.5 ATM and ATR

The relationship between ATM and ATR in the DDR pathway is not a simple, mutually exclusive one. There is considerable interdependence and crosstalk between the pathways at multiple levels. At the upstream level, although ATM responds primarily to DSBs and ATR to ssDNA at replication forks, they have both been demonstrated to respond to a variety of DNA damages. ATR can also respond to DSBs after the induction of ATM as the ATM-mediated process requires DSB end-resection which reveals ssDNA (Jazayeri A *et al*, 2006; Myers and Cortez, 2006). For instance, ATM and ATR are both activated in response to ionizing radiation. However, ATM is activated quickly and throughout the cell cycle whereas ATR is slower and occurs predominantly at the G2/M checkpoint.

Whereas ATR can also be activated by DSBs, there is some evidence that ATM can also be activated at stalled replication forks but it is unclear whether this signalling occurs specifically due to ssDNA in the absence of the generation of DSBs at replication forks (Brown and Baltimore, 2003). It can be difficult to establish causality with certainty because one type of DNA damage can be converted to another during the process of repair. For instance, ssDNA can be converted to DSBs by the action of nucleases downstream of ATM and ATR, there is crosstalk at multiple levels. One early interaction is at the level of TOPBP1, which is phosphorylated by ATM, and phosphorylated TOPBP1, in turn, results in the phosphorylation of ATR (Yoo HY et al, 2007). Further downstream, many proteins such as BRCA1 and p53 are phosphorylated by both ATM and ATR (Cortez D *et al*, 1999; Tibbetts RS *et al*, 1999). However, there appears to be some substrate specificity in that ATM targets Chk2 and ATR targets Chk1.

1.3.6 ATM and Chk2

ATM, once induced by DSBs, phosphorylates Chk2 at threonine 68 (T68) (Ahn JY *et al*, 2000). Following activation, Chk2 undergoes homo-dimerisation to become more activated. Activated Chk2 subsequently phosphorylates CDC25 phosphatases (**Figure 1.6**) (Blasina A *et al*, 1999; Falk J *et al*, 2001). CDC25 phosphatases regulate cell cycle transitions by removing inhibitory phosphorylations on cyclin dependent kinases (CDKs); therefore, their inhibition by phosphorylation by Chk2 ultimately results in slowing of the cell cycle. Chk2 has also been suggested to cause p53-mediated cell cycle arrest because activated Chk2 has been shown to phosphorylate p53 (Shieh SY *et al*, 2000). Furthermore, Chk2 has been implicated in inducing apoptosis in a p53-independent manner by phosphorylation of transcription factor E2F-1 (Yang S *et al*, 2002).

1.3.7 ATR and Chk1

ATR activates Chk1 by phosphorylating it at serine 317 (S317) and S345 (Liu Q *et al*, 2000; Lopez-Girona A *et al*, 2001). ATR and Chk1 are brought into proximity at sites of replication fork arrest by Claspin, a "mediator" protein which is found at replication forks (Kumagai and Dunphy, 2000). Once phosphorylated, however, Chk1 is liberated from chromatin to inhibit CDC25 phosphatases (**Figure 1.6**) (Smits VA *et al*, 2006; Sanchez Y *et al*, 1997). Thus, ATR-dependent Chk1 activation leads to an overall reduction in cell cycle progression through activation of the CDC25 phosphatase-CDK pathway.

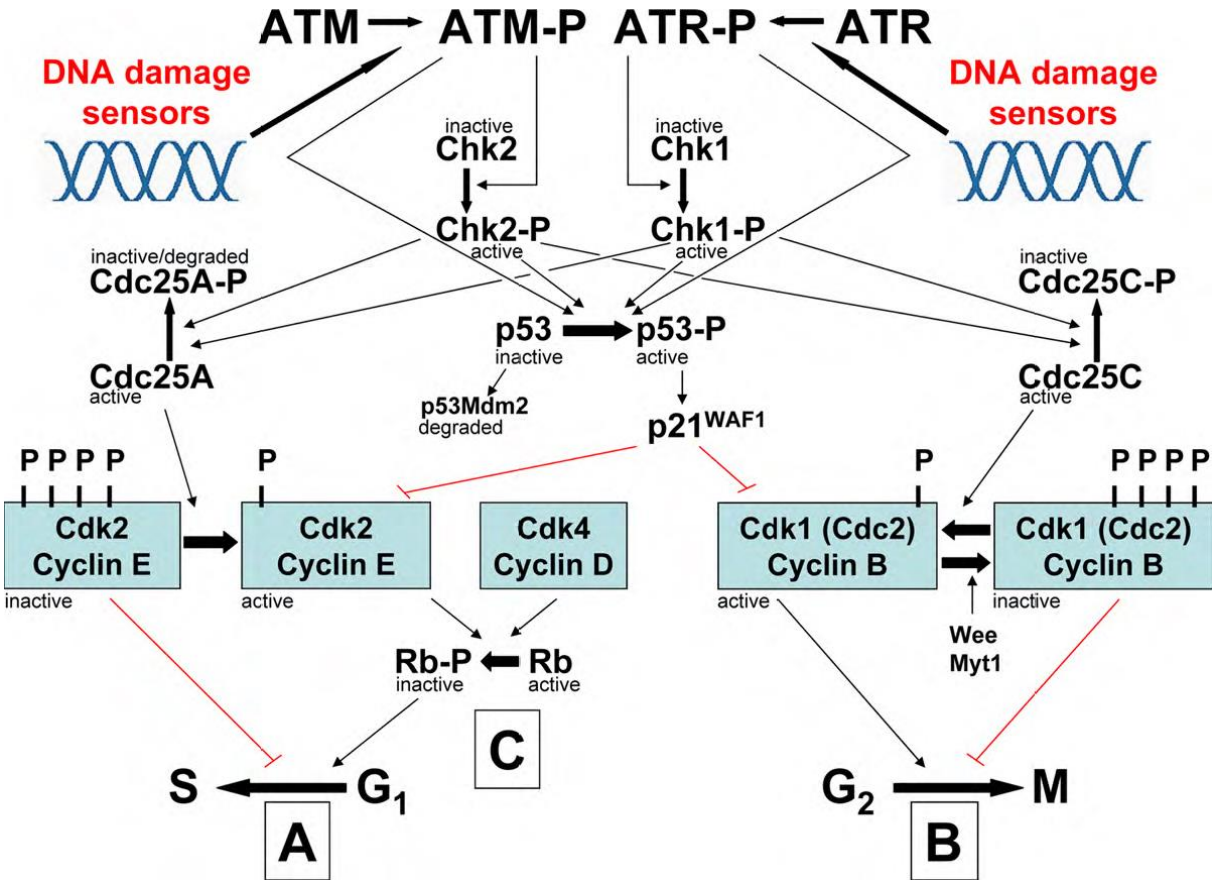

Figure 1.6: The G1/S and G2/M checkpoint regulation network following upstream ATM/ATR activation. Detection of DNA damage results in the activation of ATM/ATR followed by activation of Chk2/Chk1. Cell cycle regulatory proteins (for example, Cyclins, CDKs and CDC25 phosphatases) are then activated/deactivated to influence progression through the G1/S and G2/M cell cycle checkpoints (taken from: Poehlmann and Roessner, 2010).

1.3.8 DNA damage repair of cisplatin lesions

Cisplatin (cis-diamminedichloroplatinum, CDDP) is a platinum compound that was accidentally discovered to inhibit the growth of *Escherichia coli* and was subsequently found to kill tumor cells as well (Rosenberg B, 1973). It is commonly used as an anti-tumour agent to treat a variety of malignancies including bladder cancer. It is one of the most potent anti-tumour agents available on account of its ability to induce DNA damage via the formation of intra-strand and inter-strand cross-links (ICLs) which result in the blockage of cellular processes such as replication and transcription, particularly in highly replicating cells such as tumour cells (Siddik ZH, 2003; Wang and Lippard, 2005; Kelland L, 2007). Due to its mechanism of forming DNA-adducts, it is commonly classified as an alkylating agent; however, it does not possess an alkyl-group and is more accurately referred to as "alkylating-like" anti-tumour agent. Cisplatin's mechanism is believed to be cell cycle-independent; however, in some cases, a prolongation of the G2 phase cell-cycle arrest may occur (Roberts and Pascoe, 1972; Siddik ZH, 2003; Kelland L, 2007).

Cisplatin induces toxicity in a concentration-dependent manner and cell death is caused by both necrosis and apoptosis mechanisms (Gonzalez et al, 2001; Nguewa, et al, 2003). Necrosis is reported to involve the hyper-activation of Poly (ADP ribose) polymerase (PARP) (Nguewa PA *et al*, 2003). Apoptosis is reported to occur as a result of activation of caspases (Gonzalez VM *et al*, 2001).

Repair of cisplatin-induced DNA lesions occurs via different mechanisms in the DDR pathway. It is established that intra-strand adducts are excised and repaired by

the nucleotide excision repair (NER) pathway using the other DNA strand as a template (Jalal S *et al*, 2011). Inter-strand cross-links (ICLs) represent a major challenge for repair as both strands are damaged and other repair enzymes are required. Two major pathways are involved in ICL repair. One involves homologous recombination (HR) which is cell cycle dependent and the other is cycle-independent and occurs via DNA polymerases (Jalal S *et al*, 2011). DDR mediators such as DNA-PK, ATM and ATR have been implicated in the process of cisplatin-adduct repair (Liu S et al, 2012; 66. Cruet-Hennequart S *et al*, 2008). Chk1 and Chk2 phosphorylation are also thought to occur directly or indirectly as a result of cisplatin-induced DNA damage (Colton SL *et al*, 2006). ATR is responsible for Chk1 activation (**Figure 1.6**) and ATR has been implicated in cell cycle arrest and apoptosis in cisplatin-induced DNA damage response (Lewis KA *et al*, 2009). This DDR pathway via ATR, in cisplatin-induced damage repair, has also been reported to be p53-dependent (Sangster-Guity N *et al*, 2011). However, where p53 status is concerned, there are conflicting reports of cisplatin sensitivity (da Silva GN *et al*, 2010).

1.3.9 ERCC1

DNA damage caused by genotoxic agents, such as Cisplatin or radiation, requires the interplay of a complex group of DDR factors for repair. Amongst the many factors involved, excision repair cross-complementation group protein -1 (ERCC1) is considered to play an important role, particularly in the NER pathway (Parker RJ *et al*, 1991). The interplay of ERCC1 with xeroderma pigmentosum (XPF) protein, via hetero-dimerisation into the ERCC1-XPF complex, is thought to play a key role in excising and repairing bulky DNA-adducts (Li L *et al*, 1994; Bessho T *et al*,

1995; Choi YJ *et al*, 2005; Tripsianes K *et al*, 2005; Tsodikov OV *et al*, 2005). In addition to the NER pathway, ERCC1-XPF is also thought to be important in the repair of inter-strand crosslinks (ICLs) and DNA double-strand breaks (DSBs) commonly induced by ionising irradiation (Kuraoka I *et al*, 2000; Niedernhofer LJ *et al*, 2004).

Expression of *ERCC1* in tumours has been correlated to survival outcome due to the altered sensitivity to cisplatin mediated DNA damage (Shirota Y *et al*, 2001). Polymorphisms in *ERCC1* have been demonstrated to alter ERCC1 expression and affect cisplatin sensitivity (Chen P *et al*, 2000; Zhou W *et al*, 2004). In the clinical setting of cisplatin treatment, survival has been correlated to ERCC1 expression status in a variety of cancers including testis, lung, gastric, head and neck, and melanoma (Olaussen K *et al*, 2005; Simon GR *et al*, 2005; Jun HJ *et al*, 2008; Kim MK *et al*, 2008; Matsubara J *et al*, 2008; Usanova S *et al*, 2010; Song L *et al*, 2011). In bladder cancer, ERCC1 expression status has been correlated with survival outcome following cisplatin treatment in a number of studies (Bellmunt J *et al*, 2007; Hoffmann AC *et al*, 2010; Kim KH *et al*, 2010; Kawashima A *et al*, 2011; Sun JM *et al*, 2012; Ozcan MF *et al*, 2013; Sakano S *et al*, 2013). However, a few studies have not found a significant correlation between ERCC1 expression and survival in cisplatin treated bladder cancer (Matsumura M *et al*, 2011; Choueiri TK *et al*, 2014; Shilkrut M *et al*, 2014).

1.4 The role of radiation in the treatment of bladder cancer

1.4.1 Introduction to bladder cancer: epidemiology, pathological staging and treatment options for muscle-invasive disease

In the UK, bladder cancer is the second most common urological malignancy after prostate cancer, with approximately 12,000 new cases annually and accounts for around 5,000 deaths annually (CRUK cancer statistics). Treatment depends upon the grade and stage of the disease. **Table 1.1** outlines the 2002 Tumour, Nodes, Metastases (TNM) classification approved by the Union for International Cancer Control (UICC) (Sobin DH *et al*, 2002).

Table 1.1: 2002 TNM classification of urinary bladder cancer

T	**Primary tumour**
Tx	Primary tumour cannot be assessed
T0	No evidence of primary tumour
Ta	Non-invasive papillary carcinoma
Tis	Carcinoma in situ: 'flat tumour'
T1	Tumour invades subepithelial connective tissue
T2	Tumour invades muscle:
T2a	Tumour invades superficial muscle (inner half)
T2b	Tumour invades deep muscle (outer half)
T3	Tumour invades perivesical tissue:
T3a	Microscopically
T3b	Macroscopically (extravesical mass)
T4	Tumour invades any of the following: prostate, uterus, vagina, pelvic wall, abdominal wall

T4a	Tumour invades prostate, uterus or vagina
T4b	Tumour invades pelvic wall or abdominal wall
N	**Lymph nodes**
NX	Regional lymph nodes cannot be assessed
N0	No regional lymph node metastasis
N1	Metastasis in a single lymph node 2 cm or less in greatest dimension
N2	Metastasis in a single lymph node more than 2 cm but not more than 5 cm in greatest dimension, or multiple lymph nodes, none more than 5 cm in greatest dimension
N3	Metastasis in a lymph node more than 5 cm in greatest dimension
M	**Distant metastasis**
MX	Distant metastasis cannot be assessed
M0	No distant metastasis
M1	Distant metastasis

Grading of tumours is based on a classification (**Table 1.2**) proposed by the World Health Organization (WHO) and the International Society of Urological Pathology (ISUP) (1998 WHO/ISUP classification) and published by the WHO in 2004 (Sauter G *et al*, 2004). The 2004 WHO classification was an update from the 1973 WHO classification. The majority of trials reported in the literature are based on the 1973 version and the 1973 version is still widely used internationally.

Table 1.2: WHO grading of bladder cancer in 1973 and 2004

1973 WHO grading
Urothelial papilloma
Grade 1: well differentiated
Grade 2: moderately differentiated
Grade 3: poorly differentiated
2004 WHO grading
Flat lesions
Hyperplasia (flat lesions without atypia or papillary aspects)
Reactive atypia (flat lesion with atypia)
Atypia of unknown significance
Urothelial dysplasia
Urothelial CIS
Papillary lesions
Urothelial papilloma (completely benign lesion)
Papillary urothelial neoplasm of low malignant potential (PUNLMP)
Low-grade papillary urothelial carcinoma
High-grade papillary urothelial carcinoma

The mainstay of treatment of non-muscle invasive (<T2) disease is by trans-urethral resection of the bladder tumour (TURBT) with or without adjuvant treatment depending upon the risk profile of the disease. For instance, non-muscle invasive bladder cancer (NMIBC) with a "high risk" profile such as high-grade (G3), multiple foci of tumours or recurrence of tumours may receive adjuvant treatment (e.g. with intravesical BCG) following TURBT. On the other hand, NMIBC with a "low risk" profile such as a new tumour which is solitary, small (<1cm diameter) and is histologically low-grade (G1), TURBT alone may suffice but one dose of

intravesical mitomycin instillation immediately following TURBT is usually recommended. For muscle-invasive bladder cancer (MIBC) which is "organ-confined" (T2-4a without nodal involvement or metastasis), radical cystectomy (RC) is currently accepted as the "gold standard" modality for treatment. RC involves removal of the bladder along with adjacent organs, i.e. prostate and seminal vesicles in men, and uterus and adnexa in females. However, such radical treatment, delivered with a curative intent, still imparts only around 50% survival at 5 years post-cystectomy (Bassi P *et al*, 1999; Dalbagni G *et al*, 2001; Ghoneim MA *et al*, 1997; Stein JP *et al*, 2001; Stein and Skinner, 2006). Furthermore, the peri-operative mortality is around 3%; early complications (within 3 months of cystectomy) occur in around 25%; and there are notable late complications depending upon the type of urinary diversion such as stomal complications in those with ileal conduits and anastomotic strictures in those with continent orthotopic neobladder urinary diversions. In addition, radical surgery can have an adverse impact on the psycho-social status of patients due to urinary incontinence and erectile dysfunction, body image dissatisfaction and difficulties with activities of daily living (Zietman AL *et al*, 2003; Shipley WU *et al*, 2003; Zietman AL *et al*, 2001).

1.4.2 Radical radiotherapy and radio-chemotherapy as organ-preserving options

In view of the issues discussed above, there is an ongoing effort to develop means of improving the treatment modality of muscle-invasive, organ-confined disease such that survival is improved and the morbidity reduced. In this regard, rather than radical surgery, radiation exposure has been explored in the last few decades as an alternative, radical treatment modality for bladder cancer. However, there are no

randomised, controlled trials (RCT) which compare RC with radiotherapy (RT). One recent attempt to examine this issue, in a RCT setting, was the SPARE (selective bladder preservation against radical excision) trial, which closed prematurely due to poor accrual of patients (Huddart RA *et al*, 2010). However, there is a recent Cochrane review of published clinical series which suggested that RT alone, as a mono-therapy, confers less survival benefit compared to RC (Shelley MD *et al*, 2002). Therefore, RC remains the "gold standard" option under normal circumstances (Stenzl A *et al*, 2009). However, if the patient is deemed unfit for surgery or if the patient chooses not to have surgery, most centres regard RT as a valuable curative alternative. A recent retrospective study comparing RC with RT, in 169 patients in a large U.K. teaching hospital, found that there were indeed no significant differences in overall, cause-specific, and distant recurrence-free survival between the two groups even though those in the RT group were significantly older (Kotwal S *et al*, 2008). Given that bladder cancer patients are an increasingly elderly population, this study highlighted the need for RT to be considered a viable radical treatment modality.

There is also a drive towards incorporating irradiation as part of a multimodal treatment in an effort to cure organ-confined MIBC (T2-4a) with the rationale of providing bladder preservation. Such bladder-sparing multimodal therapies often involve an initial TURBT followed by irradiation and systemic chemotherapy. These multimodal treatments (MMTs) are often also referred to as "trimodality treatment (TMT)" or "combinational modality treatment (CMT)". Chemotherapy is usually with a cisplatin-containing regimen, usually combined with paclitaxel or fluorouracil, and is given at the time of RT to increase the radiosensitisation of

tumours. A few weeks following TURBT and concomitant chemo-RT, a cystoscopy is performed to evaluate the response. If there is complete response (CR), either macroscopically or microscopically, further consolidation chemo-RT is usually given with the intent of sparing the bladder. However, if there is microscopic or macroscopic tumour on cystoscopy, the multimodal regimen is abandoned and salvage cystectomy is usually performed. The 5-year survival (overall survival, OS) with such MMTs has been reported to be 45-54% (Rodel C *et al*, 2002; Shipley WU *et al*, 2002; Shipley WU *et al*, 2003). Such series have also reported the achievement of CR in 60-85% of patients and, after accounting for those who undergo salvage cystectomy for poor response to chemo-RT, 5-year survival rates with an intact bladder are quoted to be around 40-45% in these patients undergoing bladder-sparing MMT.

When considering bladder-preservation, the drive towards MMT comes from an accumulation of evidence that mono-therapy with either TURBT, radiotherapy or chemotherapy alone does not produce acceptable oncological outcomes. Mono-therapy measures are unlikely to cure muscle-invasive disease compared to RC. When "limited surgery" (as opposed to RC) with either TURBT or partial cystectomy alone was used, local disease control was only possible in approximately 20% of cases (Hall HW, 1987; Henry K *et al*, 1998). When systemic chemotherapy alone was used, with a combination of cisplatin, epirubicin, vinblastine and methotrexate, the outcomes were not much better with only around 19% of patients enjoying a 3-year recurrence-free survival (Hall RR *et al*, 1990). When RT alone was used, local control was surprisingly better at about 40% but was still significantly lower compared to RC (around 80-90%) and the 5-year survival rates

were 38-59% for T2 disease and 14-39% for T3-4a disease (Jenkins BJ *et al*, 1988; Gospodarowicz MK *et al*, 1989; De Neve W *et al*, 1995; Mameghan H *et al*, 1995). However, there have been improvements in delivering RT in the last decade and this has reflected in better outcomes whereby the results are similar to RC (Kotwal S *et al*, 2008; Hoskin PJ *et al*, 2009; Huddart RA *et al*, 2013;).

When a combination of modalities is considered, comparing RT alone against a combination of RT and cisplatin, in patients with T3 disease in a randomised controlled trial, there was an improvement in local disease control from 47% (radiotherapy) to 67% (radiotherapy and cisplatin) (Coppin CM *et al*, 1996). In a similar vein, combining TURBT and chemotherapy nearly doubled the CR rate to 33-56%, compared to either modality alone but was still significantly less than radical cystectomy (80-90%) (Hall RR *et al*, 1984; Prout GR *et al*, 1990; Herr HW *et al*, 1998). Following these encouraging outcomes resulting from a combinational approach, the North American Radiation Therapy Oncology Group (RTOG) conducted a phase II study involving 42 patients (Tester W *et al*, 1993). The patients were treated with cisplatin and once-daily RT (40Gy) concurrently. Complete responders were treated with further cisplatin and consolidation RT (24Gy). Non-responders underwent RC. The CR rate was 66% and the 5-year survival was 52% with 42% surviving with an intact bladder. Other groups, such as those at Massachusetts General Hospital (MGH) and the Medical Research Council (MRC), have looked at the potential benefit of neoadjuvant chemotherapy prior to RT or prior to chemo-RT (Kaufman DS *et al*, 1993; International Collaboration of Trialists, 1999). The results did not demonstrate a clear benefit in favour of administering chemotherapy in a neoadjuvant fashion. However, it is noteworthy

that, when considering chemotherapy in a neoadjuvant setting prior to radical cystectomy (not as part of MMT regimen), there is an approximately 5% absolute improvement in survival at 5 years (Stenzl A *et al*, 2009). This has led many Urological societies to issue a firm recommendation advocating the use of cisplatin-based, neoadjuvant chemotherapy to all eligible patients with bladder cancer undergoing radical treatment (RC or RT).

Following lack of evidence in support of neoadjuvant (versus concurrent chemotherapy), for the purpose of MMT, groups have also looked into optimising the protocol of RT delivery. Twice-daily, fractionated RT has been investigated as an alternative to the once-daily RT regimen but there does not appear to be a clear benefit in favour of a twice-daily regimen (Housett M *et al*, 2005; Horwich A *et al*, 2005). The rationale for fractionation is that there is potential for increased biological response and faster completion of induction rendering quicker identification of non-responders; however, due to lack of clear benefit, different groups tend to prefer one or the other RT strategy.

There have also been trials attempting to improve the efficacy of chemotherapy by adding other chemotherapeutic agents such as paclitaxel and gemcitabine to cisplatin. RTOG investigated a concurrent chemotherapy regimen involving cisplatin and paclitaxel followed by adjuvant cisplatin and gemcitabine (Kaufman DS *et al*, 2009). They demonstrated an impressive CR of 81% with a 5-year overall survival of 56% and disease specific survival of 71%. Others, such as the University of Erlangen group, which has one of the oldest series on multimodal treatment, have added 5FU (5-fluorouracil) to cisplatin and have found an increase in CR from 82%

to 87% and an improvement in overall survival from 62% to 65%, at 5 years (Weiss C *et al*, 2007). RTOG are currently investigating the relative efficacies of paclitaxel against 5FU when added to cisplatin. In a recently published study, where patients were randomised to RT alone versus RT with concurrent 5FU and mitomycin, there was no significant difference in survival but there was a significant difference in loco-regional recurrence (James ND *et al*, 2012).

However, complete response (CR) is not achieved in approximately 12-40% of patients undergoing MMT; consequently, they are candidates for immediate salvage cystectomy (reviewed in: Rene NJ *et al*, 2009). However, even in those deemed to have achieved CR and have completed MMT, approximately 14-50% will go on to fail locally with most recurrences occurring within 12-24 months. Most local recurrences are superficial (non-muscle invasive), occurring in approximately 60% of patients, and are usually managed with TURBT. The remaining 40% are muscle-invasive and are considered for salvage cystectomy. Overall, following MMT, 5-year survival with an intact bladder is approximately 38-51% which represents around 80% of those who had committed to a bladder-sparing regimen.

One of the main objectives of current MMT trials is to improve the selection of patients such that those selected are likely to have a CR to chemo-RT. There is a suggestion that completeness of response to chemo-RT is predictive of the likelihood of the development of metastases and, therefore, predictive of survival. The University of Erlangen group found that in those who had achieved CR, the 5-year and 10-year survival, free from metastases, were 79% and 70% respectively. However, if response was incomplete, these figures

decreased to 52% and 48% respectively (Rodel C *et al*, 2002). Similarly, Housset *et al* demonstrated that 5-year overall survival decreased significantly from 78% in those with CR to 29% in whom the response was incomplete (Housset M *et al*, 2005). These results suggest that the biological behaviour of tumours can be predicted on the basis of their response to chemo-RT. If tumours respond well to chemo-RT, the patients are likely to do well long-term in terms of survival. Therefore, it can be argued that, if tumours can be selected which are likely to respond well to chemo-RT, those patients can be subjected to MMT. Those which are unlikely to respond well to MMT can be stratified into RC straight away so that there is no delay to their definitive treatment and also that they are not exposed to the possibility of adverse effects of a treatment (MMT) which is ultimately unlikely to benefit them. For instance, there is a concern that RT can cause tissue change and render orthotopic substitution cystoplasty very difficult when patients undergo salvage RC after MMT.

In this regard, there are several biological markers, involved in the DNA damage response (DDR) pathway, which have been reported to predict biological responsiveness to chemotherapy and/or radiotherapy. X-ray repair cross complement group 1 protein (XRCC1) and human apurinic/apyrimidinic endonuclease (APE1) are proteins involved in the base excision repair (BER) process following ionising radiation-induced DNA base damage (Vidal AE *et al*, 2001). XRCC1 acts as a scaffold for APE1 which has enzymatic activity in producing BER (Mortusewicz and Leonhardt, 2007). High levels of XRCC1 or APE1 have been shown to be predictive of responsiveness to RT and to overall survival (Sak SS *et al*, 2005). Similarly, the excision-repair cross-complementing

group 1 (ERCC1) protein expression has been shown to correlate with efficacy of response to chemo-RT (Kawashima A *et al*, 2010). ERCC1 is important in the nucleotide excision repair (NER) pathway and its deficiency has been demonstrated to result in sensitivity to ionising radiation (Park CH *et al*, 1995; Ahmad A *et al*, 2008). Lack of ERCC1 is also reported to correlate with sensitivity to cisplatin treatment because ERCC1, as part of the NER pathway, is involved in the removal of cisplatin from DNA adducts (Olaussen KA *et al*, 2006; Bellmunt J *et al*, 2007).

Another DDR pathway protein reported to have predictive value in radiosensitivity to bladder cancer treatment is Mre11 (Choudhury A *et al*, 2010). Mre11 is part of the MRN complex and plays a crucial role in the detection and repair of DNA double strand breaks. Choudhury *et al* demonstrated reduced expression of Mre11 to correlate with poor outcomes in patients who had undergone radical radiotherapy for MIBC. However, protein expression of Rad51 and Nbs1, also part of the MRN complex, did not have similar predictive value. Other proteins involved in the DDR pathway, such as ATM, γH2AX and p53, also did not reveal a correlation with outcomes in their study. The lack of correlation between p53 expression and radiosensitivity or treatment outcomes is not novel as there are conflicting reports in the literature. Some studies have demonstrated a correlation of *TP53* mutations with radio-sensitivity and improved outcomes (Ribeiro JC *et al*, 1997; Rotterud R *et al*, 2001). In contrast, other studies have reported radio-resistance and poor outcomes as a result of *TP53* mutations (Hinata N *et al*, 2003; Poeta ML *et al*, 2007). A recent systematic review of the literature on p53 status and outcomes in colorectal cancers concluded that a definitive correlation could not be made due to publication bias and heterogeneity of reports (Munro AJ *et al*, 2005).

Specifically in relation to multiple modality treatment (MMT) in bladder cancer, one RTOG study has demonstrated a significant correlation between Her-2 expression and poor response to chemo-RT (Chakravarti A *et al*, 2005). Others have reported that the apoptotic index and Ki-67 expression, but not p53 or bcl-2 expression, are related to complete response (CR) after MMT (Rodel C *et al*, 2002). Matsumoto *et al* have reported that Ki-67 expression and Bax to Bcl-2 ratio are predictive of CR following MMT (Matsumoto H *et al*, 2004).

There is therefore a rationale for formulating a panel of biomarkers which can have predictive or prognostic value in determining the outcomes of MMT in a bladder-sparing regimen. It is worth interrogating the predictive value of a panel of biomarkers, incorporating ones listed above as well as those involved in the DDR pathway, such as AIMP3, in the selection of appropriate patients for MMT. Selection of those patients likely to respond well to MMT would ensure preservation of bladder, reduction of side-effects attributable to radical surgery, without necessarily compromising the oncological outcomes. This strategy may lead to a shift in the paradigm of bladder cancer management, from radical surgery to a less-invasive one, akin to the recent shift in the management of breast cancer from radical surgery to a far less aggressive regimen involving lumpectomy, local irradiation and systemic chemotherapy with the addition of anti-Her-2 depending upon expression status of Her-2.

1.5 Background work by group: identification of AIMP3 as a dysregulated gene in bladder cancer suitable for investigation

The current project builds upon work carried out by our group in discovering and investigating novel biomarkers in bladder cancer. Leading up to this project, our group had completed a genomic analysis of muscle invasive bladder cancer (MIBC) and non-muscle invasive bladder cancer (NMIBC) by expression array and array comparative genomic hybridisation (aCGH). In an initial genome-wide survey, using aCGH at 1Mb resolution, our group identified copy number gains and amplifications of Mouse Double Minute 4 (MDM4) and gain of Aurora kinase A (AURKA) associated with an aggressive phenotype in bladder cancer (Veerakumarasivam A *et al*, 2008; Veerakumarasivam A *et al*, 2008). These genes are currently the subject of early phase trials in advanced bladder cancers. In order to identify potential tumour suppressor genes (TSGs), copy number loss (regions with hemi and homozygous deletions) was annotated across the dataset. By this method, multiple potential hits were identified; however, it was noted that many loci spanned gene-poor regions which were less likely to harbour significant TSGs. Using a bioinformatic approach, the search strategy was altered to combine CGH along with expression array data generated using an Agilent human 21K chip; the datasets were analysed by incorporating independent sets and whole genome libraries.

In addition, through collaboration with Oncomethylome Sciences (OMS), a methylation library containing a whole genome map representing CpG-rich gene promoter sites was interrogated. For the analysis, expression array data was normalised and ranked to identify low level transcript expression in MIBC and

NMIBC; ranked transcripts were screened using the CpG promoter site library. It was postulated that the targets identified by this process may be TSGs which are epigenetically silenced, especially if accompanied by hemizygous deletions. Using this strategy, a number of potential targets were identified which warrant further analysis (**Table 1.3**). Table 1.3 lists the gene ontologies (GOs) that represent the identified targets; expressed as molecular function of gene products, their role in multi-step biological processes, and their localization to cellular compartments. Many of the identified target genes are involved in basic cellular homeostasis processes.

One such target was amino acyl tRNA synthetase (ARS) – interacting protein 3 (AIMP3). *AIMP3* was confirmed, by quantitative RTPCR, as demonstrating low expression in bladder cancer (unpublished, **Figure 1.7**). Furthermore, *AIMP3* was found to have a CpG-rich promoter which was potentially methylated. In collaboration with OMS, a pilot study was conducted on a small number of cases which confirmed that *AIMP3* was indeed hyper-methylated in bladder cancer (unpublished, **Figure 1.7**). Although copy loss was not identified using aCGH (unpublished), the analysis suggested that hypermethylation of *AIMP3* may play a role in the development of an aggressive phenotype and potentially in the progression from NMIBC to MIBC.

Table 1.3: List of non-redundant gene ontologies (GOs) of lowest expressing genes.

Gene Ontology (GO)	Example of genes
Biological Process	
Regulation of nucleobase, nucleoside, nucleotide and nucleic acid metabolic process	*C20orf100,RBM15B,MTERF,NPAS2,RARB,*
RNA biosynthetic process	*C20orf100,MTERF,NPAS2,RARB,TCEA3,*
Intracellular transport	*IMMP2L,MRPL32,TRAPPC1,BNIP1,STARD3*
Protein modification	*STK11,PRKCD,CHM,ARD1A,MINK1,CASK*
Translation	*PELO,PABPC4,MRPL13,**AIMP3**,MRPL32*
Cell death	*TPT1,IFNB1,BNIP1,SCIN,EEF1E1*
Phosphorylation	*MINK1,CASK,STK11,PRKCD*
Blood coagulation	*ENTPD2,PABPC4,TBXAS1,FGA*
DNA packaging	*CHAF1B,L3MBTL2,ARD1A*
Cellular secretion	*BNIP1,SCIN,TRAPPC1*
Molecular Function	
Zinc ion binding	*L3MBTL2,ZNF138,APOBEC3G,PRKCD,TCEA3*
Protein kinase activity	*CASK,PRKCD,STK11,MINK1*
ATP binding	*STK11,MINK1,CASK,PRKCD*
Pyrophosphatase activity	*RRAS,ENTPD2*
Symporter activity	*SLC16A4,SLC25A18*
Iron ion binding	*SC5DL,TBXAS1*
Double-stranded DNA binding	*MTERF*
Phosphatidylinositol binding	*SCIN*
Chloride transporter activity	*SLC26A1*
Phosphatidylinositol-4,5-bisphosphate binding	*SCIN*
Cellular Component	
Intracellular organelle	*PRKCD,TCEA3,ZZZ3,NPAS2,NUP37,IMMP2L*
Intrinsic to membrane	*JAM2,RNF133,LIME1,SLC25A36,GRIK3*

Cytoplasm	*SC5DL,CHAF1B,STARD3,**AIMP3**,SCIN*
Plasma membrane part	*SLC16A4,PELO,FLRT3,AQP4,JAM2,CASK*
Ribonucleoprotein complex	*MRPL13,MRPL32*
Synaptosome	*CASK*
Aminoacyl-tRNA synthetase multienzyme complex	***AIMP3***
Outer membrane	*AQP4*
SNARE complex	*BNIP1*
Basal lamina	*ENTPD2*

In a separate pilot study, the focus was on the optimisation of immunohistochemistry (IHC) using the AIMP3 polyclonal antibody (Abcam) on sections of normal (n=12) and cancer cases (n=123) embedded into a tissue microarray (TMA) (**Figure 1.7**). AIMP3 immunostaining was strongly positive in normal bladder and other normal tissues; however, staining was weaker in MIBC (**Figure 1.7A**). This corroborated the AIMP3 gene expression findings at protein level; a trend was observed of a generalised reduction in AIMP3 expression in cancer compared to normal urothelium (**Figure 1.7B**). The experiment was also useful to establish the staining methodology, appropriate controls and scoring method.

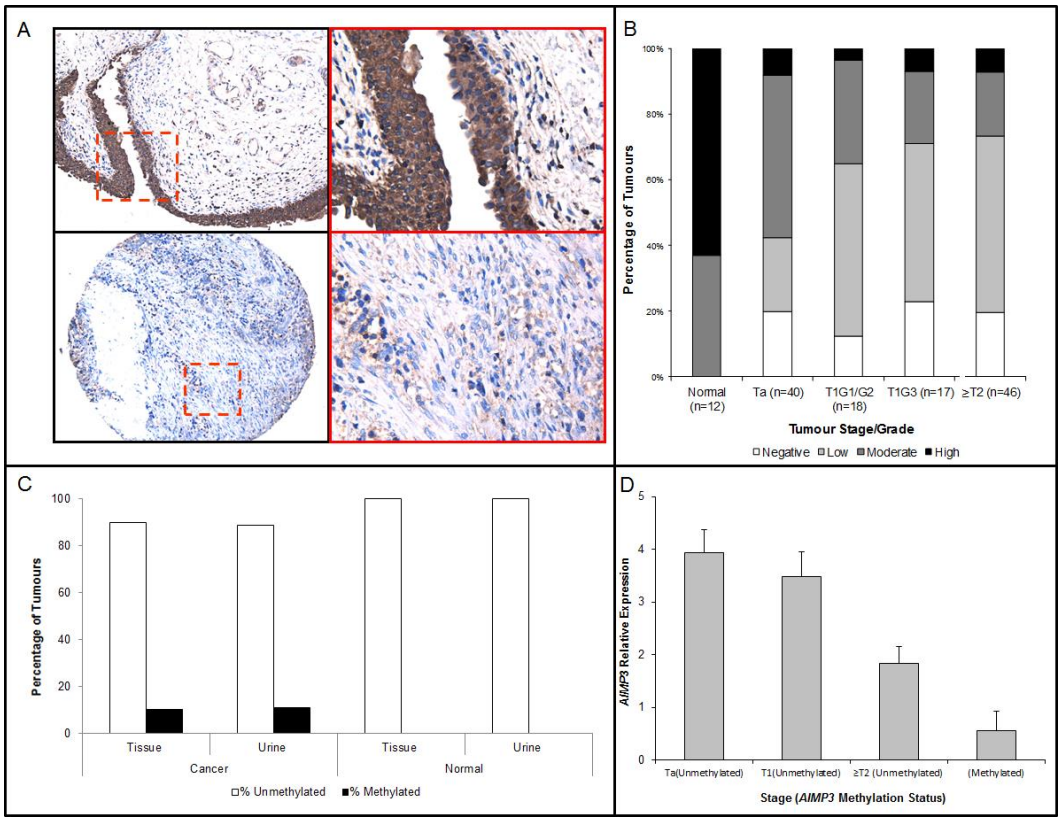

Figure 1.7: Loss of AIMP3 is a feature of invasive bladder cancer and AIMP3 promoter methylation is cancer-exclusive. **(*A*)** Top: Normal urothelium demonstrating high expression of AIMP3 (Left x20 magnification; Right x60 magnification); Bottom: Expression of AIMP3 is lost in an invasive T2G3 tumour (Left x20 magnification; Right x60 magnification). **(*B*)** There is a general loss of AIMP3 expression in cancer as compared to normal urothelium and a downward shift in the percentage of moderate/high expressing tumours exists with stage/grade progression. **(*C*)** Promoter methylation of AIMP3 was detected in about 10% of tumours as well as cells in urine sediments derived from patients with tumours but was not detected in corresponding normal cells. **(*D*)** Relative AIMP3 mRNA expression stratified by tumour stage/grade and methylation status. Methylated tumours demonstrated a significant loss in expression, while a marked difference was observed between Ta/T1 and T2/higher tumours ($p<0.001$). Bars, (standard error) SE

1.6 Research hypothesis and objectives

The foregoing review of the role of AIMP3 as a tumour suppressor involved in the DDR pathway, the main components of the DDR pathway, the need for biomarkers to predict outcomes of chemo/radio-therapy in bladder cancer and our preliminary findings of AIMP3 expression in bladder cancer resulted in the formulation of the following hypotheses:

"*AIMP3 is predictive of response to chemo- or radio-therapy in vitro in bladder cancer cell lines"*

"AIMP3 expression status may be predictive of clinical outcome following radio- or chemo-therapy in patients with muscle-invasive bladder cancer."

The main objectives of the research were as follows:

A) To demonstrate whether downregulation of AIMP3 by siRNA transfection in a panel of bladder cancer cell lines impacts on functional outcomes (e.g. alters clonogenic survival) following exposure to radiotherapy.

B) To demonstrate whether expression status of AIMP3 predicts survival following radical radiotherapy in patients with muscle-invasive disease (e.g. in a cohort of patients enrolled in a radical radiotherapy trial such as BCON).

C) To investigate whether expression status of AIMP3 is predictive or prognostic by correlating expression status with survival in an "untreated/control" set of patients undergoing radical cystectomy (i.e. not treated with concurrent or adjunctive radical radiotherapy; not treated with either neoadjuvant or adjunctive chemotherapy).

D) To investigate the predictive or prognostic value of other DDR proteins (e.g. p53, Mre11, ERCC1) which are reported to be significant.

E) To investigate whether siRNA downregulation of AIMP3 impacts on functional outcome (e.g. alters clonogenic survival) following cisplatin exposure in a panel of cisplatin-sensitive and cisplatin-resistant bladder cancer cell lines (e.g. RT112 and RT112CP).

F) To investigate the predictive or prognostic value of AIMP3 in a group of patients treated with cisplatin-based neoadjuvant chemotherapy prior to radical treatment (e.g. either radical radiotherapy or radical cystectomy).

Chapter 2

Materials and Methods

2.1 Cells

The choice of bladder cancer cell lines was as follows, with HeLa being used as a reported positive control for AIMP3 in most experiments (David A *et al*, 2011; Kwon NH *et al*, 2011; Park BJ *et al*, 2005):

- T24
- RT112
- RT112CP
- 253J
- RT4

- HeLa

All cell lines were obtained in-house from Professor John Masters with identities checked through STR (short tandem repeat) profiling. All the cells were maintained as monolayers using RPMI 1640 media (Gibco Invitrogen, Paisley, UK) supplemented with 10% heat-inactivated FBS (fetal bovine serum) (Flow Laboratories, Irvine, UK) and 2mM L-glutamine (Gibco Invitrogen). Cells were incubated at 37^{o}C in a humidified atmosphere of 5% CO_2 in air. When sub-culturing was required, the monolayers were detached using trypsin (0.01%) (Difco Laboratories, London, England) with versene (0.003%) (BDH Chemicals, Poole, England) in PBS (phosphate buffered saline) (Gibco Invitrogen). Mycoplasma was not demonstrable in nutrient agar culture and with indirect fluorescent staining.

The characteristics of the bladder cancer cell lines are summarised in **Table 2.1**. T24 cell lines were originally derived from a grade III transitional cell bladder carcinoma in 1970 in Sweden from an 82 year old woman (Bubenik J *et al*, 1973). RT112 cells were originally established at the Institute of Oncology, University of London, from a grade I-II transitional cell carcinoma of the bladder (Masters JRW *et al*, 1986). RT4 was originally derived from a recurrent grade I transitional cell bladder carcinoma (Rigby and Franks, 1970). T24 is not tumorigenic in nude mice (Marshall CJ *et al*, 1977). RT112 is clonogenic in nude mice (Marshall CJ *et al*, 1977). RT4 is not tumorigenic in nude mice (Marshall MJ *et al*, 1994). T24 contains p53 mutant protein while RT112 contains wild-type p53 (Cooper MJ *et al*, 1994; Warenius HM *et al*, 2000). RT4 was found to produce wild-type p53 (Cooper MJ *et al*, 1994). RT4, RT112, 253J and T24 are reported to display phenotypes representative of a spectrum of well-differentiated, moderately-differentiated and poorly-differentiated urothelial carcinoma respectively where RT4 is well-differentiated and T24 the least well-differentiated (Booth C *et al*, 1997). RT4 and RT112 are reported to demonstrate a superficial pattern of growth and are regarded by some as models of non-invasive models of bladder cancer (Booth C *et al*, 1997). In contrast, T24 and 253J demonstrate aggressive, invasive growth patterns and are regarded as models of invasive bladder cancer (Davies G *et al*, 1999; Elliott AY *et al*, 1977). RT112CP is a cisplatin-resistant subline of RT112 (Bedford P *et al*, 1987).

Table 2.1: Original characteristics of bladder cancer cell lines used

Cell line	Origin	Clinical stage	Histological grade	Year culture established	Sex of patient	Patient's prior therapy	Population doubling time (hours)	Tumorigenecity in nude mice	P53 status
T24	Recurrence in bladder	NR	G3	1970	F	None	21	No	mut
253J	Retroperitoneal lymph node metastasis	T4	G4	1972	M	NR	28	Yes	mut
RT112	Bladder primary	NR	G1-2	1973	F	None	24	Yes	wt
RT112CP	Bladder primary (RT112 subline)	NR	G1-2	1987	F	None	24	NR	NR
RT4	Recurrence in bladder	T2	G1	1967	M	Gold grains 2 years earlier	37	Yes	wt

F=female; M=male; mut=mutant; NR=not recorded; wt=wild-type

2.2 Western blot analysis

2.2.1 Protein extraction

Cells for protein extraction were washed with cold PBS (phosphate buffered saline) (Gibco Invitrogen, Paisley, UK). The cells were lysed in appropriate volumes (e.g. 200 µl for T25 flasks; 600 µl for T75 flasks) of modified radioimmunoprecipitation (RIPA) buffer [50 mM Tris-HCl, pH 7.4, 1% TritonX-100, 150 mM NaCl, 1 mM EDTA, 1 mM NaF, 1 mM Na_3VO_4, 1 protease inhibitor cocktail tablet per 10 ml of RIPA buffer (Complete Mini, Roche Diagnostics, Mannheim, Germany). The lysed cells were removed from the flasks using cell scrapers (BD Falcon, Bedford, MA, USA) and transferred into 1.5 ml Eppendorf tubes. The lysates were left on ice for 15 minutes and then centrifuged at 13,000 rpm for 15 minutes at 4°C. After centrifugation, the supernatants were collected in pre-chilled Eppendorf tubes ready for subsequent studies or for storage at -80°C.

2.2.2 Protein concentration measurement

The total protein concentrations of the lysates extracted from the cells were measured using the Modified Lowry Protein Assay Kit (PIERCE, Rockford, IL). Serial dilutions of Bovine Serum Albumin (BSA) were made from the BSA standard solution (2 mg/ml, supplied in the PIERCE Kit) as listed in **Table 2.2**. Briefly, 125 µl of the original BSA standard (2 mg/ml) is diluted with 375 µl of distilled water to obtain the initial concentration standard of 500 µg/ml (0.5 mg/ml) in Vial A; 200 µl of BSA from Vial A is diluted with 200 µl of distilled water to obtain 250 µg/ml standard in Vial B and so on in a serial dilutional method down to 31.25 µg/ml

standard in Vial E. Vial F contains no BSA (0 µg/ml) making it the "blank" for spectrophotometric purposes.

Table 2.2: BSA standards preparation

Vials	Volume of BSA (µl)	Volume of diluents (µl)	Final BSA concentration (µg/ml)
A	125	375	500
B	200	200	250
C	200	200	125
D	200	200	62.5
E	200	200	31.25
F	0	200	0 (blank)

Ten microliters (10 µl) of each lysate sample was diluted 20 fold with 190 µl of distilled water (total volume 200 µl). One millilitre (1 ml) of Modified Lowry Protein Assay Reagent was added to each diluted sample or BSA standard and mixed gently. The mixture was then incubated for exactly 10 minutes at room temperature. 2N Folin-Ciocalteu Reagent (supplied by the Kit) was diluted 50:50 with distilled water (e.g. 2 ml reagent with 2 ml distilled water) to make the final reagent concentration of 1N. At the end of the 10 minute incubation period, 100 µl of 1N Folin-Ciocalteu Reagent was added to each lysate sample or BSA standard and mixed gently. The mixture was incubated for 30 minutes at room temperature. Afterwards, the samples were measured using the UV/Visible Spectrophotometer (Ultrospec 3100 Pro). Standard curve was plotted automatically by the machine

based on absorbance readings against the concentrations of BSA standards. Readings of lysate samples were taken from the machine and concentrations were calculated by multiplying ×20 on account of the original 1:20 dilution of the lysates.

2.2.3 SDS PAGE and protein blotting

Equal amounts of total protein from lysate samples were normalized to the same volume using RIPA buffer. Appropriate volume of 6x Sample Buffer (200 mM Tris, pH6.8, 60% glycerol, 12 mM EDTA, 12% SDS, 864 mM β-mercaptoethanol, 0.05% bromophenol blue) were added to the protein samples to reach the final concentration of 1x SB. The mixture was heated at 95°C for 5 minutes. The denatured protein samples were then ready to be loaded onto the sodium dodecyl sulphate (SDS)-polyacrylamide gel with the concentration of acrylamide tailored to the size of the protein being investigated (e.g. 14% gel for p18; 8% for ATM/ATR). The recipe of SDS-polyacrylamide gel is listed in **Table 2.3**.

Table 2.3: Recipe of SDS-polyacrylamide gel. (***A***) Resolving gel, (***B***) Stacking gel

A **Resolving gel**					
	6%	**8%**	**10%**	**12%**	**14%**
1 M Tris, pH8.8	3.75 ml	3.75 ml	3.75 ml	3.75 ml	3.75 ml
30% Acrylamide	2 ml	2.67 ml	3.33 ml	4 ml	4.67 ml
H_2O	4.2 ml	3.53 ml	2.87 ml	2.2 ml	1.53 ml
20% SDS	50 µl	50 µl	50 µl	50 µl	50 µl
10% (APS)	100 µl	100 µl	100 µl	100 µl	100 µl
TEMED	6 µl	6 µl	6 µl	6 µl	6 µl

B **Stacking gel**	
1 M Tris, pH 6.8	375 µl
30% Acrylamide	374 µl
H_2O	2.24 ml
20% SDS	15 µl
10% APS	30 µl
TEMED	5 µl

For one SDS-polyacrylamide gel, around 8 ml of resolving gel solution was poured into the assembled Mini-PROTEAN III (Bio-Rad) gel cassette. Isopropranolol was added to the top of the resolving gel to ensure a sharp and uniform interface between the resolving and loading gels. When the resolving gel was set, the isopropanolol layer was poured off, washed a few times with distilled water and the stacking gel solution was prepared and poured onto the top of the resolving gel. The comb was

placed into the stacking gel before the gel was set. When the whole gel was set, boiled protein samples (in the sample buffer mixture) were loaded into the separated wells. Ten microliters (10 µl) of Rainbow Molecular Weight Marker (Amersham, GE Healthcare) was loaded as the reference for molecular sizes.

The gel was then subjected to electrophoresis using the Mini PROTEAN III Electrophoresis System (Bio-Rad) at a constant current (20 mA per gel) in running buffer (diluted to 1x from 5x stock containing 37 g Trizma base, 7.5 g Glycine and 0.5 g SDS made up to 500 ml distilled water) for 1-2 hours until the dye, from the sample buffer in the loaded samples, was running out from the bottom of the gel.

2.2.4 Western blotting

Immediately after the SDS-PAGE, proteins on the SDS-polyacrylamide gel were transferred onto a Polyvinylidene fluoride (PVDF) membrane (Millipore, Sigma-Aldrich, St Louis, MO). The transfer sandwich, including the sponge, filter paper, gel and PVDF membrane, was assembled as illustrated below (**Figure 2.1**):

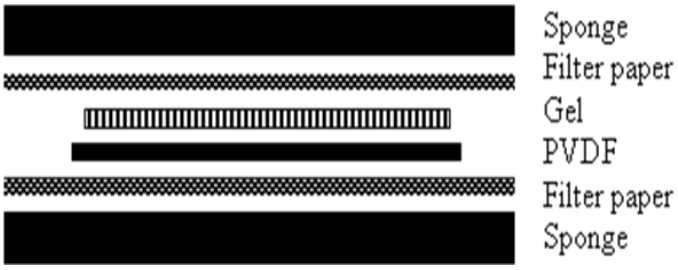

Figure 2.1: Western blot transfer sandwich

Every component of the transfer sandwich was rinsed in transfer buffer (diluted to 1 x from 10 x stock containing: 37 g glycine and 7.5 g Trizma base made up to 500 ml with distilled water). The PVDF membrane was pre-wet in 100% methanol for 15 seconds and then rinsed in transfer buffer. The transfer sandwich was placed into the assembly tray of the Mini Trans-Blot Cell (Bio-Rad) which was filled with transfer buffer. The gel was closed to the cathode and the electrotransfer was carried out at a constant voltage of 20 V overnight at 4 °C. After electrotransfer, the membrane was rinsed briefly in PBS-Tween 20 (PBS-T, 0.1% Tween-20 in 1x PBS) and blocked in 5% non-fat milk (in PBS-T) for 1 hour at room temperature. After blocking, the membrane was probed with 5 ml of appropriately diluted primary antibody (the details of the antibodies used are listed in **Table 2.4**) in 1% non-fat milk (in PBS-T) and incubated for 1-2 hours at room temperature or over-night at 4 °C.

After primary antibody incubation, the membrane was washed with PBS-T for 2 minutes four times. After washing, the membrane was incubated with 5 ml of horseradish peroxidase (HRP)-conjugated secondary antibody diluted in 1% non-fat milk (in PBS-T) for 1 hour. The membrane was then washed with PBS-T for 2 minutes four times after which it was ready for enhanced chemi-luminescent (ECL) development.

Table 2.4: Details of the antibodies used.

Antigen against -	Manufacturer	Catalogue Number	Dilution Factor
AIMP3 (p18/EEF1E1)	AbCam	Ab31543	1:10,000
p53	Cell Signaling	2982	1:1,000
Beta-Actin	AbCam	Ab6276	1:20,000
GAPDH	Sigma-Aldrich	G9545	1:10,000
Anti-Rabbit IgG-HRP	Santa Cruz	sc-2314	1:5,000
Anti-Mouse IgG-HRP	Santa Cruz	sc-2030	1:5,000

2.2.5 Chemi-luminescence

The chemi-luminescent signals were detected using Pierce ECL Western Blotting Substrate (PIERCE). Appropriate volume of mixture of Detection Reagents 1 and 2 at a 1:1 ratio was added to the membrane and incubated for 5 minutes at room temperature. The membrane was then placed between two transparency plastic sheets and set into a Kodak BioMax Cassette (Kodak). The membrane was exposed to X-ray films (Kodak) in a dark-room and the films were developed and fixed using pre-diluted developer and fixer solutions respectively (Kodak). The films were washed in water and dried in a drying-cupboard.

2.2.6 Image blot analysis

Developed images, of the Western blot bands on the X-ray films, were scanned as JPEG in 8bit grayscale format at 600dpi, and the pixel intensities were measured using ImageJ freeware from the National Institutes of Health (http://rsb.info.nih.gov/ij). Pixel intensities were measured with corrections for background. Digitised gel intensity data were exported into a database (Excel, Microsoft).

2.3 Clonogenic survival assay

Cells were plated in T75 flasks until approximately 90% confluent. After removing the media from the flasks and washing the cells with PBS, 3 ml of trypsin was added per flask and the cells were re-suspended in media, pipetting several times, to obtain a single cell solution. A suitable volume (e.g. 200 µl) of single cell suspension was treated with Trypan Blue (e.g. 200 µl) and the concentration of cells was counted using a haemocytometer under microscopy. The cells were then plated in 60 mm petri dishes (Nunc), in triplicates, at different numbers ranging from 0 to 1000 (i.e. 0 cells per petri dish, 100 cells, 200 cells, 500 cells, 750 cells, 1000 cells). Five millilitres (5 ml) of RPMI 1640 media (Invitrogen) (supplemented with L-glutamine and FBS) were added to each dish and the dishes shaken gently to allow even mixing and distribution of cells. The cells were then incubated for approximately 14 days with a change of media at day 7. Following the incubation period, the media was discarded from the dishes and the cells fixed with 70% IMS (industrial methylated spirit) for 5 minutes. The IMS was replaced with 1% crystal violet to

stain the cells. After approximately 30 minutes, the crystal violet solution was washed off under gentle running tap water. When dry, the colonies stained were counted under the dissecting microscope.

The serial plating of cells allowed the optimal plating number for each of the cell lines to be deduced. This was based on the maximal number of individual colonies (each colony consisting of >50 cells) that could be counted on each petri dish. This was variable between cell lines due to the differing plating efficiencies of the cell lines as well as the size of their colonies.

2.4 Irradiation

Cells were grown to a logarithmic phase of growth at approximately 80% confluence in either T25 or T75 flasks. The cells were then exposed to the dose of X-ray irradiation required (for instance, 0 Gy, 2 Gy, 5 Gy – see **Table 2.5** below) using a CP320 Bipolar X-ray machine (Gulmay, Kent, UK). Doses were adjusted by varying the duration of irradiation (2 Gy/min) while the voltage (250 kV), current (12.5 mA), X-ray filter (Sn, Cu, Al) and distance from X-ray source (30 cm) remained constant.

Following irradiation, cells were incubated to the length of time required (time points: 0 hours, 1 hour, 6 hours, 24 hours, 48 hours) post irradiation. At the appropriate time-point, the cells were subjected to either Western blot analysis or Clonogenic assays. For Western analysis, cells were washed with cold PBS quickly and lysed with appropriate volumes of modified RIPA buffer. Cells were then

scraped with cell scraper and the protein extracted, quantified and either used or stored as described above. For Clonogenic assays, cells were washed with PBS, trypsinised into single-cell suspensions, counted and plated onto petri dishes at the relevant plating numbers.

Table 2.5: Irradiation parameters

kV	* mA	Filter	Distance	Dose Rate Gy/min
215	12.5	**1**	30	1.31
			60	0.33
			90	0.14
215	12.5	**2**	30	3.30
			60	0.82
			90	0.37
215	12.5	**3**	30	6.40
			60	1.60
			90	0.71
250	12.5	**1**	30	2.04
			60	0.51
			90	0.23
250	12.5	**2**	30	4.52
			60	1.13
			90	0.50
250	12.5	**3**	30	9.90
			60	2.47
			90	1.1
200	10	**2**	30	2.08
			60	0.52
			90	0.23

*The mA is proportional to the dose rate therefore halving the mA will halve the dose rate

Filter 1 is 0.4 mm Sn + 0.15 mm Cu + 1.0 mm Al

Filter 2 is 0.25 mm Cu + 1.0 mm Al

Filter 3 is 1.0 mm Al

Sn: selenium; Cu: copper; Al: aluminium; mA: milliamps; kV: kilovolts; Gy: grays

2.5 Immunofluorescence

Twenty-two millimetres (22 mm) X 22 mm coverslips were sterilised by exposing to ethanol & heat (Bunsen burner). The coverslips were placed in 6-well plates (Nunc). The cells for immunofluorescence studies were trypsinised so as to obtain single-cell suspensions. Cells were plated onto the coverslips in the 6-well plates and incubated overnight with 2 ml of RPMI media such that, after overnight incubation, approximately 40-80% confluence was achieved.

On Day 2, after checking for viability and appropriate confluence, the cells were washed briefly with 2 ml of PBS and fixed by adding 2 ml of formaldehyde into each well. After incubating at room temperature for 30 minutes, the formaldehyde was pipetted off and the wells washed with 2 ml of PBS. The fixed cells were then ready for immediate use or could be stored at 4 degrees for subsequent studies.

For immunofluorescence, the cells were incubated with 2 ml of Permeabiliser Buffer (0.5% TritonX, 1% BSA (bovine serum albumin), PBS) into each well. After at least 10 minutes of incubation, the Permeabiliser buffer was washed off. On clean strips of paraffin membranes, about 150 µl of primary antibody solution drops were

placed separated out such that each drop would accommodate the 22 mm X 22 mm coverslips easily. The Primary Antibody (AIMP3/p18) solution was prepared at 1:500 dilution (e.g. 4 µl of AIMP3/p18 into 2 ml of Permeabiliser buffer). The coverslips were removed from the 6-well plates and placed face-down onto the primary antibody drops on the paraffin strips such that the cells were in direct contact with the antibody solution.

After incubating for at least 1 hour at room temperature, the coverslips were held with forceps and washed several times in PBS making sure of the orientation of the cells on the coverslips. Incubation with secondary antibody solution was then carried out in a similar method on paraffin strips. Appropriate FITC (fluorescein isothiocyanate) (e.g. Anti-rabbit FITC for AIMP3/p18 raised in rabbit) was prepared at 1:500 dilution as above (e.g. 4 µl of anti-rabbit FITC into 2 ml of Permeabiliser buffer). After incubation for at least an hour at room temperature, the secondary antibody solution was washed off as previously by immersing several times into a beaker of PBS. Further immunolabelling (e.g. with TRITC-phylloidin for Actin) was either carried out or fixation of the coverslips onto the microscope slides was performed. For this, 20 µl of DAPI was added onto the microscope slides and the coverslips were placed face-down onto the microscope slides containing DAPI. Confocal microscopy was then performed.

2.6 siRNA transfection

Cells were trypsinised into single-cell suspensions and plated onto 6-well plates with 2 ml RPMI (Gibco, Invitrogen) media (supplemented with FCS & L-Glutamine) such that approximately 40-60% confluence was achieved overnight.

For transfection work, 1X siRNA Buffer was prepared from the stock 5X siRNA Buffer (Thermo Fischer Scientific). Final 5 nM concentrations, from 100 nM stock, of the siRNA (Thermo Fisher Scientific) were prepared for the 4 test conditions:

(1) AIMP3/p18 siRNA

(2) Non Targeting siRNA (negative control)

(3) GAPDH siRNA (positive control)

(4) No Treatment (only Dharmafect as a negative control)

Tube 1 & Tube 2 were prepared (1.5 ml eppendorfs). Into Tube 1 (siRNA), 10 µl of 5 nM siRNA was added into 190 µl of Optimem (serum-free transfection medium) (Gibco, Invitrogen). Into Tube 2 (DharmaFECT), 10 µl of DharmaFECT was added into 190 µl of Optimem. Four-fold (4X) volumes, accounting for pipetting errors, of Tube 2 were prepared to account for each test condition (1) AIMP3/p18 siRNA; (2) Non-targeting negative control; (3) GAPDH positive control; (4) Untreated negative control with only Dharmafect.

Each Tube was gently mixed by pippetting 3-5X. The Tubes were incubated at room temperature for 5 minutes. Then Tube 1 was mixed with the corresponding Tube 2 (= 400 µl final volume of mixture). After gently mixing by pippetting 3-5X, the mixtures were incubated for 20 minutes at room temperature. The mixtures (400 µl) were then added into respective wells (6-well plates). Sixteen hundred micorlitres (1600 µl) of Optimem was added onto each well (final volume 2 ml per well) and the cells incubated. After 12-24 hours of incubation with siRNA-containing Optimem media, the cells were checked for viability. The Optimem (serum-free) media was replaced with 2 ml of complete media containing serum (RPMI supplemented with FCS & L-glutamine). At appropriate time-points (24, 48, 72, 96, 120 hours), cells were checked for viability (to ensure >80% survival for optimal effects) and subjected to further studies as appropriate. For example, Western blot analysis could be carried out at 48-72 hours to demonstrate optimal downregulation of AIMP3/p18 protein expression following siRNA knock-down of AIMP3/p18 in the cells. For clonogenic survival assays, the 6-well plates were exposed to X-ray irradiation at appropriate doses, trypsinised within an hour and replated at appropriate numbers onto petri dishes to allow colony formation to be counted at day 14.

2.7 Cisplatin exposure

2.7.1 Cisplatin dose response

RT112 and RT112CP cells were trypsinised and seeded at 750 cells per 60 mm x 15 mm petri dishes with 5 ml per dish of RPMI media supplemented with 10% FBS and L-glutamine. Plating in petri dishes were done in triplicates. Following incubation overnight, cells were treated with a range of doses of cisplatin (for example, 0

µg/ml, 1 µg/ml, 2 µg/ml, 3 µg/ml, 4 µg/ml, 5 µg/ml, 10 µg/ml, 25 µg/ml, 50 µg/ml). Cisplatin (Sigma, UK) was prepared immediately prior to treatment by dissolving in sterile water to give a concentration of 1 mg/ml. Treatment was for 1 hour by incubating the cisplatin-treated cells at 36.5^0C. Following treatment, cells were washed with PBS and incubated in RPMI media for 14 days with media change at day 7. At day 14, colonies were fixed in IMS, stained with crystal violet and counted (as described in **Section 2.3** above). Experiments were repeated at least 3 times.

2.7.2 Cisplatin sensitivity with AIMP3 knockdown

RT112 and RT112CP cells were trypsinised into single-cell suspensions and plated onto 6-well plates with 2 ml RPMI (Gibco, Invitrogen) media (supplemented with FCS & L-Glutamine) to achieve sub-confluence after overnight incubation.

For transfection work, 1X siRNA Buffer was prepared from the stock 5X siRNA Buffer (Thermo Fischer Scientific). Final 5 nM concentrations, from 100 nM stock, of the siRNA (Thermo Fisher Scientific) were prepared for the 4 test conditions:

(1) AIMP3/p18 siRNA

(2) Non Targeting siRNA (negative control)

(3) GAPDH siRNA (positive control)

(4) No Treatment (only Dharmafect as a negative control)

siRNA transfection was carried out according to the protocol described above in **Section 2.6**. Following transfection, at appropriate time-points (e.g. 24, 48, 72, 96, 120 hours), cells were checked for viability and subjected to further studies as appropriate. For example, Western blot analysis could be carried out at 48-72 hours to demonstrate optimal downregulation of AIMP3/p18 protein expression following siRNA knock-down.

For cisplatin-sensitivity following siRNA knock-down, the 6-well plates were exposed to IC50 doses of cisplatin for 1 hour, washed with PBS, trypsinised into single-cell suspensions, replated at appropriate numbers onto petri dishes and incubated to allow colony formation to be counted on day 14. Media changes were performed on day 7.

2.8 Radiotherapy tissue specimens from the BCON trial

2.8.1 Patient demographics

The Bladder Carbogen Nicotinamide (BCON) trial was a Phase III, RCT which investigated the outcomes of patients with organ-confined bladder cancer randomised to treatment with either radical radiotherapy alone or radical radiotherapy supplemented with carbogen nicotinamide (CON). The full clinical and pathological characteristics of all the enrolled patients are summarised in the original report (Hoskin PJ *et al*, 2010). Of the 333 patients enrolled into the trial, adequate pathological tissues and complete clinical outcome data were available for 217 cases – these are the subject of the current research analyses. Only those cases with adequate tumour with detrusor muscle in the specimen and those without diathermy artefact were selected. Hematoxylin and eosin (H&E) stained cores were

examined with the pathologist. Relevant clinico-pathological data for the 217 cases are summarised below (**Table 2.6**).

Table 2.6: Clinical and pathological characteristics of patients enrolled into the BCON trial included in the current research analyses

Characteristic	All patients (n=217)	Percentage %
Age (years)		
Median age	74	
Range	51-90	
Sex		
Male	174	80
Female	43	20
Tumour Stage		
1	22	10
2	144	66
3	41	19
4	10	5
Grade		
2	33	15
3	184	85
Preceding Tumour		
No	186	86
Yes	31	14
Preceding Tumour treatment		
TURBT		
- Complete	90	42
- Partial	66	30
- Biopsy only	53	24
- Unknown	8	4
BCON randomisation		
RT alone	113	52
RT + CON	104	48
Hb (g/dL)		
Median	13.6	
Range	9.3-17.2	

RT: radiotherapy; CON: carbogen nicotinamide; Hb: haemoglobin; TURBT: transurethral resection of bladder tumour; g/dL: grams per decilitre

2.8.2 Tissue microarray characteristics

Tissue microarray cores of 0.6 mm diameter were organised in quadruplicates in paraffin blocks; in other words, each case was represented by four cores on the TMA block. The cores for the 217 cases included spanned four blocks in total. Tissue cores from liver, lung and brain were embedded as orientation markers in each block. At least one of the quadruplicate cores was available in all cases for the current analysis. Sample "maps" of the BCON TMA blocks are included in **Appendix A-(i)**.

2.9 Radical cystectomy tissue specimens

2.9.1 Patient demographics

All cases pertained to radical cystectomies performed at Southampton General Hospital (University of Southampton, UK) between the period 1st January, 2001 and 1st March, 2012. Cases performed for bladder cancer were included. For the purpose of this study, all cases where patients had received neoadjuvant chemotherapy, adjuvant chemotherapy or adjuvant radiotherapy were excluded. The rationale for this exclusion was to reduce the confounding effects of such treatments (i.e. chemotherapy and/or radiotherapy) on clinical outcome following radical cystectomy when comparing against a radical radiotherapy cohort (i.e. the BCON cohort). Ideally, a true "control cohort" to compare the BCON cohort against would have been patients with the same disease but who did not receive any form of treatment at all; this was not possible because any such practice would be completely unethical. Hence, the use of a "surgical cohort" as control which is valid because surgery achieves favourable clinical outcome based on the physical removal

of the tumour rather than through the DNA-damaging, cytotoxic mechanism associated with radiotherapy or chemotherapy.

With the inclusion of patients who had only had radical cystectomy, there were 151 cases available for analysis for the present study. The clinic-pathologic demographics of these cases are summarised below (**Table 2.7**).

Table 2.7: Clinical and pathological characteristics of patients in the radical cystectomy set

Characteristic	All patients (n=151)	Percentage %
Age, years		
Median age	73	
Range	33-87	
Gender		
Male	118	78
Female	33	22
Stage [x]		
0	7	5
is	24	16
1	8	5
2	23	15
3	58	38
4	10	7
Node +ve	21	14
Grade [¥]		
2	10	7
3	129	85

x pathological staging from radical cystectomy; 0 (pT0): no residual tumour following previous TURBT; is (pTis or CIS): carcinoma in situ

¥ does not include pT0 and cases which were exclusively pTis

2.9.2 Tissue microarray characteristics

Tissue cores were obtained from pre-cystectomy TURBT specimens. Tissue cores for each case were organised in triplicates on the TMA blocks. Each core was 1 mm in diameter. Sample "maps" of the radical cystectomy TMA are included in **Appendix A-(ii)**.

2.10 Neoadjuvant chemotherapy tissue specimens

2.10.1 Patient demographics

Ethics approval (reference: EC06.1; see **Appendix B**) was obtained from University College London (UCL) to collate pathology materials related to patients who had undergone cisplatin-based neoadjuvant chemotherapy prior to definitive radical treatment (either radical cystectomy or radical radiotherapy) for bladder cancer (see **Appendix A-iii**). In order to match the Neoadjuvant cohort closely to the BCON and radical cystectomy cohorts, cases were selected from a similar era from January 1st 2000 to January 1st 2012. Similar to the Radical Cystectomy cohort, in order to reduce the confounding effects of other treatments, patients who subsequently received adjuvant treatments following definitive treatments were excluded. In total, there were 86 patients from 6 institutions within the UK. The clinico-pathologic details are summarised below (**Table 2.8**).

Table 2.8: Clinical and pathological characteristics of patients in the Neoadjuvant set

Characteristic	All patients (n=84)	Percentage %
Age, years		
Median age	66	
Range	35-82	
Gender		
Male	64	76
Female	20	24
Stage [x]		
0	38	45
is	6	7
1	2	2
2	16	19
3	11	13
4	0	0
Node +ve	11	13
Grade [¥]		
2	2	2
3	39	46
Treatment		
Cystectomy	46	55
Radiotherapy	38	45

x pathological staging from radical cystectomy; 0 (pT0): no residual tumour following previous TURBT; is (pTis or CIS): carcinoma in situ

¥ does not include pT0 and cases which were exclusively pTis

2.10.2 Tissue microarray characteristics

Tissue cores for each patient were organised as duplicates on the TMA blocks. Each core was 1 mm in diameter. Other tissue cores, such as from prostate, were used as orientation markers on the blocks. Sample TMA maps are included in **Appendix A-(iii)**.

2.11 LaMB trial tissue specimens

2.11.1 Patient demographics

LaMB is a phase II/III double-blind, randomised-control trial (RCT) (ISRCTN35418671) which assigns patients with locally-advanced or metastatic bladder cancer to receive, along with their systemic chemotherapy, either lapatinib or placebo. Lapatinib is a tyrosine kinase inhibitor which inhibits tumour proliferation by blocking the epidermal growth factor receptors, HER1 and HER2. LaMB is a multi-centre trial within the UK and commenced accrual from 27th January, 2009 and completed recruitment on 31st December, 2013. Full details of the trial are available online from the Cancer Research UK clinical trials website (http://cancerhelp.cancerresearchuk.org/trials/a-trial-looking-at-lapatinib-for-people-with-bladder-cancer-that-has-spread).

For the purpose of the current study, patients included in LaMB, regardless of whether they received Lapatinib or placebo, were considered provided they had adequate initial-diagnostic tissue specimens available to be included onto a TMA. There were 72 patients available for TMA purposes. Their clinic-pathologic demographics are summarised below (**Table 2.9**).

Table 2.9: Clinical and pathological characteristics of patients in the LaMB set

Characteristic	All patients (n=72)	Percentage %
Age, years Median age Range	 67 42-82	
Gender Male Female	 59 13	 82 18
Treatment Standard Standard + Lapatinib	 33 39	 46 54

2.11.2 Tissue microarray characteristics

Tissue cores were organised in duplicates or triplicates on the TMA blocks. Cores were 1 mm in diameter. Other tissue cores, such as from appendix, were included as orientation markers within the blocks. The TMA slides were obtained from the LaMB triallists (Dr T Powles). Sample maps of the LaMB TMA are included in **Appendix A-(iv)**.

2.12 Control TMA

A separate "control" TMA was created in order to incorporate other tissue cores which were reported positive or negative immunostaining controls for the various antibodies interrogated. Secondly, the "control" TMA also included cases of bladder cancer with a broad range of pathological grades and stages. The purpose of this was to investigate how the immunostaining for any particular antibody altered according to the pathological grade/stage of bladder cancers. Cores were 1 mm in diameter. Where adequate tissue material was available, some cases were included

as duplicate cores. A sample map for the Control TMA is included in **Appendix A-(v)**.

2.13 Immunohistochemistry of tissue microarray slides

2.13.1 Immunohistochemistry protocol

Immunohistochemistry of all the TMAs (BCON, Radical Cystectomy, Neoadjuvant, and LaMB) were performed by the University College London Advanced Diagnostics (UCL-AD) laboratory. UCL-AD is part of the UCL Cancer Institute and provides accredited research and clinical laboratory services internationally (http://www.uclad.com/).

Immunohistochemistry was performed using the Bond Polymer Refine Detection kit with Bond-III automated immunostaining system (Leica Microsystems, Milton Keynes, UK) following the manufacturer's instructions. In brief, the TMA slides were deparaffinized, rehydrated, washed and endogenous peroxidase was blocked using Bond-III "*Dewax Protocol D*" following the manufacturer's instructions (Leica Biosystems, Newcastle, UK). Epitope retrieval was achieved using Bond-III "*Protocol H1(30)*" (Leica).

The slides were incubated with antibodies against AIMP3 (1:25) (Atlas Antibodies, Sigma-Aldrich, UK) at room temperature for 1 hour. Incubation dilutions for the other antibodies were as follows: Mre11 (1:200) (Atlas Antibodies); ERCC1 (1:300) (Clone 8F1, Neomarkers, Thermo-Fisher Scientific, Cheshire, UK); p53 (prediluted)

(Clone D07, Novocastra, Leica Biosystems, Newcastle, UK). Antibody binding was detected using diaminobenzidine (DAB) with haemotoxylin counterstaining following Bond-max and Bond-x "*IHC protocol F*" (Leica).

External positive controls for the markers were as follows: non-cancer colon tissue (AIMP3); non-cancer prostate tissue (Mre11); non-cancer tonsil tissues (ERCC1 and p53). Non-cancer liver tissues were used as external negative controls.

2.13.2 Immunohistochemistry image analyses

The stained TMA cores were examined under a light microscope at 400x magnification, standardising the scoring according to the reference control cores. The reference material was assigned a staining intensity of 2, graded on a scale of 0 to 3, against which the bladder cancer cores were compared. Three independent investigators, blinded to the clinical data, assessed the cores with the primary investigator scoring the staining a second time, after a time gap of at least one week, to assess intra-observer variance. The whole area of each core was viewed and the proportion of cells in each core staining positively was assigned a proportion score (0 if 0%, 0.1 if 1% to 9%, 0.5 if 10% to 49%, and 1 if 50% to 100%). A semi-quantitative histopathology (H) score was obtained by multiplying the staining intensity with the proportion score. The median value of all H scores was defined as the cut-off value to categorize antibody staining in the cores as either positive or negative. Cores with discordant scores, resulting in H values that altered the staining status stratification were assessed by a third investigator to reach a consensus.

2.14 Outcome data for TMA sets

Overall survival (OS) was taken as the primary outcome measure for all TMA (BCON trial, Cystectomy series, Neoadjuvant series, LaMB trial) datasets. Overall survival was chosen as this was felt likely to be the least biased measure in terms of definitive, objective outcome. However, OS can be limited by the requirement of long periods of follow-up meaning that most randomised trials cannot be adequately powered to detect significant differences between arms. This point considered, OS data were available for all the cases in the current study making its choice as outcome measure easier. Cancer specific survival (CSS) data was incomplete in most datasets and was also felt likely to have inaccuracies in terms of attribution of cause of death. Other outcome measures such as recurrence-free survival and progression-free survival were also not used as primary outcome measures for the same reasons. Where recurrence data was available (e.g. BCON trial dataset) and appropriate to analyse, it was measured as a secondary outcome.

2.15 Statistical analysis

2.15.1 Laboratory data

Statistical analyses were performed using SPSS, version 17.0 (SPSS Inc, IL, US). For *in vitro* work, differences in means between groups (at least 3 independent experiments) were measured using a two-tailed Student's t-test. Standard deviations (SD) and standard error of means (SE) were calculated where appropriate. Graphical plots were constructed using either Microsoft Excel 2010 or Sigmaplot (version 10) packages.

2.15.2 TMA data

Statistical analyses were performed using SPSS, version 17.0 (SPSS Inc, IL, US). For the TMA datasets, agreement in the scoring of the stained TMA cores (inter- and intra- observer agreement) was measured using Kappa statistics. Overall survival (OS) was estimated using the Kaplan-Meier method. The effect of the tested antibody (e.g. AIMP3, ERCC1) by staining status was measured using a Cox proportional hazards model adjusted for relevant covariates such as age, gender, tumor grade (G2 or G3) and tumour stage (T1, T2, T3 or T4). Hazard ratio (HR) and confidence interval (CI) calculations were based on the Cox model; p values of <0.05 were used to denote statistical significance.

Chapter 3

Expression of AIMP3 in bladder cancer cell lines and altered sensitisation to irradiation following siRNA knockdown of AIMP3

3.1 Introduction to Chapter 3

AIMP3 (p18/EEF1E1) is a multifunctional protein, which in addition to its role in protein synthesis, behaves as a tumour suppressor (Park BJ *et al*, 2005). Altered expression of AIMP3 was demonstrated in both human cancer cell lines and biopsy specimens (Park BJ *et al*, 2005). Cell line studies demonstrated that AIMP3 is implicated in the DNA damage repair (DDR) pathway following exposure to irradiation and chemicals (Park BJ *et al*, 2005; Park BJ *et al*, 2006). Alteration in AIMP3 expression, by gene transfection in cell lines, demonstrated altered cell survival in response to these DDR agents; downregulation of AIMP3 resulted in reduced survival and upregulation resulted in increased survival (Park BJ *et al*, 2005; Han JM *et al*, 2008). AIMP3 knockout (AIMP -/-) mice are embryonically lethal and heterozygosity (AIMP3 +/-) leads to early susceptibility to a broad range of common cancers, indicating that AIMP3 is an important gene with tumour suppressor function (Park BJ *et al*, 2005).

The broad aim the current project was to investigate the role of AIMP3 in bladder cancer. In the UK, bladder cancer is the second most common urological malignancy accounting for around 12000 new cases and 5000 deaths in 2010 (http://www.cancerresearchuk.org/cancer-info/cancerstats/types/bladder/). Radical surgery is currently the "gold standard" treatment for the curative management of organ-confined, muscle-invasive bladder cancer (Stenzl A *et al*, 2009). However, disease-specific survival following radical surgery is still low and has improved little over the last few decades. Radical radiotherapy is the second-line treatment option in most countries for patients who are unfit for surgery or choose not to have

surgery; however, survival is slightly less with radiotherapy alone and there is radiation-specific morbidity (Shelley MD *et al*, 2002). Hence, the rationale for and increasing popularity of less radical treatment modalities, incorporating radiation and chemotherapy, in this setting to achieve similar, if not better, survival in these patients (Rodel C *et al*, 2002; Shipley WU *et al*, 2002; Shipley WU *et al*, 2003; Housset M *et al*, 2005). Irradiation and chemotherapy (neoadjuvant or adjuvant) have the potential to be of curative value in the treatment of organ-confined, muscle-invasive bladder cancer. Furthermore, chemotherapy and radiotherapy already have a role in the palliative management of metastatic bladder cancer.

The primary objective of our study was to measure the expression of AIMP3 in a panel of bladder cancer cell lines and correlate protein expression to outcomes in response to DDR agents such as irradiation and chemotherapy. The translational relevance of any observed correlation (either decreased expression correlating to improved cell survival or vice versa) would be that bladder tumours in clinical practice may be stratified into those either likely or unlikely to respond to treatment with irradiation and chemotherapy. The secondary objective was to localise AIMP3 in the cell lines. This would help provide a mechanistic explanation for any correlations in outcomes such as altered cell survival.

3.2 AIMP3 expression in bladder cancer cell lines

3.2.1 AIMP3 protein expression

Western blot analyses demonstrated protein expression of AIMP3 in a panel of bladder cancer lines (**Figure 3.1*A***); T24, 253J, RT112 and RT4 lines were chosen to

represent a spectrum from aggressive (T24) to low-grade (RT4) disease respectively. When comparing AIMP3 expression between the cell lines, there was a significant difference in the mean expression in between the groups (p=0.0001, F=19.01, one-way ANOVA).

When compared to HeLa cells (positive control for AIMP3 expression), RT4 (0.54 +/- 0.02) and 253J (0.70 +/- 0.13) cells expressed the most AIMP3 with approximately five-fold amount of AIMP3 relative to HeLa (**Figure 3.1*B***); the difference in expression between HeLa (0.12 +/- 0.01) and RT4 was statistically significant (p=0.001, two-tailed T-test) and, the difference in expression between HeLa and 253J was also statistically significant (p=0.04, two-tailed T-test). There was no significant difference in AIMP3 expression between RT4 and 253J (p=0.32, two-tailed T-test).

Of the bladder cancer cell lines, T24 expressed the least amount of AIMP3 (0.21 +/- 0.05). This was not statistically different to AIMP3 expression by HeLa (p=0.21, two-tailed T-test). In other words, both T24 and HeLa expressed the least amount of AIMP3 and were similar in terms of AIMP3 expression. As explained above, RT4 and 253J expressed the highest level of AIMP3 in the panel of cell lines and they were similar in terms of AIMP3 expression. When T24 was compared against RT4 and 253J, there was a significant difference relative to each (p=0.01 and p=0.04, respectively). In the panel of cell lines, RT112 was intermediate in terms of AIMP3 expression with an expression level (0.32 +/- 0.06) between the low-expressing cell lines (HeLa and T24) and the high-expressing cell lines (RT4 and 253J); however,

there was no statistically significant difference when comparing RT112 against each of the other cell lines (Hela, p=0.07; T24, p=0.24; 253J, p=0.08; RT4, p=0.05).

Figure 3.1*A*:

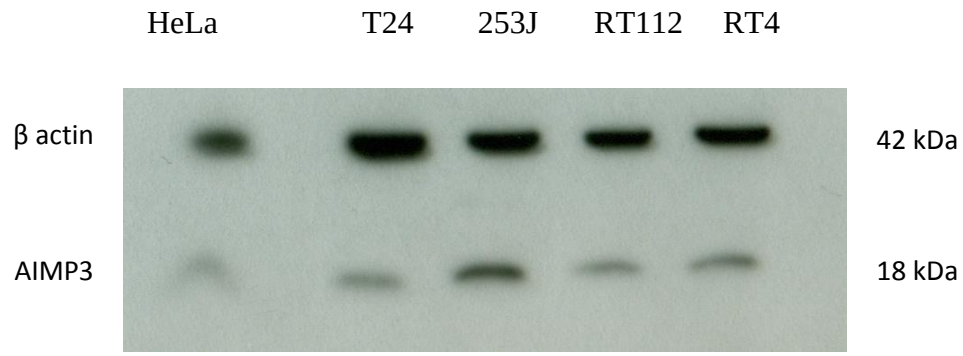

Figure 3.1*B*:

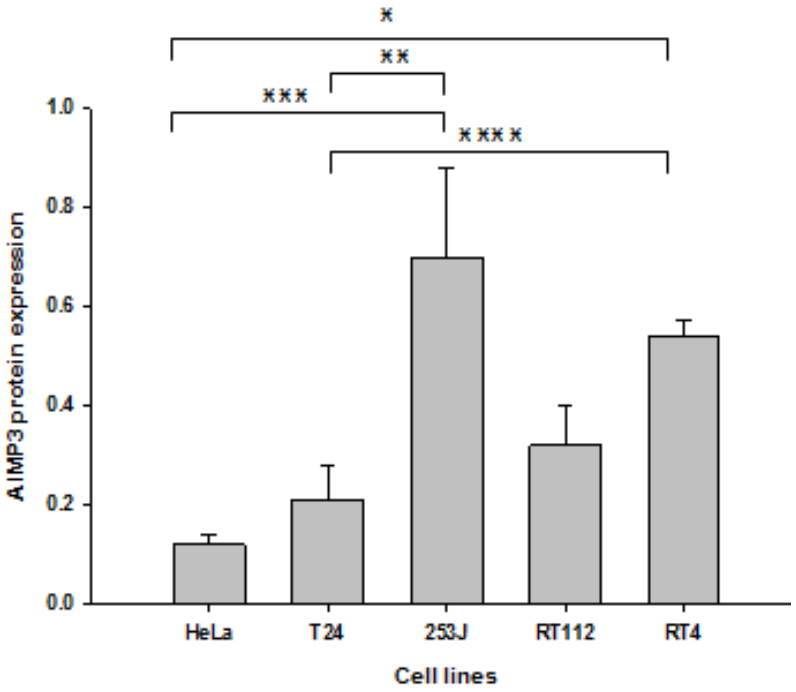

Figure 3.1: Western blot analysis of AIMP3 expression in the bladder cancer cell lines and quantitation of expression.

3.1*A*: Western blot analysis of AIMP3 protein expression in T24, 253J, RT112 and RT4 bladder cancer cell lines (with HeLa in Lane 1 used as the positive control for AIMP3).

3.1*B*: Quantitation of AIMP3 protein expression in T24, 253J, RT112 and RT4 bladder cancer cell lines relative to HeLa. Quantitation for AIMP3 for each cell line was calculated as ratio of Actin. The experiments were repeated independently three times. The mean and standard error of means (SEM) (error bars) from the three experiments are represented. HeLa (0.12 +/- 0.01); T24 (0.21 +/- 0.05); 253J (0.70 +/- 0.13); RT112 (0.32 +/- 0.06); RT4 (0.54 +/- 0.02). x indicates significant differences where: x is p=0.001 (between HeLa and RT4), xx is p=0.01 (between T24 and 253J), xxx is p=0.04 (between HeLa and 253J), and xxxx is p=0.04 (between T24 and RT4).

3.2.2 AIMP3 protein expression after irradiation

Colony survival assays were performed to characterise the dose-response radiosensitivity characteristics of the cell lines used and to calculate their IC50 values (**Figure 3.2**). When T24 cells were irradiated (X rays) at their IC50 values, there was no significant increase in the level of AIMP3 protein expression out to 120 hours following irradiation (**Figures 3.3*A*** and **3.3*B***). When comparing the mean AIMP3 expression between the time-points (0 to 120 hours), there was no significant difference in the means in between the groups (p=0.37, F=1.18, one-way ANOVA). Relative to the reference time-point (untreated or 0 hours), where AIMP3 protein expression was 0.25 +/- 0.06 (mean and SEM), AIMP3 expression at 24 hours (0.30 +/- 0.10) was not significantly different (p=0.55, two-tailed T test). Similarly, relative to the reference time-point of 0 hours, expressions at 48 hours (0.43 +/- 0.08; p=0.57), 72 hours (0.53 +/- 0.11; p=0.38), 96 hours (0.52 +/- 0.12; p=0.36) and, 120 hours (0.47 +/- 0.16; p=0.19) were not significantly different. In short, in T24 cells, following irradiation at IC50 dose, there appeared to be a marginal increase in protein expression, particularly after 48 hours, but any increase or change in the level of expression was not statistically significant.

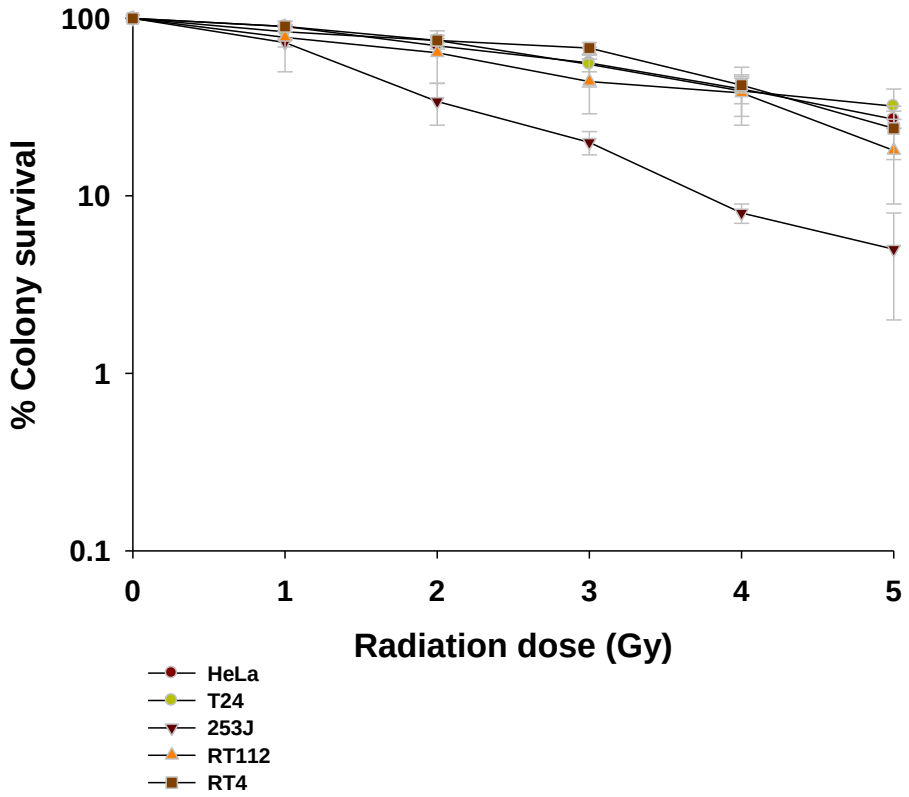

Figure 3.2: Log-linear plot of percentage colony survival at a range of doses (0-5Gy) of irradiation in the panel of bladder cancer cell lines (T24, 253J, RT112 and RT4; with HeLa used as control). Untreated (not irradiated) cells were used as reference (100% survival) to calculate the proportion of surviving colonies at each irradiation dose (1, 2, 3, 4 and 5Gy). IC50 value was taken as the dose of irradiation at which there was 50% colony survival compared to the reference point of no irradiation (0Gy). The IC50 values were: RT4 (4.6Gy), T24 (3.9Gy), RT112 (2.9Gy), 253J (2.7Gy); and HeLa (3.4Gy). Three independent experiments were performed.

Figure 3.4: Western blot analysis of AIMP3 expression in T24 cells following irradiation and quantitation of time-course changes in expression.

Fig 3.4*A*: Western blot analysis of AIMP3 protein expression in T24 cells following irradiation. Cells were irradiated at the IC50 dose and lysates extracted at 24 hour intervals out to 120 hours.

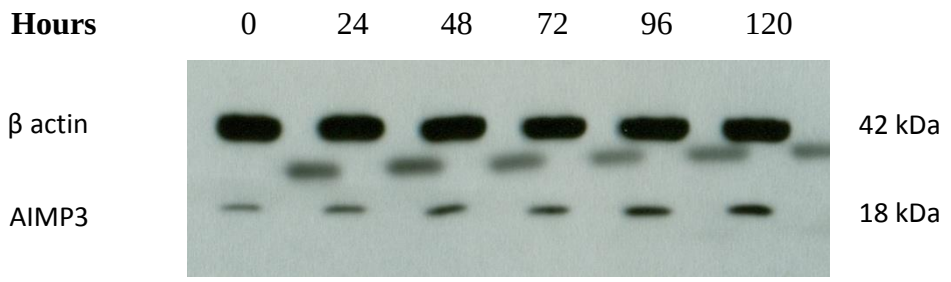

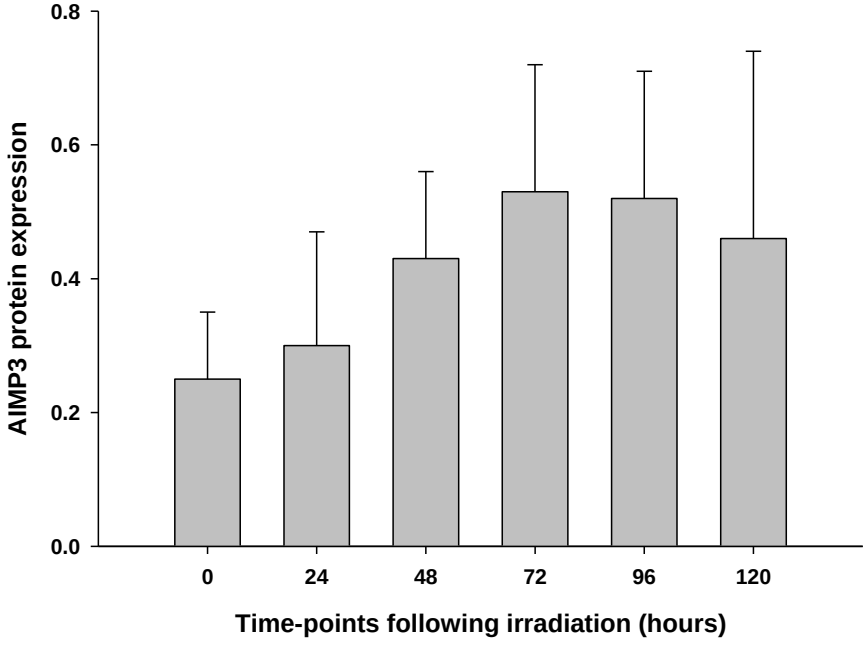

Fig 3.4*B* Relative change in AIMP3 protein expression from 24 to 120 hours compared to the reference time-point 0 (not irradiated) in T24 cells. There was no significant change in AIMP3 expression (mean +/- SEM) out to 120 hours.

3.3 Subcellular trafficking of AIMP3 following irradiation

Immunofluorescence was performed to characterise the sub-cellular localisation of AIMP3 in the cell lines used. Immunofluorescence demonstrated a pan-cellular distribution of AIMP3 protein within both the cytosolic and nuclear compartments (**Figure 3.5**). However, there appeared to be an increased localisation of AIMP3 protein in the nuclear compartment relative to the cytosolic compartment at 1 hour following irradiation (X rays at IC50 doses). This finding, together with the finding that there was negligible increase in the amount of AIMP3 protein expression out to 120 hours following irradiation, suggests that AIMP3 is likely translocated from the cytosolic compartment into the nuclear compartment at an early time-point (within hours) following irradiation presumably to take part in the DNA damage response (DDR) pathway within the nucleus, the site of DNA damage (**Figure 3.5**). In addition, following the sub-lethal dose of irradiation (IC50 dose), there is increased transcription of AIMP3 which is significantly apparent after 72 hours.

A.

IR -

AIMP3-FITC

DAPI

TRITC

Merge

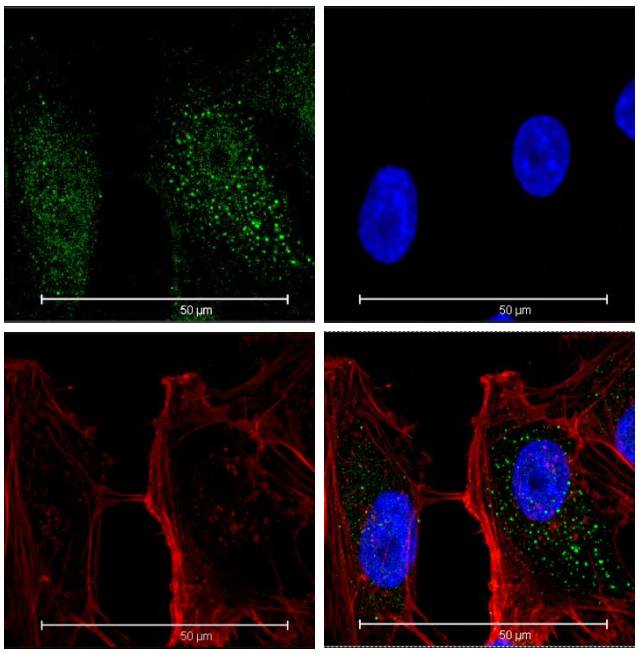

IR +

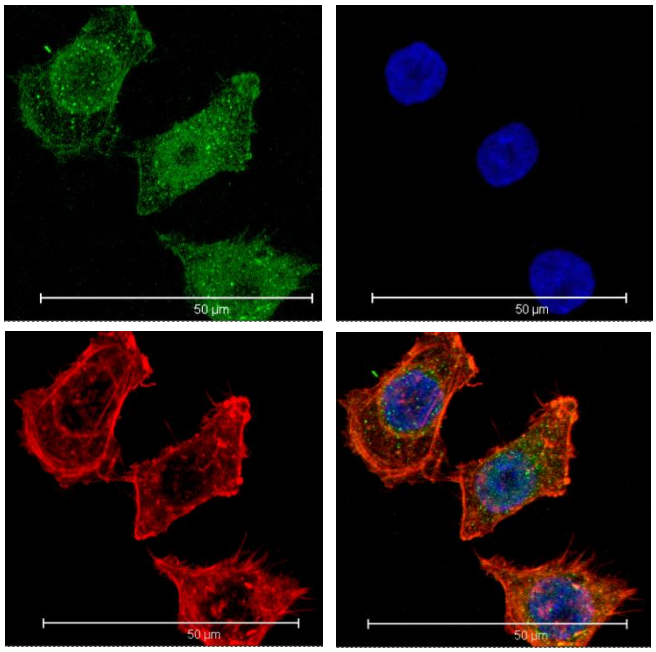

B.

IR -

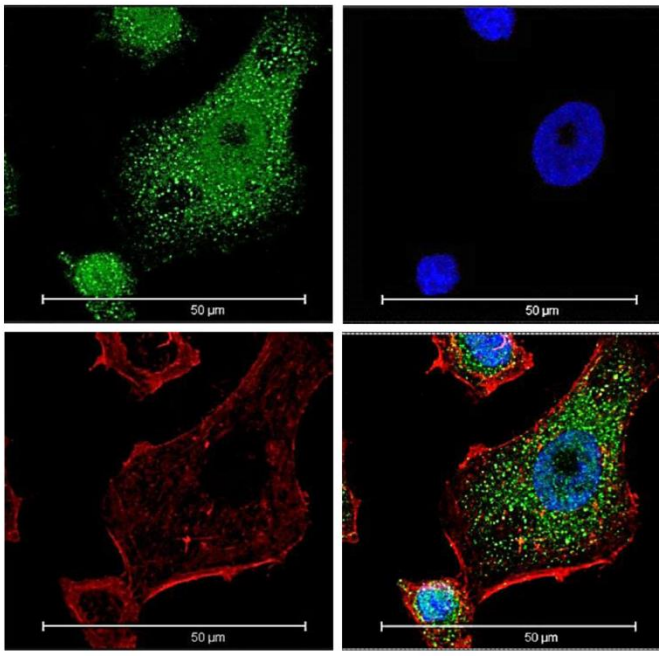

IR +

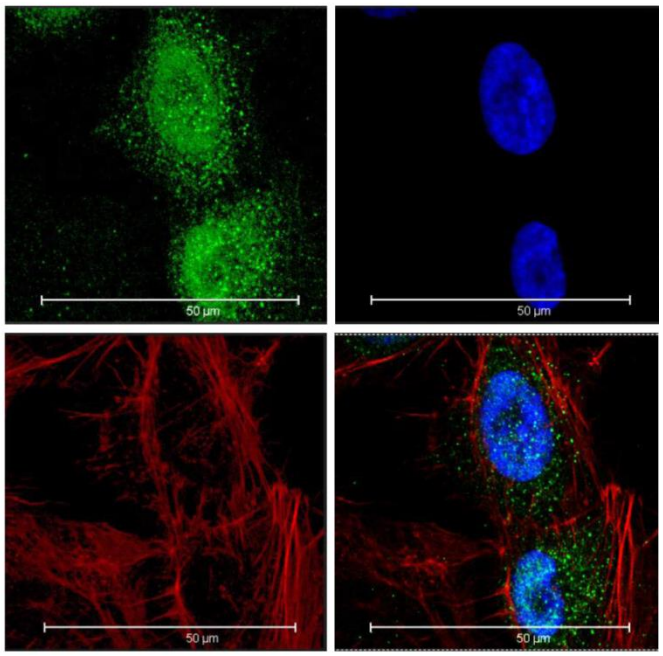

C.

IR -

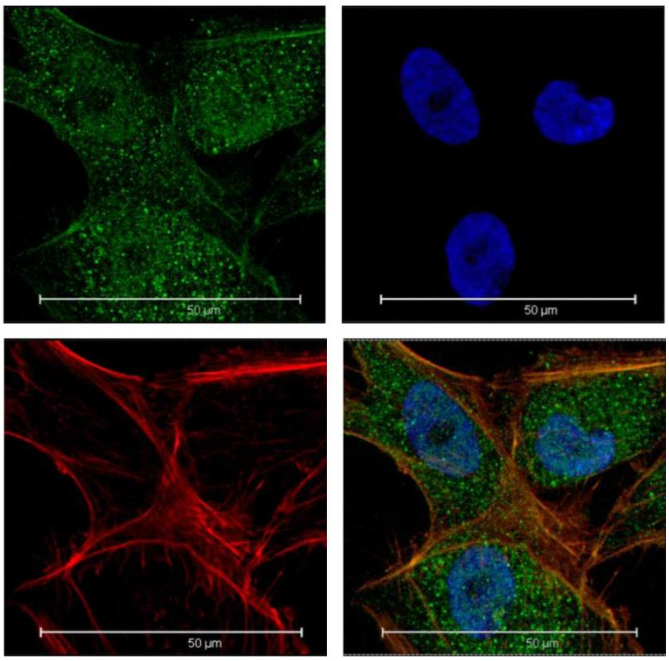

IR +

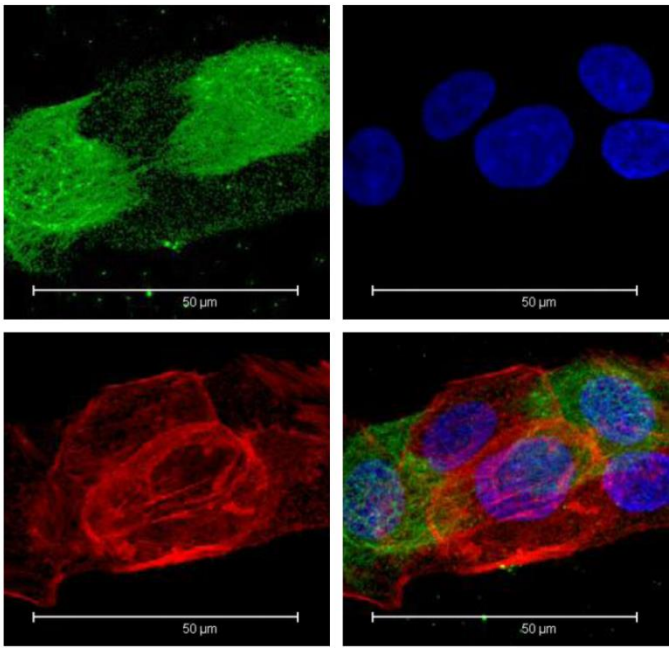

D.

IR -

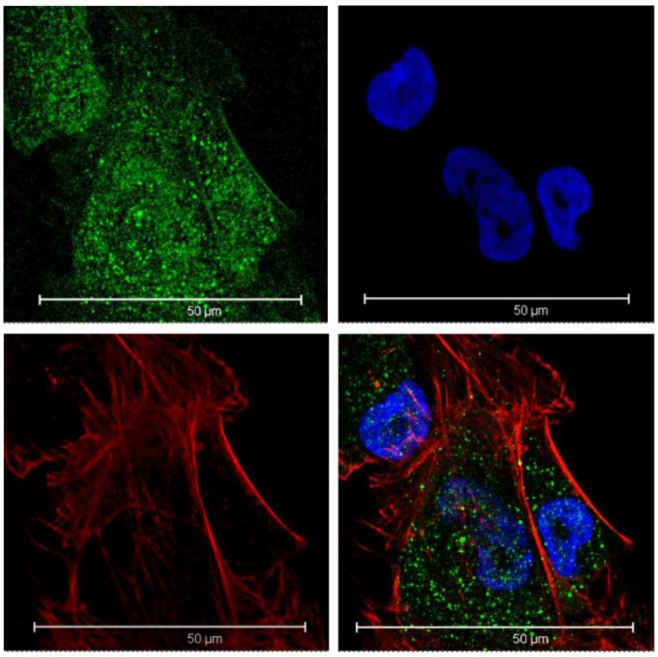

IR +

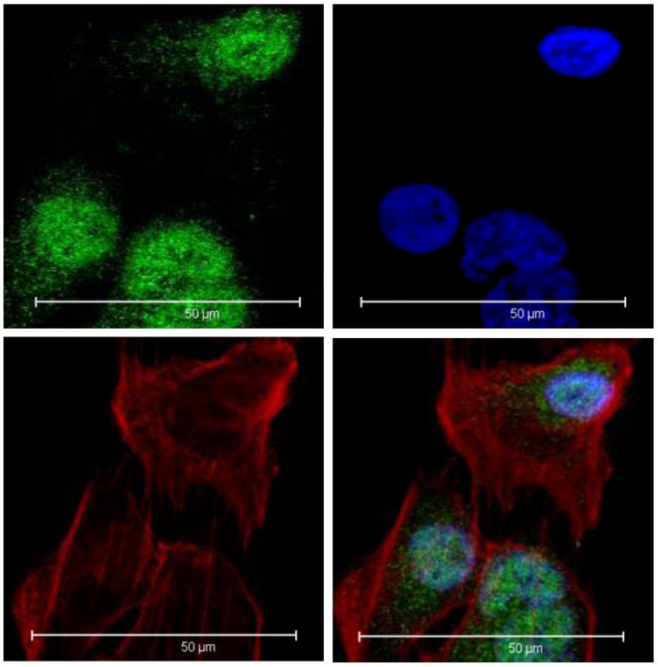

Figure 3.5: Confocal immunofluorescence images demonstrating subcellular localisation of AIMP3 in bladder cancer cells with (IR+) and without (IR-) irradiation (x600). AIMP3 was conjugated with FITC (green-yellow); cytoskeletal actin was stained with TRITC (red-pink); nuclear staining was with DAPI (blue); and, merged images were acquired of the three. Following irradiation, there is increased AIMP3 staining corresponding to the nuclear compartment in the bladder cancer cell lines: (***A***) T24, (***B***) 253J, (***C***) RT112, (***D***) RT4.

3.4 Clonogenic survival following siRNA knock-down of AIMP3 and treatment with irradiation

Downregulation of AIMP3 protein expression was achieved using 5nM siRNA to AIMP3 and was compared to AIMP3 expression in untreated (culture media only) cells, cells treated with siRNA to GAPDH and cells treated with non-targeting, scrambled siRNA (**Figure 3.6**). Time-course experiments demonstrated maximal downregulation between 48 to 72 hours following transfection with siRNA (**Figures 3.7*A*** and 3.7***B***). After 96 hours, there was gradual reconstitution of AIMP3 expression.

The earliest time-point of 48 hours was chosen as the optimal time-point, for functional studies interrogating the effects of AIMP3 downregulation on outcomes such as clonogenic survival following treatment with irradiation or chemotherapy, as cell-death and off-target effects of siRNA transfection were reasoned to be likely to be lower at an earlier time-point compared to later time-points such as 72 hours or 96 hours. Therefore, 48 hours following siRNA knockdown of AIMP3, cells were irradiated at their IC50 doses and their clonogenic survival measured at day 14 (**Figure 3.8**). Relative to those irradiated at their IC50 dose, there was an increase in

the clonogenic survival of all cells when AIMP3 expression was reduced. This increase in survival was statistically significant in T24 (p=0.03), RT112 (p=0.01) and RT4 cells (p=0.02). In 253J cells, there was an increase in survival from 56% +/- 7% (irradiated at IC50 dose) to 61% +/- 15% (siRNA AIMP3 and irradiated at IC50 dose) but this increase was not significant (p=0.62).

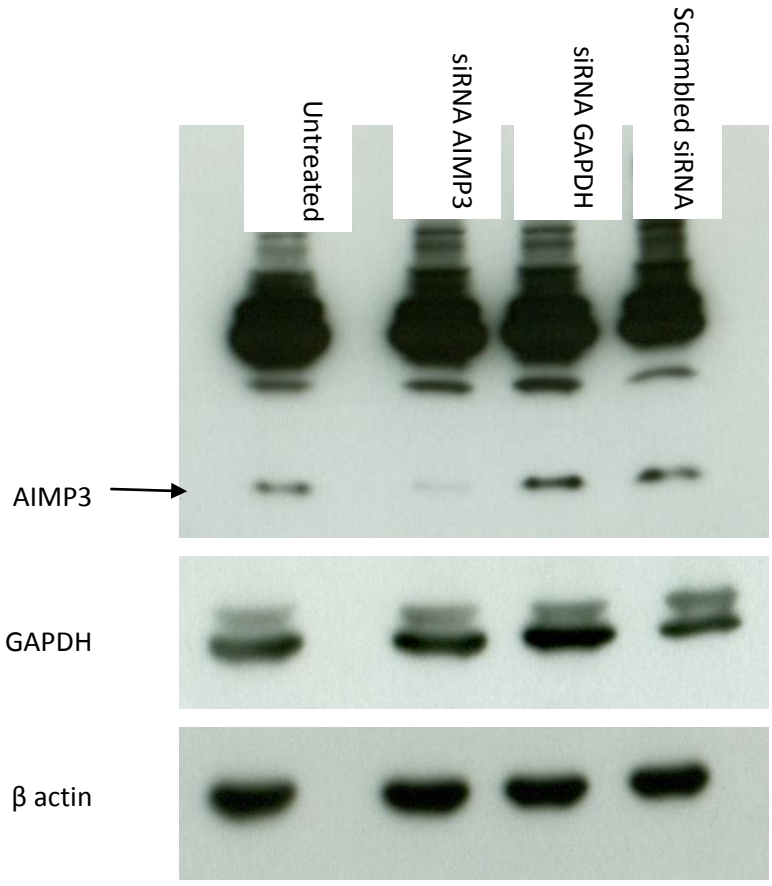

Figure 3.6: Western blot analysis of reduction in the expression of AIMP3 (lane 2) 72 hours after siRNA knockdown in T24 cells. Negative controls are in Lane 1 (untreated cells) and Lane 4 (scrambled, non-targeting siRNA). siRNA to GAPDH is the positive control in Lane 3. β-actin is also demonstrated as a loading control as GAPDH expression may have been altered in Lane 3 (siRNA to GAPDH).

Figure 3.7*A*

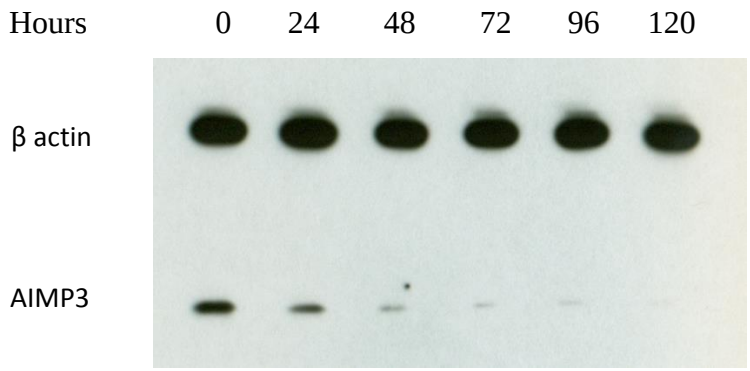

Figure 3.7*B*:

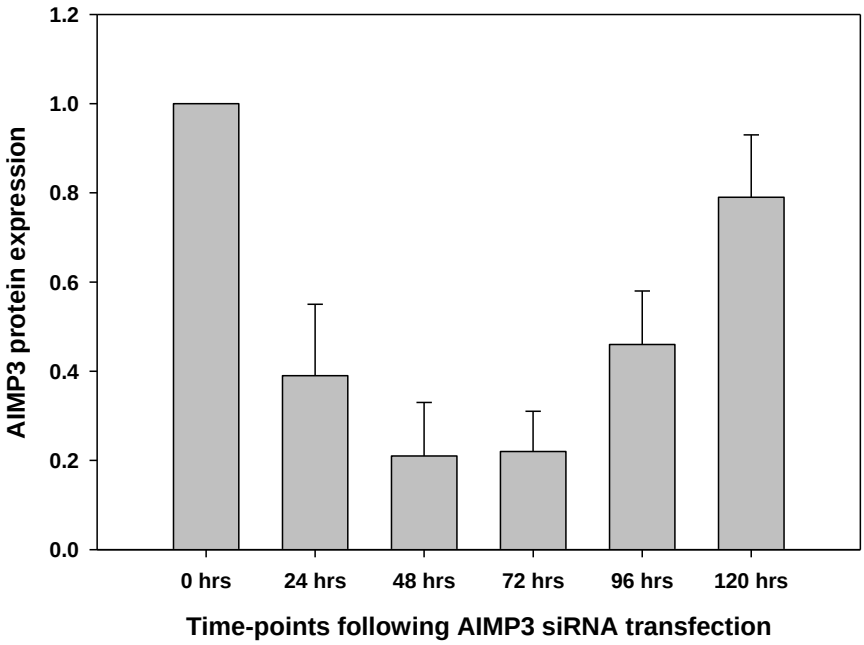

Figure 3.7: Western blot and quantitation of siRNA knockdown of AIMP3 expression in T24 cells

3.7*A*: Time-course of AIMP3 expression following siRNA knockdown of AIMP3 at 5nM in T24 cells. There is significant (>50%) reduction in the level of AIMP3 from 24 to 96 hours following siRNA transfection.

3.7B: Quantitation of change in AIMP3 protein expression at 24 hour intervals out to 120 hours following siRNA transfection (reference time-point 0) in T24 cells. There was approximately 80% reduction in AIMP3 expression at time-points 48 hours and 72 hours following siRNA transfection of AIMP3. By time-point 120 hours, there was 79% +/- 14% reconstitution of AIMP3 expression relative to time-point 0.

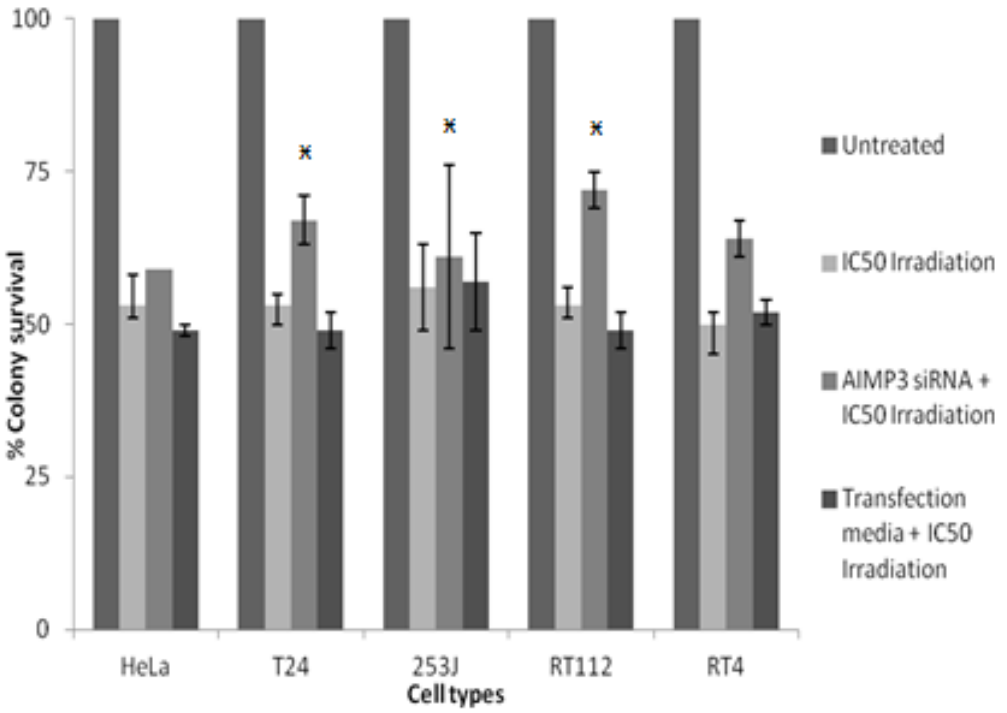

Figure 3.8: Colony survival following siRNA knockdown of AIMP3 and irradiation at IC50 value. There is an increase in colony survival when AIMP3 is reduced (Lane 3) compared to when AIMP3 is present (Lane 2). Lane 4 represents cells which have only been treated with the transfection media (-ve control) and Lane 1 represents cells plated at their optimal plating numbers but not irradiated (referenced as 100% for subsequent irradiation at IC50 dose).

3.5 Discussion of results

The findings outlined above in this chapter demonstrate a number of points in relation to AIMP3 in the panel of cell lines used. Firstly, AIMP3 protein expression, as measured by Western blot analyses, was constitutively different in the panel of cell lines used. T24 and HeLa expressed significantly lower levels of AIMP3 compared to RT4 and 253J; RT112 expressed intermediate levels in this spectrum. HeLa was used as a reported positive control cell line for the expression of AIMP3. In the panel of bladder cancer cell lines, T24 is considered by some to be the least differentiated (high grade) and it was notable that AIMP3 expression was the lowest in T24 relative to the other bladder cancer cell lines used. This finding was in keeping with our preliminary finding that AIMP3 mRNA and protein expression was low in high-grade bladder cancer tissues compared to low-grade bladder cancer tissues. These observations allude to the possibility that AIMP3 expression may be altered or reduced during bladder cancer pathogenesis; however, our findings do not provide unequivocal proof of this. Further supportive evidence will be required to prove this.

Secondly, the radiosensitivity dose-response characteristics of the cell lines were plotted using clonogenic survival assays as the functional readouts. This allowed IC50 values to be calculated for the cell lines. RT4 was the most radioresistant with an IC50 value of 4.6Gy and 253J was the most radiosensitive with an IC50 value of 2.7Gy. The IC50 values for the other cell lines were as follows: T24 (3.9Gy), RT112 (2.9Gy), and HeLa (3.4Gy). If radiosensitivity was dependent on AIMP3 expression levels, one would expect either a positive or negative correlation. This was not the

case. Therefore, AIMP3 expression levels do not adequately explain the radiosensitivity characteristics of the cell lines.

When the expression of AIMP3 protein following irradiation was measured in T24 cells, time-course experiments demonstrated that AIMP3 levels did rise marginally after 48 hours suggesting that irradiation may have induced increased transcription of AIMP3. However, the increase was not statistically significant. Therefore, it cannot be said conclusively that irradiation induces increased transcription of AIMP3 in bladder cancer cell lines. Certainly, similar experiments would need to be performed in all the bladder cancer cell lines used. Consequently, it cannot be assumed that increased AIMP3 transcription following irradiation is one of the mechanism by which cells may respond to DNA damage.

Instead, the immunofluorescence experiments suggest that, rather than increased transcription as a possible mechanism of DNA damage response following irradiation, sub-cellular translocation of AIMP3 may be a possible mechanism. At one hour following irradiation, there appears to be increased staining of AIMP3 corresponding to the nuclear compartment relative to the cytosolic compartment. This suggests that nuclear translocation of AIMP3 occurs as an "early event" following irradiation so that AIMP3 can take part in the DNA damage response pathway within the nucleus where DNA damage is occurring. The immunofluorescence experiments above have not quantitated the extent to which the cytosolic to nuclear translocation occurred. This was largely due to technical difficulties such as cellular and subcellular damage upon irradiation, even at sub-lethal IC50 doses, precluding accurate quantitations of fluorescence of different

subcellular compartments. However, a recent study has elegantly demonstrated that AIMP3 is anchored to methionyl-tRNA synthetase (MRS) in the cytosol but is released to translocate to the nucleus upon DNA damage for DNA repair (Kwon NH *et al*, 2011).

As AIMP3 is a reported tumour suppressor, it was important to interrogate whether alterations in AIMP3 expression would lead to any change in tumourogenic functional outcomes following irradiation. The hypothesis was that reduction in AIMP3 levels within the cell lines would lead to increased survival when exposed to DNA damaging stimuli such as irradiation. AIMP3 levels were knocked-down with the lowest level of siRNA feasible (5nM siRNA) and irradiation performed at the earliest time-point where knockdown was maximal (48 hours) so as to minimise off-target effects and toxicity of siRNA transfection. All cell lines were exposed to their standardised IC50 doses of irradiation. There was a significant increase in clonogenic survival following irradiation in all cell lines when AIMP3 was knocked down except for 253J. This lends support to the notion that AIMP3 may be an important tumour suppressor in bladder cancer as the above observations suggest that dimunition in AIMP3 enables cancerous cells to survive significant exposure to DNA damaging agents such as ionising radiation. With respect to 253J, it is not entirely clear why there was no significant difference in survival. There was an increase in survival but the increase was not statistically significant. One possible explanation is that the 253J cell colonies are less discrete ("fuzzy") meaning that the standard errors whilst counting the colonies are liable to be higher. Consequently, the confidence intervals of the errors between the comparisons overlap resulting in non-significance.

The implication of these findings is that tumour cell survival in response to DNA damaging agents such as irradiation may be influenced by expression of AIMP3. In the clinical setting, it may be possible to predict likelihood of responsiveness to radiotherapy by the level of AIMP3 expressed in the tumour. This would in turn mean that it may be possible to individualise therapy for patients with bladder cancer, depending on the AIMP3 expression status of their tumours, by allowing them to receive radiotherapy in the knowledge that they would most likely respond favourably to it. Thus, correct stratification of patients likely to respond to a particular type of treatment modality such as radiotherapy, chemotherapy or surgery might be achieved. Such a stratified approach would help change the current paradigm of the management of organ-confined, muscle-invasive bladder cancer.

Chapter 4

AIMP3 expression is predictive of survival in patients treated with radical radiotherapy for muscle-invasive disease

4.1 Introduction to Chapter 4

The *in vitro* findings discussed in the preceding chapter (**Chapter 3**) indicated that, at the cell line level using our panel of bladder cancer cell lines (T24, RT112, 253J and RT4), AIMP3 expression status was predictive of cell survival following irradiation. Specifically, when AIMP3 expression was reduced, by siRNA transfection, clonogenic survival in the bladder cancer cell lines was increased following irradiation at the respective IC50 doses for the cell types. The implication of this was that the loss of expression of an important tumour suppressor gene such as *AIMP3*, during bladder cancer pathogenesis, may confer a survival advantage to the AIMP3-deficient tumour cells by decreasing their radiosensitivity. Conversely, in AIMP3-proficient cells, where siRNA transfection was not carried out or where only scrambled, non-interfering siRNA transfection was performed, clonogenic cell survival was not altered following irradiation at the same IC50 dose for the cell type.

Therefore, it was hypothesised that AIMP3 expression in bladder cancer tissues would be predictive of response to radiation treatment and may be prognostic for patient survival following radiotherapy. The main objective was to test this hypothesis by correlating the expression of AIMP3 in cancer tissue cores, obtained from 217 patients enrolled into the BCON radiotherapy trial (ISRCTN45938399), to clinical outcomes such as tumour status at 6 months and overall survival.

4.2 Characteristics of BCON patients stratified by AIMP3 status

Table 2.5 summarises the clinico-pathologic demographics of all BCON patients tested in the current study. The characteristics of the 217 patients, as stratified by their AIMP3 staining status, are summarised below in Table 4.1.

Table 4.1: Characteristics of patients in the BCON trial stratified by AIMP3 status

Demographics	All patients treated in BCON (n=326)	All patients tested in current study (n=217)	AIMP3 negative (n=106)	AIMP3 positive (n= 111)	P value
	Number (percent)				
Age, years					
Median age	74	74	75	74	0.06 α
Range	51-90	51-90	53-88	51-90	
Sex					0.497 ‡
Male	260 (80)	174 (80)	83 (78)	91 (82)	
Female	66 (20)	43 (20)	23 (22)	20 (18)	
Stage					0.997 ‡
1	30 (9)	22 (10)	11 (10)	11 (10)	
2	214 (66)	144 (66)	70 (66)	74 (67)	
3	68 (21)	41 (19)	20 (19)	21 (19)	
4	14 (4)	10 (5)	5 (5)	5 (4)	
Grade					
2	46 (14)	33 (15)	19 (18)	14 (13)	0.345 ‡
3	280 (86)	184 (85)	87 (82)	97 (87)	
Preceding Tumour					
No	276 (85)	186 (86)	87 (82)	99 (89)	0.174 ‡
Yes	50 (15)	31 (14)	19 (18)	12 (11)	
Preceding Tumour treatment					0.405 ‡
TURBT					
-Complete	126 (39)	90 (42)	35 (33)	55 (50)	
-Partial	100 (31)	66 (30)	36 (34)	30 (27)	
-Biopsy only	87 (26)	53 (24)	28 (26)	25 (22)	
-Unknown	13 (4)	8 (4)	7 (7)	1 (1)	
BCON randomisation					0.446 ‡
RT alone	163 (50)	113 (52)	58 (55)	55 (50)	
RT + CON	163 (50)	104 (48)	48 (45)	56 (50)	
Hb, g/dL					0.08 α
Median	13.7	13.6	13.5	13.9	
Range	9.3-17.2	9.3-17.2	9.3-17.2	9.8-17.0	

Abbreviations: TURBT, transurethral resection of bladder tumour; RT, radiotherapy; CON, carbogen and nicotinamide; Hb, haemoglobin

α Mann-Whitney U test ‡ Fisher's Exact Test

4.3 AIMP3 immuno-staining in the BCON TMA set

AIMP3 protein expression was variable in the tissue microarray (TMA) cores obtained from the 217 patients in the BCON trial set. As described in the "Materials and Methods" section (**2.13.2** "Immunohistochemistry Image Analysis"), TMA cores were assigned staining scores based on the proportion of cells staining positive and the intensity of staining in order to obtain a semi-quantitative H score. TMA cores were stratified as positive or negative using a median H score cut-off. Examples of AIMP3-negative and AIMP3-positive TMA cores are demonstrated below (**Figure 4.1**).

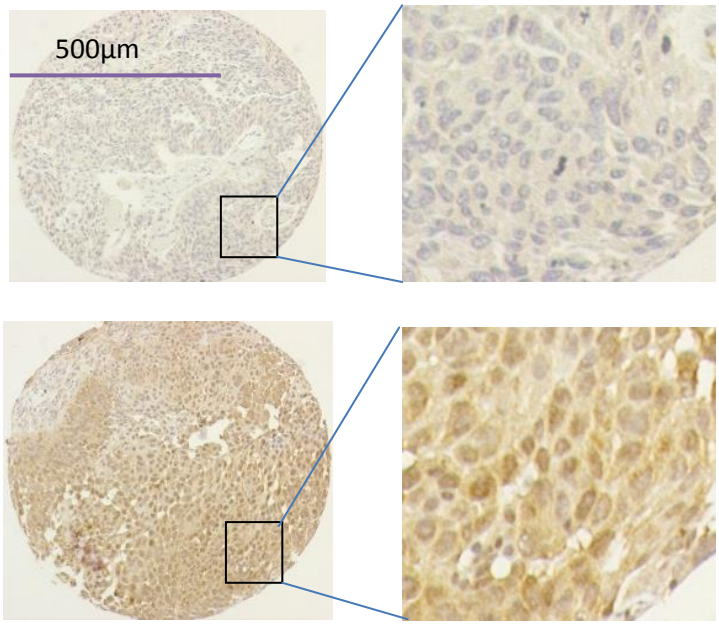

Figure 4.1: Differential expression of AIMP3 protein in the BCON TMA cores demonstrating weak staining (Top panel) and strong staining (Bottom panel) (Left panel images10x magnification; expanded Right panel images 200x magnification). The tissue core in the Top panel is classified as AIMP3-negative as there is weak staining (H score of 0.2 due to a weak staining score of 1 out of 3 in less than 50% of cells, i.e., 1 multiplied by 0.2) below the median H score of 1 (range of H score is 0 to 3). The tissue core in the Bottom panel is AIMP3-positive as it has strong AIMP3 staining (H score of 3 due to a staining strength score of 3 out of 3 in greater than 50% of cells, i.e., 3 multiplied by 1) above the median H score of 1.

4.4 Intra-observer and Inter-observer agreements of immunostaining scoring

The immunostaining measurements of the TMA cores were performed by different observers. Where scorings were repeated by the same observer in different experiments, intra-observer agreements were obtained. Inter-observer agreements could be evaluated when scorings from different observers were available.

4.4.1 Intra-observer scoring

The scoring, as AIMP3-positive and AIMP3-negative, for each of the 217 TMA cores, for the same observer, is tabulated in Table 4.2.

Table 4.2: Cross-tabulation of Intra-observer scores. Cross-tabulation of AIMP3-positive (-) and AIMP3-negative scores (+) in experiments 1 (Expt 1) and 2 (Expt 2) for the same observer

AIMP3Expt2 and AIMP3Expt1 Scores Cross-tabulation				
		AIMP3 Expt1		Total
		Negative (-)	Positive (+)	
AIMP3 Expt2	Negative (-)	88	18	106
	Positive (+)	20	91	111
Total		108	109	217

The Kappa value was calculated for the above (**Table 4.2**) scores to measure the intra-observer agreement. There was good intra-observer agreement as demonstrated by a Kappa value of 0.650 ($p<0.001$) – see Table 4.3 below.

Table 4.3: Cross-tabulation for Kappa value calculation in the intra-observer scores

	Kappa Value	**Standard Error**	**Significance**
Measure of Agreement (Kappa)	.650	.052	.000
Number of cases	217		

4.4.2 Inter-observer scoring

AIMP3 scorings between different observers are tabulated below in Table 4.4 and Table 4.5.

Table 4.4: Inter-observer cross-tabulation. Cross-tabulation of Observer 1 (Expt 2) versus Observer 2

AIMP3Expt2 * AIMP3Observer2 Scores Cross-tabulation				
		AIMP3 Observer 2		**Total**
		Negative (-)	**Positive (+)**	
AIMP3 Expt2	**Negative (-)**	67	39	106
	Positive (+)	20	91	111
Total		87	130	217

Kappa value calculation for the above (**Table 4.3**) scoring is tabulated below in Table 4.4. There was good agreement (Kappa value of 0.450) between the different observers ($p<0.001$).

Table 4.5: Kappa value calculation for inter-observer (Table 4.3) scores

	Kappa Value	**Standard Error**	**Significance**
Measure of Agreement (Kappa)	.454	.060	.000
Number of cases	217		

Inter-observer scoring between Observer 2 (PCRC) and Observer 3 (ST) is tabulated in Table 4.6 below.

Table 4.6: Cross-tabulation of AIMP3-positive and AIMP3-negative scores between Observer 2 and Observer 3

AIMP3Observer3 and AIMP3Observer2 Scores Cross-tabulation				
		AIMP3Observer2 (AIMP3 negative)	**(AIMP3 positive)**	**Total**
AIMP3Observer3	**(AIMP3 negative)**	70	23	93
	(AIMP3 positive)	17	107	124
Total		87	130	217

Kappa value calculations for the above inter-observer scores (**Table 4.5**) are cross-tabulated in Table 4.6 below. There was good inter-observer agreement (Kappa value of 0.621) and this was significant ($p<0.001$).

Table 4.7: Cross-tabulation for Kappa value calculation between Observer 2 and Observer 3

	Kappa Value	**Standard Error**	**Significance**
Measure of Agreement (Kappa)	.621	.054	.000
Number of Cases	217		

4.5 AIMP3 expression status and Overall Survival in the BCON set

4.5.1 Kaplan-Meier estimates of Survival

Kaplan-Meier plot of Overall Survival (OS), stratified by AIMP3 staining status, is depicted below (**Figure 4.2**). There was a significant difference in OS ($p<0.001$) with higher survival in the AIMP3-positive group compared to the AIMP3-negative group. Table 4.7A outlines the distribution of cases stratified by AIMP3 status and Table 4.7B tabulates the log-rank estimates for the Kaplan-Meier plot in Figure 4.2. The estimates for the median survivals for the AIMP3-positive and AIMP3-negative groups are calculated in Table 4.7C.

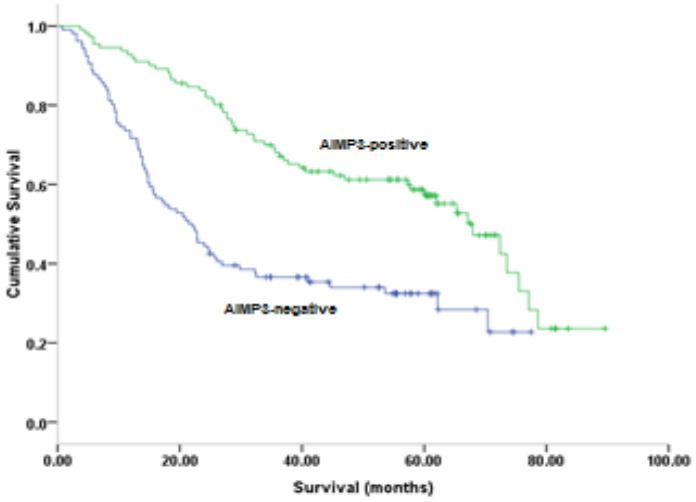

Numbers at risk

AIMP3-positive	111	95	67	40	5	0
AIMP3-negative	106	56	32	13	0	0

Figure 4.2: Kaplan-Meier plot of Overall Survival by AIMP3 staining status. Survival is greater in the AIMP3-positive group (green survival curve) relative to the AIMP3-negative group (blue survival curve). The numbers at risk, for each time-point interval (e.g. 0, 20, 40 months) are tabulated below the figure.

The calculations for the K-M estimates above are tabulated below in Table 4.7 (A, B and C). As evident from the K-M plots, there was a significant difference in the median survival estimates between the AIMP3-positive and AIMP3-negative cases. In the AIMP3-positive group, median survival was 67.9 +/- 5.0 months (95% CI: 58.0 to 77.8 months) compared to 21.5 +/- 3.0 months (95% CI: 15.7 to 27.3 months) in the AIMP3-negative group (**Table 4.7C**). The p value for this log rank estimate was <0.001 (**Table 4.7B**).

Table 4.7: Case-processing summary, log-rank estimates and median survival estimates in the BCON set stratified by AIMP3 status

Table 4.7A: Case-processing summary for K-M calculations

AIMP3 status	Total	Number of Events	Censored	
			Number	Percentage
Negative (-)	106	72	34	32.1%
Positive (+)	111	54	57	51.4%
Overall	217	126	91	41.9%

Table 4.7B: Log-rank of the K-M estimates and significance

	Chi-Square	Significance
Log Rank (Mantel-Cox)	22.277	.000

Table 4.7C: Median survival estimates and 95% Confidence Intervals around the estimates stratified by AIMP3 staining status

Means and Medians for Survival Time								
AIMP3 Status	Mean				Median			
	Estimate	Standard Error	95% Confidence Interval		Estimate	Standard Error	95% Confidence Interval	
			Lower Bound	Upper Bound			Lower Bound	Upper Bound
Negative	34.945	2.892	29.277	40.614	21.500	2.960	15.698	27.302
Positive	57.301	2.967	51.487	63.116	67.900	5.043	58.015	77.785
Overall	47.266	2.346	42.668	51.865	40.800	9.423	22.330	59.270

4.5.2 Univariate analysis by Cox proportional hazards method

When univariate analysis was performed based on AIMP3 staining status (**Table 4.8**), there was a 57% survival advantage (0.57 = 1 minus 0.43) in favour of those in the AIMP3-positive group compared to the AIMP3-negative group. The 95% confidence interval around this estimate (0.430) ranged from 0.300 to 0.617. This was statistically significant (p<0.001)

Table 4.8: Univariate Cox modelling by AIMP3 staining status

Variable	Standard Error	Significance	Hazard Ratio (HR)	95.0% CI for Hazard Ratio	
				Lower	Upper
AIMP3	.184	.000	.430	.300	.617

4.5.3 Multivariate analysis by Cox proportional Hazards method

When multivariate analysis was performed, taking into account all the relevant clinic-pathologic variables, AIMP3 staining status was still a significant predictive factor for survival (**Table 4.9**). AIMP3-positivity conferred a 47% survival advantage (1 minus 0.53); 95% CI: 0.358 to 0.784 (p<0.002).

Age and tumour status at 6 months were also significantly predictive of overall survival. For every year of increase in age, there was a 4% increase in the risk of death in this cohort (p=0.003).

Table 4.9: Multivariate modelling of AIMP3 staining status

Variables in Cox modelling					
	Standard Error	Significance	Hazard Ratio (HR)	95.0% CI for Hazard Ratio	
				Lower	Upper
Randomisation	.197	.851	.964	.655	1.417
Tumour recurrence	.246	.000	8.841	5.462	14.311
Previous cancer	.254	.055	1.630	.990	2.683
Hb	.197	.417	.174	.797	728
Stage		.545			
Stage 1	.415	.247	1.617	.717	3.648
Stage 2	.459	.664	1.220	.496	3.000
Stage 3	.603	.414	1.636	.502	5.330
Grade	.63	.847	1.052	.628	1.763
TURBT		.873			
TURBT complete	.267	.615	1.144	.678	1.931
TURBT partial	.252	.674	1.112	.678	1.823
Gender	.241	.327	.790	.492	1.266
Age	.013	.003	1.040	1.013	1.068
AIMP3 status	.200	.001	.530	.358	.784

4.6 AIMP3 expression status and Tumour Recurrence in the BCON set

In terms of tumour recurrence, cystoscopic recurrence at 6 months conferred an 8.8-fold increase in the risk of death (HR: 8.84; 95%CI: 5.5 to 14.3; p<0.001). Figure 4.3 depicts a K-M plot of differences in survival in those with recurrence compared to those without recurrence.

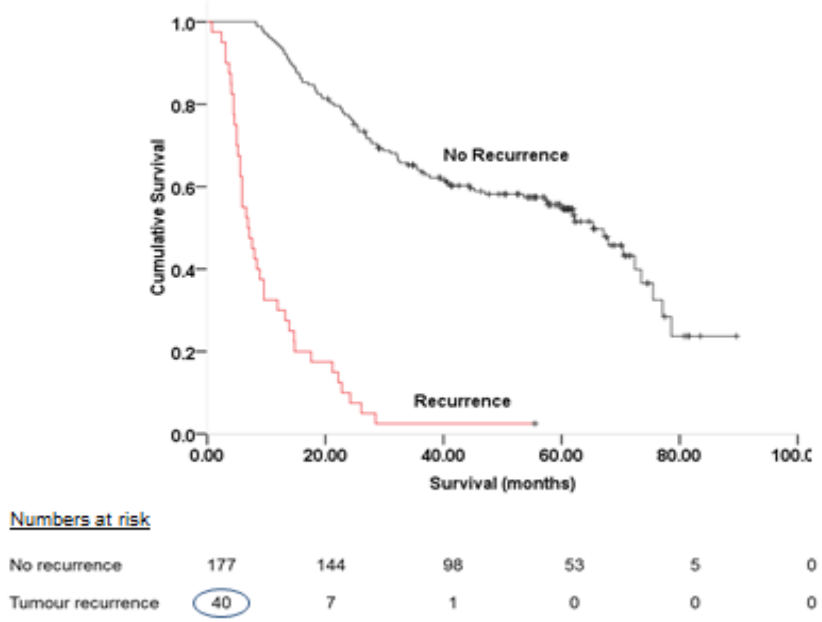

Figure 4.3: Difference in survival comparing those with tumour recurrence at 6 months (red) against those with no recurrence at 6 months (black)

When tumour recurrence status was evaluated against AIMP3 staining status, there was a significant difference in the likelihood of recurrent tumours also being AIMP3-negative (**Table 4.10**). Of the 40 cases (out of 217) with tumour recurrence, 30 were in the AIMP3-negative group and 10 were in the AIMP3-positive group. This difference was statistically significant ($p<0.001$).

Table 4.10: Cross-tabulation of tumour recurrence and AIMP3-status

Cystoscopic tumour recurrence status	All patients	Patients with AIMP3-negative tumours *Number (percent)*	Patients with AIMP3-positive tumours	p value
				<0.001 [α]
No recurrence	177 (82)	76 (35)	101 (47)	
Recurrence	40 (18)	30 (14)	10 (4)	

[α] Fisher's Exact Test

4.7 Discussion of results

The main objectives of the work presented in this chapter were to analyse the BCON dataset in relation to AIMP3 immunostaining, analyse AIMP3 immunostaining on the BCON TMA cores and to correlate the immunostaining status with clinical outcomes on the dataset. The distribution of the clinico-pathological characteristics of the patients in the BCON are summarised previously (**Table 2.5**). In brief, of the 217 patients, 174 were males (80%) and 43 (20%) females, with a median age of 74 years (range: 55 to 90 years). When analysing by AIMP3 staining status, these patients were stratified into 106 in the AIMP3-negative group and 111 in the AIMP3-positive group (**Table 4.1**). When analysing the differences in the clinic-pathological characteristics between the AIMP3-negative and AIMP3-positive groups, there were no statistically significant differences between the variables (**Table 4.1**).

The immuno-staining properties of AIMP3 in the TMA cores were as expected. The AIMP3-negative cores had negligible staining in the cells (**Figure 4.1**). In contrast, AIMP3-positive cores had unequivocal staining of both the nuclear and cytoplasmic compartments (**Figure 4.1**). In the AIMP3-positive cores, there was no false-positive staining of cellular membranes and extracellular matrix. There were strong intra-observer and inter-observer agreements in the scorings (**Tables 4.2 to 4.5**).

Survival analyses demonstrated a significant difference between the AIMP3-positive and AIMP3-negative groups in the BCON set. Median survival in the AIMP3-positive group was estimated at 67.9 +/- 5.0 months (95% CI: 58.0 to 77.8 months) and this was significantly higher than 21.5 +/- 3.0 (95% CI: 15.7 to 27.3 months) in the AIMP3-negative group ($p<0.001$). On multivariate analysis, AIMP3-positivity conferred a 47% survival advantage (1 minus 0.53); 95% CI: 0.358 to 0.784 ($p<0.002$). Of the other variables, "Age" and "Tumour Status at 6 Months" were also significant on multivariate analysis (**Table 4.9**). The hazard ratio for Age was 1.04 (95% CI: 1.01 to 1.07) suggesting a 4% increased risk of death for every year increase in age ($p=0.003$). The hazard ratio for "Tumour Status at 6 Months" was 8.8 (95% CI: 5.5 to 14.3) suggesting an almost 9-fold increased risk of death if there was tumour recurrence at 6 months following radical radiotherapy in the BCON cohort ($p<0.001$). Of those who had tumour recurrences (30 cases), significantly more were observed in the AIMP3-negative group ($p<0.001$). The findings support the hypothesis that AIMP3 may be a significant predictor of clinical outcomes in patients who undergo radical radiotherapy for MIBC.

Chapter 5

AIMP3 expression is not prognostic of survival in patients who have undergone Radical Cystectomy

5.1 Introduction to Chapter 5

In the previous chapter (**Chapter 4**), immunostaining analyses of the BCON radiation trial TMA set demonstrated that AIMP3 expression is predictive of outcome in patients with MIBC who had undergone radical radiotherapy. AIMP3 staining status was significantly correlated to the risk of tumour recurrence and overall survival. However, to answer the question whether AIMP3 was predictive of radiotherapy outcome or whether it was simply predictive of survival from MIBC in this cohort, it was necessary to interrogate AIMP3 staining in a "control" patient cohort with MIBC who had not been treated with radiotherapy. The best "control" cohort would be one where patients with similar clinicopathologic characteristics were not exposed to any treatment. However, to randomise MIBC patients to "no treatment" would be unethical and indeed, there is no such "control" cohort available. Therefore, we used a cohort of patients with MIBC who had undergone radical cystectomy. Radical cystectomy achieves survival benefit by a different mechanism to radical radiotherapy. Whereas in radiotherapy the mechanism of tumour eradication involves exposure to ionising radiation and interference with the DDR pathway, radical surgery achieves tumour eradication by surgical excision of the whole organ (cystectomy) containing the tumour and surrounding lymph nodes (lymphadenectomy).

A TMA comprising cores from 151 TURBT biopsies from patients who subsequently underwent radical cystectomy was obtained from the University of Southampton. All cases were diagnosed and treated between January 2000 and

January 2011. Cases exposed to neoadjuvant chemotherapy, adjuvant chemotherapy or radiotherapy were excluded.

5.2 Characteristics of patients in the Radical Cystectomy cohort

The clinicopathologic characteristics of the radical cystectomy cohort, stratified by AIMP3 staining, are summarised below **(Table 5.1**).

Table 5.1: AIMP3 staining status in the Radical Cystectomy cohort

	All patients (n=151)	**AIMP3 negative** (n=94)	**AIMP3 positive** (n=57)
		Number (percent)	
Age, years			
Median age	73	73	74
range	33-87	33-87	47-86
Sex			
Male	118 (78)	71 (60)	47 (40)
Female	33 (22)	21 (64)	12 (36)
Stage [x]			
0	7 (5)	7 (100)	0 (0)
is	24 (16)	9 (40)	15 (60)
1	8 (5)	3 (40)	5 (60)
2	23 (15)	14 (61)	9 (39)
3	58 (38)	45 (78)	13 (22)
4	10 (7)	5 (50)	5 (50)
Node +ve	21 (14)	9 (43)	12 (57)
Grade [¥]			
2	10 (7)	6 (60)	4 (40)
3	120 (79)	70 (58)	50 (42)

x pathological staging from radical cystectomy; 0 (pT0): no residual tumour following previous TURBT; is (pTis or CIS): carcinoma in situ

¥ does not include pT0 and cases which were exclusively pTis

5.3 AIMP3 immunostaining in the Radical Cystectomy cohort

AIMP3 immunostaining was scored using the same methodology described for the BCON TMA set. Examples of AIMP3-negative and AIMP3-positive TMA cores from the Radical Cystectomy set are shown below (**Figure 5.1**).

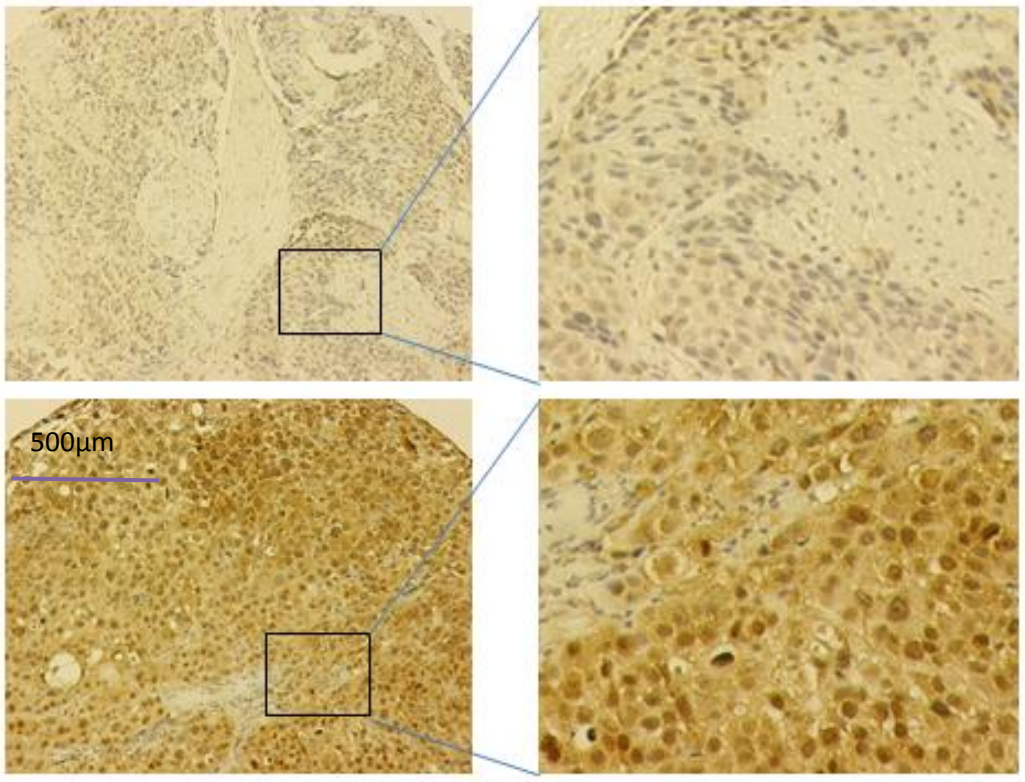

Figure 5.1: AIMP3-negative cores (top panel) and AIMP3-positive cores (bottom panel). Left panel cores are at 10X magnification and Right panel cores are at 200X magnification.

5.4 Kaplan-Meier estimates of survival in the Radical Cystectomy cohort

Survival estimates by Kaplan-Meier method demonstrated no significant difference in survival between the AIMP3-positive and AIMP3-negative cases in the Radical Cystectomy set (**Figure 5.2**).

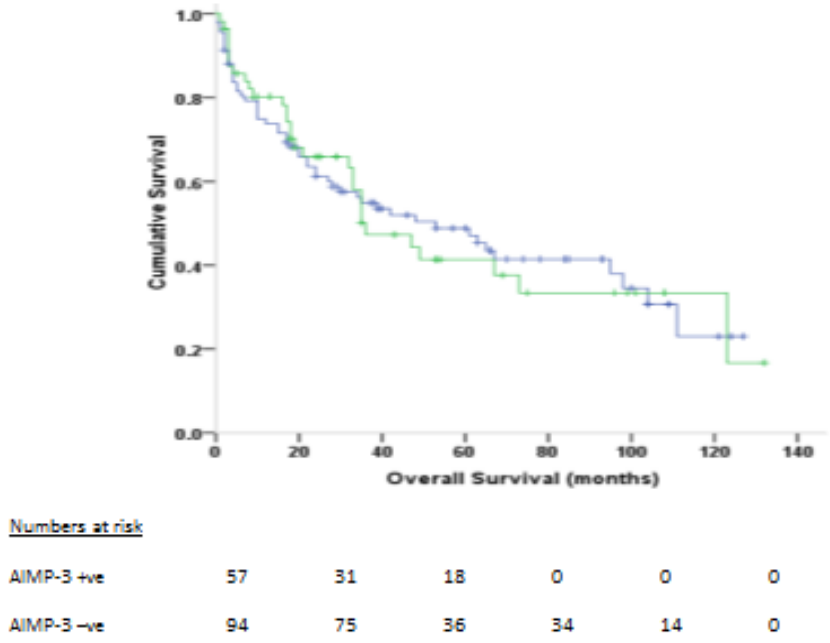

Figure 5.2: Kaplan-Meier plots for survival in the AIMP3-postive (green) and AIMP3-negative (blue) groups

5.5 Univariate analysis

Univariate analysis of AIMP3 staining status in the Radical Cystectomy set (**Table 5.2**) confirmed the above Kaplan-Meier estimated that AIMP3 is not predictive of survival outcome in this set (p=0.986).

Table 5.2: Univariate analysis of AIMP3 in the Radical Cystectomy set

Variable	Standard Error	Significance	Hazard Ratio (HR)	95.0% CI for Hazard Ratio	
				Lower	Upper
AIMP3 status	.221	.986	1.004	.650	1.549

5.6 Multivariate analysis

Multivariate analyses by Cox proportional hazards modelling, taking into account all relevant clinico-pathologic variables, confirmed that AIMP3 is not prognostic for survival in the Radical Cystectomy cohort. The results are summarised below (**Table 5.3)**. The size effect for AIMP3 in this analysis was 0.91, equating to a 9% survival advantage in the AIMP3-positive group; however, this was not significant (p=0.702; 95% CI: 0.562 to 1.474).

The statistically significant clinic-pathologic factors were Tumour Stage (p<0.001), Patient Age (p=0.045) and Patient Sex (p=0.046). With respect to Tumour Stage, relative to those with Stage 1 disease (G3pT1), those who had Stage 4 disease (G3pT4) had a 5.756-fold increased risk of death (95% CI: 2.645 to 12.523; p<0.001). With respect to Age, there was a 2.3% increased risk of death per year increase in a patient's age (95% CI: 1.000 to 1.046; p=0.046). With respect to Sex, there was a 77% increased risk of death for Male patients compared to Female patients (95%: 1.012 to 3.097; p=0.045).

Table 5.3: Multivariate analysis of AIMP3 staining status in the Radical Cystectomy cohort

	Variables in Cox modelling				
	Standard Error	Significance	Hazard Ratio (HR)	95.0% CI for Hazard Ratio	
				Lower	Upper
Stage		.000			
Stage 1	.420	.856	.927	.406	2.112
Stage 2	.350	.005	2.685	1.353	5.329
Stage 3	.505	.008	3.782	1.405	10.185
Stage 4	.397	.000	5.756	2.645	12.523
Grade		.996			
Grade 2	.899	.989	.988	.170	5.754
Grade 3	.793	.957	.958	.203	4.528
Gender	.285	.045	1.770	1.012	3.097
Age	.011	.046	1.023	1.000	1.046
AIMP3 status	.246	.702	.910	.562	1.474

5.7 Discussion of results

The main objectives of the work presented in this chapter were to analyse the Radical Cystectomy dataset, analyse the immunostaining of the TMA cores and to correlate the immunostaining status to the clinical outcomes in the dataset. With respect to the sample size of the dataset, a total of 64 cases were required to detect a

50% difference (e.g. 40 months versus 30 months) in the survival between two groups (AIMP3-positive versus AIMP3-negative) with a power of 80% and a p-value of 0.05. The sample size of the Radical Cystectomy set was good with a cohort of 151 patients. This compared to 217 patients in the BCON set and this meant that both the cohorts were similar in terms of sample size for adequately powered statistical analyses.

The Radical Cystectomy set was obtained from within the UK which has advantages in terms of allowing a better comparison to the BCON cohort. Firstly, the risk profile of a population within the same country for a particular disease (bladder cancer) is likely to have less variability than when comparing the risk profile of populations from different countries. For instance, the demographics of bladder cancer in the UK are not comparable to Egypt. There is a far higher incidence of schistosomiasis-related bladder cancer and a higher incidence of squamous cell-type bladder cancer in Egypt. Secondly, the clinical management of a disease from the same country is likely to hold less variability. National guidelines mean that clinicians in the UK are less likely to deviate from agreed standards. Therefore, in terms of managing patients with organ-confined MIBC, clinicians in the UK would be expected to adopt similar practices. Hence, selection of patients for radiotherapy or surgery would be expected to be reasonably similar throughout the UK. In this respect, the BCON cohort selection is robust by virtue of strict criteria inherent in a large randomised clinical trial. Ideally, the radical cystectomy cohort would also have been derived from a clinical trial set but this was not available. In fact, the only clinical trial devised to randomise patients to either radical radiotherapy or radical cystectomy (SPARE trial: selective bladder preservation against radical

excision trial) was unsuccessful (Huddart RA *et al*, 2010). In the absence of such a trial cystectomy cohort, a large series from within the UK was felt to be a suitable "control set" to compare against the BCON "treatment set".

Another advantage of the radical cystectomy set used was that it was contemporary to the BCON series. This allows for a better comparison for most of the reasons explained above - the disease demographics within the population and the clinical practices in managing the disease at a given period in time are likely to be less variable. One criticism of the control set may be that a larger series could have been obtained by incorporating contemporary cohorts from multiple centres. However, this task was beyond the scope of this current project. In any case, the sample size of 151 was deemed adequately powered for statistical analyses.

An important concern with the radical cystectomy set was to ensure that any confounding factors for radiotherapy effect would be minimised. In this respect, patients who had undergone chemotherapy or radiotherapy either in the neoadjuvant, adjuvant or salvage setting were excluded from the radical cystectomy series. For instance, cisplatin-based neoadjuvant chemotherapy prior to radical treatment was being increasingly introduced in the earlier part of the era of this series and is currently the established standard. Similarly, patients who had had prior radical radiotherapy as the primary treatment and subsequently radical cystectomy as salvage treatment had to be excluded. Also, patients who had had salvage radiotherapy following radical cystectomy or patients who had received adjuvant radiotherapy or chemotherapy had to be excluded. Thus, by excluding any radical

cystectomy patient who had had radiotherapy or chemotherapy, the confounding effects these DNA damaging modalities would have in terms of allowing a comparison with the BCON "treatment set" is minimised.

When the characteristics of the patients in the radical cystectomy set (**Table 5.1**) are analysed, the clinic-pathological demographics are what would be expected of a large radical cystectomy series. The median age was 73 years (range: 33 to 87 years) in this series. This compares to a median age of 74 years (range: 51 to 90 years) in the BCON set (**Table 2.5**). The female to male gender distribution was 20% and 80% in the BCON set; this was 28% (females) and 72% (males) in the Radical Cystectomy set. Therefore, both the BCON and Radical Cystectomy sets are similar in terms of Age and Gender distribution. However, there was a difference with respect to the Stage distribution of the treated patients. In the BCON set, 76% (166/217) of the tumours were Stage T2 or less (T0, Tis, T1, and T2 inclusive were 62 out of the total sample size of 217). In the Radical Cystectomy set, 41% (62/151) of the tumours were Stage T2 or less. In other words, there were more tumours of higher Stages (T3, T4) in the Radical Cystectomy set compared to the BCON set. This would be expected to translate to a relatively better survival outcome in the BCON set. The estimated median survival of the Radical Cystectomy set was 49.0 +/- 9.9 months (95% CI: 29.6 to 68.4 months); this was greater than the estimated median survival in the BCON set which was 40.8 +/- 9.4 months (95% CI: 22.3 to 59.3 months). However, the difference in the median survival estimates between the two groups, taking into account the standard errors in the estimates and the 95% confidence intervals, was not statistically significant.

In terms of assessing the potential prognostic value of AIMP3 staining status in the Radical Cystectomy set, it was important that there were no significant differences between the AIMP3-positive and AIMP3-negative groups as far as the distribution of clinic-pathological characteristics were concerned (**Table 5.1**). There were 94 patients in the AIMP3-negative group and 57 in the AIMP3-positive group. The median ages in the two groups were similar – 73 years (range: 33 to 87 years) in the AIMP3-negative group compared to 74 years (range: 47 to 86 years) in the AIMP3-positive group. 22% (21/94) were females in the AIMP3-negative group compared to 21% (12/57) in the AIMP3-positive group. 35% (33/94) patients in the AIMP3-negative group had tumours which were Stage T2 or less compared to 51% (29/57) in the AIMP3-positive group.

In the Radical Cystectomy set, there was no significant difference in survival between the AIMP3-negative and AIMP3-positive groups (**Figure 5.2**). Univariate (**Table 5.2**) and multivariate (**Table 5.3**) confirmed this lack of significant difference in survival. The findings indicate that AIMP3 status is not a prognostic factor for survival in patients with MIBC. In fact, in conjunction with the findings of the previous chapter demonstrating that AIMP3 was predictive of survival in the BCON set, the lack of significance in survival difference in the "control" Radical Cystectomy set, suggests that AIMP3 is a predictive factor for radiotherapy response. In other words, AIMP3 status is predictive of radiotherapy outcome as hypothesised rather than just being a prognostic factor of survival in all patients with organ-confined MIBC regardless of the radical treatment modality received.

Chapter 6

Immunostaining profiling of Mre11, ERCC1 and p53 in the BCON and Radical Cystectomy TMA sets

6.1 Introduction to Chapter 6

The previous two results chapters demonstrated that AIMP3 is a predictive factor for radiotherapy response and that it is not simply prognostic for survival in patients with bladder cancer; this was based on interrogation of both the BCON radiotherapy set and the control Radical Cystectomy set. We wanted to investigate whether other biomarkers, which are reported to be predictive of radiotherapy outcome based on TMA immunostaining platforms used, could be interrogated on the BCON and Radical Cystectomy TMA sets. This would help to ascertain the predictive and/or prognostic value of the tested biomarkers.

Mre11 and ERCC1 were chosen as described previously. p53 expression was also interrogated as p53 is reported to be an important prognostic factor for survival in many cancers including bladder. In a radical cystectomy series including 243 patients, nuclear accumulation of p53 was strongly correlated to decreased recurrence-free survival and overall survival (Esrig D *et al*, 1994). In another series of 164 patients who had undergone radical cystectomy, p53 was demonstrated to be an independent predictor of tumour recurrence and overall survival (Chatterjee SJ *et al*, 2004). However, others have argued that p53 expression may be significant in the pT1 disease subset of patients undergoing radical cystectomy in terms of stratifying the risk of disease recurrence and disease-specific mortality (Shariat SF *et al*, 2009). Adding p53 status into a multi-marker model was also found to improve prognostication in a large series comprising 692 patients with locally-advanced, non-metastatic bladder cancer (Shariat SF *et al*, 2010). Furthermore, other studies have

suggested that p53 expression may be predictive of clinical outcome following chemotherapy or radiotherapy for bladder cancer. In a series of 82 consecutive patients undergoing combined-modality treatment, incorporating cisplatin-based systemic chemotherapy and radical radiotherapy, p53 expression was found to be significantly correlated with bladder-preservation and cancer-specific survival (Garcia del Muro X *et al*, 2004). Similarly, another series of 96 patients undergoing cisplatin-based chemo-radiotherapy, demonstrated a significant correlation between p53 expression and both cancer-specific and cystectomy-free survival (Shinohara A *et al*, 2009). However, p53 was not found to be a significant predictor of outcome in another series of 73 patients undergoing cisplatin-based chemo-radiotherapy as part of the Radiation Therapy Oncology Group trial (Chakravarti A *et al*, 2005).

6.2 Mre11 expression

Mre11 immunostaining was performed as described previously in the Materials & Methods section. Whereas for AIMP3, a median H score was used as the cut-off threshold to stratify into AIMP3-positive and AIMP3-negative groups, a 25th percentile threshold was used for Mre11 as described by Choudhury A *et al*.

6.2.1 Mre11 expression in the BCON set

Mre11 immunostaining in the BCON TMA cores is exemplified below (**Figure 6.1**). Mre11 staining was present only in the nucleus as expected.

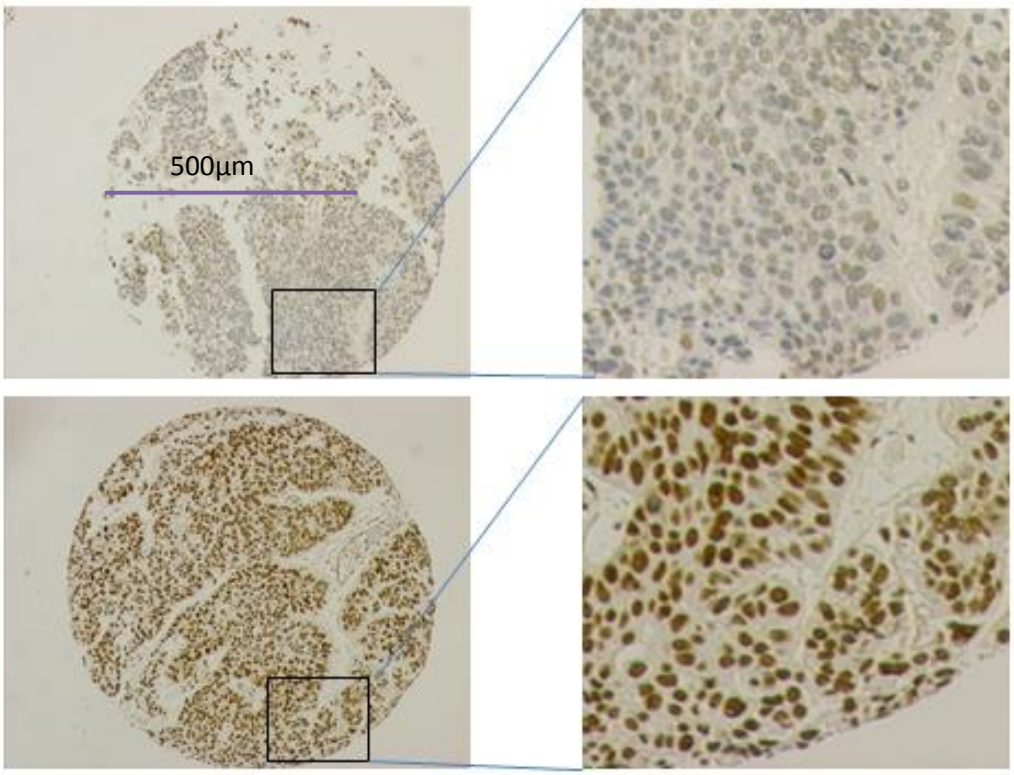

Figure 6.1: Mre11 immunostaining in the BCON TMA cores. Mre11-negative (Top panel) and Mre11-positive (Bottom panel) are demonstrated at 10x (Left panel) and 200x (Right panel) magnification.

6.2.2 Mre11 expression in the Radical Cystectomy set

Mre11 immunostaining in the Radical Cystectomy TMA cores is exemplified below (**Figure 6.2**).

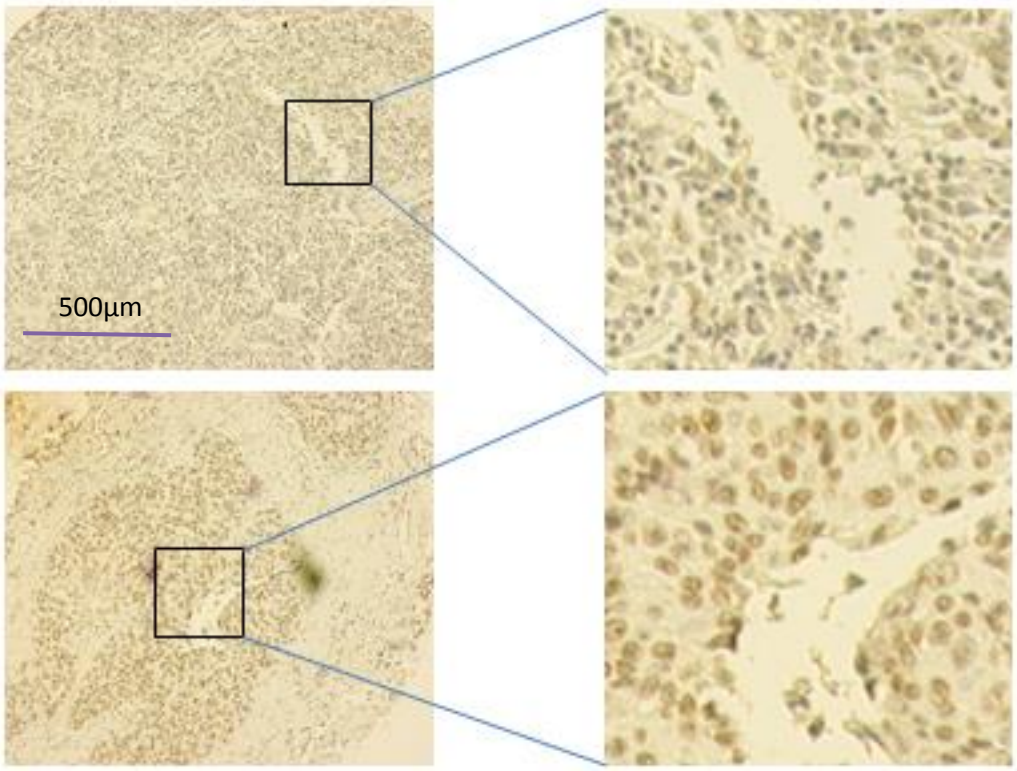

Figure 6.2: Mre11 expression in the Radical Cystectomy TMA cores. Mre11-negative (Top panel) and Mre11-positive (Bottom panel) are demonstrated at 10x (Left panel) and 200x (Right panel) magnification.

6.2.3 Mre11 is predictive of radiotherapy outcome in the BCON set

Kaplan-Meier estimates of survival outcome differences, between Mre11-positive and Mre11- negative groups, are demonstrated below. Using the 25th percentile cut-off method, of Choudhury *et al* as explained above, there was a significant survival advantage in the Mre11-positive group compared to the Mre11-negative group. The median survival in the Mre11-positive group was 53.6+/- 9.6 months (95% CI: 34.9 to 72.3 months) as compared to 19.5 +/- 3.4 months (95% CI: 12.8 to 26.2 months) in the Mre11-negative group (**Table 6.1B**). This difference was statistically significant (p=0.03) (**Table 6.1C**) and was evident in the Kaplan-Meier plots for the two groups (**Figure 6.3**).

Table 6.1: Case-processing summary (Table 6.1A), survival estimates (Table 6.1B) and log rank estimates (Table 6.1C) based on Mre11 immunostaining status in the BCON TMA set

Table 6.1A: The distribution of Mre11-negative (-) and Mre11-positive (+) cases is tabulated below.

Mre11 status	Number	Number of Events	Censored	
			Number	Percent
Mre11 (-)	35	23	12	34.3%
Mre11 (+)	182	103	79	43.4%
Overall	217	126	91	41.9%

Table 6.1B: The survival estimates for the Mre11-negative (-) and Mre11-positive (+) cases are tabulated below. For the whole cohort (217 patients), the median survival was 40.8 +/- 9.4 months (95% CI: 22.3 to 59.3 months).

Means and Medians for Survival Time								
Mre11 status	Mean				Median			
	Estimate	Standard Error	95% Confidence Interval		Estimate	Standard Error	95% Confidence Interval	
			Lower Bound	Upper Bound			Lower Bound	Upper Bound
Mre11 (-)	35.676	5.223	25.439	45.913	19.500	3.430	12.777	26.223
Mre11 (+)	49.102	2.507	44.188	54.016	53.600	9.549	34.884	72.316
Overall	47.266	2.346	42.668	51.865	40.800	9.423	22.330	59.270

Table 6.1C: Log-rank of the K-M estimates and significance. The significance (p value) for the above survival estimates (Table 6.1B) is calculated at 0.03 meaning that there is a significant difference in survival between the Mre11-negative and Mre11-positive cases.

	Chi-Square	Significance
Log Rank (Mantel-Cox)	4.714	.030

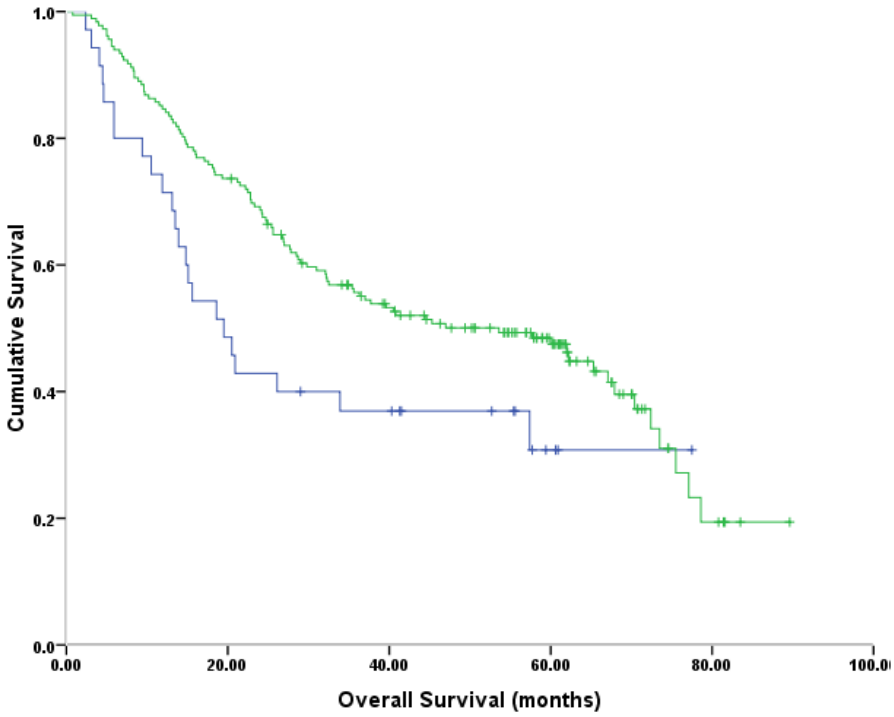

Figure 6.3: Kaplan-Meier plots for Mre11 staining status in the BCON set. Mre11-negative (blue) and Mre11-positive (green) cases suggesting a greater survival in the Mre11-positive group; this is confirmed on the log rank estimates (see **Table 6.1C**)

6.2.4 Univariate and multivariate modelling of Mre11 immunostaining and outcome in the BCON set

Cox proportional hazards modelling demonstrated that Mre11 status, on univariate analysis, was a significant predictor of radiotherapy outcome in the BCON set (**Table 6.2**). Mre11-positivity conferred a 39% (1 minus 0.61) survival advantage relative to those with Mre11-negative status (95% CI: 0.39 to 0.96; p=0.032).

On multivariate analysis, with all clinical variables in the model, this statistical significance was lost (p=0.372) (**Table 6.3**). Therefore, as opposed to AIMP3, where significance was retained on multivariate analysis, Mre11 status could not be confirmed as being significantly predictive of radiotherapy outcome in the BCON set.

Table 6.2: Univariate analysis of Mre11 immunostatining in the BCON set demonstrating significance (p=0.032).

Variable	Standard Error	Significance	Hazard Ratio	95.0% CI for Hazard Ratio	
				Lower	Upper
Mre11	.232	.032	.608	.386	.957

Table 6.3: Multivariate analysis of Mre11 immunostaining in the BCON set demonstrating loss of significance (p=0.372) when the known clinic-pathological variables are input into the model.

Variables in Cox modelling					
	Standard Error	**Significance**	**Hazard Ratio**	**95.0% CI for Hazard Ratio**	
				Lower	**Upper**
Randomisation	.198	.758	.941	.638	1.387
Tumour Recurrence	.246	.000	9.619	5.940	15.577
Previous Cancer	.257	.056	1.632	.987	2.697
Hb	.200	.344	1.208	.817	1.787
Stage		.339			
Stage 1	.416	.202	1.701	.752	3.846
Stage 2	.463	.771	1.145	.461	2.839
Stage 3	.606	.391	1.681	.513	5.510
Grade	.268	.779	1.078	.637	1.824
TURBT		.828			
TURBT complete	.279	.553	1.180	.683	2.037
TURBT partial	.253	.799	1.066	.649	1.751
Gender	.240	.250	.759	.475	1.214
Age	.013	.004	1.039	1.012	1.067
Mre11 status	.262	.372	.791	.473	1.323

6.2.5 Mre11 immunostaining analyses using the median H score method

To investigate whether Mre11 status may be predictive of outcome in the BCON set, the dataset was further interrogated using the median H score method as per AIMP3. Given that Mre11 status demonstrated significance, in the Kaplan-Meier method and also on Univariate analysis, which was subsequently lost on multivariate analysis, it was important to investigate whether there was truly a significant finding which was only lost due to the immunoscoring methodology used. Hence, the decision to analyse additionally by using the median H score method too.

Analyses of survival outcomes stratified by Mre11 status based on the median H-score method is illustrated below (**Figure 6.4**). In the Mre11-positive group, the median survival estimate was 53.6 months (95% CI: 32.2 to 79.9 months). This was greater than the median survival estimate in the Mre11-negative group (33.9 months; 95% CI: 7.2 to 60.6 months) (**Table 6.4B**). Kaplan-Meier plots of the two groups suggested a difference which may be significant (**Figure 6.4**). However, this difference was not statistically significant (p=0.254) (**Table 6.4C**). This was confirmed on Cox analysis where the hazard ratio for Mre11 status was 0.815 (95% CI: 0.573 to 1.159; p=0.255) (**Table 6.5**).

Table 6.4: Case-processing summary (Table 6.4A), survival estimates (Table 6.4B), and log rank estimates (Table 6.4C) for Mre11 immunostaining status as per the median H score method, in the BCON set, are tabulated below.

Table 6.4A: The distribution of Mre11-negative (-) and Mre11-positive (+) cases is tabulated below.

Mre11 status	Number	Number of Events	Censored	
			Number	Percent
Mre11 (-)	99	58	41	41.4%
Mre11 (+)	118	68	50	42.4%
Overall	217	126	91	41.9%

Table 6.4B: The survival estimates for the Mre11-negative (-) an Mre11-positive (+) cases is tabulated below. For the whole cohort (217 patients), the median survival is 40.80 +/- 9.42 months (95% CI: 22.33 to 59.27 months).

Means and Medians for Survival Time								
Mre11 status	Mean				Median			
	Estimate	Standard Error	95% Confidence Interval		Estimate	Standard Error	95% Confidence Interval	
			Lower Bound	Upper Bound			Lower Bound	Upper Bound
Mre11 (-)	42.946	3.140	36.792	49.101	33.900	13.605	7.235	60.565
Mre11 (+)	49.732	3.100	43.656	55.809	53.600	10.915	32.207	74.993
Overall	47.266	2.346	42.668	51.865	40.800	9.423	22.330	59.270

Table 6.4C: The significance (p value) for the above survival estimates (Table 6.4B) is calculated at 0.254 meaning that there is no significant difference in survival between the Mre11-negative and Mre11-positive cases (see Figure 6.4).

	Chi-Square	Significance
Log Rank (Mantel-Cox)	1.302	.254

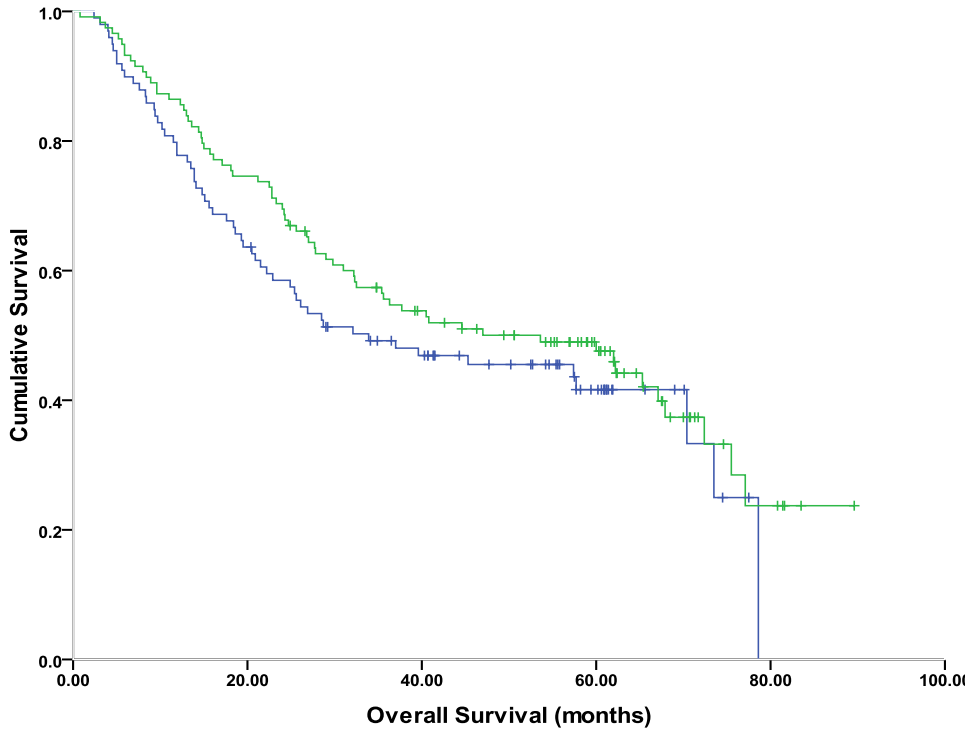

Figure 6.4: Kaplan-Meier plots for Mre11 staining status in the BCON set based on median H score method. Mre11-negative (blue) and Mre11-positive (green) cases suggesting the possible trend of greater survival in the Mre11-positive group; however, this is not confirmed on the log rank estimates (see Table 6.3C) or univariate analysis (see Table 6.4).

Table 6.5: Univariate analysis of Mre11 status, by H score method, demonstrating lack of significant survival differences (p=0.255) in the BCON set.

Variable	Standard Error	Significance	Hazard Ratio	95.0% CI for Hazard Ratio	
				Lower	Upper
Mre11 status	.180	.255	.815	.573	1.159

6.2.6 Mre11 status is not predictive of outcome in the Radical Cystectomy set

Interrogation of Mre11 expression status in the BCON set demonstrated that Mre11 status was not predictive of radiotherapy outcome. In order to answer the question whether Mre11 status was prognostic of survival in patients with bladder cancer, as for AIMP3, the Radical Cystectomy "control" set was interrogated. There was suggestion of a survival difference between the Mre11-negative and Mre11-positive groups but the difference narrowly missed statistical significance (p=0.063) (**Table 6.6C**). The estimated median survival in the Mre11-negative group was 63.00 +/- 20.68 months (95% CI: 22.47 to 103.53 months) which was greater than that in the Mre11-positive group which was 35.00 +/- 10.71 months (95% CI: 14.01 to 55.99 months) (**Table 6.6B**).

Table 6.6: Case processing summary (Table 6.6A), median survival estimates (Table 6.6B), and log rank estimates (Table 6.6C) for Mre11 expression status in the radical cystectomy set are tabulated below.

Table 6.6A: The distribution of Mre11-negative (-) and Mre11-positive (+) cases is tabulated below.

Mre11 status	Number	Number of Events	Censored	
			Number	Percent
Mre11 (-)	90	48	42	46.7%
Mre11 (+)	61	38	23	37.7%
Overall	151	86	65	43.0%

Table 6.6B: The survival estimates for the Mre11-negative (-) an Mre11-positive (+) cases is tabulated below. For the whole cohort (151 patients), the median survival is 49.00 +/- 9.92 months (95% CI: 20.68 to 10.71 months).

Means and Medians for Survival Time								
Mre11 status	Mean				Median			
	Estimate	Standard Error	95% Confidence Interval		Estimate	Standard Error	95% Confidence Interval	
			Lower Bound	Upper Bound			Lower Bound	Upper Bound
Mre11 (-)	72.096	6.434	59.485	84.706	63.000	20.678	22.471	103.529
Mre11 (+)	47.349	5.643	36.288	58.410	35.000	10.710	14.009	55.991
Overall	64.583	4.947	54.886	74.280	49.000	9.919	29.559	68.441

Table 6.5C: The significance (p value) for the above survival estimates (Table 6.3B) is calculated at 0.063 meaning that there is no significant difference in survival between the Mre11-negative and Mre11-positive cases (**Figure 6.5**).

	Chi-Square	Significance
Log Rank (Mantel-Cox)	3.470	.063

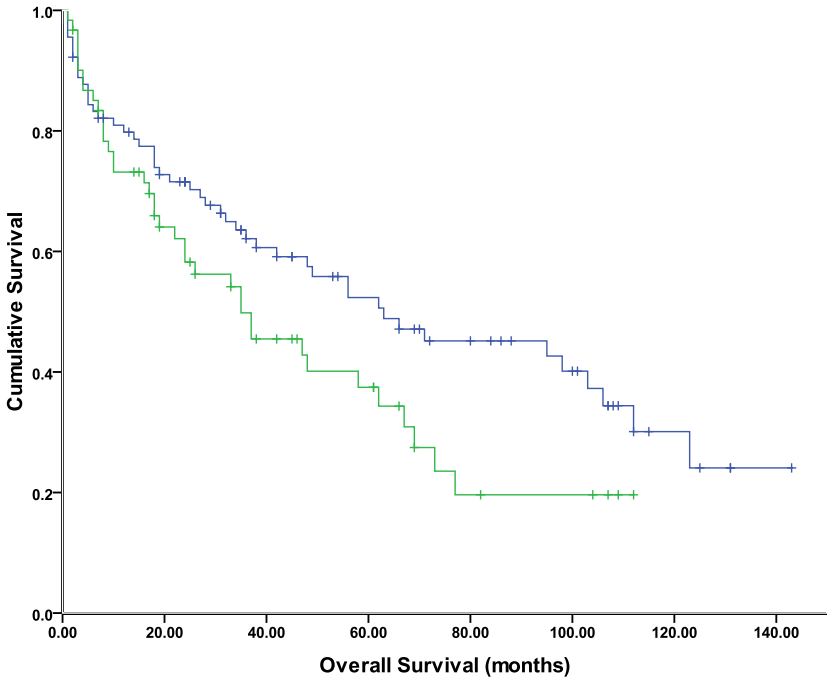

Figure 6.5: Kaplan-Meier plots for Mre11 staining status in the Radical Cystectomy set. Mre11-negative (blue) and Mre11-positive (green) cases suggesting a likelihood of greater survival in the Mre11-positive group; however, this is not confirmed on the log rank estimates (Table 6.6C) or univariate analysis (Table 6.7).

Table 6.7: Univariate analysis of Mre11 expression in the radical cystectomy set demonstrating that the difference in survival between groups is not significant (p=0.066).

Variables					
	Standard Error	Significance	Hazard Ratio	95.0% CI for Hazard Ratio	
				Lower	Upper
Mre11 status	.221	.066	1.500	.973	2.311

6.3 ERCC1 expression

ERCC1 immunostaining was performed as described previously in the Materials and methods section. As with AIMP3, a median H score cut-off was used to stratify cases into ERCC1-positive and ERCC1-negative groups. As expected, ERCC1 immunostaining was exclusively nuclear.

6.3.1 ERCC1 expression in the BCON set

ERCC1 immunostaining in the BCON TMA cores is exemplified by the ERCC1-negative and ERCC1-positive cores below (**Figure 6.6**).

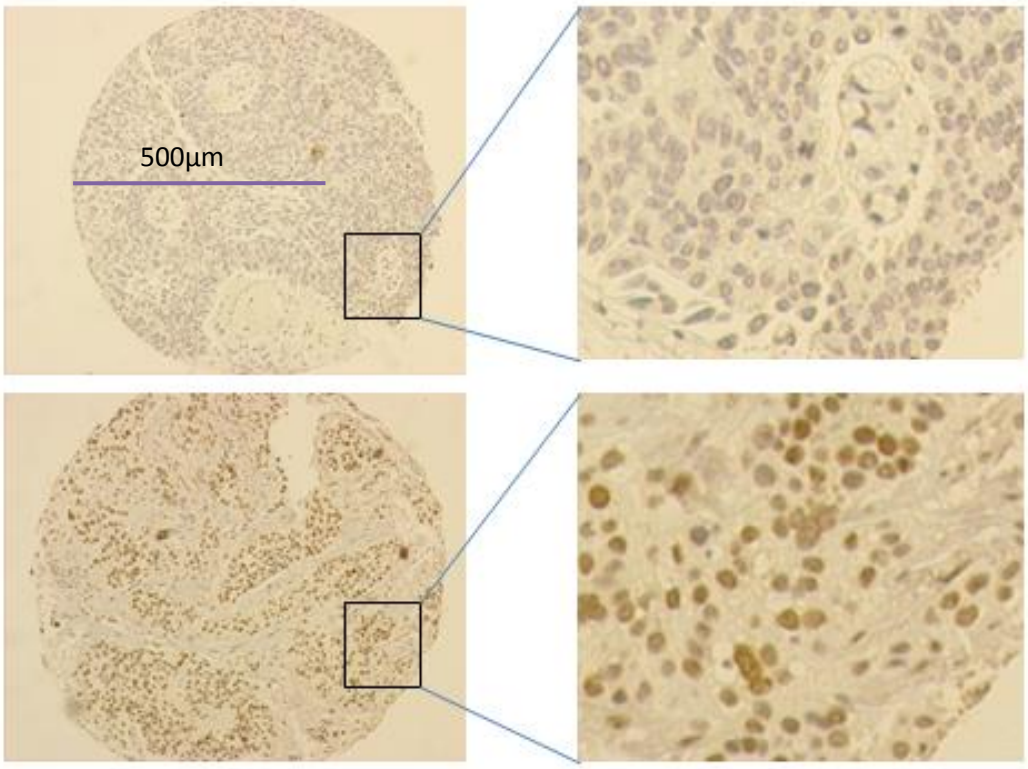

Figure 6.6: ERCC1 immunostaining in the BCON set. ERCC1-negative (Top panel) and ERCC1-positive (Bottom panel) are demonstrated at 10x (Left panel) and 200x (Right panel) magnification.

6.3.2 ERCC1 expression in the Radical Cystectomy set

ERCC1 immunostaining in the Radical Cystectomy cores is exemplified by the ERCC1-negative and ERCC1-positive cores below (**Figure 6.7**).

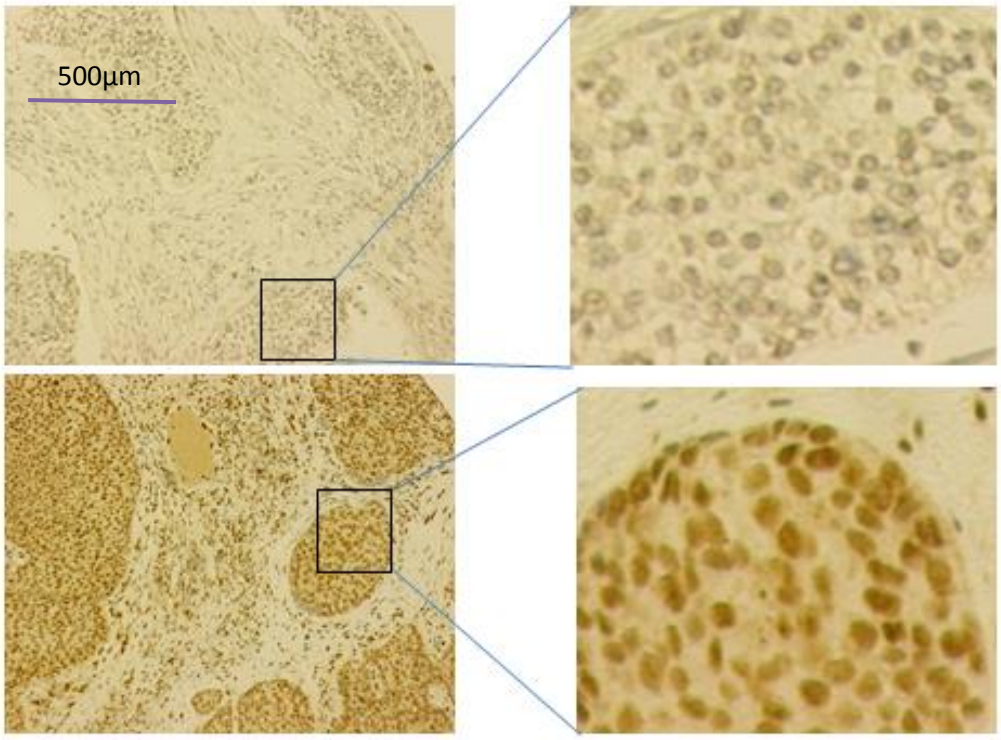

Figure 6.7: ERCC1 immunostaining in the Radical Cystectomy TMA cores. ERCC1-negative (Top panel) and ERCC1-positive (Bottom panel) are demonstrated at 10x (Left panel) and 200x (Right panel) magnification.

6.3.3 ERCC1 is predictive of radiotherapy outcome in the BCON set

ERCC1 immunostaining status was found to be strongly predictive of overall survival in the BCON set. In contrast to AIMP3, where positivity conferred a survival advantage, ERCC1-negativity was strongly correlated with a survival advantage.

The log rank estimates for the median survival in the ERCC1-negative group was 72.4 months (95% CI: 64.8 to 80.0; $p<0.001$) (**Table 6.8B**). This was significantly

greater than the ERCC1-positive group where the estimate was 22.9 months (95% CI: 16.5 to 29.4 months; p<0.001) (**Table 6.8B**).

Table 6.8: Case processing summary (Table 6.8A), median survival estimates (Table 6.8B), and log rank estimates (Table 6.8C) for ERCC1 expression status in the BCON set are tabulated below.

Table 6.8A: The distribution of ERCC1-negative (-) and ERCC1-positive (+) cases is tabulated below.

ERCC1 status	Number	Number of Events	Censored	
			Number	Percent
ERCC1 (-)	93	34	59	63.4%
ERCC1 (+)	124	92	32	25.8%
Overall	217	126	91	41.9%

Table 6.8B: The survival estimates for the ERCC1-negative (-) an ERCC1-positive (+) cases is tabulated below. For the whole cohort (217 patients), the median survival is 40.80 +/- 9.42 months (95% CI: 22.33 to 59.27 months).

Means and Medians for Survival Time								
ERCC1 status	Mean				Median			
	Estimate	Standard Error	95% Confidence Interval		Estimate	Standard Error	95% Confidence Interval	
			Lower Bound	Upper Bound			Lower Bound	Upper Bound
ERCC1 (-)	63.992	3.406	57.315	70.668	72.400	3.889	64.777	80.023
ERCC1 (+)	34.536	2.651	29.340	39.732	22.900	3.293	16.446	29.354
Overall	47.266	2.346	42.668	51.865	40.800	9.423	22.330	59.270

Table 6.8C: The significance (p value) for the above survival estimates (Table 6.8B) is calculated at <0.001 meaning that there is a significant difference in survival between the ERCC1-negative and ERCC1-positive cases (see Figure 6.8).

	Chi-Square	Significance
Log Rank (Mantel-Cox)	38.07	.00

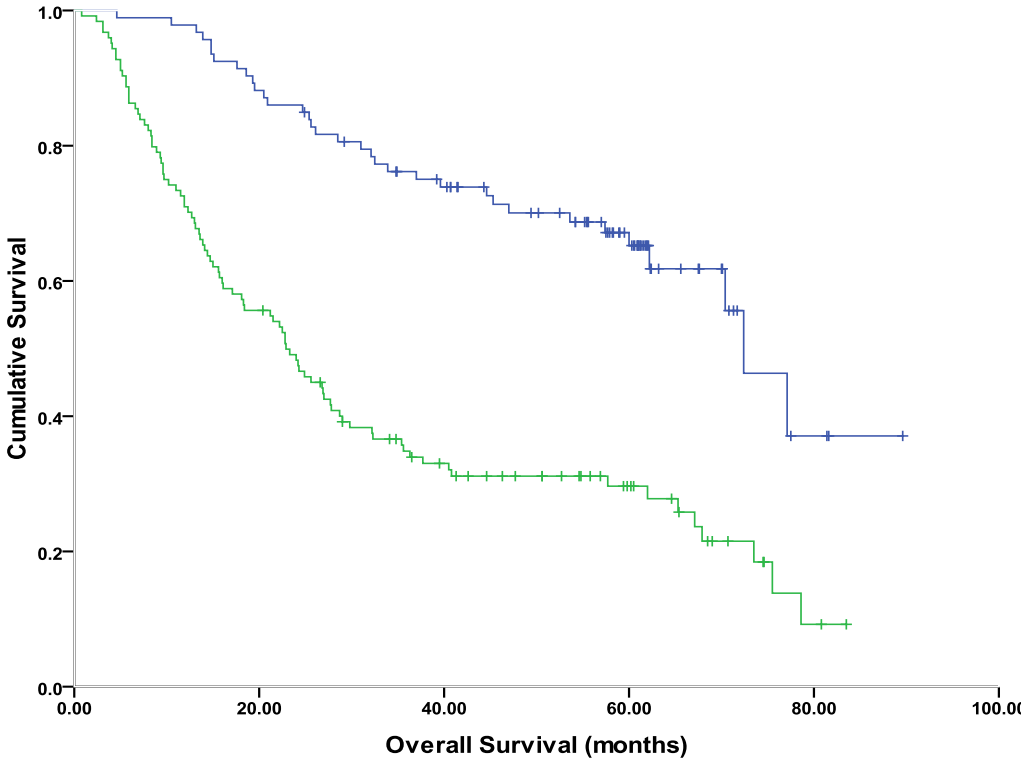

Figure 6.8: Kaplan-Meier plots for ERCC1 staining status in the BCON set. ERCC1-negative (blue) and ERCC1-positive (green) cases demonstrating a greater survival in the ERCC1-negative group. This is confirmed on the log rank estimates (see Table 6.8C) and univariate analysis (see Table 6.9).

6.3.4 Univariate analysis of ERCC1 in the BCON set

The highly significant difference in the median survival estimates between the ERCC1-negative and ERCC1-positive groups was confirmed on Cox proportional hazards modelling. On univariate analysis, the hazard ratio was 3.22 (95% CI: 2.17

to 4.79) and this was highly significant (p<0.001) (**Table 6.9**). This indicated that, relative to those who were ERCC1-negative, there was a 3.22-fold increased risk of death in those who were ERCC1-positive.

Table 6.9: Univariate analysis of ERCC1 expression in the BCON set demonstrating that the difference in survival between groups is significant (p<0.001). The hazard ratio is 3.22 (95% CI: 2.17 to 4.79) indicating a 3-fold risk of death in the ERCC1-positive group relative to the ERCC1-negative group.

Variables					
	Standard Error	Significance	Hazard Ratio	95.0% CI for Hazard Ratio	
				Lower	Upper
ERCC1 status	.202	.000	3.224	2.169	4.791

6.3.5 Multivariate analysis of ERCC1 in the BCON set

When all clinical variables were input into the Cox model for multivariate analysis, ERCC1 status was found to retain statistical significance in the model (**Table 6.10**). This was similar to AIMP3 where significance was retained on multivariate analysis and different to Mre11, where significance found on univariate analysis was lost in a multivariate model.

The hazard ratio on multivariate analysis (**Table 6.10**) was 3.15 (95% CI: 2.05 to 4.84) which suggested that, relative to those in the ERCC1-negative group, those

who were ERCC1-positive had a 3.15-fold increased risk of death and this was highly significant ($p<0.001$).

Table 6.10: Multivariate analysis for ERCC1 in the BCON set demonstrating that ERCC1 status retains significance ($p<0.001$) when all other known clinic-pathological factors are input into the model. The hazard ratio is 3.15 (95% CI: 2.05 to 4.84).

Variables in Cox modelling					
	Standard Error	Significance	Hazard Ratio	95.0% CI for Hazard Ratio	
				Lower	Upper
ERCC1	.219	.000	3.147	2.047	4.839
Age	.014	.024	1.031	1.004	1.059
Gender	.238	.367	.807	.506	1.286
TURBT		.330			
TURBT complete	.270	.501	1.199	.707	2.033
TURBT partial	.249	.532	.856	.525	1.395
Stage		.447			
Stage 1	.413	.154	1.801	.801	4.048
Stage 2	.463	.465	1.402	.566	3.473
Stage 3	.603	.368	1.719	.528	5.600
Hb	.196	.615	1.104	.751	1.622
Previous Cancer	.252	.063	1.598	.975	2.620
Randomisation	.197	.699	.927	.631	1.363
Tumour Recurrence	.254	.000	11.045	6.712	18.176

6.4 ERCC1 validation with intra- and inter-observer analyses

As with AIMP3, it was necessary to test the validity of the observed significant findings for ERCC1, through repeated experiments, performed by both the primary observer as well as different observers.

6.4.1 ERCC1: intra-observer

The survival analyses from a different experiment, for the primary observer, are presented below. In this experiment, the median survival estimate for the ERCC1-negative group was 73.5 +/- 3.2 months (95% CI: 67.2 to 79.8 months) compared to 21.5 +/- 3.0 months (95% CI: 15.5 to 27.5 months) in the ERCC1-positive group (**Table 6.11B**). This difference was significant ($p<0.001$) (**Table 6.11C**). The significant difference in survival between the groups is easily appreciable in the Kaplan-Meier survival plots for the two groups (**Figure 6.9**).

Table 6.11: Case processing summary (Table 6.11A), median survival estimates (Table 6.11B), and log rank estimates (Table 6.11C) for ERCC1 expression status in the BCON set are tabulated below.

Table 6.11A: The distribution of ERCC1-negative (-) and ERCC1-positive (+) cases is tabulated below.

ERCC1	Total Number	Number of Events	Censored	
			Number	Percent
ERCC1 (-)	94	33	61	64.9%
ERCC1 (+)	123	93	30	24.4%
Overall	217	126	91	41.9%

Table 6.11B: The survival estimates for the ERCC1-negative (-) and ERCC1-positive (+) cases is tabulated below. For the whole cohort (217 patients), the median survival is 40.80 +/- 9.42 months (95% CI: 22.33 to 59.27 months).

Means and Medians for Survival Time								
ERCC1 status	Mean				Median			
	Estimate	Standard Error	95% Confidence Interval		Estimate	Standard Error	95% Confidence Interval	
			Lower Bound	Upper Bound			Lower Bound	Upper Bound
ERCC1 (-)	66.530	3.090	60.474	72.587	73.500	3.198	67.233	79.767
ERCC1 (+)	32.109	2.581	27.050	37.169	21.500	3.042	15.537	27.463
Overall	47.266	2.346	42.668	51.865	40.800	9.423	22.330	59.270

Table 6.11C: The significance (p value) for the above survival estimates (Table 6.11B) is calculated at <0.001 meaning that there is a significant difference in survival between the ERCC1-negative and ERCC1-positive cases (see Figure 6.9).

	Chi-Square	Significance
Log Rank (Mantel-Cox)	54.760	.000

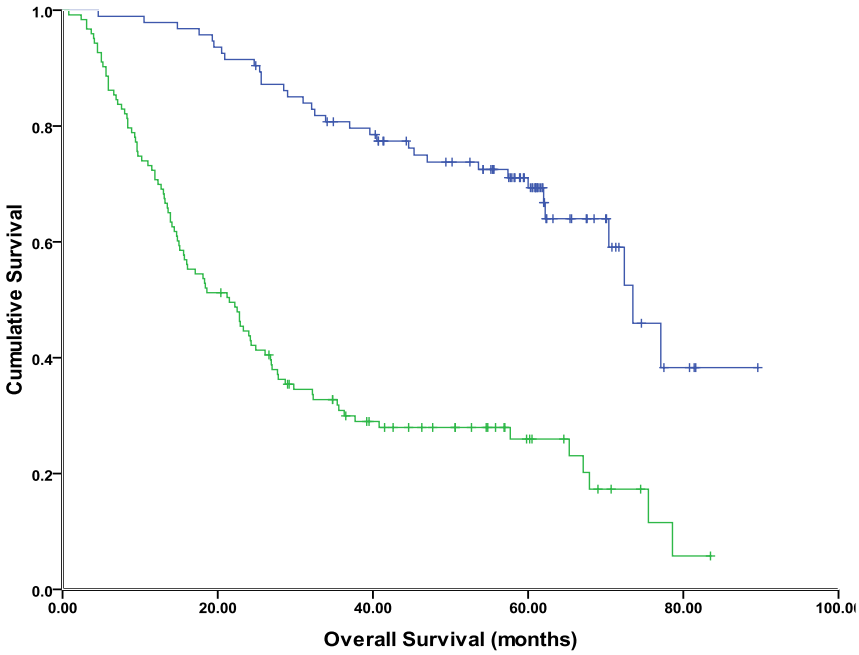

Figure 6.9: Kaplan-Meier plots for ERCC1 staining status in the BCON set: intra-observer. ERCC1-negative (blue) and ERCC1-positive (green) cases demonstrating a greater survival in the ERCC1-negative group.

The significant difference in survival between the ERCC1-negative and ERCC1-positive groups is confirmed on univariate analysis (**Table 6.12**). The hazard ratio was 4.11 (95% CI: 2.75 to 6.16) indicating a 4-fold increased risk of death in the ERCC1-positive group relative to the ERCC1-negative group.

Table 6.12: Univariate analysis of ERCC1 expression in the BCON set demonstrating that the difference in survival between groups is significant ($p<0.001$).

Variables					
	Standard Error	Significance	Hazard Ratio	95.0% CI for Hazard Ratio	
				Lower	Upper
ERCC1 status	.206	.000	4.113	2.747	6.156

When multivariate analysis was performed, the significance of ERCC1 status was maintained (**Table 6.13**). The hazard ratio was calculated at 3.48 (95% CI: 2.23 to 5.46) indicating a 3-fold increased risk of death in the ERCC1-positive group relative to the ERCC1-negative group. The level of significance was maintained at $p<0.001$.

Table 6.13: Multivariate analysis for ERCC1 in the BCON set demonstrating that ERCC1 status retains significance ($p<0.001$) when all other known clinic-pathological factors are input into the model.

Variables in Cox modelling					
	Standard Error	Significance	Hazard Ratio	95.0% CI for Hazard Ratio	
				Lower	Upper
ERCC1 status	.229	.000	3.482	2.223	5.456
Randomisation	.197	.912	.978	.665	1.440
Tumour Recurrence	.253	.000	8.951	5.450	14.702
Previous Cancer	.255	.020	1.807	1.096	2.979
Hb	.199	.720	1.074	.727	1.588
Stage		.594			
Stage 1	.412	.192	1.713	.763	3.844
Stage 2	.466	.410	1.469	.589	3.664
Stage 3	.599	.407	1.642	.508	5.310
TURBT		.517			
TURBT complete	.267	.730	1.096	.649	1.851
TURBT partial	.250	.519	.851	.522	1.389
Gender	.241	.771	.932	.581	1.496
Age	.014	.031	1.030	1.003	1.057

6.4.2 ERCC1: inter-observer

Analyses of ERCC1 scoring for a different observer are presented below. In this experiment, the median survival estimate for the ERCC1-negative group was 72.4 +/- 9.6 months (95% CI: 53.6 to 91.2 months) compared to 27.0 +/- 3.8 months (95% CI: 19.5 to 34.5 months) in the ERCC1-positive group (**Table 6.14B**). This difference was significant ($p<0.001$) (**Table 6.14C**). The significant difference in survival between the groups is easily appreciable in the Kaplan-Meier survival plots for the two groups (**Figure 6.10**).

Table 6.14: Case processing summary (Table 6.14A), median survival estimates (Table 6.14B), and log rank estimates (Table 6.14C) for ERCC1 expression status in the BCON set are tabulated below.

Table 6.14A: The distribution of ERCC1-negative (-) and ERCC1-positive (+) cases is tabulated below.

ERCC1 status	Number	Number of Events	Censored	
			Number	Percent
ERCC1 (-)	106	47	59	55.7%
ERCC1 (+)	111	79	32	28.8%
Overall	217	126	91	41.9%

Table 6.14B: The survival estimates for the ERCC1-negative (-) an ERCC1-positive (+) cases is tabulated below. For the whole cohort (217 patients), the median survival is 40.80 +/- 9.42 months (95% CI: 22.33 to 59.27 months).

Means and Medians for Survival Time								
ERCC1 status	Mean				Median			
	Estimate	Standard Error	95% Confidence Interval		Estimate	Standard Error	95% Confidence Interval	
			Lower Bound	Upper Bound			Lower Bound	Upper Bound
ERCC1 (-)	53.525	3.019	47.608	59.442	72.400	9.613	53.559	91.241
ERCC1 (+)	39.349	3.012	33.446	45.252	27.000	3.839	19.476	34.524
Overall	47.266	2.346	42.668	51.865	40.800	9.423	22.330	59.270

Table 6.14C: The significance (p value) for the above survival estimates (Table 6.10B) is calculated at <0.001 meaning that there is a significant difference in survival between the ERCC1-negative and ERCC1-positive cases (see Figure 6.10).

	Chi-Square	Significance
Log Rank (Mantel-Cox)	13.058	.000

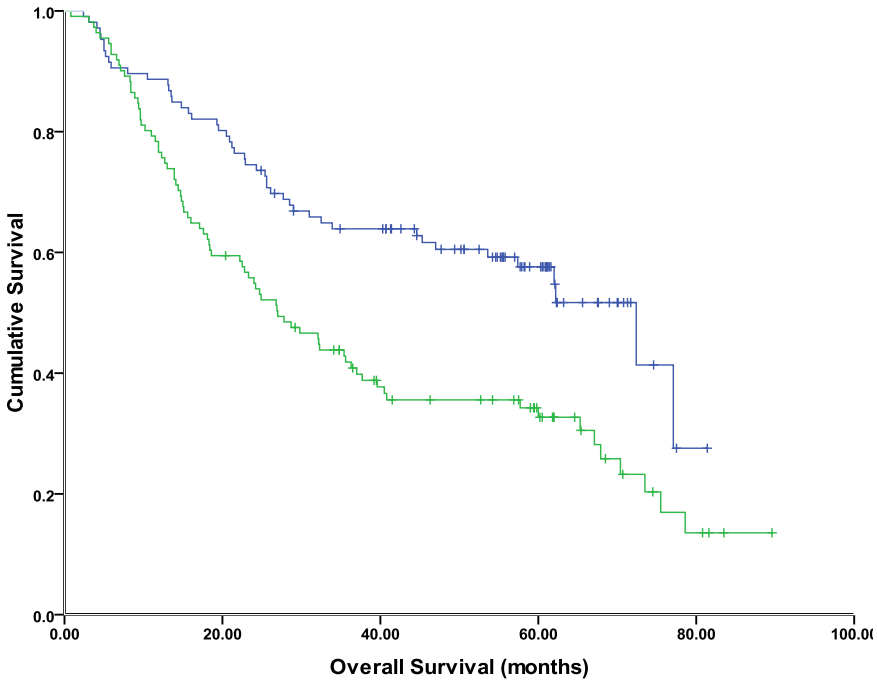

Figure 6.10: Kaplan-Meier plots for ERCC1 staining status on the BCON set: inter-observer. ERCC1-negative (blue) and ERCC1-positive (green) cases demonstrating a greater survival in the ERCC1-negative group.

The observed significant difference in survival between the ERCC1-negative and ERCC1-positive groups was confirmed on univariate analysis (**Table 6.15**). The hazard ratio was 1.93 (95% CI: 1.34 to 2.78) indicating a 2-fold increased risk of death in the ERCC1-positive group relative to the ERCC1-negative group.

Table 6.15: Univariate analysis of ERCC1 expression in the BCON set: inter-observer. demonstrating that the difference in survival between groups is significant ($p<0.001$).

	Variables				
	Standard Error	Significance	Hazard Ratio	95.0% CI for Hazard Ratio	
				Lower	Upper
ERCC1 status	.185	.000	1.931	1.343	2.777

On multivariate analysis, ERCC1 status maintained significance. The hazard ratio was calculated at 1.79 (95% CI: 2.05 to 4.84) indicating an almost 2-fold increased risk of death in the ERCC1-positive group relative to the ERCC1-negative group. The level of significance was $p<0.004$.

Table 6.16: Multivariate analysis for ERCC1 in the BCON set: inter-observer. demonstrating that ERCC1 status retains significance ($p<0.004$) when all other known clinic-pathological factors are input into the model.

Variables in Cox modelling					
	Standard Error	Significance	Hazard Ratio	95.0% CI for Hazard Ratio	
				Lower	Upper
Randomisation	.197	.917	.980	.666	1.442
Tumour Recurrence	.246	.000	10.000	6.178	16.187
Previous Cancer	.255	.053	1.638	.994	2.699
Hb	.197	.455	1.158	.788	1.703
Stage		.394			
Stage 1	.414	.198	1.704	.757	3.836
Stage 2	.464	.665	1.222	.493	3.032
Stage 3	.604	.326	1.810	.554	5.918
TURBT		.833			
TURBT 1	.270	.624	1.142	.672	1.938
TURBT 2	.249	.965	1.011	.620	1.647
Gender	.239	.394	.815	.510	1.304
Age	.013	.005	1.038	1.011	1.066
ERCC1 status	.198	.003	1.790	1.215	2.638

6.4.3 ERCC1: Kappa analyses

Cross tabulations of the scores for the different experiments were performed to evaluate the level of agreement in the scoring between the experiments (**Table 6.17**, **Table 6.19**, **Table 6.21**). As previously described, Kappa scores were calculated to quantitate the level of agreement (**Table 6.18**, **Table 6.20**, **Table 6.22**). The crosstabulation comparisons were as follows: two different experiments (experiments 1 and 2) for the same primary observer 1 (**Table 6.17** and **Table 6.18**); two different observers 1 and 2 (**Table 6.19** and **Table 6.20**); and, two different observers 1 and 3 (**Table 6.21** and **Table 6.22**).

Table 6.17: Kappa analyses - cross-tabulation of ERCC1-positive (+) and ERCC1-negative scores (-) in experiments 1 (Expt 1) and 2 (Expt 2) for the same observer

ERCC1Expt1 and ERCC1Expt2 Scores Cross-tabulation				
		ERCC1Expt2		Total
		(-)	(+)	
ERCC1Expt1	(-)	82	12	94
	(+0	11	112	123
Total		93	124	217

The Kappa value was calculated for the above (**Table 6.17**) scores to measure the intra-observer agreement. There was strong intra-observer agreement as demonstrated by a Kappa value of 0.784 and this was highly significant ($p<0.001$) (**Table 6.18**).

Table 6.18: Cross-tabulation for Kappa value calculation in the intra-observer scores

	Kappa Value	Standard Error	Significance
Measure of Agreement **Kappa**	.784	.043	.000
Number of Cases	217		

When analysing the observations for Observer 1 against Observer 2 (**Table 6.19**), there was good inter-observer agreement as demonstrated by a Kappa value of 0.436 (**Table 6.20**). This was highly significant ($p<0.001$).

Table 6.19: Kappa analyses - cross-tabulation of ERCC1-positive (+) and ERCC1-negative scores (-) in experiments in between different observers (Observer 1-Expt2 and Observer 2).

ERCC1observer2 and ERCC1Expt2 Scores Cross-tabulation			
	ERCC1Expt2		**Total**
	(-)	**(+)**	
ERCC1observer2 (-)	69	37	106
(+)	24	87	111
Total	93	124	217

Table 6.20: Cross-tabulation for Kappa value calculation in the inter-observer (Observer 1-Expt2 and Observer2-Expt2) scores

	Value	Standard Error	Significance
Measure of Agreement **Kappa**	.436	.061	.000
Number of Cases	217		

When analysing the observations for Observer 1 against Observer 3 (**Table 6.21**), there was good inter-observer agreement with a Kappa value of 0.568 (**Table 6.22**). This was highly significant ($p<0.001$).

Table 6.21: Kappa analyses - cross-tabulation of ERCC1-positive (+) and ERCC1-negative scores (-) in experiments in between different observers (Observer 1-Expt 2 and Observer 3).

ERCC1observer2 and ERCC1Expt2 Scores Cross-tabulation Count			
	ERCC1Expt2		**Total**
	(-)	**(+)**	
ERCC1observer3 (-)	71	24	95
(+)	22	100	122
Total	93	124	217

Table 6.22: Cross-tabulation for Kappa value calculation in the inter-observer (Observer 1-Expt2 and Observer3) scores

	Kappa Value	Standard Error	Significance
Measure of Agreement **Kappa**	.568	.056	.000
Number of Cases	217		

6.4.4 ERCC1 may be predictive of outcome in the radical cystectomy set

Interrogation of ERCC1 expression in the BCON set indicated that ERCC1 status was significantly predictive of radiotherapy outcome (**Section 6.3**). In the BCON set, those who were ERCC1-positive were approximately 3-fold more likely to die following radiotherapy than those who were ERCC1-negative. As for AIMP3, ERCC1 expression was interrogated in the Radical Cystectomy set in order to answer the question whether ERCC1 status was simply prognostic of survival in bladder cancer or whether it was truly predictive of radiotherapy outcome.

Survival analyses in the Radical Cystectomy set, stratified by ERCC1 status, demonstrated that there was a difference in outcome. The median survival estimate for those who were ERCC1-positive was 66.0 +/- 13.4 months (95% CI: 39.8 to 92.2 months) compared to 37.0 +/- 9.3 (18.7 to 55.3 months) for those who were ERCC1-negative (**Table 6.23B**). Interestingly, as opposed to ERCC1-negativity conferring survival advantage in the BCON set, the opposite observation was true in the Radical Cystectomy set. However, the difference in survival in the Radical Cystectomy set was just statistically significant with a p value of 0.049 (**Table 6.23C**).

Table 6.23: Case processing summary (Table 6.23A), median survival estimates (Table 6.23B), and log rank estimates (Table 6.24C) for ERCC1 expression status in the Radical Cystectomy set are tabulated below.

Table 6.23A: The distribution of ERCC1-negative (-) and ERCC1-positive (+) cases is tabulated below.

ERCC1 status	Number	Number of Events	Censored	
			Number	Percent
ERCC1 (-)	78	52	26	33.3%
ERCC1 (+)	73	34	39	53.4%
Overall	151	86	65	43.0%

Table 6.23B: The survival estimates for the ERCC1-negative (-) an ERCC1-positive (+) cases is tabulated below. For the whole cohort (151 patients), the median survival is 49.00 +/- 9.92 months (95% CI: 29.56 to 68.44 months).

Means and Medians for Survival Time								
ERCC1 status	Mean				Median			
	Estimate	Standard Error	95% Confidence Interval		Estimate	Standard Error	95% Confidence Interval	
			Lower Bound	Upper Bound			Lower Bound	Upper Bound
ERCC1 (-)	54.075	5.909	42.493	65.658	37.000	9.338	18.698	55.302
ERCC1 (+)	75.216	7.496	60.525	89.907	66.000	13.371	39.792	92.208
Overall	64.583	4.947	54.886	74.280	49.000	9.919	29.559	68.441

Table 6.23C: The significance (p value) for the above survival estimates (Table 6.23B) is calculated at 0.049 meaning that there is no significant difference in survival between the ERCC1-negative and ERCC1-positive cases.

	Chi-Square	Significance
Log Rank (Mantel-Cox)	3.881	.049

The difference in survival between the ERCC1-positive group and the ERCC1-negative group in the Radical Cystectomy set was also evident on the Kaplan-Meier plots (**Figure 6.11**). The difference was narrowly statistically significant (p=0.049) (**Table 6.23C**).

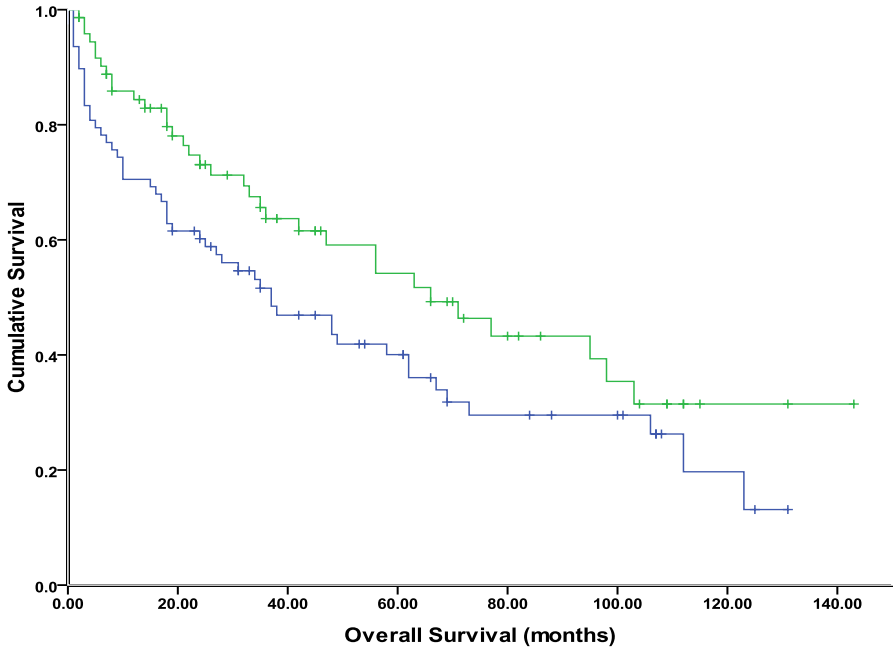

Figure 6.11: Kaplan-Meier plots for ERCC1 staining status on the Radical Cystectomy set. There appears to be better survival in the ERCC1-positive group (green survival plot) than the ERCC1-negative group (blue survival plot).

Univariate and multivariate analyses of ERCC1 status in the Radical Cystectomy set produced marginally conflicting results. On univariate analysis, ERCC1 status narrowly missed statistical significance with a p value of 0.052 (**Table 6.24**). This

calculation was in agreement with the log-rank estimates (p =0.049) (**Table 6.23C**). However, on multivariate analysis, ERCC1 status was found to be statistically significant with a p value of 0.026 (**Table 6.25**). The hazard ratio was 0.60 (95% CI: 0.38 to 0.94) indicating a 40% survival advantage in the ERCC1-positive group relative to the ERCC1-negative group.

Table 6.24: Univariate analysis of ERCC1 expression in the Radical Cystectomy set

Variables in the Equation					
	Standard Error	Significance	Hazard Ratio (HR)	95.0% CI for HR	
				Lower	Upper
ERCC1 status	.221	.052	.651	.423	1.004

Table 6.25: Multivariate analysis of ERCC1 expression in the radical cystectomy set

Variables in the Equation					
	Standard Error	Significance	Hazard Ratio (HR)	95.0% CI for HR	
				Lower	Upper
ERCC1 status	.229	.026	.601	.383	.942
Age	.012	.025	1.026	1.003	1.050
Sex	.295	.081	1.673	.938	2.983
Grade		.991			
Grade 1	.931	.966	1.040	.168	6.452
Grade 2	.832	.982	.982	.192	5.015
Stage		.000			
Stage 1	1.032	.095	5.603	.741	42.365
Stage 2	1.057	.090	6.005	.756	47.681
Stage 3	1.016	.013	12.570	1.715	92.109
Stage 4	1.113	.015	14.989	1.693	132.680
Stage 5	1.033	.001	26.974	3.563	204.205

6.5 p53 expression

p53 immunostaining was performed as described above in the Materials and Methods section. The validated method of using a 10% cut-off as the threshold for assigning p53-positive or p53-negative core was used (Esrig D *et al*, 1994). p53 immunostaining was examined in both the BCON and Radical Cystectomy TMA sets. As expected, p53 immunostaining was exclusively nuclear (**Figure 6.12** and **Figure 6.13**).

6.5.1 p53 expression in the BCON set

Examples of p53 immunostaining in the BCON cores are demonstrated below (**Figure 6.12**).

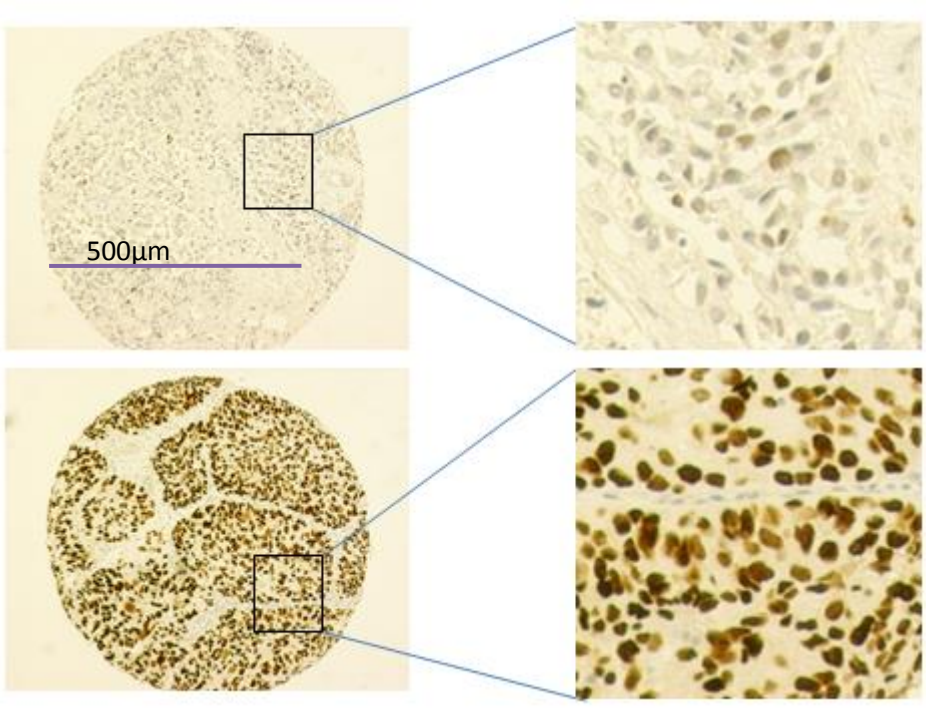

Figure 6.12: p53 immunostaining in the BCON set. Top panel shows p53-negative cores at 10x (Left panel) and 200x (Right panel) magnification. Bottom panel shows a p53-positive core at 10x (Left) and 200x (Right) magnification.

6.5.2 P53 expression in the Radical Cystectomy set

Examples of p53-positive and p53-negative cores in the Radical Cystectomy set are demonstrated below (**Figure 6.13**).

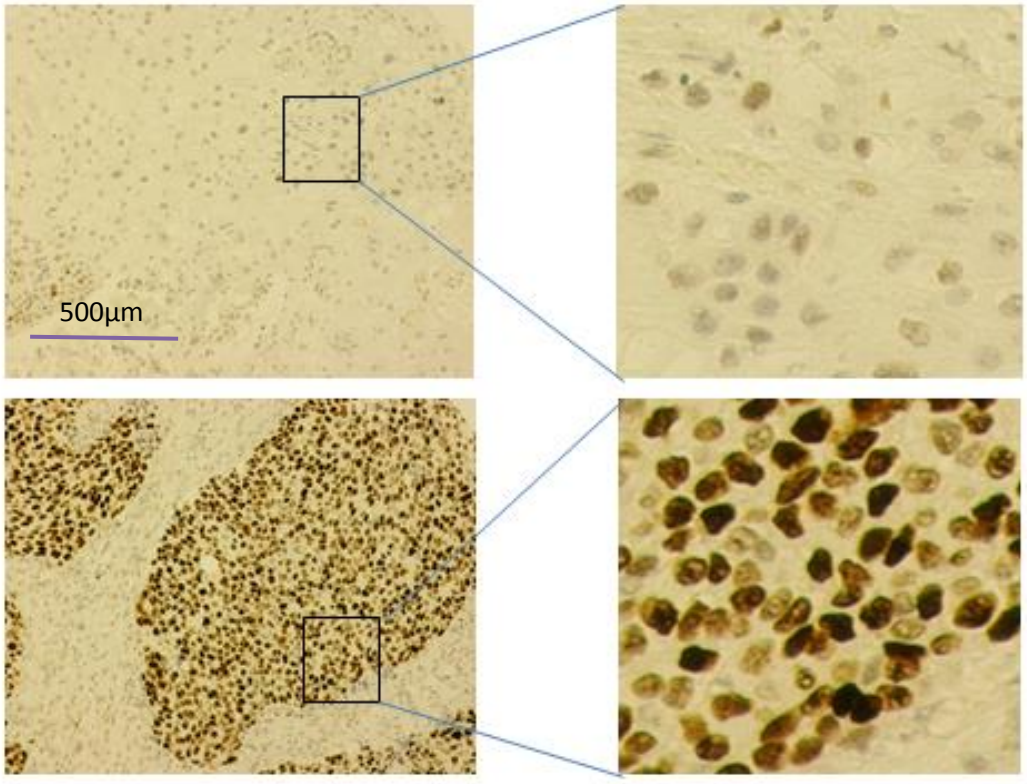

Figure 6.13: p53 immunostaining in the Radical Cystectomy TMA set. Top panel shows p53-negative cores at 10x (Left panel) and 200x (Right panel) magnification. Bottom panel shows a p53-positive core at 10x (Left) and 200x (Right) magnification.

6.5.3 P53 is not predictive of outcome in the BCON set

Survival analyses in the BCON set, stratified by p53 staining status, demonstrated a difference in survival between the p53-positive and p53-negative groups. The median survival estimate for those in the p53-positive group was 47.0 +/- 10.0

months (95% CI: 27.5 to 66.5 months) compared to 26.1 +/- 3.4 months (95% CI: 19.4 to 32.8 months) for those in the p53-negative group (**Table 6.26B**). This difference was appreciable in the Kaplan-Meier plots (**Figure 6.14**). However, the difference was not statistically significant (p=0.103) (**Table 6.26C**).

Table 6.26: Case processing summary (Table 6.26A), median survival estimates (Table 6.26B), and log rank estimates (Table 6.26C) for p53 expression status in the BCON set are tabulated below.

Table 6.26A: The distribution of p53-negative (-) and p53-positive (+) cases is tabulated below.

p53 status	Number	Number of Events	Censored	
			Number	Percent
p53 (-)	63	41	22	34.9%
p53 (+)	154	85	69	44.8%
Overall	217	126	91	41.9%

Table 6.26B: The survival estimates for the p53-negative (-) and p53-positive (+) cases are tabulated below. For the whole cohort (217 patients), the median survival is 40.80 +/- 9.42 months (95% CI: 22.33 to 59.27 months).

Means and Medians for Survival Time								
p53 status	Mean				Median			
	Estimate	Standard Error	95% Confidence Interval		Estimate	Standard Error	95% Confidence Interval	
			Lower Bound	Upper Bound			Lower Bound	Upper Bound
p53 (-)	40.352	3.802	32.900	47.804	26.100	3.401	19.434	32.766
p53 (+)	49.680	2.815	44.161	55.198	47.000	9.966	27.467	66.533
Overall	47.266	2.346	42.668	51.865	40.800	9.423	22.330	59.270

Table 6.26C: The significance (p value) for the above survival estimates (Table 6.25B) is calculated at 0.103 meaning that there is no significant difference in survival between the p53-negative and p53-positive cases.

	Chi-Square	Significance
Log Rank (Mantel-Cox)	2.664	.103

The suggestion of a difference in survival between the p53-positive and p53-negative groups in the BCON set was appreciable in the Kaplan-Meier plots (**Figure 6.14**). However, the difference missed statistical significance with a p value of 0.103 (**Table 6.26C**).

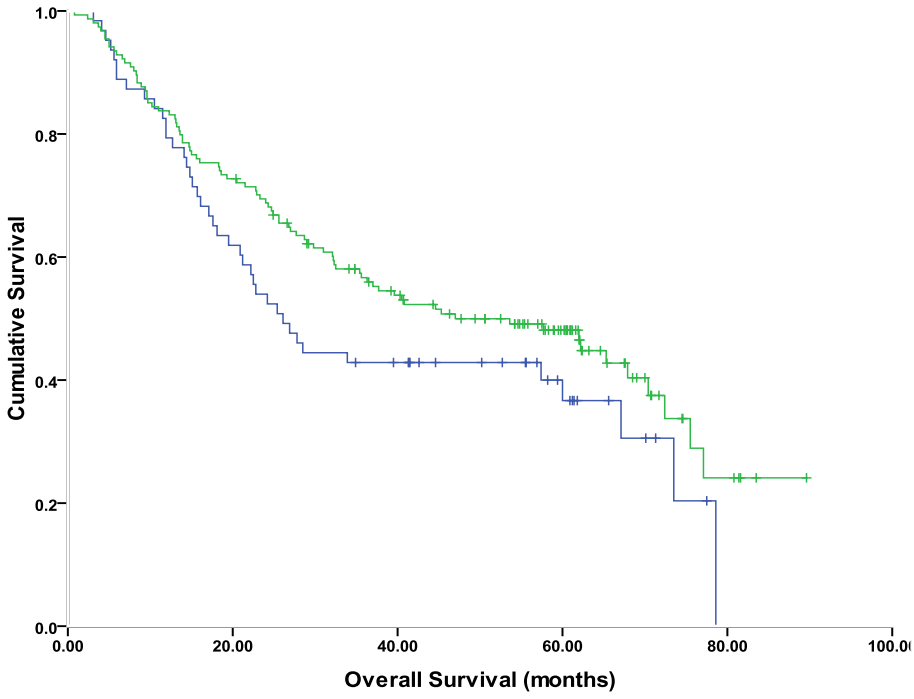

Figure 6.14: Kaplan-Meier plots for p53 staining status in the BCON set. Survival appears to be greater in the p53-positive group (green survival plot) compared to the p53-negative group (blue survival plot).

The absence of a statistically significant difference in survival between the p53-positive and p53-negative groups in the BCON set was confirmed by univariate analysis (**Table 6.27**). The hazard ratio was 0.73 (95% CI: 0.51 to 1.1) and the p value for this was 0.104.

Table 6.27: Univariate analysis of p53 expression in the BCON set

Variables					
	Standard Error	Significance	Hazard Ratio (HR)	95.0% CI for Hazard Ratio	
				Lower	Upper
p53 status	.191	.104	.734	.505	1.066

6.5.4 P53 expression by the median H score method in the BCON set

As there was a suggestion of a small difference in outcomes between the p53-positive and p53-negative, an alternative analysis of staining status was performed using the median H score method, as for AIMP3 and ERCC1 (**Table 6.28**). By this method, survival outcomes between the groups were also not significantly different. The estimated median survival in the p53-negative group was 37.7 +/- 13.1 months (95% CI: 12.0 to 63.4 months) compared to 44.6 +/- 10.1 months (95% CI: 24.9 to 64.3 months) in the p53-positive group (**Table 6.28B**). There was no difference in survival between the groups (p=0.775) (**Table 6.28C**). In fact, the size effect of the difference in survival between the groups was far less pronounced for the median H score method; in other words, there was less difference between the groups when the H score method was used.

Table 6.28: Case-processing summary (Table 6.28A), survival estimates (Table 6.28B), and log rank estimates (Table 6.28C) for p53 immunostaining status, as per the median H score method, in the BCON set.

Table 6.28A: The distribution of p53-negative (-) and p53-positive (+) cases is tabulated below.

p53 status	Number	Number of Events	Censored	
			Number	Percent
p53 (-)	129	77	52	40.3%
p53 (+)	88	49	39	44.3%
Overall	217	126	91	41.9%

Table 6.28B: The survival estimates for the p53-negative (-) and p53-positive (+) cases are tabulated below. For the whole cohort (217 patients), the median survival is 40.80 +/- 9.42 months (95% CI: 22.33 to 59.27 months).

Means and Medians for Survival Time								
p53 status	Mean				Median			
	Estimate	Standard Error	95% Confidence Interval		Estimate	Standard Error	95% Confidence Interval	
			Lower Bound	Upper Bound			Lower Bound	Upper Bound
p53 (-)	46.159	2.952	40.373	51.946	37.700	13.104	12.017	63.383
p53 (+)	47.248	3.467	40.452	54.044	44.600	10.072	24.859	64.341
Overall	47.266	2.346	42.668	51.865	40.800	9.423	22.330	59.270

Table 6.28C: The significance (p value) for the above survival estimates (Table 6.28B) is calculated at 0.775 meaning that there is no significant difference in survival between the p53-negative and p53-positive cases.

	Chi-Square	Significance
Log Rank (Mantel-Cox)	.082	.775

The absence of difference in the survival outcomes between the p53-positive and p53-negative groups in the BCON set, analysed by the median H score method, was appreciable in the Kaplan-Meier plots for the two groups (**Figure 6.15**).

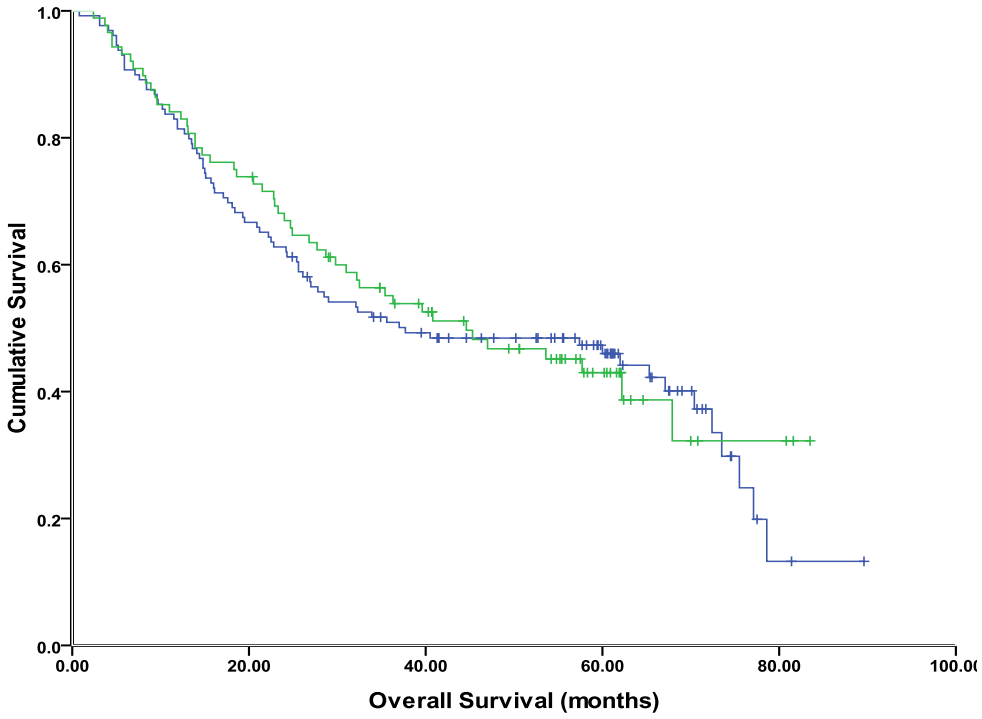

Figure 6.15: Kaplan-Meier plots for p53 staining status, by the median H score method, in the BCON set.

Univariate analysis confirmed the observed lack of difference between the groups. The hazard ratio was 0.95 (95% CI: 0.66 to 1.36) with a p value of 0.775 (**Table 6.29**).

Table 6.29: Univariate analysis of p53 expression, by the median H score method, in the BCON set

Variables					
	Standard Error	Significance	Hazard Ratio (HR)	95.0% CI for Hazard Ratio	
				Lower	Upper
p53 status	.183	.775	.949	.662	1.360

6.5.5 p53 expression in the radical cystectomy set

In order to evaluate the prognostic value of p53 staining status, the Radical Cystectomy set was interrogated (**Table 6.30**). There was a difference in the survival outcomes between the p53-positive and p53-negative groups in this set. The estimated median survival for the p53-negative group was 62.0 +/- 12.2 months (95% CI: 31.1 to 86.0 months) compared to 37.0 +/- 7.6 months (95% CI: 22.1 to 51.9 months) for the p53-positive group (**Table 6.30B**). However, the difference in survival was not statistically significant (**Table 6.30C**).

Table 6.30: Case-processing summary (Table 6.30A), survival estimates (Table 6.30B), and log rank estimates (Table 6.30C) for p53 immunostaining status in the Radical Cystectomy set

Table 6.30A: The distribution of p53-negative (-) and p53-positive (+) cases is tabulated below.

p53 status	Number	Number of Events	Censored	
			Number	Percent
P53 (-)	73	36	37	50.7%
P53 (+)	77	49	28	36.4%
Overall	150	85	65	43.3%

Table 6.30B: The survival estimates for the p53-negative (-) and p53-positive (+) cases are tabulated below. For the whole cohort (150 patients), the median survival is 56.00 +/- 10.43 months (95% CI: 35.55 to 76.45 months).

Means and Medians for Survival Time								
p53 status	Mean				Median			
	Estimate	Standard Error	95% Confidence Interval		Estimate	Standard Error	95% Confidence Interval	
			Lower Bound	Upper Bound			Lower Bound	Upper Bound
p53 (-)	69.448	6.717	56.283	82.613	62.000	12.221	38.047	85.953
p53 (+)	57.199	6.414	44.628	69.769	37.000	7.584	22.136	51.864
Overall	64.987	4.964	55.256	74.717	56.000	10.432	35.554	76.446

Table 6.30C: The significance (p value) for the above survival estimates (Table 6.29B) is calculated at 0.148 meaning that there is no significant difference in survival between the p53-negative and p53-positive cases.

	Chi-Square	Significance
Log Rank (Mantel-Cox)	2.093	.148

The difference in survival between the p53-negative and p53-positive groups on the Radical Cystectomy set, suggested by the median estimates (**Table 6.30B**), was appreciable on the Kaplan-Meier plots for the groups (**Figure 6.16**). However, the difference was not statistically significant (p=0.148) (**Table 6.30C**).

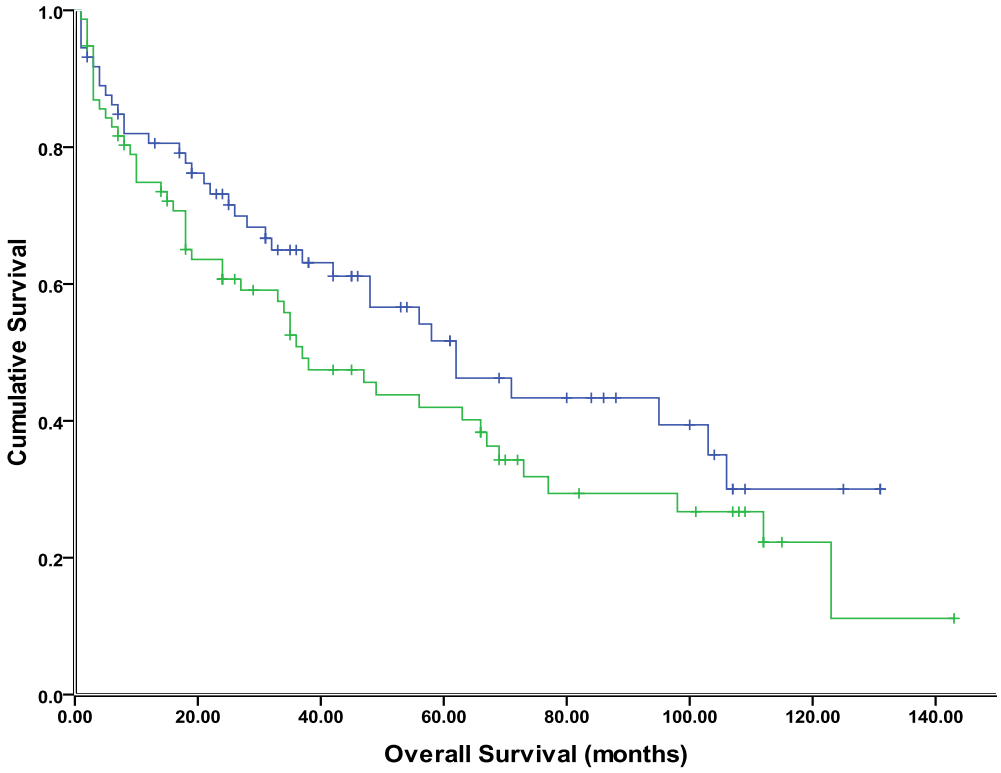

Figure 6.16: Kaplan-Meier plots for p53 staining status in the Radical Cystectomy set. Those in the p53-neagtive group (blue survival plot) appear to have greater survival compared to those in the p53-positive group (green survival plot).

The absence of a significant difference in survival outcomes between the p53-negative and p53-positive groups was confirmed on univariate analysis. The hazard ratio was 1.37 (95% CI: 0.89 to 2.11) with a p value of 0.152 (**Table 6.31**).

Table 6.31: Univariate analysis of p53 expression in the Radical Cystectomy set

Variables					
	Standard Error	Significance	Hazard Ratio	95.0% CI for Hazard Ratio	
				Lower	Upper
p53 status	.220	.152	1.370	.890	2.109

6.6 Discussion of results

The main objectives of the work outlined in this chapter were to evaluate the predictive or prognostic value of Mre11, ERCC1 and p53. Therefore, these markers were interrogated on both the BCON radiotherapy set as well as the Radical Cystectomy set.

Firstly, interrogation of Mre11status on the BCON set intially appeared to be significant. In the BCON set, those in the Mre11-positive group had a greater survival compared to those in the Mre11-negative group. This was observed on the Kaplan-Meier median survival estimates as well as on univariate anlysis with the level of significance calculated at p=0.03. This finding was in agreement with the findings of Choudhury *et al* where Mre11 status was found to be significantly predictive of radiotherapy outcome. Furthermore, in agreement with the findings of Choudhury *et al*, Mre11-positive patients were found to have greater survival relative to those in the Mre11-negative group. However, on multivariate analysis of the BCON set, the difference in survival outcomes between the two groups was not found to be significant (p=0.37). It is noteworthy that the levels of significance (p values), for the findings of Choudhury *et al*, were p=0.01 and p=0.02 for their test and validation sets, respectively. When the findings of this chapter are analysed in the context of the findings of Choudhury *et al*, one of the conclusions that may be drawn is that Mre11 is indeed a predictive marker of radiotherapy outcome. However, the clinico-pathological demographics of the BCON set, being a clinical trial set, may be slightly different to the Choudhury *et al* radiotherapy series, and this may have led to the loss of significance on multivariate analysis of Mre11 in the

BCON set when all the clinico-pathologic variables were input into the model for proportional hazards modelling. It is unlikely that the loss of significance is due to an inadequate sample size in the BCON set, with 217 patients, given that the Choudhury *et al* series had 86 and 93 patients each in their test and validation radiotherapy sets, respectively.

It was important to pose the question whether the immunoscoring methodology used may have influenced the outcomes; in other words, a potential significance was lost due to the 25^{th} percentile cutoff method used as per Choudhury *et al*. Therefore, additional analyses were peformed for Mre11 using the median H score method as for AIMP3 previously. However, the difference in survival between the groups was even less pronounced when using the median H score method lending credence to the validity of Choudhury *et al*'s 25^{th} percentile method to optimally assign patients into the Mre11-positive and Mre11-negative groups.

Next, Mre11 status was interrogated on the Radical Cystectomy set in order to evaluate whether Mre11 was a prognostic factor for survival in patients with bladder cancer. Interestingly, Mre11 status narrowly missed significance, on both Kaplan-Meier estimates ($p=0.06$) and univariate anlysis ($p=0.07$), in terms of differentiating a survival difference between the groups. Furthermore, as opposed to a greater survival in the Mre11-positive group in the BCON set, the converse was found to be the case in the Radical Cystectomy set. In other words, those in the Mre11-negative group, in the Radical Cystectomy set, had an improved survival. These observations narrowly missed significance and therefore, strong conclusions cannot be drawn

from them. However, it is noteworthy that this finding, of Mre11-negativity conferring improved survival in the Radical Cystectomy set, was in agreement with *Choudhury et al*'s finding in their study. Although not supported by statistically significant findings in the present study, there is a suggestion that Mre11 is a predictive marker of radiotherapy outcome and that it is not prognostic of survival in those with bladder cancer.

Next, ERCC1 status was interrogated in the BCON set. The findings suggested that ERCC1-negativity conferred a highly significant survival advantage in the BCON set. Those in the ERCC1-positive group had an approximately 3-fold increased risk of death compared to those in the ERCC1-negative group. The findings were highly significant ($p<0.001$). The significance was maintained on multivariate analyses. The experiments were repeated for the same observer and compared with the scoring pattern of different observers. The agreements in the scorings in between the same observer and different observers were also evaluated to ensure strong concordance in the measurements. The level of significance was maintained for the survival analyses arising from the different observations for ERCC1 in the BCON set. There were two obvious findings with respect to ERCC1 when compared to the findings of AIMP3 in the BCON set. Firstly, ERCC1 was a stronger predictor of survival outcome than AIMP3. This was based on the size effect of the findings. Whereas for AIMP3, the survival advantage was approximately 47% (0.47) for one group relative to another, this was approximately 300% (3-fold) for ERCC1. However, both findings were highly significant ($p<0.001$ for both). Secondly, as opposed to AIMP3, where AIMP3-positivity conferred a survival advantage, the converse was true for ERCC1. In the case of ERCC1, ERCC1-negativity conferred a survival

advantage. This finding was in agreement with validated reports from a large, multi-national, randomised controlled trial confirming that ERCC1-negativity confers a survival advantage (Olaussen KA *et al*, 2006). The findngs of Olaussen *et al* were in the context of lung cancer and the expanation provided for this observation was that tumours with reduced levels of ERCC1 were likely to have reduced capacity for repair of DNA damage leading in turn to reduced likelihood of survival of the tumours. Consequently, this would result in better survival outcomes for the patients with the tumours. Conversely, tumours with higher expression of ERCC1 (ERCC1-positive) would have the capacity to repair DNA damage and survive thereby leading to poor survival outcome for the patients with such tumours. The predictive value of ERCC1 in the context of radical radiotherapy for bladder cancer has not yet been reported. However, Kawashima *et al* have reported that ERCC1 may predict the efficacy of chemoradiation therapy for muscle-invasive bladder cancer (Kawashima A *et al*, 2011). The conclusions of Kawashima *et al* were based mainly on the basis of their *in vitro* assays interrogating siRNA knock-down of ERCC1 in bladder cancer cell lines; however, they did interrogate ERCC1 staining status on a small clinical set of 22 patients with organ-confined MIBC and found that ERCC1-negativity was likely to confer a survival advantage.

When ERCC1 was interrogated on the Radical Cystectomy set, some intriguing findings were observed. Firstly, survival analyses appreared to indicate that ERCC1-positivity conferred a survival advantage (**Table 6.23**). This was appreciable on the Kaplan-Meier plots for the two groups (**Figure 6.11**). However, the log rank estimates (p=0.049) and univariate analysis (p=0.052) seemed to indicate that the difference in survival observed was not statistically significant.

However, on multivariate analysis, ERCC1 status was found to retain statistical significance with a p value of 0.026 (**Table 6.23**). The hazard ratio was 0.60 (95% CI: 0.38 to 0.94) indicating that not only was the difference significant but that there was a 40% survival advantage in the ERCC1-positive group relative to the ERCC1-negative group. The observation that ERCC1-positivity, rather than ERCC1-negativity, conferred survival advantage in the Radical Cystectomy set suggests that ERCC1 is truly predictive of radiotherapy outcome rather than just being a prognostic marker of survival outcome in MIBC. If ERCC1-negativity, as in the BCON set, had instead been found to have conferred survival advantage in the Radical Cystectomy set, it might have suggested that ERCC1 was only a prognostic factor of survival in MIBC.

Survival analyses for p53 status in the BCON and Radical Cystectomy sets did not reveal any statistically significant findings. In the BCON set, there was a non-significant survival advantage in favour of the p53-positive group (p=0.103 and p=0.104 on log rank estimates and univariate analysis, respectively). Additional survival analyses, by using the median H score method, did not demonstrate any statistically significant results (p=0.775). In the Radical Cystectomy set, there was a non-significant survival advantage in favour of the p53-negative group (p=0.148). As the findings in both the BCON and Radical Cystectomy sets were clearly statistically non-significant, it would be reasonable to conclude that p53 is neither predictive of radiotherapy outcome nor prognostic of survival in bladder cancer.

Chapter 7

Combinational modelling of AIMP3 and ERCC1 stratifies patients into groups with differential responses to radiotherapy

7.1 Introduction to Chapter 7

The previous chapters demonstrated that, amongst the molecular markers tested on the BCON and Radical Cystectomy sets, AIMP3 and ERCC1 predicted response to radiotherapy. This was true of AIMP3 and ERCC1 when analysed separately by the Kaplan-Meier method and by univariate analysis or when analysed by multivariate analysis with the other clinic-pathological variables. Mre11 was also predictive of radiotherapy outcome in the BCON set on Kaplan-Meier and univariate analysis but the statistical significance was marginal and was lost on multivariate analysis.

The primary objective of this chapter was to identify whether a combination of the four markers could be used to improve the prediction of response to radiotherapy. In order to explore this, the markers were input into a Cox proportional hazards combinational model in a step-wise fashion. Step-wise entry into the model was interrogated by both the "forward" as well as "backward" methods where variables were either added into the model in the case of "forward" or removed step-wise from a combination of all variables in a "backward" manner, respectively. The consistent finding was that only AIMP3 and ERCC1, in combination, improved prediction with statistical significance. In other words, any combinational permutation which included Mre11 or p53 was found not to yield statistically significant outcomes when applied on the BCON set to interrogate survival outcomes.

7.2 AIMP3 and ERCC1 combination

When AIMP3 and ERCC1 were combined, four possible permutations were obtained: (1) AIMP3-positive and ERCC1-negative (AIMP3+ERCC1-); (2) AIMP3-negative and ERCC1-positive (AIMP3-ERCC1+); (3) AIMP3-positive and ERCC1-positive (AIMP3+ERCC1+); and, (4) AIMP3-negative and ERCC1-positive (AIMP3-ERCC1+) (**Table 7.1A**). Of these permutations, based on the findings of the previous chapters, the combination that would be expected to confer the highest survival advantage in the BCON set would be AIMP3+ERCC1- and that which would be expected to confer the lowest survival advantage would be AIMP3-ERCC1+, respectively. In terms of survival advantage, the sequence of combinations expected to predict survival, from highest survival to lowest, would be expected to be (1), (2), (3) and (4), respectively.

7.2.1 Log rank and Kaplan-Meier estimates

As hypothesised, the estimates of the median survival for the four combinations were in the sequence (1), (2), (3) and (4), respectively, where (1) had the highest median survival at 77.1 +/- 5.3 months (95% CI: 66.7 to 87.5 months) and (4) had the lowest median survival at 13.5 +/- 1.5 months (95% CI: 10.5 to 16.5 months) (**Table 7.1B**). The estimated median survival for combination (2) was 62.2 +/- 7.5 months (95% CI: 47.4 to 77.0 months) and that for combination (3) was 40.5 +/- 13.0 months (95% CI: 15.1 to 66.0 months). The differences between the groups was significant on the log rank estimates ($p<0.001$) (**Table 7.1C**).

Table 7.1: Case-processing summary (Table 7.1A), survival estimates (Table 7.1B), and log rank estimates (Table 7.1C) for AIMP3 and ERCC1 combinations in the BCON set

Table 7.1A: The distribution of AIMP3+ERCC1- (1), AIMP3-ERCC1- (2), AIMP3+ERCC1+ (3) and AIMP3-ERCC1+ (4) cases is tabulated below.

AIMP3 and ERCC1 status	Number	Number of Events	Censored	
			Number	Percent
1 (AIMP3+ERCC1-)	51	16	35	68.6%
2 (AIMP3-ERCC1-)	42	18	24	57.1%
3 (AIMP3+ERCC1+)	60	38	22	36.7%
4 (AIMP3-ERCC1+)	64	54	10	15.6%
Overall	217	126	91	41.9%

Table 7.1B: The survival estimates for the AIMP3-ERCC1 combinations are tabulated below. For the whole cohort (217 patients), the median survival is 40.80 +/- 9.42 months (95% CI: 22.33 to 59.27 months)

Means and Medians for Survival Time								
AIMP3 and ERCC1 status	Mean				Median			
	Estimate	Standard Error	95% Confidence Interval		Estimate	Standard Error	95% Confidence Interval	
			Lower Bound	Upper Bound			Lower Bound	Upper Bound
1	69.637	4.040	61.720	77.555	77.100	5.322	66.670	87.530
2	52.908	4.280	44.519	61.297	62.200	7.535	47.430	76.970
3	46.743	3.706	39.479	54.006	40.500	12.965	15.089	65.911
4	22.473	2.924	16.741	28.205	13.500	1.511	10.538	16.462
Overall	47.266	2.346	42.668	51.865	40.800	9.423	22.330	59.270

Table 7.1C: The significance (p value) for the above survival estimates (Table 7.1B) is calculated at $p<0.001$ meaning that there is a significant difference in survival between the AIMP3 and ERCC1 combination of cases (see Figure 7.1).

	Chi-Square	Significance
Log Rank (Mantel-Cox)	78.554	.000

The difference in survival outcomes between the four combinations was appreciable on the Kaplan-Meier plots (**Figure 7.1**). Combination (1), depicted by the blue survival plot, had the highest survival followed by combination (2), depicted by the green survival plot, and then combination (3), depicted by the light-yellow survival plot. Combination (4), depicted by the purple survival plot, had the lowest survival.

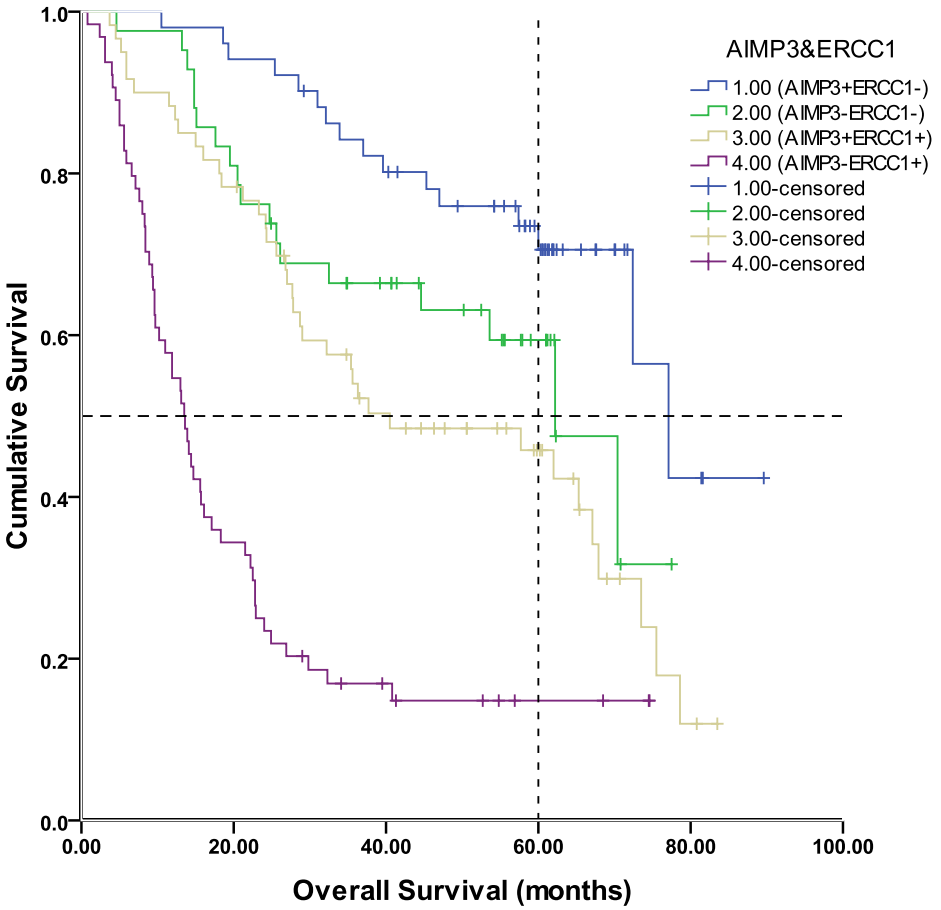

Figure 7.1: Kaplan-Meier plots for the AIMP3 and ERCC1 combinations in the BCON set. Combination (1) is AIMP3+ERCC1- depicted in blue. Combination (2) is AIMP3-ERCC1- depicted in green. Combination (3) is AIMP3+ERCC1+ depicted in light-yellow. Combination (4) is AIMP3-ERCC1+ depicted in purple. Horizontal perforated line represents the median survival (50% cumulative survival) cut-off. Vertical perforated line represents the 5-year (60 months) overall survival cut-off.

The above Kaplan-Meier plot was analysed in Life Table format to ascertain the exact proportion of patients, in each combination, surviving at designated time intervals (**Table 7.2**). For instance, at 12 months, 98% of patients in the combinations (1) and (2) were still alive compared to 88% and 55% of patients in the combinations (3) and (4), respectively. In other words, 45% of patients had

already died within one year in the worst prognostic combination (AIMP3-ERCC1+) compared to only 2% of patients in the best prognostic combination (AIMP3+ERCC1-). Similarly, when looking at the 3-year (36 months) time interval, the cumulative survival was only 15% (i.e. 85% dead) in the worst prognostic combination (AIMP3-ERCC1+) compared to 76% cumulative survival (i.e. 24% dead) in the best prognostic combination (AIMP3+ERCC1-). Likewise, when looking at the 5-year (60 months) time interval, the cumulative survival was 15% in the worst prognostic combination (AIMP3-ERCC1+) compared to 69% cumulative survival (i.e. 31% dead) in the best prognostic combination (AIMP3-ERCC1+). When comparing the best (AIMP3+ERCC1-) and worst (AIMP3-ERCC1+) prognostic groups, it was notable that, from both the Kaplan-Meier plots (**Figure 7.1**) as well as the Life Table (**Table 7.2**), the median survival in the best prognostic group (AIMP3+ERCC1-) was more than 5 years whereas it was less than 2 years in the worst prognostic group (AIMP3-ERCC1+).

Table 7.2: Life table tabulation of the cumulative proportion of cases surviving at the end of each designated interval for the AIMP3-ERCC1 combinations in the BCON set. (1) AIMP3+ERCC1- (2) AIMP3-ERCC1- (3) AIMP3+ERCC1+ (4) AIMP3-ERCC1+

Life Table									
Statistics = Cumulative Proportion Surviving at End of Interval									
First-order Controls		**Interval Start Time (months)**							
		0	**12**	**24**	**36**	**48**	**60**	**72**	**84**
AIMP3 and ERCC1 status	**PN (1)**	.98	.94	.84	.76	.74	.69	.34	.34
	NN (2)	.98	.76	.66	.63	.59	.41	.41	
	PP (3)	.88	.75	.54	.48	.46	.30	.08	
	NP (4)	.55	.25	.17	.15	.15	.15	.15	

7.2.2 Multivariate analysis

When the four combinations were analysed in combination with all the known clinic-pathologic variables, there were statistically significant survival differences between the groups (**Table 7.3**). When group (1) (AIMP3+ERCC1-) was compared to group (4) (AIMP3-ERCC1+), there was an approximate 6-fold difference in survival. The hazard ratio for this comparison was 6.10 (95% CI: 3.27 to 11.29) indicating a 6.1-fold increased risk of death in group (4) (AIMP3-ERCC1+) compared to group (1) (AIMP3+ERCC1-). This was statistically highly significant ($p<0.001$). When group (1) (AIMP3+ERCC1-) was compared to group (3) (AIMP3+ERCC1+), there was an approximate 3-fold difference in survival. The hazard ratio for the comparison was 3.05 (95% CI: 1.62 to 5.75) indicating a 3.1-fold increased risk of death in group (3) (AIMP3+ERCC1+) relative to group (1) (AIMP3+ERCC1-). This comparison was also highly significant ($p<0.002$). However, there was no statistically significant difference when comparing the survival outcomes between group (1) (AIMP3+ERCC1-) and group (2) (AIMP3-ERCC1-). The hazard ratio for this comparison was 1.85 (95% CI: 0.90 to 3.81) and this was not significant ($p=0.095$). Although direct comparisons between group (2) (AIMP3-ERCC1-) and group (3) (AIMP3+ERCC1+) could not be made on this modelling, the 95% confidence intervals for both hazard ratios overlapped; therefore, it was likely that the survival differences between the two groups was unlikely to be significant.

Table 7.3: Multivariate analysis of AIMP3-ERCC1 combinations in the BCON set. For AIMP3-ERCC1combinations: (1) AIMP3+ERCC1-, (2) AIMP3-ERCC1-, (3) AIMP3+ERCC1+, (4) AIMP3-ERCC1+

Variables					
	Standard Error	Significance	Hazard Ratio (HR)	95.0% CI for Hazard Ratio	
				Lower	Upper
Randomisation	.196	.796	1.052	.716	1.546
Tumour Recurrence	.261	.000	.105	.063	.175
Previous Cancer	.251	.045	.605	.370	.989
Hb	.195	.779	.947	.646	1.387
Stage		.536			
Stage 1	.600	.367	.582	.180	1.885
Stage 2	.469	.939	1.037	.413	2.601
Stage 3	.517	.785	.868	.315	2.390
TURBT		.707			
TURBT complete	.251	.744	1.085	.664	1.774
TURBT partial	.233	.405	1.214	.769	1.917
Gender	.243	.542	1.160	.720	1.869
Age	.014	.023	1.032	1.004	1.060
(1) AIMP3+ERCC1-		.000			
(2) AIMP3-ERCC1-	.368	.095	1.850	.899	3.807
(3) AIMP+ERCC1-	.323	.001	3.052	1.621	5.745
(4) AIMP3-ERCC1+	.319	.000	6.095	3.262	11.391

7.3 Discussion of results

In this chapter, step-wise modelling of the markers demonstrated AIMP3 and ERCC1 to be a compatible combination in order to discriminate radiotherapy outcome in the BCON set. Mre11 and p53 were rejected from the combinational modelling as any permutation with their presence did not yield statistical significance to allow discrimination in survival outcomes. In the panel of the four markers tested, ERCC1 was the strongest, in terms of predicting radiotherapy outcome in the BCON set, followed by AIMP3, Mre11 and p53. p53 was not significant and Mre11 was significant but narrowly missed significance on multivariate analysis. Ideally, a molecular selection panel would comprise of a number of markers, rather than just two (here, AIMP3 and ERCC1), so that the discriminatory power of any cases selected through such a panel would be greater. One of the limitations of the current study was that more markers were not evaluated on the BCON set. However, the panel used in this study comprised of AIMP3, which had a sound in vitro basis from the initial work conducted in the study, as well as ERCC1, Mre11 and p53 which have been recently reported in the literature as having predictive value in the context of radiotherapy outcome in bladder cancer. Other markers, reported as predictors of radiotherapy outcomes, albeit in other cancers, could have been explored but that was beyond the scope of the current project due to limitations of time and resources.

Allowing for the above points, what was noteworthy from the findings of this chapter was that a dual marker panel, comprising ERCC1 and AIMP3, was able to segregate the BCON set into four prognostic sub-groups such that there were

significant differences in the radiotherapy survival outcomes between the groups. The best prognostic group (AIMP3+ERCC1-) had an approximate 6-fold reduced risk of death following radiotherapy compared to the worst prognostic group (AIMP3-ERCC1+). The second-best prognostic group (AIMP3-ERCC1-) had an approximate 3-fold reduced risk of death following radiotherapy compared to the worst prognostic group (AIMP3-ERCC1+). These findings were statistically highly significant ($p<0.001$ and $p<0.002$, respectively). Looking at the actual estimates of survival duration, rather than the odds of survival described above, the median survival of the best prognostic group (AIMP3+ERCC1-) was approximately 77 months. This compared to 62 months in the second-best prognostic group (AIMP3-ERCC1-) and only 14 months in the worst prognostic group (AIMP3-ERCC1+). In other words, patients in the best prognostic group would be expected to live over 5 years longer than those in the worst prognostic group. These findings suggest that the dual panel of AIMP3 and ERCC1 is sufficiently discriminatory in selecting patients into good or poor radiotherapy outcome groups in the BCON set.

Chapter 8

AIMP3 expression predicts response to cisplatin-exposure *in vitro* but AIMP3 and ERCC1 are not predictive of cisplatin-based chemotherapy outcome in the Neoadjuvant chemotherapy or the LaMB trial chemotherapy sets

8.1 Introduction to Chapter 8

In Chapter 3, the functional impact of downregulation of AIMP3, through siRNA transfection, on radiation exposure outcome was explored. In the panel of bladder cancer cells used (T24, 253J, RT112 and RT4; including HeLa as control), siRNA knockdown of AIMP3 resulted in an increase in the clonogenic survival following respective IC50 doses of irradiation of the cell lines. The findings led to the hypothesis that AIMP3 expression status may be predictive of survival outcome in patients who had been treated with radical radiotherapy for bladder cancer. This hypothesis was tested in the preceding chapters with the conclusion that, in the BCON set, AIMP3 and ERCC1 were significant predictors of survival.

As discussed in the introductory chapter (**Chapter 1, section 1.5**), radical radiotherapy and radical cystectomy are the established curative treatment modalities for organ-confined muscle-invasive bladder cancer (MIBC). Systemic chemotherapy alone cannot offer cure. However, cisplatin-based chemotherapy, in the neoadjuvant setting, is increasingly being offered to patients with MIBC, prior to radical treatment (with either surgery or radiotherapy), as there is an improvement in survival. In addition, organ-preservation strategies such as multi-modality treatment, that incorporate cisplatin-based systemic chemotherapy concurrently with radical radiotherapy, are also gaining popularity. Furthermore, cisplatin-based systemic chemotherapy is the mainstay of management of metastatic bladder cancer where disease control and improved progression-free survival are the aims. However, not all patients respond well to cisplatin. Any biomarker which could

help select patients who are likely to respond to cisplatin treatment would help stratify patients into treatment algorithms.

The primary objective of this chapter was to investigate whether downregulation of AIMP3 expression, by siRNA transfection, would influence cisplatin sensitivity in bladder cancer cell lines. Cisplatin causes DNA damage by forming cisplatin-DNA adducts and, AIMP3, by virtue of its role in the DNA damage response pathway, can be hypothesised to mediate response to this. The bladder cancer cell lines used were RT112 and RT112CP (**Table 2.1**). As described previously (**Chapter 2, section 2.1**), RT112CP is a cisplatin-resistant subline of RT112. They were chosen as a panel to represent a spectrum of cisplatin-sensitive and cisplatin-resistant bladder cancer cell lines. The methodology used, to investigate the primary objective of whether AIMP3 downregulation would influence cisplatin-response, was similar to the one used to investigate radiotherapy response (**Chapter 3**). Firstly, the respective IC50 doses for RT112 and RT112CP were calculated by profiling their dose-response characteristics to cisplatin exposure. Then, their respective clonogenic survivals, with or without (control with scrambled siRNA) siRNA knockdown of AIMP3, were measured following IC50 dose exposure to cisplatin. With controls for cisplatin exposure (transfection media without cisplatin), the differences in survival outcomes, by colony forming assays, were measured.

The secondary objective of this chapter was to investigate the predictive value of AIMP3 and ERCC1 expression status on survival outcomes in the Neoadjuvant and LaMB sets. As described previously (**Chapter 2, sections 2.10 and 2.11**), the

Neoadjuvant and LaMB sets were collated to provide platforms, of patients treated with cisplatin-based systemic chemotherapy for bladder cancer, for analyses of clinical outcomes. In the Neoadjuvant set, patients with organ-confined MIBC were administered cisplatin-based chemotherapy in the neoadjuvant setting. In the LaMB set, patients with metastatic bladder cancer were administered cisplatin-based chemotherapy as a palliative measure in a trial setting. As for the BCON and Radical Cystectomy sets, the methodology used was to stratify the clinical sets by AIMP3 and ERCC1 immunostaining status and to perform survival analyses to ascertain whether there was improved predictive performance of the markers in these sets.

8.2 Cisplatin-sensitivity in RT112 and RT112CP cells

Dose-response measurements to cisplatin exposure in RT112 and RT112CP cells confirmed that RT112CP was more resistant to cisplatin than RT112 (**Figure 8.1**). The IC50 value for RT112CP was calculated at 8.8 µg/mL and that for RT112 was 1.6 µg/mL. This meant that RT112CP was approximately 5.5-fold more resistant to cisplatin than RT112. At the IC50 dose for RT112 (1.6 µg/mL), there was no effect on the clonogenic survival of RT112CP cells. In other words, all RT112CP cells would be expected to survive at 1.6 µg/mL (**Figure 8.1**). Similarly, it was also observed that exposure to the IC50 dose of cisplatin for RT11CP (8.8 µg/mL) would result in all RT112 cells to be exterminated.

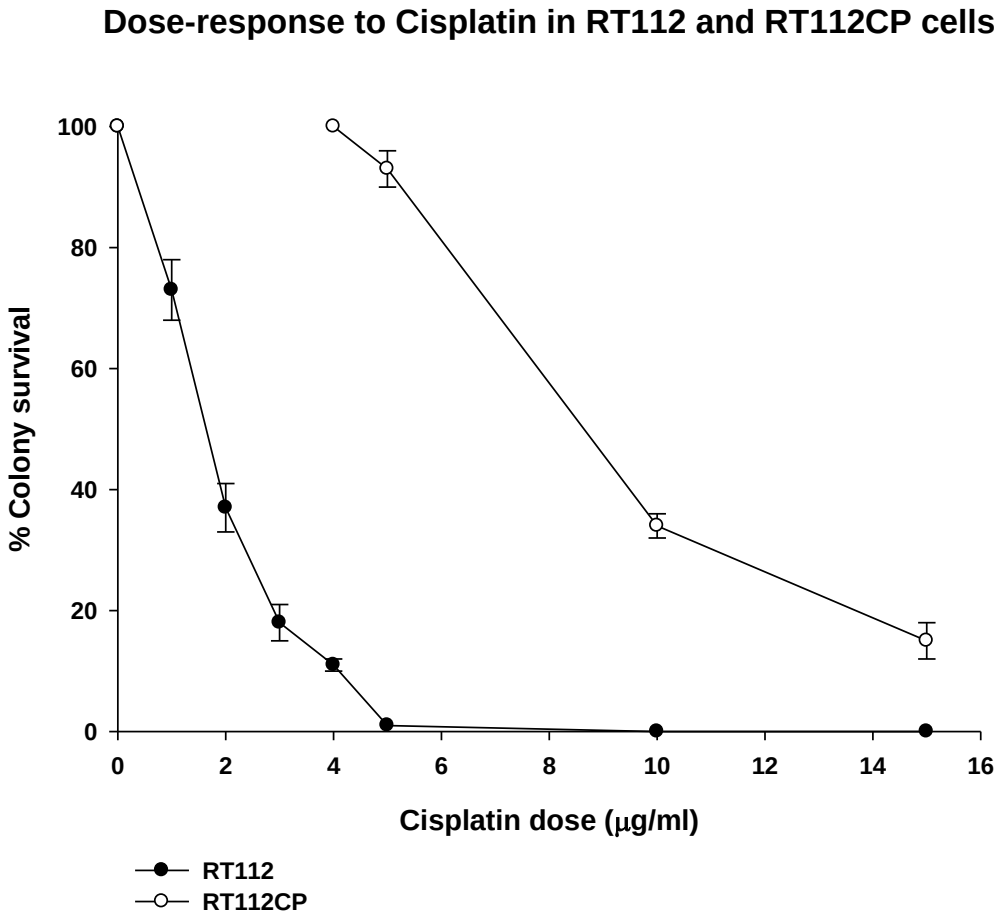

Figure 8.1: Dose-response to cisplatin in RT112 and RT112CP cell lines. RT112 cells are more sensitive to cisplatin than RT112CP cells. The results are based on 3 independent experiments. In each experiment, cells were plated in triplicate dishes. Values indicate the means and the error bars indicate the standard errors of the means.

8.3 AIMP3 expression in RT112 and RT112CP

Western blot analyses of AIMP3 expression were compared from lysates obtained from RT112 and RT112CP. The rationale behind this was to explore whether differences in AIMP3 expression may provide an explanation for the differing cispatin chemosensitivity in these cell lines. There was no significant difference in

the protein expression of AIMP3 between RT112 and RT112CP at differing loading doses of lysates (**Figure 8.2**).

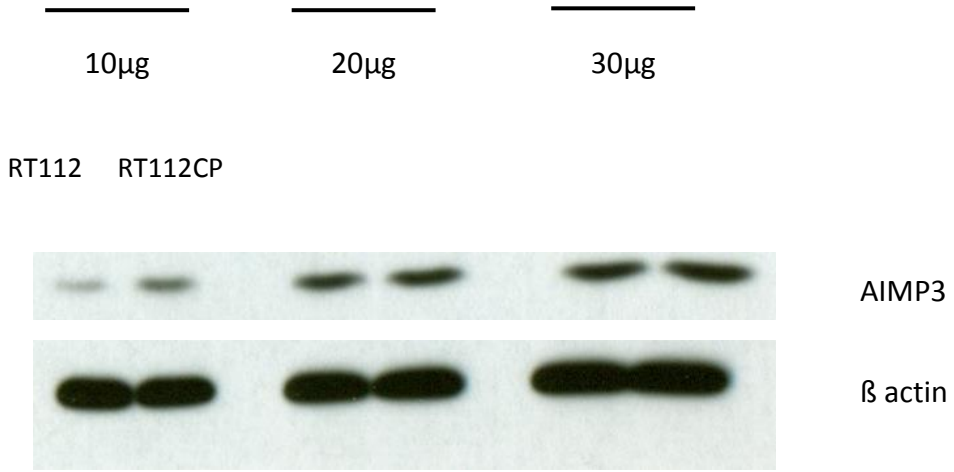

Figure 8.2: Western blot comparison of AIMP3 expression in RT112 and RT112CP cells. Levels of AIMP3 protein expression are compared at lysate loading doses of 10µg, 20µg and 30µg. For comparison at each lysate loading dose, RT112 lysates are on the left panel and RT112CP on the right panel. Experiments were repeated independently three times.

8.4 AIMP3 knockdown and cisplatin-sensitivity

In RT112, when comparing the cisplatin-sensitivity following siRNA knockdown of AIMP3, there was a significant difference between the treated and control groups (one-way ANOVA) (**Figure 8.3**). Relative to the control groups (IC50 cisplatin; scrambled siRNA), there was a significant increase in clonogenic survival in the treated group (AIMP3 siRNA + IC50 cisplatin) in Experiment 2 ($p=0.001$) and Experiment 3 ($p=0.007$). In Experiment 1, the difference was not statistically significant ($p=0.066$).

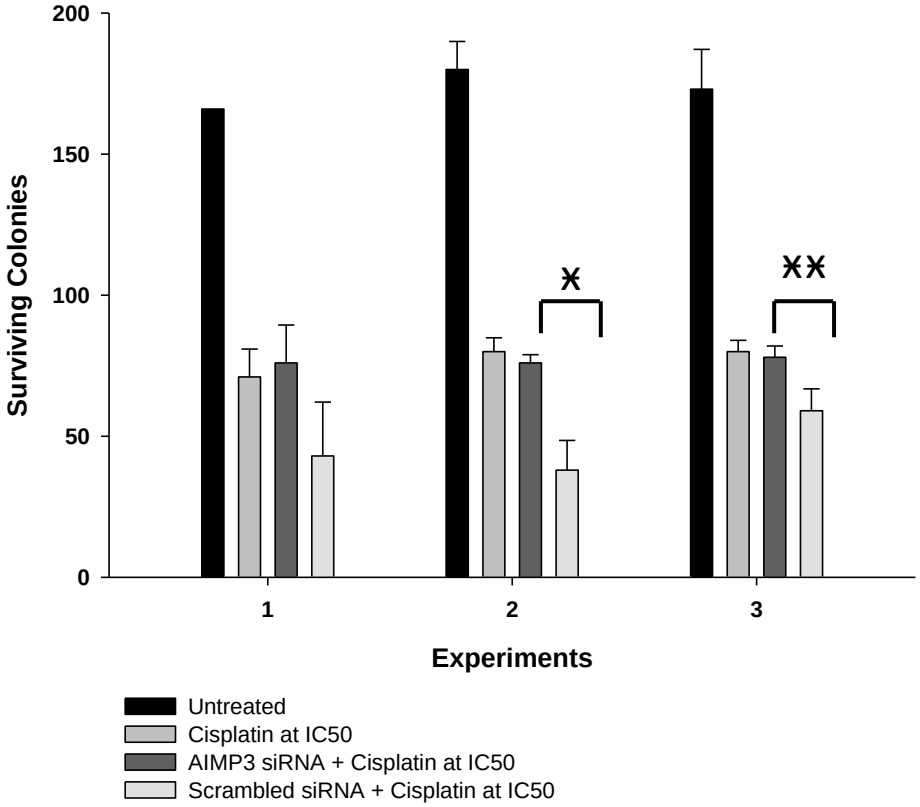

Figure 8.3: Clonogenic survival in RT112 cells after siRNA knockdown of AIMP3 and IC50 cisplatin exposure. The results for three independent experiments are presented. The total surviving colony counts are presented in the y-axis. For each experiment, four treatment groups are presented: (i) *Untreated* – no treatment with either cisplatin or siRNA, (ii) *Cisplatin at IC50* – treatment with IC50 dose (1.6 µg/mL) of cisplatin, (iii) *AIMP3 siRNA + Cisplatin at IC50* – knockdown of AIMP3 with siRNA followed by treatment with IC50 dose (1.6 µg/mL) of cisplatin, (iv) *Scrambled siRNA + Cisplatin at IC50* – treatment with non-targeting, scrambled siRNA followed by treatment with IC50 dose of cisplatin. ⁎ (p=0.001); ⁎⁎ (p=0.007)

In RT112CP, when comparing the cisplatin-sensitivity following siRNA knockdown of AIMP3, there was a significant difference between the groups (one-way ANOVA) (**Figure 8.4**). Relative to the control groups (IC50 cisplatin; scrambled siRNA), there was a significant increase in clonogenic survival in the treatment

group (AIMP3 siRNA + IC50 cisplatin) in Experiment 1 (p=0.003) and Experiment 2 (p=0.006). In Experiment 3, the difference was not statistically significant (p=0.102).

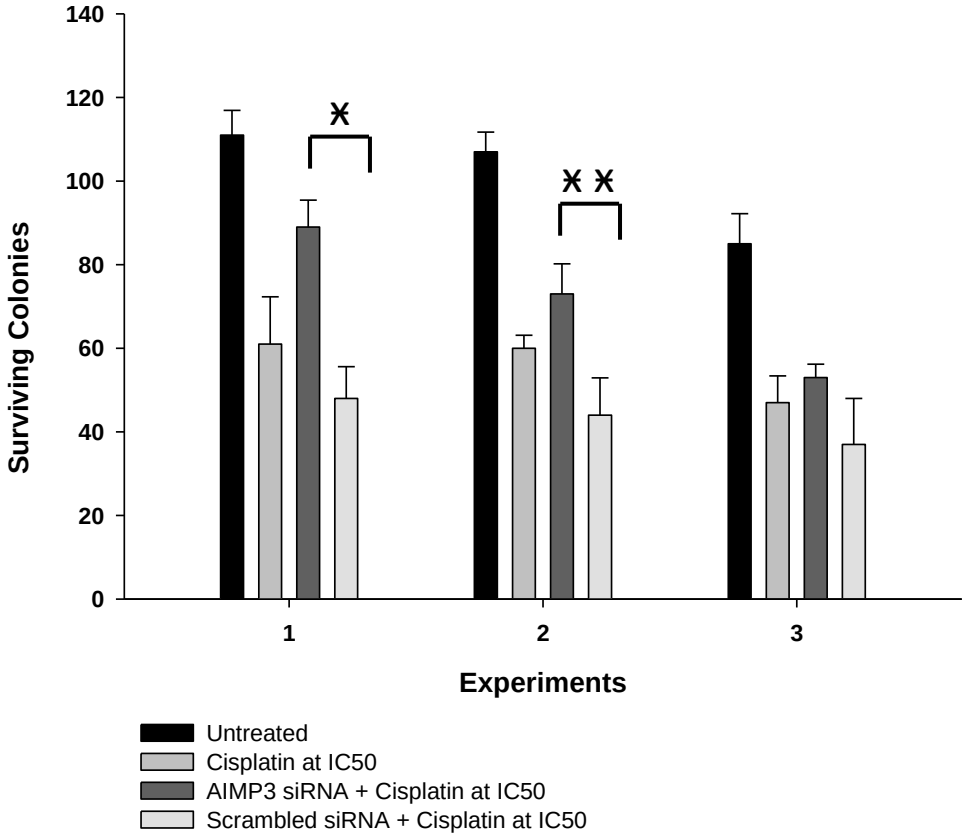

Figure 8.4: Clonogenic survival in RT112CP cells after siRNA knockdown of AIMP3 and IC50 cisplatin exposure. The results for three independent experiments are presented. The total surviving colony counts are presented in the y-axis. For each experiment, four treatment groups are presented: (i) *Untreated* – no treatment with either cisplatin or siRNA, (ii) *Cisplatin at IC50* – treatment with IC50 dose (8.8 µg/mL) of cisplatin, (iii) *AIMP3 siRNA + Cisplatin at IC50* – knockdown of AIMP3 with siRNA followed by treatment with IC50 dose (8.8 µg/mL) of cisplatin, (iv) *Scrambled siRNA + Cisplatin at IC50* – treatment with non-targeting, scrambled siRNA followed by treatment with IC50 dose of cisplatin (8.8 µg/mL). * (p=0.003); * * (p=0.006)

8.5 AIMP3 and ERCC1 in the Neoadjuvant chemotherapy TMA set

8.5.1 Patient characteristics and immuno-staining characteristics of the Neoadjuvant set

The clinico-pathological characteristics of the Neoadjuvant set are previously summarised (**Table 2.7**). In brief, there were a total of 84 patients; mean age was 66 years (range: 35 to 82 years); 64 were males and 20 females. Following neoadjuvant cisplatin-based chemotherapy, 46 patients (55%) underwent Radical Cystectomy compared to 38 patients (45%) who received Radical Radiotherapy.

The immuno-staining characteristics of AIMP3, ERCC1, Mre11 and p53 are shown below (**Figure 8.5**).

A

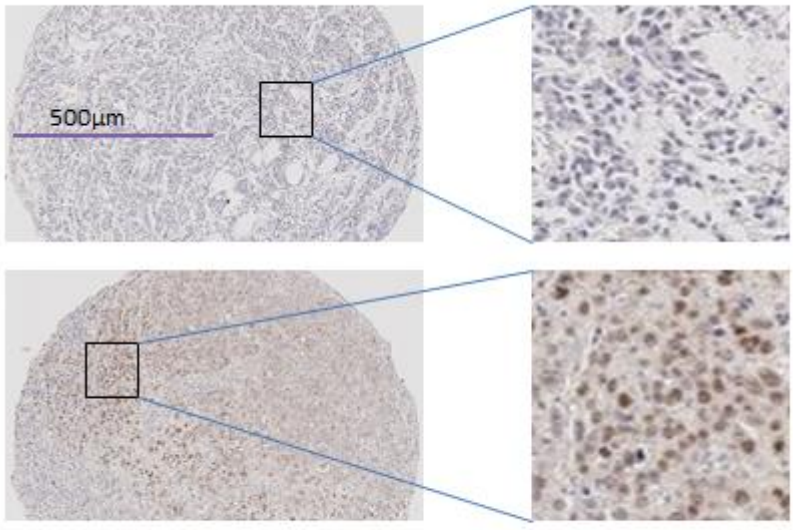

B

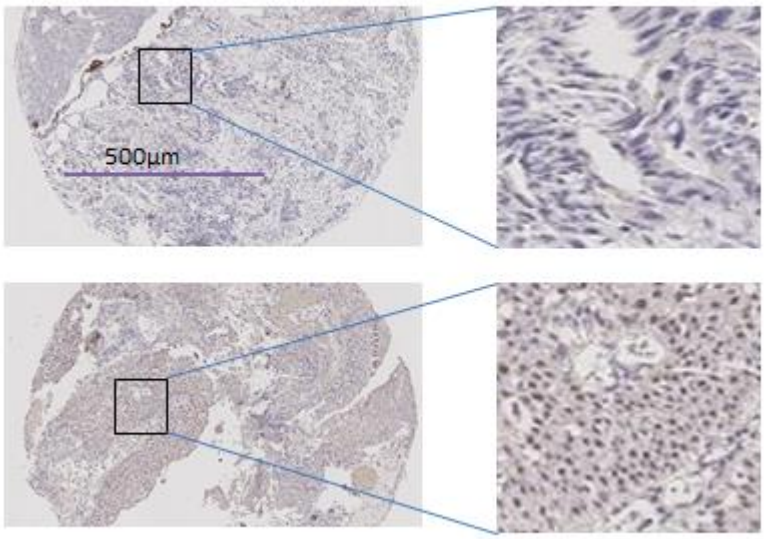

C

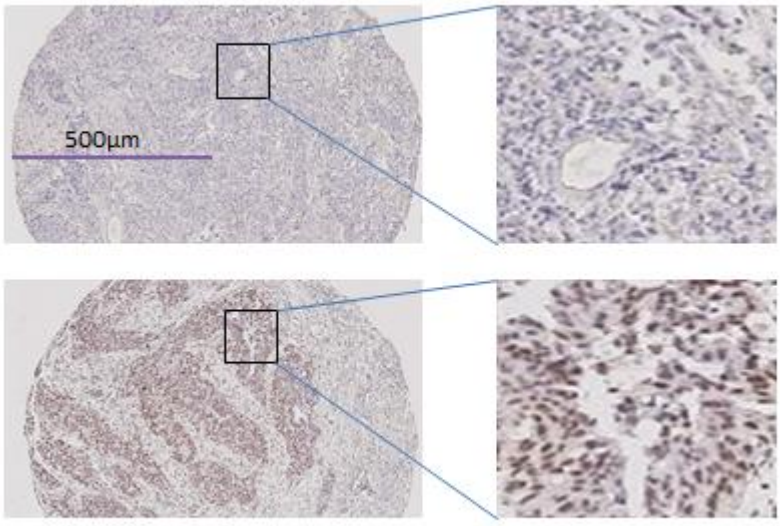

D

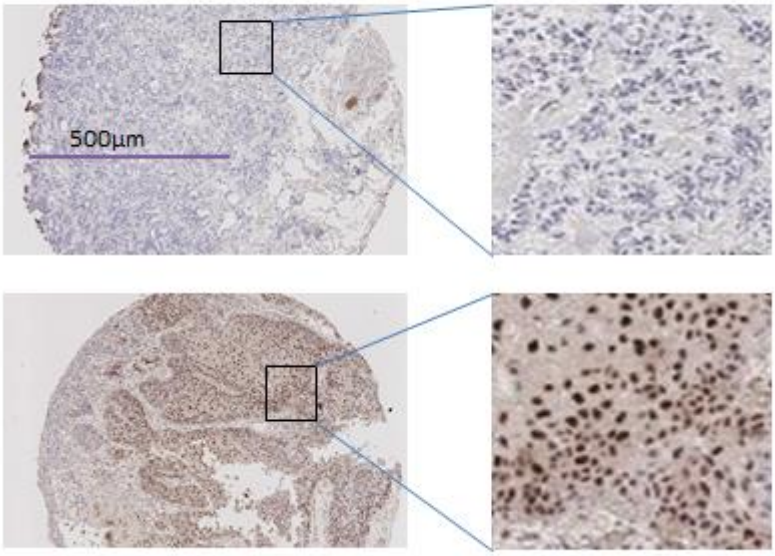

Figure 8.5: Neoadjuvant set: Negative cores (top panel) and Positive cores (bottom panel). Left panel cores are at 10X magnification and Right panel cores are at 200X magnification. (**A**) AIMP3, (**B**) ERCC1, (**C**) Mre11, (**D**) p53.

8.5.2 AIMP3 in the Neoadjuvant set

Kaplan-Meier analysis of the survival differences in the Neoadjuvant set, stratified by AIMP3 status, demonstrated no significant differences between the AIMP3-positive and AIMP3-negative groups (**Table 8.1**). The estimated median survival in the AIMP3-negative group was 62.0 +/- 12.2 months (95% CI: 38.0 to 86.0 months) compared to 51.0 +/- 8.1 months (95% CI: 35.2 to 66.8 months) (**Table 8.1B**). This

difference was not significant (p=0.660) (**Table 8.1C**). The absence of a significant difference was appreciable on the Kaplan-Meier survival plots (**Figure 8.6**).

Table 8.1: Case-processing summary (Table 8.1A), survival estimates (Table 8.1B) and log rank estimates (Table 8.1C) based on AIMP3 immunostaining status in the Neoadjuvant TMA set

Table 8.1A: The distribution of AIMP3-negative (-) and AIMP3-positive (+) cases is tabulated below.

AIMP3 status	Number	Number of Events	Censored	
			Number	Percent
AIMP3 (-)	46	22	24	52.2%
AIMP3 (+)	38	18	20	52.6%
Overall	84	40	44	52.4%

Table 8.1B: The survival estimates for the AIMP3-negative (-) and AIMP3-positive (+) cases are tabulated below. For the whole cohort (84 patients), the median survival was 53.0 +/- 8.2 months (95% CI: 36.9 to 69.1 months).

Means and Medians for Survival Time								
AIMP3 status	**Mean**				**Median**			
	Estimate	**Standard Error**	**95% Confidence Interval**		**Estimate**	**Standard Error**	**95% Confidence Interval**	
			Lower Bound	**Upper Bound**			**Lower Bound**	**Upper Bound**
AIMP3 (+)	63.942	7.766	48.721	79.162	62.000	12.242	38.006	85.994
AIMP3 (-)	61.263	9.474	42.694	79.832	51.000	8.051	35.220	66.780
Overall	62.358	5.954	50.689	74.028	53.000	8.236	36.858	69.142

Table 8.1C: Log-rank of the K-M estimates and significance. The significance (p value) for the above survival estimates (Table 8.1B) is calculated at 0.660 meaning that there is no significant difference in survival between the AIMP3-negative and AIMP3-positive cases.

	Chi-Square	Significance
Log Rank (Mantel-Cox)	.194	.660

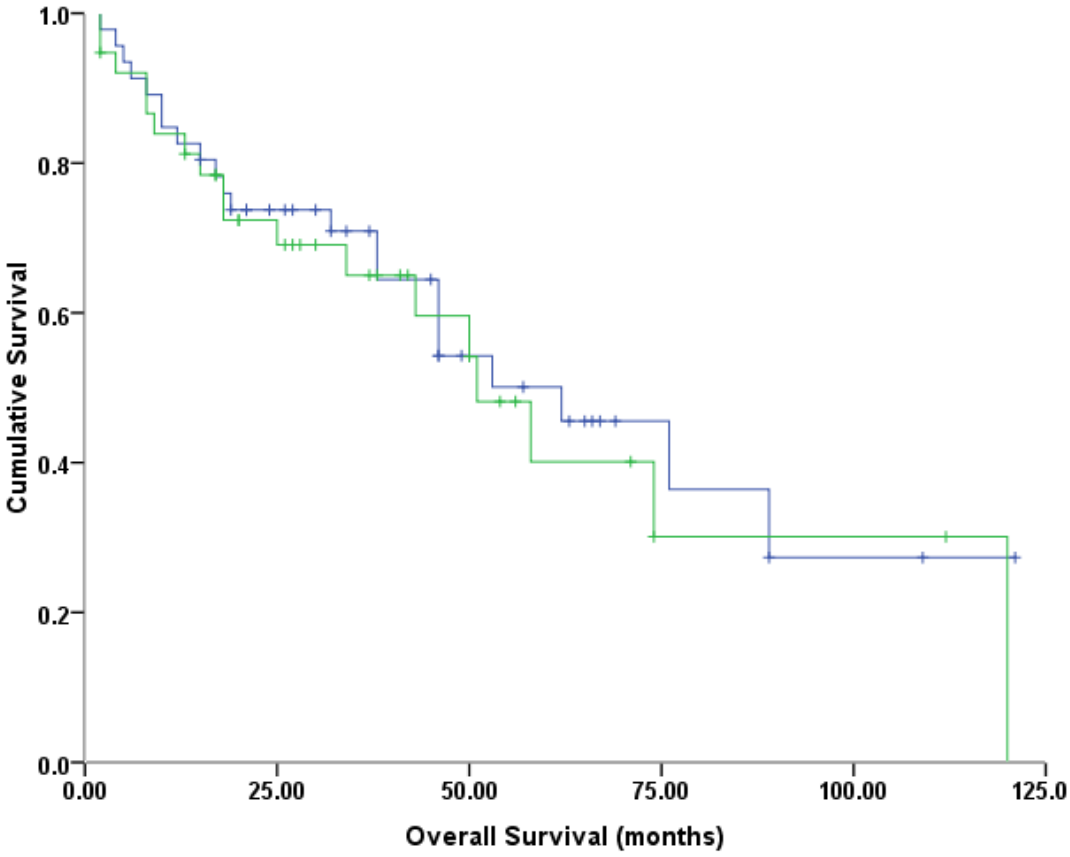

Figure 8.6: Kaplan-Meier plots for the AIMP3 in the Neoadjuvant set. There is no difference in survival between the AIMP3-negative group (blue survival plot) and the AIMP3-positive group (green survival plot).

Univariate analysis confirmed the lack of significant difference in survival outcomes between the AIMP3-positive and AIMP3-negative groups (**Table 8.2**). The hazard ratio was 1.15 (95% CI: 0.62 to 2.15) (p=0.663).

Table 8.2: Univariate analysis of AIMP3 in the Neoadjuvant set

Variables					
	Standard Error	Significance	Hazard Ratio (HR)	95.0% CI for Hazard Ratio	
				Lower	Upper
AIMP3 status	.319	.663	1.149	.615	2.148

8.5.3 ERCC1 in the Neoadjuvant set

Kaplan-Meier analysis of the survival differences in the Neoadjuvant set, stratified by ERCC1 status, demonstrated no significant differences between the ERCC1-positive and ERCC1-negative groups (**Table 8.3**). The estimated median survival in the ERCC1-negative group was 53.0 +/- 7.8 months (95% CI: 37.7 to 68.3 months) compared to 62.0 +/- 21.8 months (95% CI: 19.4 to 104.7 months) (**Table 8.3B**). This difference was not significant (p=0.304) (**Table 8.3C**). The absence of a significant difference was appreciable on the Kaplan-Meier survival plots (**Figure 8.7**).

Table 8.3: Case-processing summary (Table 8.3A), survival estimates (Table 8.3B) and log rank estimates (Table 8.3C) based on ERCC1 immunostaining status in the Neoadjuvant TMA set

Table 8.3A: The distribution of ERCC1-negative (-) and ERCC1-positive (+) cases is tabulated below.

ERCC1 status	Number	Number of Events	Censored	
			Number	Percent
ERCC1 (-)	49	26	23	46.9%
ERCC1 (+)	35	14	21	60.0%
Overall	84	40	44	52.4%

Table 8.3B: The survival estimates for the ERCC1-negative (-) and ERCC1-positive (+) cases are tabulated below. For the whole cohort (84 patients), the median survival was 53.0 +/- 8.2 months (95% CI: 36.9 to 69.1 months).

Means and Medians for Survival Time								
ERCC1 status	**Mean**				**Median**			
	Estimate	**Standard Error**	**95% Confidence Interval**		**Estimate**	**Standard Error**	**95% Confidence Interval**	
			Lower Bound	**Upper Bound**			**Lower Bound**	**Upper Bound**
ERCC1 (-)	54.179	6.081	42.260	66.097	53.000	7.809	37.695	68.305
ERCC1 (+)	73.402	9.679	54.430	92.373	62.000	21.758	19.354	104.646
Overall	62.358	5.954	50.689	74.028	53.000	8.236	36.858	69.142

Table 8.3C: Log-rank of the K-M estimates and significance. The significance (p value) for the above survival estimates (Table 8.3B) is calculated at 0.304 meaning that there is no significant difference in survival between the ERCC1-negative and ERCC1-positive cases.

	Chi-Square	Significance
Log Rank (Mantel-Cox)	1.058	.304

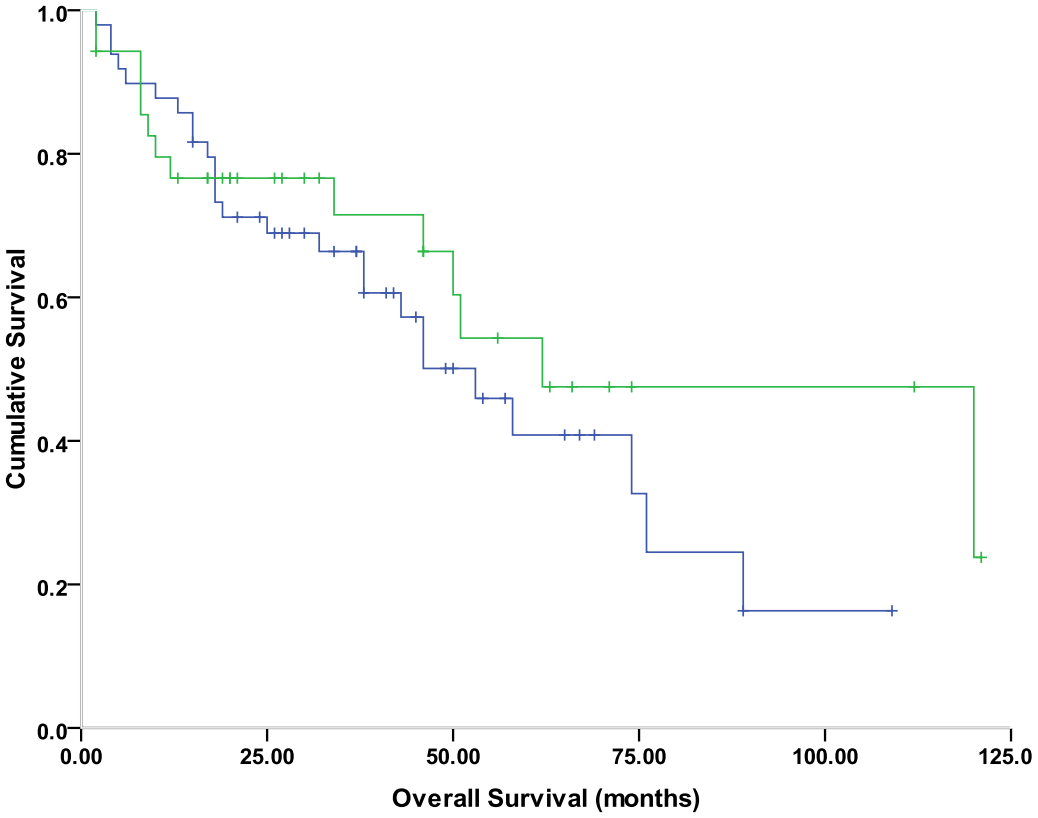

Figure 8.7: Kaplan-Meier plots for ERCC1 in the Neoadjuvant set. There is no difference between the ERCC1-negative (blue survival plot) and ERCC1-positive (green survival plot) groups.

Univariate analysis confirmed the lack of significant difference in survival outcomes between the ERCC1-positive and ERCC1-negative groups (**Table 8.4**). The hazard ratio was 0.71 (95% CI: 0.36 to 1.38) (p=0.310).

Table 8.4: Univariate analysis of ERCC1 in the Neoadjuvant set

Variables					
	Standard Error	Significance	Hazard Ratio (HR)	95.0% CI for Hazard Ratio	
				Lower	Upper
ERCC1 status	.341	.310	.708	.363	1.379

8.5.4 Mre11 in the Neoadjuvant set

Kaplan-Meier analysis of the survival differences in the Neoadjuvant set, stratified by Mre11 status, demonstrated no significant differences between the Mre11-positive and Mre11-negative groups (**Table 8.5**). The estimated median survival in the Mre11-negative group was 58.0 +/- 10.0 months (95% CI: 38.5 to 77.5 months) compared to 51.0 +/- 14.0 months (95% CI: 23.5 to 78.5 months) (**Table 8.5B**). This difference was not significant (p=0.400) (**Table 8.5C**). The absence of a significant difference was appreciable on the Kaplan-Meier survival plots (**Figure 8.8**).

Table 8.5: Case-processing summary (Table 8.5A), survival estimates (Table 8.5B) and log rank estimates (Table 8.5C) based on Mre11 immunostaining status in the Neoadjuvant TMA set

Table 8.5A: The distribution of Mre11-negative (-) and Mre11-positive (+) cases is tabulated below.

Mre11 status	Number	Number of Events	Censored	
			Number	Percent
Mre11 (-)	28	13	15	53.6%
Mre11 (+)	56	27	29	51.8%
Overall	84	40	44	52.4%

Table 8.5B: The survival estimates for the Mre11-negative (-) and Mre11-positive (+) cases are tabulated below. For the whole cohort (84 patients), the median survival was 53.0 +/- 8.2 months (95% CI: 36.9 to 69.1 months).

Means and Medians for Survival Time								
Mre11 status	Mean				Median			
	Estimate	Standard Error	95% Confidence Interval		Estimate	Standard Error	95% Confidence Interval	
			Lower Bound	Upper Bound			Lower Bound	Upper Bound
Mre11 (-)	68.929	9.927	49.473	88.386	58.000	9.949	38.501	77.499
Mre11 (+)	56.380	6.489	43.661	69.099	51.000	14.008	23.543	78.457
Overall	62.358	5.954	50.689	74.028	53.000	8.236	36.858	69.142

Table 8.5C: Log-rank of the K-M estimates and significance. The significance (p value) for the above survival estimates (Table 8.5B) is calculated at 0.03 meaning that there is a significant difference in survival between the Mre11-negative and Mre11-positive cases.

	Chi-Square	Significance
Log Rank (Mantel-Cox)	.708	.400

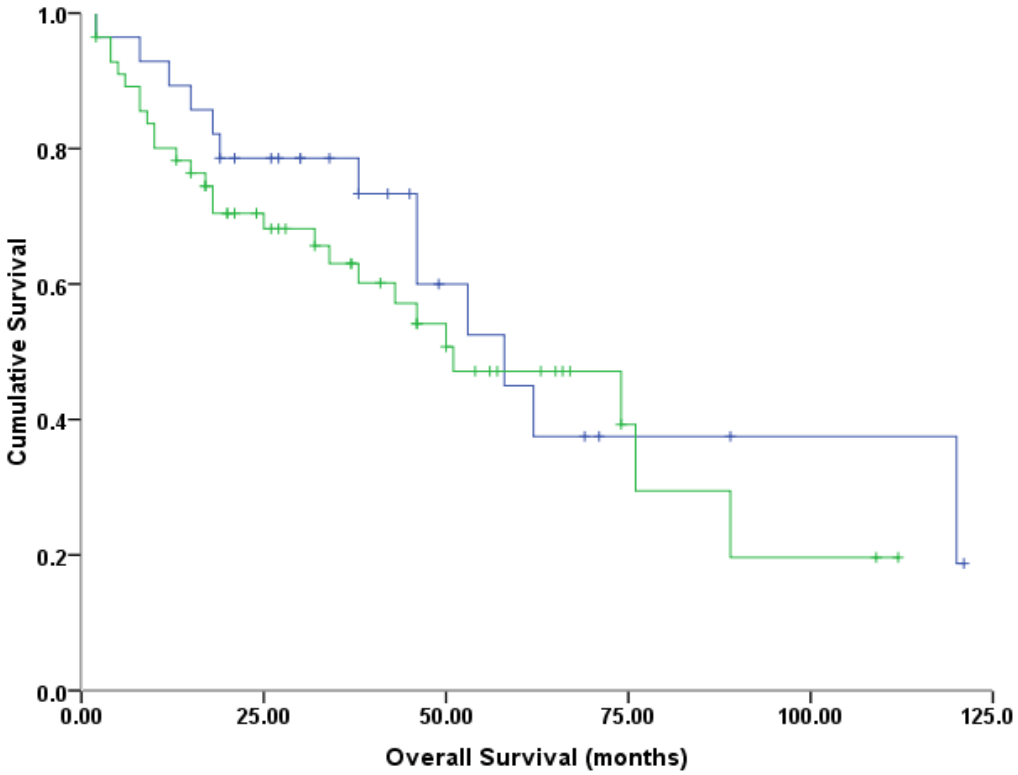

Figure 8.8: Kaplan-Meier plots for the Mre11 in the Neoadjuvant set. There is no significant difference between the Mre11-negative group (blue survival plot) and the Mre11-positive group (green survival plot).

Univariate analysis confirmed the lack of significant difference in survival outcomes between the AIMP3-positive and AIMP3-negative groups (**Table 8.6**). The hazard ratio was 1.34 (95% CI: 0.68 to 2.64) (p=0.405).

Table 8.6: Univariate analysis of Mre11 in the Neoadjuvant set

Variables					
	Standard Error	Significance	Hazard Ratio (HR)	95.0% CI for Hazard Ratio	
				Lower	Upper
Mre11 status	.348	.405	1.335	.676	2.639

8.5.5 p53 in the Neoadjuvant set

Kaplan-Meier analysis of the survival differences in the Neoadjuvant set, stratified by p53 status, demonstrated a significant difference between the p53-positive and p53-negative groups (**Table 8.7**). The estimated median survival in the p53-negative group was 38.0 +/- 14.1 months (95% CI: 10.4 to 65.6 months) compared to 74.0 +/- 9.5 months (95% CI: 55.4 to 90.7 months) (**Table 8.7B**). This difference was statistically significant (p=0.016) (**Table 8.7C**). The presence of a probable significant difference was appreciable on the Kaplan-Meier survival plots (**Figure 8.9**).

Table 8.7: Case-processing summary (Table 8.7A), survival estimates (Table 8.7B) and log rank estimates (Table 8.7C) based on p53 immunostaining status in the Neoadjuvant TMA set

Table 8.7A: The distribution of p53-negative (-) and p53-positive (+) cases is tabulated below.

p53 status	Number	Number of Events	Censored	
			Number	Percent
p53 (-)	34	18	16	47.1%
p53 (+)	50	22	28	56.0%
Overall	84	40	44	52.4%

Table 8.7B: The survival estimates for the p53-negative (-) and p53-positive (+) cases are tabulated below. For the whole cohort (84 patients), the median survival was 53.0 +/- 8.2 months (95% CI: 36.9 to 69.1 months).

Means and Medians for Survival Time								
p53 status	Mean				Median			
	Estimate	Standard Error	95% Confidence Interval		Estimate	Standard Error	95% Confidence Interval	
			Lower Bound	Upper Bound			Lower Bound	Upper Bound
p53 (-)	44.971	8.796	27.731	62.210	38.000	14.075	10.414	65.586
p53 (+)	70.656	7.309	56.330	84.982	74.000	9.515	55.351	92.649
Overall	62.358	5.954	50.689	74.028	53.000	8.236	36.858	69.142

Table 8.7C: Log-rank of the K-M estimates and significance. The significance (p value) for the above survival estimates (Table 8.7B) is calculated at 0.016 meaning that there is a significant difference in survival between the p53-negative and p53-positive cases.

	Chi-Square	Significance
Log Rank (Mantel-Cox)	5.810	.016

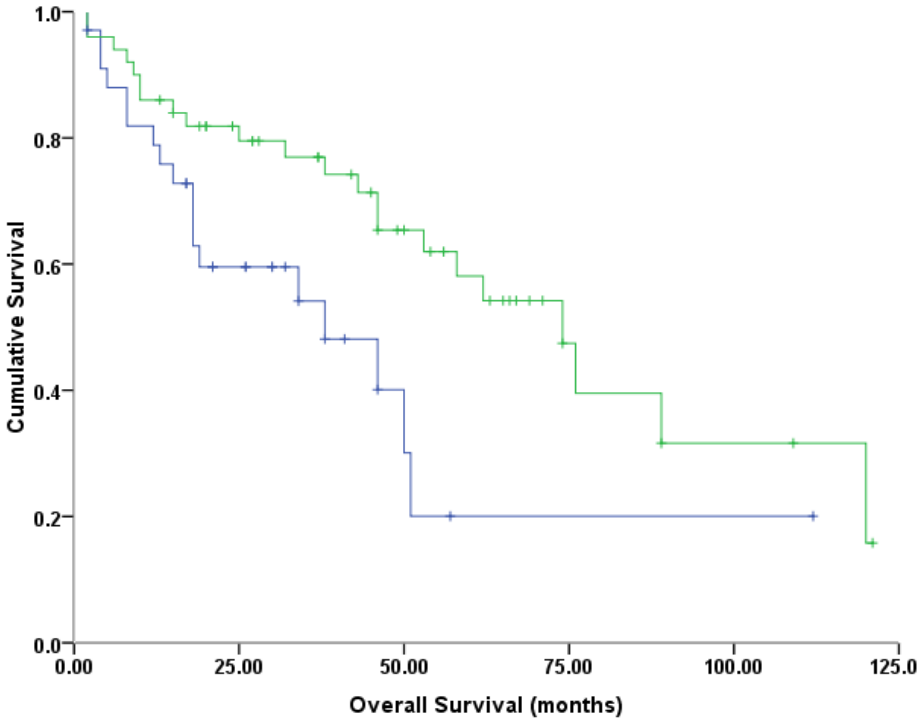

Figure 8.9: Kaplan-Meier plots for p53 in the Neoadjuvant set. There appears to be a significant difference between the p53-positive group (green survival plot) and the p53-neagtive group (blue survival plot).

Univariate analysis confirmed the above findings that there was a significant difference in survival between the p53-negative and p53-positive groups (**Table 8.8**). The hazard ratio was 0.46 (95% CI: 0.24 to 0.88) indicating that there was a 64% (1 minus 46) survival advantage in the p53-positive group relative to the p53-negative group. The statistical significance was maintained (p=0.019).

Table 8.8: Univariate analysis of p53 in the Neoadjuvant set

Variables					
	Standard Error	Significance	Hazard Ratio (HR)	95.0% CI for Hazard Ratio	
				Lower	Upper
p53 status	.336	.019	.456	.236	.880

8.5.6 Multivariate analysis in the Neoadjuvant set

Multivariate analysis was performed to investigate whether p53 status retained statistical significance with all other variables included in the analysis (**Table 8.9**). p53 status narrowly missed statistical significance (p=0.051). The hazard ratio for p53 was 0.51 (95% CI: 0.26 to 1.00); the inclusion of 1 in the upper limit of the confidence interval denoted non-significance.

The only variable to demonstrate statistical significance was "pT0" status. The hazard ratio was 4.01 (95% CI: 1.58 to 10.17) (p=0.003) suggesting a 4-fold increased risk of death in the "pT0"-positive group. In other words, in those who

had persistence of tumour post-treatment (either cystectomy or radiotherapy), there was a 4-fold increased risk of death. There was no significant difference in survival between radical treatment modalities (surgery or radiotherapy) (p=0.321).

Table 8.9: Multivariate analysis in the Neoadjuvant set

Variables					
	Standard Error	Significance	Hazard Ratio (HR)	95.0% CI for Hazard Ratio	
				Lower	Upper
Age	.018	.403	1.015	.980	1.051
Gender	.391	.353	.695	.323	1.496
Surgery	.495	.321	.612	.232	1.615
pT0	.475	.003	4.007	1.579	10.167
AIMP3	.349	.648	.852	.430	1.691
ERCC1	.371	.094	.537	.259	1.113
Mre11	.369	.675	1.167	.566	2.408
p53	.347	.051	.507	.257	1.002

8.6 AIMP3 and ERCC1 in the LaMB trial TMA set

8.6.1 Patient characteristics and immuostaining characteristics of the LaMB set

The clinico-pathological characteristics of the LaMB trial (ISRCTN35418671) set are previously summarised (**Table 2.8**). In brief, there were a total of 72 patients; mean age was 67 years (range: 42 to 82 years); 59 were males (82%) and 18 females (18%). In this group of 72 patients, 33 (46%) were randomised to the "standard"

treatment arm and 39 (54%) were randomised to the “experimental” arm comprising treatment with Lapatinib + standard.

The immune-stainining characteristics of AIMP3, ERCC1, Mre11 and p53 in the LaMB TMA cores are illustrated below (**Figure 8.10**).

A

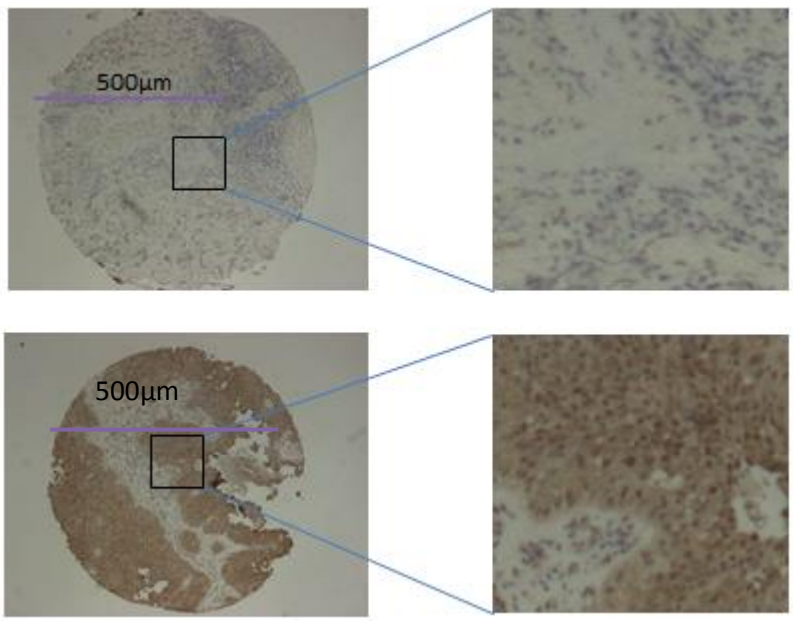

B

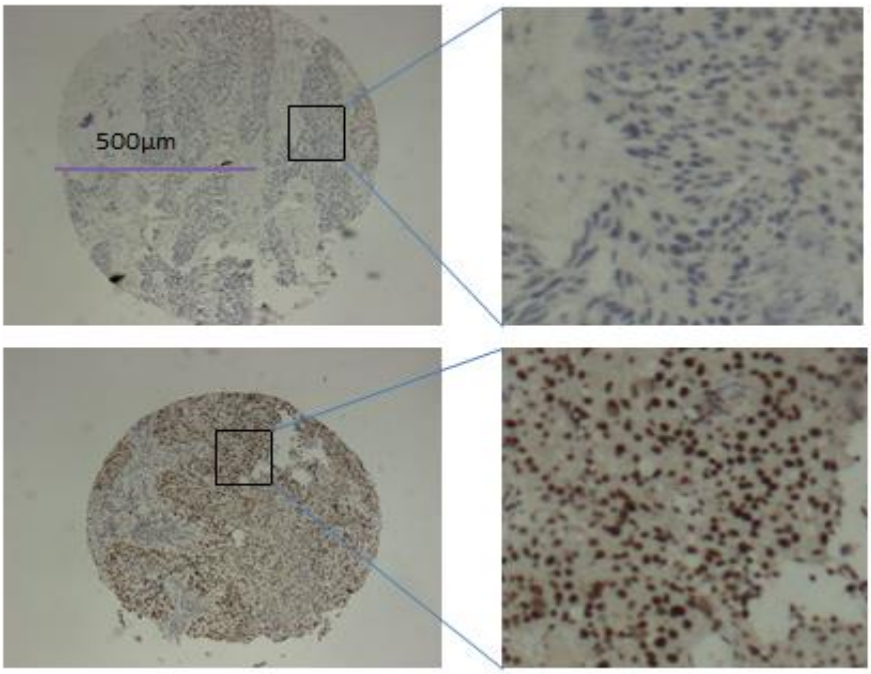

C

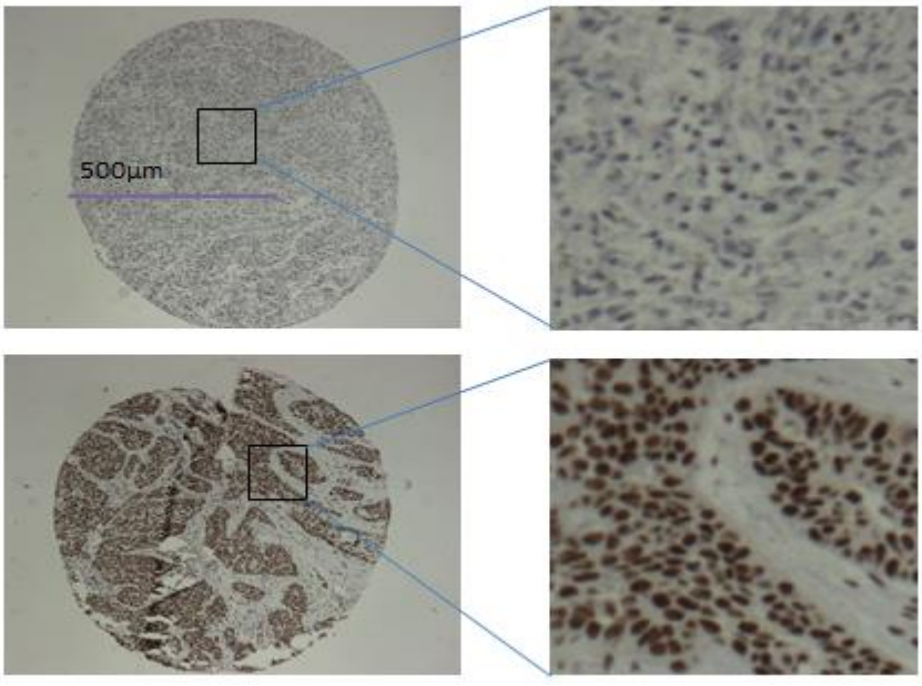

D

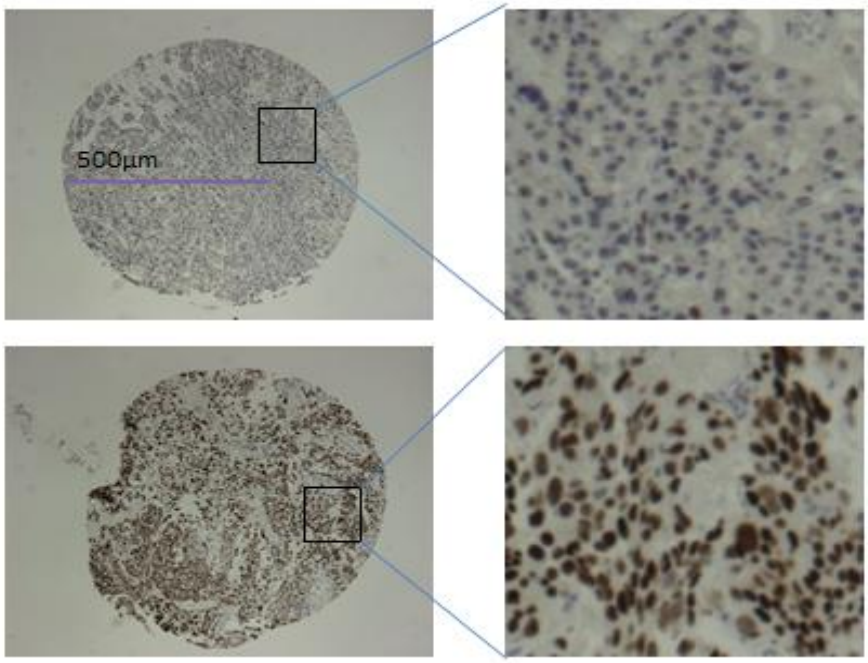

Figure 8.10: LaMB set: Negative cores (top panel) and Positive cores (bottom panel). Left panel cores are at 10X magnification and Right panel cores are at 200X magnification. (**A**) AIMP3, (**B**) ERCC1, (**C**) Mre11, (**D**) p53.

8.6.2 AIMP3 in the LaMB set

Kaplan-Meier analysis of the survival differences in the LaMB set, stratified by AIMP3 status, demonstrated no significant differences between the AIMP3-positive and AIMP3-negative groups (**Table 8.10**). The estimated median survival in the AIMP3-negative group was 15.0 +/- 2.0 months (95% CI: 11.2 to 18.9 months) compared to 23.0 +/- 7.3 months (95% CI: 8.8 to 37.2 months) in the AIMP3-

positive group (**Table 8.10B**). This difference was not significant (p=0.883) (**Table 8.10C**). The absence of a significant difference was appreciable on the Kaplan-Meier survival plots (**Figure 8.11**).

Table 8.10: Case-processing summary (Table 8.10A), survival estimates (Table 8.10B) and log rank estimates (Table 8.10C) based on AIMP3 immunostaining status in the LaMB TMA set

Table 8.10A: The distribution of AIMP3-negative (-) and AIMP3-positive (+) cases is tabulated below.

AIMP3 status	Number	Number of Events	Censored	
			Number	Percent
AIMP3 (-)	38	11	27	71.1%
AIMP3 (+)	34	12	22	64.7%
Overall	72	23	49	68.1%

Table 8.10B: The survival estimates for the AIMP3-negative (-) and AIMP3-positive (+) cases are tabulated below. For the whole cohort (72 patients), the median survival was 16.0 +/- 2.6 months (95% CI: 10.9 to 21.1 months).

Means and Medians for Survival Time								
AIMP3 status	Mean				Median			
	Estimate	Standard Error	95% Confidence Interval		Estimate	Standard Error	95% Confidence Interval	
			Lower Bound	Upper Bound			Lower Bound	Upper Bound
AIMP3 (-)	20.755	3.448	13.997	27.513	15.000	1.963	11.153	18.847
AIMP3 (+)	19.018	2.257	14.594	23.442	23.000	7.251	8.789	37.211
Overall	20.876	2.322	16.325	25.427	16.000	2.595	10.914	21.086

Table 8.10C: Log-rank of the K-M estimates and significance. The significance (p value) for the above survival estimates (Table 8.10B) is calculated at 0.883 meaning that there is no significant difference in survival between the AIMP3-negative and AIMP3-positive cases.

	Chi-Square	Significance
Log Rank (Mantel-Cox)	.022	.883

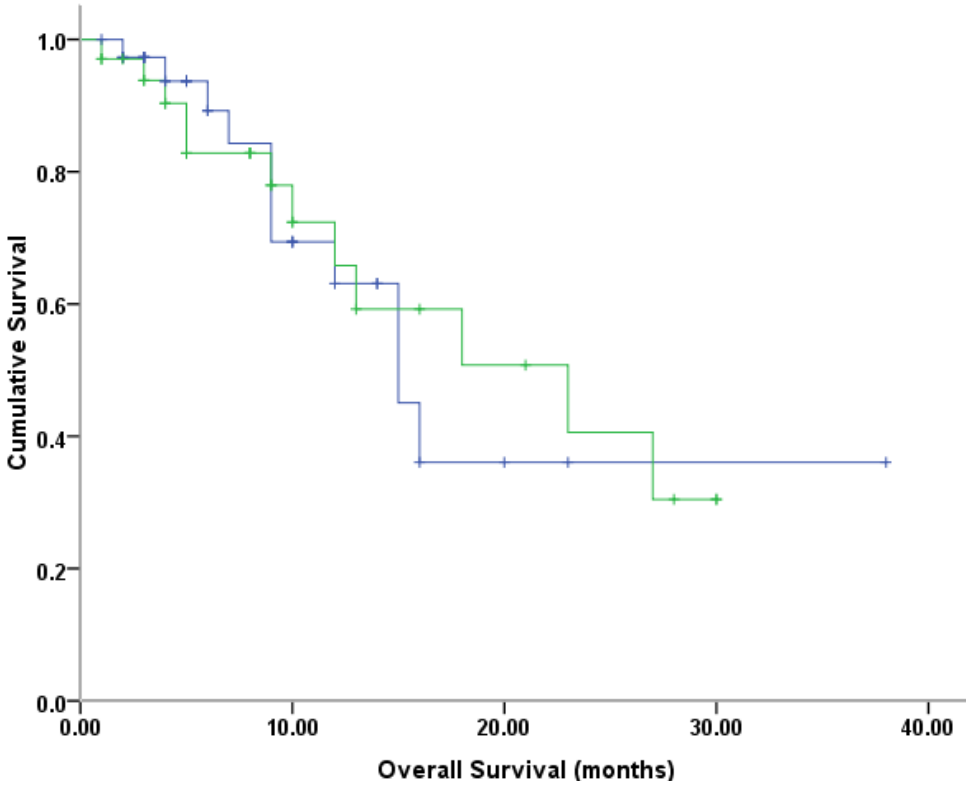

Figure 8.11: Kaplan-Meier plots for the AIMP3 in the LaMB set. There is no significant difference between the AIMP3-negative group (blue survival plot) and the AIMP3-positive group (green survival plot)

Univariate analysis confirmed the lack of significant difference in survival outcomes between the AIMP3-positive and AIMP3-negative groups (**Table 8.11**). The hazard ratio was 0.94 (95% CI: 0.41 to 2.16) (p=0.885).

Table 8.11: Univariate analysis of AIMP3 in the Neoadjuvant set

Variables					
	Standard Error	Significance	Hazard Ratio (HR)	95.0% CI for Hazard Ratio	
				Lower	Upper
AIMP3 status	.424	.885	.941	.410	2.158

8.6.3 ERCC1 in the LaMB set

Kaplan-Meier analysis of the survival differences in the Neoadjuvant set, stratified by AIMP3 status, demonstrated no significant differences between the ERCC1-positive and ERCC1-negative groups (**Table 8.12**). The estimated median survival in the ERCC1-negative group was 15.0 +/- 2.9 months (95% CI: 9.4 to 20.6 months) (**Table 8.12B**). This could not be compared directly to the ERCC1-positive group as the median survival in the group could not be calculated due to the cumulative survival in the group being more than 50% at the point of censorship (**Table 8.12B**). However, differences in survival between the groups could be estimated by log rank and this difference was not significant (p=0.660) (**Table 8.12C**). The absence of a significant difference was appreciable on the Kaplan-Meier survival plots (**Figure 8.12**).

Table 8.12: Case-processing summary (Table 8.12A), survival estimates (Table 8.12B) and log rank estimates (Table 8.12C) based on ERCC1 immunostaining status in the LaMB TMA set

Table 8.12A: The distribution of ERCC1-negative (-) and ERCC1-positive (+) cases is tabulated below.

ERCC1 status	Number	Number of Events	Censored	
			Number	Percent
ERCC1 (-)	43	15	28	65.1%
ERCC1 (+)	29	8	21	72.4%
Overall	72	23	49	68.1%

Table 8.12B: The survival estimates for the ERCC1-negative (-) and ERCC1-positive (+) cases are tabulated below. For the whole cohort (72 patients), the median survival was 16.0 +/- 2.6 months (95% CI: 10.9 to 21.1 months).

Means and Medians for Survival Time								
ERCC1 status	**Mean**				**Median**			
	Estimate	**Std. Error**	**95% Confidence Interval**		**Estimate**	**Std. Error**	**95% Confidence Interval**	
			Lower Bound	**Upper Bound**			**Lower Bound**	**Upper Bound**
ERCC1 (-)	18.739	2.690	13.467	24.011	15.000	2.853	9.408	20.592
ERCC1 (+)	20.564	2.622	15.425	25.703	.	.	.	.
Overall	20.876	2.322	16.325	25.427	16.000	2.595	10.914	21.086

Table 8.12C: Log-rank of the K-M estimates and significance. The significance (p value) for the above survival estimates (Table 8.12B) is calculated at 0.419 meaning that there is no significant difference in survival between the ERCC1-negative and ERCC1-positive cases.

	Chi-Square	Significance
Log Rank (Mantel-Cox)	.654	.419

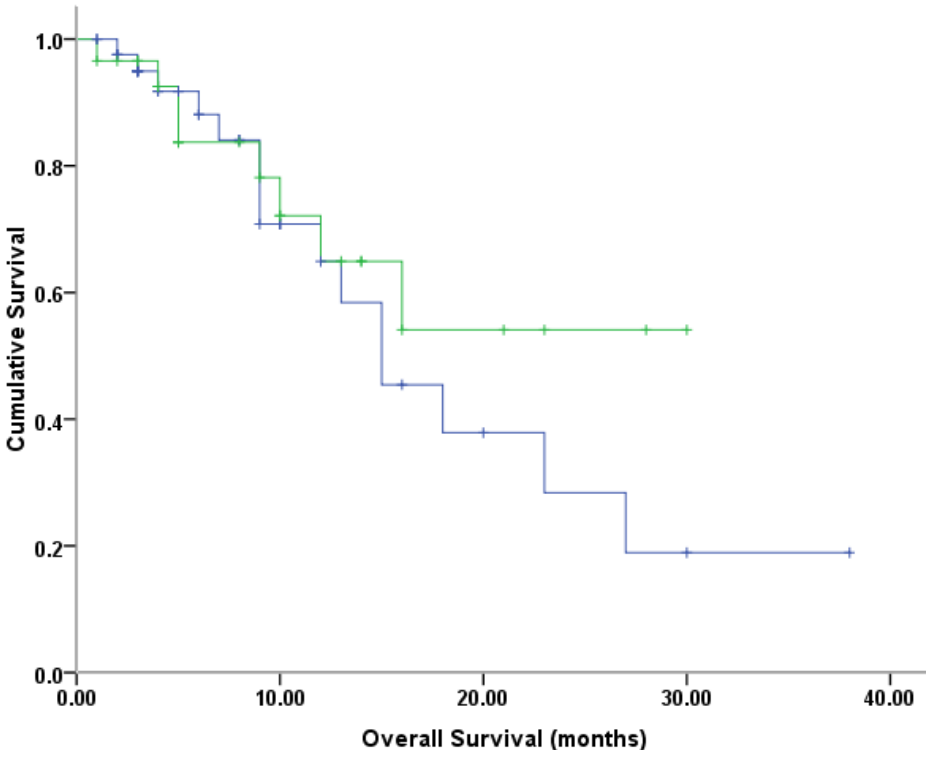

Figure 8.12: Kaplan-Meier plots for the ERCC1 in the LaMB set. There is no significant difference between the ERCC1-negative (blue survival plot) and the ERCC1-positive group (green survival plot).

Univariate analysis confirmed the lack of significant difference in survival outcomes between the ERCC1-positive and ERCC1-negative groups (**Table 8.13**). The hazard ratio was 0.71 (95% CI: 0.30 to 1.67) (p=0.428).

Table 8.13: Univariate analysis of ERCC1 in the LaMB set

Variables					
	Standard Error	Significance	Hazard Ratio (HR)	95.0% CI for Hazard Ratio	
				Lower	Upper
ERCC1 status	.438	.428	.706	.299	1.668

8.6.4 Mre11 in the LaMB set

Kaplan-Meier analysis of the survival differences in the LaMB set, stratified by Mre11 status, demonstrated no significant differences between the Mre11-positive and Mre11-negative groups (**Table 8.14**). The estimated median survival in the Mre11-negative group was 16.0 +/- 2.5 months (95% CI: 11.1 to 20.9 months). In the Mre11-positive group, the estimated median survival was 27.0 months but the confidence intervals around this estimate could not be calculated (**Table 8.14B**). However, the difference between the groups could be estimated by log rank and this difference was not significant (p=0.821) (**Table 8.14C**). The absence of a significant difference was appreciable on the Kaplan-Meier survival plots (**Figure 8.13**).

Table 8.14: Case-processing summary (Table 8.14A), survival estimates (Table 8.12B) and log rank estimates (Table 8.14C) based on Mre11 immunostaining status in the LaMB TMA set

Table 8.14A: The distribution of Mre11-negative (-) and Mre11-positive (+) cases is tabulated below.

Mre11 status	Number	Number of Events	Censored	
			Number	Percent
Mre11 (-)	48	18	30	62.5%
Mre11 (+)	24	5	19	79.2%
Overall	72	23	49	68.1%

Table 8.14B: The survival estimates for the Mre11-negative (-) and Mre11-positive (+) cases are tabulated below. For the whole cohort (72 patients), the median survival was 16.0 +/- 2.6 months (95% CI: 10.9 to 21.1 months).

Means and Medians for Survival Time								
Mre11 status	**Mean**				**Median**			
	Estimate	**Standard Error**	**95% Confidence Interval**		**Estimate**	**Standard Error**	**95% Confidence Interval**	
			Lower Bound	**Upper Bound**			**Lower Bound**	**Upper Bound**
Mre11 (-)	20.682	2.620	15.546	25.817	16.000	2.504	11.092	20.908
Mre11 (+)	19.833	3.342	13.283	26.383	27.000	.000	.	.
Overall	20.876	2.322	16.325	25.427	16.000	2.595	10.914	21.086

Table 8.14C: Log-rank of the K-M estimates and significance. The significance (p value) for the above survival estimates (Table 8.14B) is calculated at 0.821 meaning that there is no significant difference in survival between the Mre11-negative and Mre11-positive cases.

	Chi-Square	Significance
Log Rank (Mantel-Cox)	.051	.821

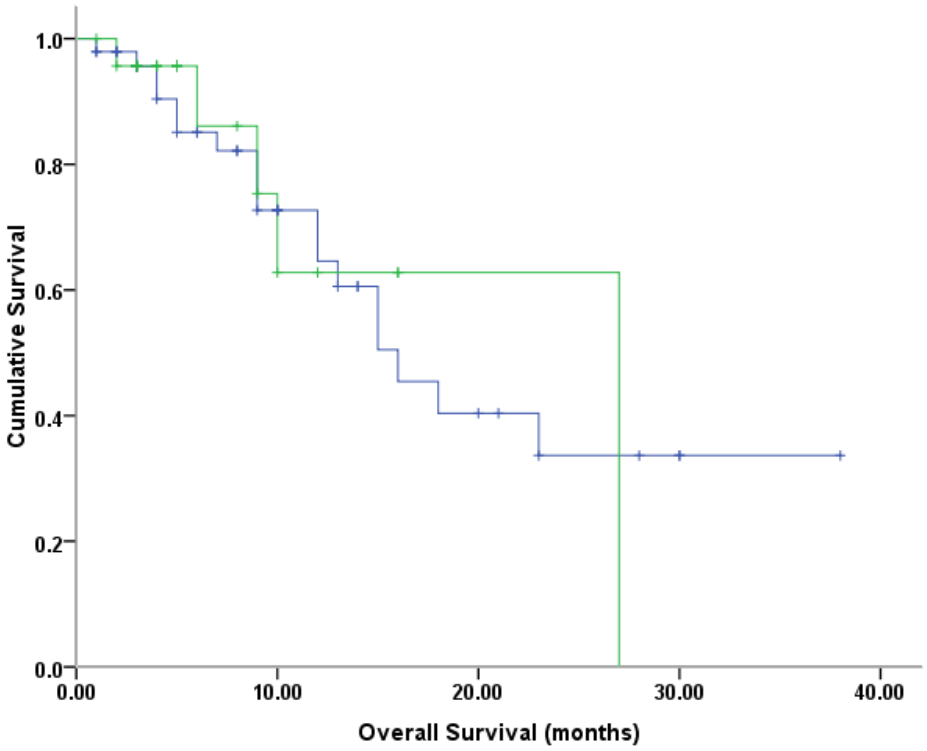

Figure 8.13: Kaplan-Meier plots for the Mre11 in the LaMB set. There is no significant difference between the Mre11-negative (blue survival plot) and the Mre11-positive group (green survival plot).

Univariate analysis confirmed the lack of significant difference in survival outcomes between the Mre11-positive and Mre11-negative groups (**Table 8.15**). The hazard ratio was 0.89 (95% CI: 0.33 to 2.43) (p=0.824).

Table 8.15: Univariate analysis of Mre11 in the LaMB set

Variables	Standard Error	Significance	Hazard ratio (HR)	95.0% CI for Hazard Ratio	
				Lower	Upper
Mre11 status	.511	.824	.892	.328	2.429

8.6.5 P53 in the LaMB set

Kaplan-Meier analysis of the survival differences in the LaMB set, stratified by p53 status, demonstrated no significant differences between the p53-positive and p53-negative groups (**Table 8.16**). The estimated median survival in the p53-negative group was 15.0 +/- 1.9 months (95% CI: 11.3 to 18.7 months) compared to 18.0 +/- 4.2 months (95% CI: 9.9 to 26.2 months) in the p53-positive group (**Table 8.16B**). This difference was not significant (p=0.692) (**Table 8.16C**). The absence of a significant difference was appreciable on the Kaplan-Meier survival plots (**Figure 8.14**).

Table 8.16: Case-processing summary (Table 8.16A), survival estimates (Table 8.16B) and log rank estimates (Table 8.16C) based on p53 immunostaining status in the LaMB TMA set

Table 8.16A: The distribution of p53-negative (-) and p53-positive (+) cases is tabulated below.

p53 status	Number	Number of Events	Censored	
			Number	Percent
p53 (-)	33	9	24	72.7%
p53 (+)	39	14	25	64.1%
Overall	72	23	49	68.1%

Table 8.16B: The survival estimates for the p53-negative (-) and p53-positive (+) cases are tabulated below. For the whole cohort (72 patients), the median survival was 16.0 +/- 2.6 months (95% CI: 10.9 to 21.1 months)

p53 status	Means and Medians for Survival Time							
	Mean				Median			
	Estimate	Standard Error	95% Confidence Interval		Estimate	Standard Error	95% Confidence Interval	
			Lower Bound	Upper Bound			Lower Bound	Upper Bound
p53 (-)	20.905	3.934	13.194	28.617	15.000	1.898	11.279	18.721
p53 (+)	18.165	2.053	14.141	22.189	18.000	4.160	9.846	26.154
Overall	20.876	2.322	16.325	25.427	16.000	2.595	10.914	21.086

Table 8.16C: Log-rank of the K-M estimates and significance. The significance (p value) for the above survival estimates (Table 8.16B) is calculated at 0.692 meaning that there is no significant difference in survival between the p53-negative and p53-positive cases.

	Chi-Square	Significance
Log Rank (Mantel-Cox)	.157	.692

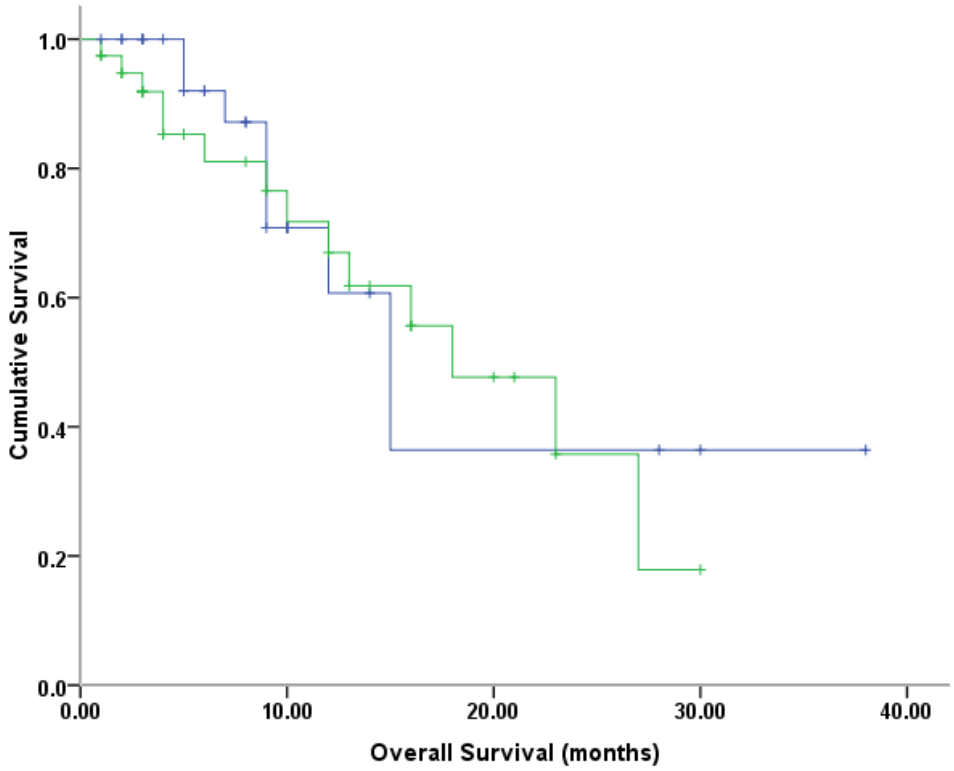

Figure 8.14: Kaplan-Meier plots for the p53 in the LaMB set. There is no significant difference between the p53-negative group (blue survival plot) and the p53-positive group (green survival plot).

Univariate analysis confirmed the lack of significant difference in survival outcomes between the p53-positive and p53-negative groups (**Table 8.17**). The hazard ratio was 1.18 (95% CI: 0.51 to 2.77) (p=0.697).

Table 8.17: Univariate analysis of p53 in the LaMB set

Variables					
	Standard Error	Significance	Hazard Ratio (HR)	95.0% CI for Hazard Ratio	
				Lower	Upper
p53 status	.434	.697	1.184	.506	2.774

8.6.6 Multivariate analysis of the LaMB set

On multivariate analysis, the findings of the Kaplan-Meier estimations and univariate analyses, for the markers, were confirmed (**Table 8.18**). None of the markers (AIMP3, ERCC1, Mre11 and p53) were found to demonstrate statistical significance in predicting survival difference in the LaMB set.

Of the available demographic clinical variables, Age (p=0.175) and Gender (p=0.436) were also not significant. In this limited cohort (n=72) of the LaMB set, Randomisation was also not significant. The hazard ratio for Randomisation was 1.06 (95% CI: 0.34 to3.35) with a p value of 0.915.

Table 8.18: Multivariate analysis in the LaMB set

Variables					
	Standard Error	Significance	Hazard Ratio (HR)	95.0% CI for Hazard Ratio	
				Lower	Upper
Age	.031	.175	1.042	.982	1.107
Gender	.569	.436	1.558	.511	4.749
AIMP3	.482	.754	.860	.334	2.210
ERCC1	.446	.569	.776	.324	1.859
Mre11	.582	.455	.647	.207	2.026
p53	.489	.708	1.201	.461	3.132
Randomisation	.586	.915	1.064	.338	3.354

8.7 Discussion of results

In this chapter, the primary objective was to investigate whether AIMP3 expression was predictive of cisplatin-exposure outcome *in vitro*. Given the previous *in vitro* findings (**Chapter 3**) where AIMP3 was predictive of radiation-exposure outcome, it was logical to hypothesise that, similarly, AIMP3 knockdown by siRNA transfection, would increase the clonogenic survival of bladder cancer cell lines following treatment with cisplatin. To answer this question, RT112 and a cisplatin-resistant subline, RT112CP, were used in conjunction as a model of the spectrum of ciplatin-sensitive to cisplatin-resistant bladder cancer cell lines. Indeed, dose-response studies demonstrated that RT112CP was approximately 5-fold more

resistant to cisplatin than RT112. In addition, their dose-response curves did not overlap indicating that their cisplatin sensitivities were at two ends of the spectrum. Therefore, the model was felt to be satisfactory in terms of testing bladder cancer cell lines with significantly different cisplatin-sensitivities. However, there is an argument to be made that it would have been more comprehensive to have incorporated other bladder cancer cell lines (e.g. T24, RT4, 253J) into the panel.

It was necessary to characterise the constitutive levels of AIMP3 expression in RT112 and RT112CP in order to explain any differences in functional outcomes that may be observed. Western blot analyses demonstrated no significant differences in AIMP3 protein expression levels between the two. Clonogenic assays were performed as the functional readouts as previously (**Chapter 3**) with RT112 and RT112CP being treated with IC50 cisplatin (and with controls; e.g. without cisplatin) following siRNA knockdown of AIMP3 (and with controls; e.g. with GAPDH siRNA and scrambled siRNA). In both RT112 and RT112CP, in two out of three experiments each, there was a significant increase in clonogenic survival when AIMP3 was downregulated suggesting that AIMP3 may be important in cisplatin-mediated DNA damage response.

The secondary objectives of this chapter were to interrogate the predictive value of the panel of markers (AIMP3, ERCC1, Mre11 and p53) in the Neoadjuvant and LaMB sets respectively. In the Neoadjuvant set, there were 84 patients included which was felt to be a reasonable sample size. Approximately half the patients had subsequently undergone radical radiotherapy and half radical cystectomy. The

median age, age range and gender distributions were not dissimilar to the BCON and Radical Cystectomy sets. In the Neoadjuvant set, only p53 demonstrated significance, in terms of differential survival outcomes, on Kaplan Meier estimates and univariate analysis. However, this significance was lost on multivariate analysis. There was no significant difference in survival outcome between the radical cystectomy and radical radiotherapy groups. This finding is in keeping with the contemporary opinion that there is little difference between survival outcomes between surgery and radiotherapy for organ-confined MIBC and that, if there is a survival advantage in favour of surgery, it is likely small. The current Neoadjuvant set, of 84 patients, would not be adequately powered to delineate this difference and this as not the objective of the current study.

In the LaMB trial set, none of the markers demonstrated significance. However, there were a number of limitations with the LaMB set. First of all, the sample size was 72 which meant that differences in survival were only likely to be detected if they were sufficiently large differences, i.e. the larger the size effect, the more likely it was to be detected with statistical significance ($p<0.05$). In other words, a larger sample size, such as that for the BCON set (n=217) would have been preferable. The main reason for the somewhat small sample size is that the LaMB trial has not been completed and the patients included in the TMA set were those who were recruited at the beginning of the trial. There were 106 cases initially identified as being suitable for incorporation into the TMA set. However, data and tissue availability were also limiting factors in committing more cases into the TMA. Furthermore, on account of the incompleteness of the study, follow-up periods for the vast majority of patients included were also short. Similarly, there were only 23

events (deaths) recorded for the 72 patients. As patients with metastatic bladder cancer are expected to have a poor prognosis, it was anticipated that a long period of follow-up may not be absolutely essential in the cohort of 72 available cases. However, with a more "mature" study, with a longer period of follow-up time, this event-rate (deaths) would be expected to be higher. Consequently, survival analyses would be more robust. In the current analysis, based on the 72 patients, there was no significant survival difference between the trial arms (standard treatment versus Lapatinib + standard treatment). For the reasons described above, it would be "premature" to conclude that there is no significant difference in the LaMB trial arms. Furthermore, the LaMB trial is set up to specifically investigate any differences in progression-free survival, as the primary objective, rather than differences in overall survival. Certainly, the LaMB set, with its full complement of recruited patients (n=204) and with a longer period of follow-up would be a more robust platform to interrogate the markers of this current study as well as to pose the question as to whether there is any significant differences in either progression-free or overall survival between the two trial arms.

Chapter 9

Final Discussion

9.1 Methodological considerations

9.1.1 Cell lines

The study of complex biological processes, such the effect of altered levels of expression of one or more genes on the response of tumours to radiotherapy or chemotherapy, is technically challenging *in vivo*. Cell lines offer a relatively simple model which allows for a quicker and more cost-effective means of interrogating questions arising from proposed hypotheses pertaining to such complex biological phenomena. On the other hand, the use of cell lines does have many limitations including the lack of genotypic and phenotypic similarities, in some cases, to the tissue or tumour that they are meant to represent. Furthermore, the complexity of biological pathways *in vivo* may mean that the observations *in vitro*, in a controlled experimental setting, may turn out to be significantly different and therefore, conclusions drawn from tumour cell lines may not be directly transferrable in the clinical setting.

In the current study, a panel of bladder cancer cell lines (T24, RT112, 253J and RT4) was used. For the initial AIMP3 expression characterisation and radiation exposure work, the panel of cell lines was felt to be satisfactorily representative of bladder cancer cells. HeLa was used as the reported positive control for AIMP3 expression. All the bladder cancer cell lines, as well as HeLa, are well established, characterised and are often reported in the literature. An argument can be made for the inclusion of more bladder cancer cell lines to have been made in the panel used in this study. This would certainly have made the findings more comprehensive. However, the addition of more cell lines would have significantly increased the

workload of each experimental protocol and this was felt, on balance, not likely to be time-efficient with respect to the remit of the project.

All the cell lines were obtained from a single, reputable source (Professor John Masters) with the passage of each cell line being documented. All cells were maintained in standardised incubation conditions, checked for mycoplasma contamination, passaged prior to confluence and used within 10 passages for experimental purposes. These measures ensured that the experimental conditions were reliable and replicable. However, there is an argument to be made for having obtained the same cell lines from a different (e.g. commercial) source and to have corroborated the experimental observations for each of the cell lines in question. Again, this exercise was felt to be not necessary for mainly the same reasons as described above.

For the cisplatin sensitivity work, RT112 and RT112CP were used as a panel to represent a spectrum of cell lines with two extremes of cisplatin sensitivity. As discussed in the preceding chapter (**Chapter 8**), this was confirmed to be the case as RT112CP was approximately 5-fold more resistant to cisplatin than RT112. Furthermore, the dose-response curves for RT112 and RT112CP did not overlap suggesting that they represented the two ends of a wide cisplatin sensitivity spectrum. Again, the use of more cell lines would have been desirable, to represent cell lines with differing cisplatin sensitivities within the spectrum (or indeed more sensitivity than RT112). However, the dual cell line model was felt to be adequate.

9.1.2 Protein expression

In this study, expression of the gene in question, *AIMP3*, was studied by the measurement of its protein product. For the cell lines-based work, Western blot analysis was used as the method of measuring AIMP3 protein expression. Expression of AIMP3 protein was successfully characterised in the panel of bladder cancer cell lines (**Chapter 3**). This meant that it was arguably not necessary to corroborate the findings at RNA level (e.g. through PCR) as proteins are the final effectors of biological processes. One of the criticisms of solely investigating gene expression through measurement of RNA levels is that mRNA transcripts may be degraded as part of the regulatory process of gene expression and may ultimately not be translated to their protein products. Hence, the decision to perform Western blot analyses in this study. Had there been issues with characterisation of AIMP3 protein expression, PCR would have been performed.

An argument can be made for having corroborated the Western findings with RTPCR measurements. However, this was not routinely performed. There was an instance when performing RTPCR was felt to be useful. When siRNA knockdown of AIMP3 was analysed by Western blot analysis (**Figure 3.6**), one of the controls included siRNA transfection with GAPDH siRNA (positive control). However, downregulation of GAPDH, at protein level, on the Western blots was not appreciable. This was most likely due to the constitutively high levels of GAPDH. To prove that the positive control (GAPDH siRNA transfection) was indeed causing a downregulation of GAPDH expression, RTPCR was performed (**Appendix C, Supplementary Figure A**). This demonstrated that there was a significant (96%) reduction in the GAPDH mRNA levels following GAPDH siRNA transfection.

Similarly, RTPCR confirmed significant downregulation of *AIMP3* expression following AIMP3 siRNA transfection (**Appendix C, Supplementary Figure B**). Therefore, it was considered satisfactory to measure AIMP3 protein expression by Western blot analysis.

9.1.3 Functional assays

Clonogenic survival assays were performed as the functional readouts for most of the experiments. Dose-response characteristics for radiation as well as cisplatin treatments were measured by this method. Following siRNA transfection, differences in radiation or cisplatin responses were also measured by this method. This methodology (i.e. clonogenic assay) was chosen as it is generally considered to be robust. Indeed, the dose-response and siRNA knockdown experimental findings were found to be consistent. Other assays (e.g. tetrazolium-based colorimetric assays) are quicker to perform but have the propensity to produce variable results based on experimental conditions affecting the metabolic status of the cells and without necessarily affecting cellular viability. Therefore, clonogenic assays were chosen as the viability readouts following cytotoxic treatments (with cisplatin or radiation) were likely to be more reliable.

In the siRNA transfection experiments, treatment arms consisted of exposure to IC50 doses of irradiation or cisplatin. This was chosen as the method as the IC50 doses calculated were consistent for the cell lines and formed the basis on which deviations in the readouts (clonogenic survival) compared to that expected (at IC50 dosing) could be readily detected. However, for each cell line, differences in the

readouts (clonogenic survival) at a range of doses would likely have been more comprehensive by demonstrating differing shifts in the dose-response curves for the different experimental conditions.

Following siRNA knockdown of AIMP3, rather than just measure the survival readouts, alternative readouts could have been performed to analyse the downstream functional effects of altered AIMP3 expression. As elaborated in the introductory chapter (**Section 1.4**), there are many key players in the DNA damage response (DDR) pathway including p53, ATM, ATR and Chek proteins. As for AIMP3, characterisation of the levels of expression of these proteins in response to radiation and cisplatin exposure in the bladder cancer cell lines is a major avenue of further research pertinent to the current project. In addition, the effects of siRNA downregulation of AIMP3 on the level of expression of these proteins or on their activities (e.g. phosphorylation of p53) could be interrogated. Although conceptualised, this body of work was considered to be beyond the scope of the current project due mainly to time-constraints.

In addition to the characterisation of AIMP3 protein levels in the panel of bladder cancer cell lines, immunofluorescence was performed to characterise the subcellular localisation of AIMP3. As previously reported in HeLa and fibroblasts, AIMP3 was demonstrated to distribute within both the cytosolic as well as nuclear compartments in the bladder cancer cell lines used. HeLa was used as the control. Following irradiation, AIMP3 was observed to be distributed relatively more in the nuclear compartment suggesting a possible nuclear translocation of AIMP3 to take part in

the DDR pathway as previously reported in HeLa and fibroblasts. However, due to technical difficulties, quantifications of the observed changes were not performed. Secondly, subcellular fractionation, following irradiation, was also technically challenging given the difficulties of extracting pure subcellular fractions in irradiate specimens. Therefore, the observed phenomenon, which is previously reported in HeLa and fibroblasts, could not be corroborated in bladder cancer cell lines in the current study.

9.1.4 TMA immunostaining, scoring and statistical analyses

Immunostaining of all the TMA sets (BCON, Radical Cystectomy, Neoadjuvant and LaMB) were performed by the UCL Advanced Diagnostics (UCLAD) laboratory. UCLAD is part of the UCL Cancer Institute and provides accredited laboratory research facilities internationally. Immunostaining was considered to be of high quality for the antibodies (AIMP3, ERCC1, Mre11 and p53) tested and the results were reproducible. This also meant that the valuable TMA sections, especially the BCON and LaMB trial materials, were used with minimal waste.

With respect to the scoring methodology, validated methods were used where previously reported. For instance, the median H score method for ERCC1, the 25th percentile cut-off for Mre11 and the 10th percentile cut-off for p53. For AIMP3, the median H score method was found to be significant. Where the results suggested a probable difference which narrowly missed significance (for instance, p53 status in the BCON set), alternative scoring methods (e.g. additional H score method for p53)

were performed in order to endure that potential significant differences were not being missed on account of the scoring method used.

The scoring process was repeated adequately by different observers to assure strong intra-observer as well as inter-observer agreements and to ensure reliability of the results. However, the significant findings, particularly with respect to AIMP3 and ERCC1 in the BCON set, must be validated externally. In other words, the findings in the BCON set must be replicated by external observers. The ideal way to achieve this would be for a different research group to replicate the entire immunostaining protocol, including staining, scoring and statistical analyses, using a fresh batch of BCON TMA sections.

9.1.5 TMA datasets

There were no major issues with the BCON trial TMA and trial dataset. The sample size was large (n=217) and the dataset was deemed to be robust, as would be expected from a reported clinical trial. However, the dataset was not considered to be large enough to divide into two large "test" and "validation" sets to detect the same level of survival differences observed. Alternatively, it would have been desirable to have validated the BCON set findings on another contemporary radical radiotherapy set. However, such a separate radiotherapy validation set was not available.

The Radical Cystectomy set was a useful "control" set to interrogate whether the significant findings of AIMP3 and ERCC1 in the BCON set indicated that they were truly predictive of radiotherapy outcome or whether they were simply prognostic of survival in bladder cancer. Ideally, this set would also have been obtained from a trial setting. However, this was not possible particularly in view of the unsuccessful SPARE trial. The advantages of the Radical Cystectomy set used were that it was large (n=151), contemporary and from a single UK institution. The dataset was deemed to be robust with characteristics that would be typically expected from a radical cystectomy series. However, for the reasons explained above with respect to BCON, it would have been desirable to either have had a larger Radical Cystectomy set or a similarly-sized separate set for validation purposes although this (a validation cystectomy set) is perhaps less important an issue compared to a validation radiotherapy set.

The Neoadjuvant set was created, following ethics approval (EC06.11), by collating tissue materials and corresponding clinical data from multiple centres in the UK. The sample size (n=84) was satisfactory but the targeted sample size (n>150 to make it comparable with the BCON and Radical Cystectomy sets) could not be achieved due primarily to the difficulties with ensuring local ethics approval at potential collaborating sites to release materials and data. Furthermore, due to the inherent nature of retrospectively identifying and collecting materials, not all materials or data were available. However, the clinic-pathological characteristics of the available Neoadjuvant set was considered to be robust to use as a platform to interrogate the predictive value of the markers in differentiating survival outcomes following neoadjuvant cisplatin-based chemotherapy. It was felt that, although it may not be

large and robust enough as the BCON trial set to demonstrate highly significant results, it might still be adequate to reveal any signal of significance with respect to the markers if there was any present. In this respect, p53 status narrowly missed significance in this set. ERCC1, AIMP3 and Mre11 were not significant. It would be interesting to investigate whether p53 demonstrated significance in a larger Neoadjuvant set. Another noteworthy point with respect to the Neoadjuvant set is that there was no significant difference in overall survival between the radical cystectomy and radical radiotherapy groups. This finding is in keeping with what would be expected. In other words, there should either not be a significant difference or, if there were any difference, there should be a marginal difference in favour of radical surgery. A significantly larger sample size would be required to demonstrate a significant difference between the two groups and this was not the purpose of the Neoadjuvant set. However, if a larger Neoadjuvant set was created, on account of inclusion of patients ultimately either undergoing surgery or radiotherapy, it might provide a validation set for both the BCON "radiation set" and the Radical Cystectomy "control set". In its current state (n=84), with 46 patients (55%) in the radical cystectomy group and 38 patients (45%) in the radical radiotherapy group, the Neoadjuvant set is not large enough to provide independent validation sets for "radiation" and "control" purposes.

The LaMB set had the advantage of arising from a clinical trial and allowed the investigation of cisplatin-based chemotherapy in bladder cancer in a different setting – palliative treatment to control the progression of locally advanced or metastatic disease. One of the main limitations of the LaMB set is that the trial is not completed. As a result, rather than a potential 214 patients, only 72 could be

included in the current TMA set. Furthermore, the event rate (deaths) was low as a significant number of patients included had not had adequate periods of follow-up. These issues make interpretation of the LaMB set findings unreliable in its current state. However, once completed and "mature" after a period of follow-up, it would be worth interrogating the markers on this set. The effects of cisplatin on progression-free or overall survival may be more pronounced on the LaMB set as compared to the Neoadjuvant set. In the neoadjuvant setting, the survival benefits of cisplatin are known to be small (but significant) with the main bulk of the survival advantage being accorded by the radical treatment modality, either surgery or radiotherapy. Therefore, the LaMB set is a worthwhile platform to interrogate in the future when trying to answer the question of cisplatin-response in the clinical setting.

9.2 Summary of the thesis' findings and future directions

The main hypothesis of the thesis was "*AIMP3 is predictive of response to chemo- or radio-therapy in vitro in bladder cancer cell lines and may be predictive of clinical outcome following radio- or chemo-therapy in patients with muscle-invasive bladder cancer*." The body of work presented in this thesis aimed to evaluate the evidence to support or refute this hypothesis.

In Chapter 3, knockdown of AIMP3 by siRNA transfection, in the panel of bladder cancer cell lines used, was demonstrated to affect their radiosensitivity as measured by clonogenic survival assays. Downregulation of AIMP3 resulted in increased clonogenic survival following IC50 irradiation supporting the notion that AIMP3

may be an important tumour suppressor involved in the radiation-induced DNA damage response pathway. AIMP3 protein expression was characterised in the cell lines by Western blot analyses. The radiation dose-response characteristics of these cell lines were also characterised by clonogenic survival assays. The trafficking of AIMP3 from a cytosolic location into the nuclear compartment, following irradiation, as explored in this study. However, conclusive evidence to support this phenomenon could not be obtained. Future lab-based work could validate these findings in a wider panel of bladder cancer cell lines. Alternative methodologies, such as RTPCR, could be performed to confirm the Western findings. Further work on refining the immunofluorescence protocol could be done in order to attempt quantitation of the subcellular AIMP3 trafficking phenomenon. Alternatively, subcellular fractionation, followed by Western blot quantitation, could be attempted to investigate this phenomenon. There is also a wide scope to investigate the role of AIMP3 in the DDR pathway. The current project focused on measuring direct outcomes (e.g. clonogenic survival following AIMP3 knockdown; AIMP3 subcellular localisation through immunofluorescence following irradiation) related to AIMP3 status. However, the effects of AIMP3 on other DDR pathway molecules such as p53, ATM, ATR, and Chek proteins could be investigated and would provide important insights into the molecular biology of the complex DDR pathway. Such studies would require substantial lab-work and could form the basis of future PhD projects.

In Chapter 4, AIMP3 immunostaining status was demonstrated to be significantly predictive of radiotherapy outcome in the BCON set. Patients who were AIMP3-positive had a 47% survival advantage compared to those who were AIMP3-

negative. This was highly significant ($p<0.002$). The other significant finding was that tumour recurrence at 6 months was highly predictive of overall survival. Those whose tumours recurred, following radiotherapy, had an approximate 9-fold increased risk of death compared to those without recurrence ($p<0.001$). Interestingly, significantly more patients with tumour recurrences were also found to be AIMP3-negative ($p<0.001$). The findings support the hypothesis that AIMP3 is a significant predictor of radiotherapy outcome in patients with organ-confined MIBC. Future work needs to focus on validating these findings. This can be done in two main ways. Firstly, the findings can be externally validated using the BCON set itself. Secondly, a separate radical radiotherapy set can be used. The two pieces of work can form the basis of a good clinical research project.

In Chapter 5, the aim was to answer the question as to whether AIMP3 is truly predictive of radiotherapy outcome or whether it is simply prognostic for survival of patients with bladder cancer. The survival analyses on the Radical Cystectomy set, used as a "control" set for radiation treatment, answered this question. AIMP3 was not predictive of survival in the Radical Cystectomy set. The corollary of this finding is that AIMP3 is a predictive marker of radiotherapy outcome. There is scope for future work on this Radical Cystectomy set. The findings can be validated externally. Further follow-up may be performed and that will allow for a more robust dataset. More importantly, a separate radical cystectomy set may also be created from one or more contemporary series in the UK. Such work will require ethics approval and can form the basis of a clinical research project.

In Chapter 6, the aim was to investigate the predictive value of an additional panel of reported radiotherapy response markers on the BCON and Radical Cystectomy sets. On the basis of the reported literature, it was hypothesised that Mre11, ERCC1 and p53 may be predictive of radiotherapy outcome. The findings in the chapter demonstrated that ERCC1 immunostaining status was a highly significant predictor of radiotherapy outcome in the BCON set. Those who were ERCC1-negative had an approximate 3-fold (300%) survival advantage relative to those who were ERCC1-positive ($p<0.001$). Interrogation of ERCC1 in the Radical Cystectomy set, as with AIMP3, confirmed that ERCC1 status was not simply prognostic of survival. There was a suggestion, on univariate analysis, that Mre11 may also be predictive of radiotherapy outcome ($p=0.03$); however, this significance was lost on multivariate analysis ($p=0.372$). p53 status was not a significant predictor in either the BCON or Radical Cystectomy set. As with AIMP3, future work needs to be conducted to validate these findings, particularly the significance of ERCC1 as a predictor of radiotherapy outcome. As explained above for AIMP3, a validation radiation set would be required. In addition, external validation on the BCON set would be important.

In Chapter 7, the main objective was to explore the potential combinational permutations of the panel of markers in order to find a combination that could help stratify the patients in the BCON set into groups that were most or least likely to respond to radiotherapy. Combinational modelling demonstrated that the only significant permutation was a dual panel of AIMP3 and ERCC1 with four possible combinations depending on marker-positivity or –negativity respectively. The best prognostic combination (AIMP3+ERCC1-) had an approximate 6-fold survival

advantage relative to the worst prognostic combination (AIMP3-ERCC1+) and this finding was highly significant ($p<0.001$). The main value of this finding is in its potential clinical utility. If patients can be stratified, on the basis of the immunostaining profile of their diagnostic TURBT specimens, into a group that is likely to do well following radiotherapy, they can be offered radical radiotherapy as the best treatment option for them. The corollary of this is that, if their immunostaining profile predicts that they are not likely to respond well to radiotherapy, they can be offered radical cystectomy instead. This type of selection strategy would help ensure that patients undergo treatments most likely to benefit them and avoid the specific side-effects of other treatments that they are not likely to benefit from in the first instance. Therefore, it is vital for future work to validate the AIMP3 and ERCC1 findings. Validation would provide the platform for the markers to be investigated formally in a clinical setting. This would be best achieved in a clinical trial setting.

In Chapter 8, the findings suggested that AIMP3 expression predicts cisplatin response *in vitro* but that AIMP3 and ERCC1 were both not predictive of outcome in the Neoadjuvant and LaMB sets. Firstly, siRNA knockdown of AIMP3 in RT112 and RT112CP cells resulted in an increase in clonogenic survival following IC50 cisplatin exposure. As with AIMP3 in the context of radiation exposure, the findings indicated that AIMP3 may play an important role in the cisplatin-mediated DNA damage response pathway. Future lab-based work would need to validate this finding preferably in a wider panel of bladder cancer cell lines. As ERCC1 is thought to play an integral role in the cisplatin-mediated DDR pathway, it would seem logical to characterise ERCC1 expression in the panel of bladder cancer cell

lines and to perform siRNA knockdown of ERCC1 to investigate any changes in functional outcome. The limitations of the Neoadjuvant and LaMB sets are already discussed above (**Sections 8.7** and **9.1.5**). In brief, there is scope to expand the Neoadjuvant set so that it serves as a robust platform in its own right. Furthermore, with a larger size, it has the potential to provide both the radiation and cystectomy validation sets. The LaMB set would be worth revisiting within a few years as this would allow the full trial cohort to be included with adequate follow-up for censoring events.

9.3 Concluding remarks

In conclusion, the body of work presented in this thesis support the central hypothesis that AIMP3 expression is predictive of radiotherapy outcome *in vitro* and that it is predictive of radiotherapy outcome in patients with organ-confined MIBC. However, future work would need to validate the *in vitro* as well as BCON set findings. AIMP3 was also demonstrated to be predictive of cisplatin-based chemotherapy outcome *in vitro*. However, it would be useful to validate this on a wider panel of bladder cancer cell lines as well as to investigate the role of ERCC1 expression in these cell lines.

The role of other key DDR pathway effectors could form the basis of future lab-based projects to improve our understanding of the pathway. Such studies may also highlight other effectors, in the DDR pathway, which may be worth interrogating in a clinical setting such as in the radiotherapy, chemotherapy or cystectomy sets. If they are found to be significant, such markers could help to augment the current

predictive panel comprising of AIMP3 and ERCC1. Future work, subsequent to validation work, would entail conducting a clinical trial to investigate the predictive panel. The eventual future direction would involve the use of such a predictive panel to effect a paradigm change in the contemporary management of organ-confined MIBC, by helping to stratify patients into effective treatment algorithms.

References

AHN, J.-Y., SCHWARZ, J. K., PIWNICA-WORMS, H. & CANMAN, C. E. 2000. Threonine 68 Phosphorylation by Ataxia Telangiectasia Mutated Is Required for Efficient Activation of Chk2 in Response to Ionizing Radiation. *Cancer Research, 60***,** 5934-5936.

AITCHISON, A. A., VEERAKUMARASIVAM, A., VIAS, M., KUMAR, R., HAMDY, F. C., NEAL, D. E. & MILLS, I. G. 2008. Promoter methylation correlates with reduced Smad4 expression in advanced prostate cancer. *The Prostate,* 68**,** 661-74.

ANAND, P., KUNNUMAKARA, A. B., SUNDARAM, C., HARIKUMAR, K. B., THARAKAN, S. T., LAI, O. S., SUNG, B. Y. & AGGARWAL, B. B. 2008. Cancer is a Preventable Disease that Requires Major Lifestyle Changes. *Pharmaceutical Research,* 25**,** 2097-2116.

ANDREASSEN, P. R., D'ANDREA, A. D. & TANIGUCHI, T. 2004. ATR couples FANCD2 monoubiquitination to the DNA-damage response. *Genes & development,* 18**,** 1958-63.

AVIGAN, M. I., STROBER, B. & LEVENS, D. 1990. A far upstream element stimulates c-myc expression in undifferentiated leukemia cells. *The Journal of biological chemistry,* 265**,** 18538-45.

BAKKENIST, C. J. & KASTAN, M. B. 2003. DNA damage activates ATM through intermolecular autophosphorylation and dimer dissociation. *Nature,* 421**,** 499-506.

BALL, H. L., EHRHARDT, M. R., MORDES, D. A., GLICK, G. G., CHAZIN, W. J. & CORTEZ, D. 2007. Function of a conserved checkpoint recruitment domain in ATRIP proteins. *Molecular and cellular biology,* 27**,** 3367-77.

BARLOW, C., HIROTSUNE, S., PAYLOR, R., LIYANAGE, M., ECKHAUS, M., COLLINS, F., SHILOH, Y., CRAWLEY, J. N., RIED, T., TAGLE, D. & WYNSHAW-BORIS, A. 1996. Atm-deficient mice: a paradigm of ataxia telangiectasia. *Cell,* 86**,** 159-71.

BARROS, L. F., COELHO, I. J., PETRINI, C. A., CHAGAS, A. C. & ROCHA E SILVA, M. 2000. Myocardial reperfusion: leukocyte accumulation in the ischemic and remote non-ischemic regions. *Shock,* 13**,** 67-71.

BARRY, S. P., TOWNSEND, P. A., KNIGHT, R. A., SCARABELLI, T. M., LATCHMAN, D. S. & STEPHANOU, A. 2010. STAT3 modulates the DNA damage response pathway. *International journal of experimental pathology,* 91**,** 506-14.

BARTOLI, G., BELLUCCI, M. C., PETRINI, M., MARCANTONI, E., SAMBRI, L. & TORREGIANI, E. 2000. An Efficient Procedure for the Diastereoselective Dehydration of beta-Hydroxy Carbonyl Compounds by CeCl(3).7H(2)O/NaI System. *Organic letters,* 2**,** 1791-1793.

BASSI, P., FERRANTE, G. D., PIAZZA, N., SPINADIN, R., CARANDO, R., PAPPAGALLO, G. & PAGANO, F. 1999. Prognostic factors of outcome after radical cystectomy for bladder cancer: a retrospective study of a homogeneous patient cohort. *The Journal of urology,* 161**,** 1494-7.

BAZZI, C., PETRINI, C., RIZZA, V., ARRIGO, G. & D'AMICO, G. 2000. A modern approach to selectivity of proteinuria and tubulointerstitial damage in nephrotic syndrome. *Kidney international,* 58**,** 1732-41.

BEDFORD, P., SHELLARD, S. A., WALKER, M. C., WHELAN, R. D. H., MASTERS, J. R. W. & HILL, B. T. 1987. Differential Expression of Collateral Sensitivity or Resistance to Cisplatin in Human Bladder-Carcinoma Cell-Lines Preexposed Invitro to Either X-Irradiation or Cisplatin. *International Journal of Cancer,* 40**,** 681-686.

BELLMUNT, J., PAZ-ARES, L., CUELLO, M., CECERE, F. L., ALBIOL, S., GUILLEM, V., GALLARDO, E., CARLES, J., MENDEZ, P., DE LA CRUZ, J. J., TARON, M., ROSELL, R. & BASELGA, J. 2007. Gene expression of ERCC1 as a novel prognostic marker in advanced bladder cancer patients receiving cisplatin-based chemotherapy. *Annals of oncology : official journal of the European Society for Medical Oncology / ESMO,* 18**,** 522-8.

BERKOVICH, E., MONNAT, R. J. & KASTAN, M. B. 2007. Roles of ATM and NBS1 in chromatin structure modulation and DNA double-strand break repair. *Nature cell biology,* 9**,** 683-90.

BESSHO, T. 1995. Purification and characterization of the XPF-ERCC1 complex of human DNA repair excision nuclease. *The Journal of biological chemistry*, 270, 22657–22660.

BEUCHER, A., BIRRAUX, J., TCHOUANDONG, L., BARTON, O., SHIBATA, A., CONRAD, S., GOODARZI, A. A., KREMPLER, A., JEGGO, P. A. & LÖBRICH, M. 2009. ATM and Artemis promote homologous recombination of radiation-induced DNA double-strand breaks in G2. *The EMBO journal,* 28**,** 3413-27.

BHASKARA, V., DUPRÉ, A., LENGSFELD, B., HOPKINS, B. B., CHAN, A., LEE, J.-H., ZHANG, X., GAUTIER, J., ZAKIAN, V. & PAULL, T. T. 2007. Rad50 adenylate kinase activity regulates DNA tethering by Mre11/Rad50 complexes. *Molecular cell,* 25**,** 647-61.

BLASINA, A., DE WEYER, I. V., LAUS, M. C., LUYTEN, W. H., PARKER, A. E. & MCGOWAN, C. H. 1999. A human homologue of the checkpoint kinase Cds1 directly inhibits Cdc25 phosphatase. *Current biology : CB,* 9**,** 1-10.

BOOTH, C., HARNDEN, P., TREJDOSIEWICZ, L. K., SCRIVEN, S., SELBY, P. J. & SOUTHGATE, J. 1997. Stromal and vascular invasion in an human in vitro bladder cancer model. *Laboratory Investigation,* 76**,** 843-57.

BROWN, E. J. & BALTIMORE, D. 2000. ATR disruption leads to chromosomal fragmentation and early embryonic lethality service ATR disruption leads to chromosomal fragmentation and early embryonic lethality. *Genes & Development***,** 397-402.

BROWN, E. J. & BALTIMORE, D. 2003. Essential and dispensable roles of ATR in cell cycle arrest and genome maintenance. *Genes & development,* 17**,** 615-28.

BRUMBAUGH, K. M., OTTERNESS, D. M., GEISEN, C., OLIVEIRA, V., BROGNARD, J., LI, X., LEJEUNE, F., TIBBETTS, R. S., MAQUAT, L. E. & ABRAHAM, R. T. 2004. The mRNA surveillance protein hSMG-1 functions in genotoxic stress response pathways in mammalian cells. *Molecular cell,* 14**,** 585-98.

BUBENIK, J., BARESOVA, M., VIKLICKY, V., JAKOUBKO.J, SAINEROV.H & DONNER, J. 1973. Established Cell Line of Urinary-Bladder Carcinoma (T-24) Containing Tumor-Specific Antigen. *International Journal of Cancer,* 11**,** 765-773.

BURKHART, D. L. & SAGE, J. 2008. Cellular mechanisms of tumour suppression by the retinoblastoma gene. *Nature Reviews Cancer,* 8**,** 671-682.

BURMA, S., CHEN, B. P., MURPHY, M., KURIMASA, A. & CHEN, D. J. 2001. ATM phosphorylates histone H2AX in response to DNA double-strand breaks. *The Journal of biological chemistry,* 276**,** 42462-7.

CARNEY, J. P., MASER, R. S., OLIVARES, H., DAVIS, E. M., LE BEAU, M., YATES, J. R., HAYS, L., MORGAN, W. F. & PETRINI, J. H. 1998. The hMre11/hRad50 protein complex and Nijmegen breakage syndrome: linkage of double-strand break repair to the cellular DNA damage response. *Cell,* 93**,** 477-86.

CARULLI, G., MARINI, A., AZZARA, A., VANACORE, R. & PETRINI, M. 2000. Cyclic oscillations of neutrophils, monocytes, and CD8-positive lymphocytes in a healthy subject. *Haematologica,* 85**,** 447-8.

CHAKRAVARTI, A., WINTER, K., WU, C.-L., KAUFMAN, D., HAMMOND, E., PARLIAMENT, M., TESTER, W., HAGAN, M., GRIGNON, D., HENEY, N., POLLACK, A., SANDLER, H. & SHIPLEY, W. 2005. Expression of the epidermal growth factor receptor and Her-2 are predictors of favorable outcome and reduced complete response rates, respectively, in patients with muscle-invading bladder cancers treated by concurrent radiation and cisplatin-based chemot. *International journal of radiation oncology, biology, physics,* 62**,** 309-17.

CHATTERJEE, S.J., DATAR, R., YOUSSEFZADEH, D., GEORGE, B., GOEBELL, P.J., STEIN, J.P., YOUNG, L., SHI, S.R., GEE, C., GROSHEN, S., SKINNER, D.G. & COTE, R.J. 2004. Combined effects of p53, p21 and pRb expression in the progression of bladder transitional cell carcinoma. *The Journal of clinical oncology,* 22, 1007-13.

CHEN, B. P. C., CHAN, D. W., KOBAYASHI, J., BURMA, S., ASAITHAMBY, A., MOROTOMI-YANO, K., BOTVINICK, E., QIN, J. & CHEN, D. J. 2005a. Cell cycle dependence of DNA-dependent protein kinase phosphorylation in response to DNA double strand breaks. *The Journal of biological chemistry,* 280**,** 14709-15.

CHEN, L., TRUJILLO, K. M., VAN KOMEN, S., ROH, D. H., KREJCI, L., LEWIS, L. K., RESNICK, M. A., SUNG, P. & TOMKINSON, A. E. 2005b. Effect of amino acid substitutions in the rad50 ATP binding domain on DNA double strand break repair in yeast. *The Journal of biological chemistry,* 280**,** 2620-7.

CHEN, P., WIENCKE, J., ALDAPE, K., KESLER-DIAZ, A., MIIKE, R., KELSEY, K., LEE, M., LIU, J. & WRENSCH, M. 2000. Association of an ERCC1 polymorphism with adult-onset glioma. *Cancer Epidemiology, Biomarkers and Prevention*, 9, 843–847.

CHOI, J. W., KIM, D. G., PARK, M. C., UM, J. Y., HAN, J. M., PARK, S. G., CHOI, E. C. & KIM, S. 2009a. AIMP2 promotes TNFalpha-dependent apoptosis via ubiquitin-mediated degradation of TRAF2. *Journal of cell science,* 122**,** 2710-5.

CHOI, J. W., UM, J. Y., KUNDU, J. K., SURH, Y.-J. & KIM, S. 2009b. Multidirectional tumor-suppressive activity of AIMP2/p38 and the enhanced susceptibility of AIMP2 heterozygous mice to carcinogenesis. *Carcinogenesis,* 30**,** 1638-44.

CHOI, Y-J., RYU, K-S., KO, Y-M., CHAE, Y-K., PELTON, J. G., WEMMER, D. E. & CHOI, B-S. 2005. Biophysical characterization of the interaction domains and mapping of the contact residues in the XPF-ERCC1 complex. *The Journal of biological chemistry*, 280, 28644–28652.

CHOUDHURY, A., NELSON, L. D., TEO, M. T. W., CHILKA, S., BHATTARAI, S., JOHNSTON, C. F., ELLIOTT, F., LOWERY, J., TAYLOR, C. F., CHURCHMAN, M., BENTLEY, J., KNOWLES, M. A., HARNDEN, P., BRISTOW, R. G., BISHOP, D. T. & KILTIE, A. E. 2010. MRE11 expression is predictive of cause-specific survival following radical radiotherapy for muscle-invasive bladder cancer. *Cancer research,* 70**,** 7017-26.

CHOUEIRI, T. K., JACOBUS, S., BELLMUNT, J., QU, A., APPLEMAN, L. J., TRETTER, C., BUBLEY, G. J., STACK, E., SIGNORETTI, S., WALSH, M., STEELE, G., HIRSCH, M., SWEENEY, C. J., TAPLIN, M. E., KIBEL, A. S., KRAJEWSKI, K. M., KANTOFF, P. W., ROSS, R. W. & ROSENBERG, J. E. 2014. Neoadjuvant dose-dense methotrexate, vinblastine, doxorubicin, and cisplatin with pegfilgrastim support in muscle-invasive urothelial cancer: pathologic, radiologic, and biomarker correlates. *Journal of clinical oncology*, 32, 1889-94.

CIMPRICH, K. A. & CORTEZ, D. 2008. ATR: an essential regulator of genome integrity. *Nature reviews. Molecular cell biology,* 9**,** 616-27.

COLTON, S.L., XU, X.S., WANG, Y.A. & WANG, G. 2006. The involvement of ataxia-telangiectasia mutated protein activation in nucleotide excision repair-facilitated cell survival with cisplatin treatment. *The Journal of Bioliological Chemistry*, 281, 27117–25.

COOPER, M. J., HALUSCHAK, J. J., JOHNSON, D., SCHWARTZ, S., MORRISON, L. J., LIPPA, M., HATZIVASSILIOU, G. & TAN, J. 1994. P53 Mutations in Bladder-Carcinoma Cell-Lines. *Oncology Research,* 6**,** 569-579.

COPPIN, C. M. L., GOSPODAROWICZ, M. K., JAMES, K., TANNOCK, I. F., ZEE, B., CARSON, J., PATER, J. & SULLIVAN, L. D. 1996. Improved local control of invasive bladder cancer by concurrent cisplatin and preoperative or definitive radiation. *Journal of Clinical Oncology*, 14**,** 2901-2907.

CORTEZ, D. 1999. Requirement of ATM-Dependent Phosphorylation of Brca1 in the DNA Damage Response to Double-Strand Breaks. *Science,* 286**,** 1162-1166.

CORTEZ, D., GUNTUKU, S., QIN, J. & ELLEDGE, S. J. 2001. ATR and ATRIP: partners in checkpoint signaling. *Science (New York, N.Y.),* 294**,** 1713-6.

COUGHLIN, C., HEANEY, J., KRALL, J., PH, D., MARTZ, K., VENNER, P. & HAMMOND, E. 1993. ?? Clinical Original Contribution COMBINED MODALITY PROGRAM WITH POSSIBLE ORGAN PRESERVATION FOR INVASIVE BLADDER CARCINOMA : RESULTS OF RTOG PROTOCOL 85-12. *Physics*.

CROCE, C. M. 2008. Molecular origins of cancer: Oncogenes and cancer. *New England Journal of Medicine,* 358**,** 502-511.

CRUET-HENNEQUART, S., GLYNN, M.T., MURILLO, L.S., COYNE, S. & CARTY, M.P. 2008. Enhanced DNA-PK-mediated RPA2 hyperphosphorylation in DNA polymerase eta-deficient human cells treated with cisplatin and oxaliplatin. *DNA Repair (Amst),* 7, 582–96.

DA SILVA, G.N., DE CASTRO MARCONDES, J.P., DE CAMARGO, E.A., DA SILVA PASSOS JUNIOR, G.A., SAKAMOTO-HOJO, E.T. & SALVADORI, D.M. 2010. Cell cycle arrest and apoptosis in *TP53* subtypes of bladder carcinoma cell lines treated with cisplatin and gemcitabine. *Experimental Biology and Medicine*, 235, 814-824.

DALBAGNI, G., GENEGA, E., HASHIBE, M., ZHANG, Z. F., RUSSO, P., HERR, H. & REUTER, V. 2001. Cystectomy for bladder cancer: a contemporary series. *The Journal of urology,* 165**,** 1111-6.

DAVIES, G., JIANG, W. G. & MASON, M. D. 1999. Cell-cell adhesion molecules and their associated proteins in bladder cancer cells and their role in mitogen induced cell-cell dissociation and invasion. *Anticancer Research,* 19**,** 547-552.

DE JAGER, M., TRUJILLO, K. M., SUNG, P., HOPFNER, K.-P., CARNEY, J. P., TAINER, J. A., CONNELLY, J. C., LEACH, D. R. F., KANAAR, R. & WYMAN, C. 2004. Differential arrangements of conserved building blocks among homologs of the Rad50/Mre11 DNA repair protein complex. *Journal of molecular biology,* 339**,** 937-49.

DE KLEIN, A., MUIJTJENS, M., VAN OS, R., VERHOEVEN, Y., SMIT, B., CARR, A. M., LEHMANN, A. R. & HOEIJMAKERS, J. H. 2000. Targeted disruption of the cell-cycle checkpoint gene ATR leads to early embryonic lethality in mice. *Current biology : CB,* 10**,** 479-82.

DE LANGE, T. & PETRINI, J. H. 2000. A new connection at human telomeres: association of the Mre11 complex with TRF2. *Cold Spring Harbor Symposia on Quantitative Biology,* 65**,** 265-73.

DE NEVE, W., LYBEERT, M. L., GOOR, C., CROMMELIN, M. A. & RIBOT, J. G. 1995. Radiotherapy for T2 and T3 carcinoma of the bladder: the influence of overall treatment time. *Radiotherapy and oncology : journal of the European Society for Therapeutic Radiology and Oncology,* 36**,** 183-8.

DOIL, C., MAILAND, N., BEKKER-JENSEN, S., MENARD, P., LARSEN, D. H., PEPPERKOK, R., ELLENBERG, J., PANIER, S., DUROCHER, D., BARTEK, J., LUKAS, J. & LUKAS,

C. 2009. RNF168 binds and amplifies ubiquitin conjugates on damaged chromosomes to allow accumulation of repair proteins. *Cell,* 136**,** 435-46.

DONEHOWER, L. A., HARVEY, M., SLAGLE, B. L., MCARTHUR, M. J., MONTGOMERY, C. A., BUTEL, J. S. & BRADLEY, A. 1992. Mice Deficient for P53 Are Developmentally Normal but Susceptible to Spontaneous Tumors. *Nature,* 356**,** 215-221.

EL AMIN, N. M., HANSON, H. S., PETTERSSON, B., PETRINI, B. & VON STEDINGK, L. V. 2000. Identification of non-tuberculous mycobacteria: 16S rRNA gene sequence analysis vs. conventional methods. *Scandinavian journal of infectious diseases,* 32**,** 47-50.

ELLIOTT, A. Y., BRONSON, D. L., CERVENKA, J., ELLIOTT, V., STEIN, N. & FRALEY, E. E. 1977. Properties of Cell Lines Established from Transitional Cell Cancers of the Human Urinary Tract Properties of Cell Lines Established from Transitional Cell Cancers of the Human UrinaryTract1. *Cancer***,** 1279-1289.

ELLIOTT, A. Y., CLEVELAN.P, CERVENKA, J., CASTRO, A. E., STEIN, N., HAKALA, T. R. & FRALEY, E. E. 1974. Characterization of a Cell Line from Human Transitional Cell Cancer of Urinary-Tract. *Journal of the National Cancer Institute,* 53**,** 1341-1349.

ELSON, A., WANG, Y., DAUGHERTY, C. J., MORTON, C. C., ZHOU, F., CAMPOS-TORRES, J. & LEDER, P. 1996. Pleiotropic defects in ataxia-telangiectasia protein-deficient mice. *Proceedings of the National Academy of Sciences of the United States of America,* 93**,** 13084-9.

ESRIG, D., ELMANJIAN, D., GROSHEN, S., FREEMAN, J.A., STEIN, J.P., CHEN, S.C., NICHOLS, P.W., SKINNER, D.G., JONES, P.A. & COTE, R.J. 1994. Accumulation of nuclear p53 and tumor progression in bladder cancer. *New England Journal of Medicine,* 331, 1259-64.

FAENZA, S. & PETRINI, F. 2000. [Mechanical ventilation in the emergency room]. *Minerva anestesiologica,* 66**,** 883-7.

FALCK, J., MAILAND, N., SYLJUÅSEN, R. G., BARTEK, J. & LUKAS, J. 2001. The ATM-Chk2-Cdc25A checkpoint pathway guards against radioresistant DNA synthesis. *Nature,* 410**,** 842-7.

FOHLMAN, J., SJOLIN, J., BENNICH, H., CHRYSSANTHOU, E., VON ROSEN, M. & PETRINI, B. 2000. Coccidioidomycosis as imported atypical pneumonia in Sweden. *Scandinavian journal of infectious diseases,* 32**,** 440-1.

GARCIA DEL MURO, X., CONDOM, E., VIGUES, F., CASTELLSAGUE, X., FIGUERAS, A., MUNOZ, J., SOLA, J., SOLER, T., CAPELLA, G. & GERMA, J.R. 2004. p53 and p21 Expression levels predict organ preservation and survival in invasive bladder carcinoma treated with a combined-modality approach. *Cancer,*100,1859-67.

GHIRARDINI, A., COSTA, A. N., VENTURI, S., RIDOLFI, L., PETRINI, F., TADDEI, S., VENTUROLI, N., MONTI, M. & MARTINELLI, G. 2000a. Evaluation of the efficiency of organ procurement and transplantation program. *Transplantation proceedings,* 32**,** 100-3.

GHIRARDINI, A., NANNI-COSTA, A., VENTURI, S., RIDOLFI, L., PETRINI, F., TADDEI, S., VENTUROLI, A., PUGLIESE, M. R., MONTI, M. & MARTINELLI, G. 2000b. Efficiency of organ procurement and transplantation programs. *Transplant international : official journal of the European Society for Organ Transplantation,* 13 Suppl 1**,** S267-71.

GHONEIM, M. A., EL-MEKRESH, M. M., EL-BAZ, M. A., EL-ATTAR, I. A. & ASHAMALLAH, A. 1997. Radical cystectomy for carcinoma of the bladder: critical evaluation of the results in 1,026 cases. *The Journal of urology,* 158**,** 393-9.

GIARDINA, A., MECOZZI, T. & PETRINI, M. 2000. Acyclic stereoselection in the reaction of nucleophilic reagents with chiral N-acyliminium ions generated from N. *The Journal of organic chemistry,* 65**,** 8277-82.

GIRARD, P. M., FORAY, N., STUMM, M., WAUGH, A., RIBALLO, E., MASER, R. S., PHILLIPS, W. P., PETRINI, J., ARLETT, C. F. & JEGGO, P. A. 2000. Radiosensitivity in Nijmegen Breakage Syndrome cells is attributable to a repair defect and not cell cycle checkpoint defects. *Cancer research,* 60**,** 4881-8.

GONZALEZ, V. M., FUERTES, M. A., ALONSO, C & PEREZ, J. M. 2001. Is cisplatin-induced cell death always produced by apoptosis? *Molecular Pharmacology*, 59, 657–663.

GORDON, G. M. & DU, W. 2011. Conserved RB functions in development and tumor suppression. *Protein & Cell,* 2**,** 864-78.

GOSPODAROWICZ, M. K., HAWKINS, N. V., RAWLINGS, G. A., CONNOLLY, J. G., JEWETT, M. A. S., THOMAS, G. M., HERMAN, J. G., GARRETT, P. G., CHUA, T., DUNCAN, W., BUCKSPAN, M., SUGAR, L. & RIDER, W. D. 1989. Radical Radiotherapy for Muscle Invasive Transitional Cell-Carcinoma of the Bladder - Failure Analysis. *Journal of Urology,* 142**,** 1448-1454.

HALL, R. R., NEWLING, D. W. W., RAMSDEN, P. D., RICHARDS, B., ROBINSON, M. R. G. & SMITH, P. H. 1984. Treatment of Invasive Bladder-Cancer by Local Resection and High-Dose Methotrexate. *British Journal of Urology,* 56**,** 668-672.

HALL, R. R., ROBERTS, J. T. & MARSH, M. M. 1990. Radical Tur and Chemotherapy Aiming at Bladder Preservation. *Neoadjuvant Chemotherapy in Invasive Bladder Cancer,* 353**,** 163-168.

HAN, J. M., LEE, M. J., PARK, S. G., LEE, S. H., RAZIN, E., CHOI, E.-C. & KIM, S. 2006a. Hierarchical network between the components of the multi-tRNA synthetase complex: implications for complex formation. *The Journal of biological chemistry,* 281**,** 38663-7.

HAN, J. M., PARK, B. J., PARK, S. G., OH, Y. S., CHOI, S. J., LEE, S. W., HWANG, S. K., CHANG, S. H., CHO, M. H. & KIM, S. 2008. AIMP2/p38, the scaffold for the multi-tRNA synthetase complex, responds to genotoxic stresses via p53. *Proceedings of the National Academy of Sciences of the United States of America,* 105**,** 11206-11.

HAN, J. M., PARK, S. G., LEE, Y. & KIM, S. 2006b. Structural separation of different extracellular activities in aminoacyl-tRNA synthetase-interacting multi-functional protein, p43/AIMP1. *Biochemical and biophysical research communications,* 342**,** 113-8.

HANAHAN, D. & WEINBERG, R. A. 2011. Hallmarks of Cancer: The Next Generation. *Cell,* 144**,** 646-674.

HARRIS, H. 1988. The Analysis of Malignancy by Cell-Fusion - the Position in 1988. *Cancer research,* 48**,** 3302-3306.

HAUPT, Y., MAYA, R., KAZAZ, A. & OREN, M. 1997. Mdm2 promotes the rapid degradation of p53. *Nature,* 387**,** 296-9.

HENRY, K., MILLER, J., MORI, M., LOENING, S. & FALLON, B. 1988. Comparison of Trans-Urethral Resection to Radical Therapies for Stage-B Bladder-Tumors. *Journal of Urology,* 140**,** 964-967.

HERR, H. W. 1987. Conservative Management of Muscle-Infiltrating Bladder-Cancer - Prospective Experience. *Journal of Urology,* 138**,** 1162-1163.

HERR, H. W., BAJORIN, D. F. & SCHER, H. I. 1998. Neoadjuvant chemotherapy and bladder-sparing surgery for invasive bladder cancer: Ten-year outcome. *Journal of Clinical Oncology,* 16**,** 1298-1301.

HINATA, N., SHIRAKAWA, T., ZHANG, Z., MATSUMOTO, A., FUJISAWA, M., OKADA, H., KAMIDONO, S. & GOTOH, A. 2003. Radiation induces p53-dependent cell apoptosis in

bladder cancer cells with wild-type- p53 but not in p53-mutated bladder cancer cells. *Urological research,* 31**,** 387-96.

HOFFMANN, A.C., WILD, P. LEICHT, C., BERTZ, S., DANENBERG, P.V., STOHR, R., STOCKLE, M., LEHMANN, J., SCHULER, M. & HARTMANN, A. 2010. MDR1 and ERCC1 expression predict outcome of patients with locally advanced bladder cancer receiving adjuvant chemotherapy. *Neoplasia,* 12, 628-36.

HOLMAN, P. J., MADELEY, J., CRAIG, T. M., ALLSOPP, B. A., ALLSOPP, M. T., PETRINI, K. R., WAGHELA, S. D. & WAGNER, G. G. 2000. Antigenic, phenotypic and molecular characterization confirms Babesia odocoilei isolated from three cervids. *Journal of wildlife diseases,* 36**,** 518-30.

HOPFNER, K. P., KARCHER, A., CRAIG, L., WOO, T. T., CARNEY, J. P. & TAINER, J. A. 2001. Structural biochemistry and interaction architecture of the DNA double-strand break repair Mre11 nuclease and Rad50-ATPase. *Cell,* 105**,** 473-85.

HOPFNER, K. P., KARCHER, A., SHIN, D. S., CRAIG, L., ARTHUR, L. M., CARNEY, J. P. & TAINER, J. A. 2000. Structural biology of Rad50 ATPase: ATP-driven conformational control in DNA double-strand break repair and the ABC-ATPase superfamily. *Cell,* 101**,** 789-800.

HORWICH, A., DEARNALEY, D., HUDDART, R., GRAHAM, J., BESSELL, E., MASON, M. & BLISS, J. 2005. A randomised trial of accelerated radiotherapy for localised invasive bladder cancer. *Radiotherapy and oncology : journal of the European Society for Therapeutic Radiology and Oncology,* 75**,** 34-43.

HOSKIN, P. J., ROJAS, A. M., BENTZEN, S. M., SAUNDERS, M. I. & INVESTIGATORS, B. 2010. Radiotherapy With Concurrent Carbogen and Nicotinamide in Bladder Carcinoma. *Journal of Clinical Oncology,* 28**,** 4912-4918.

HUDDART, R. A., HALL, E., HUSSAIN, S. A., JENKINS, P., RAWLINGS, C., TREMLETT, J., CRUNDWELL, M., ADAB, F. A., SHEEHAN, D., SYNDIKUS, I., HENDRON, C., LEWIS, R., WATERS, R. & JAMES, N. D. 2013. Randomized noninferiority trial of reduced high-dose volume versus standard volume radiation therapy for muscle-invasive bladder cancer: results of the BC2001 trial (CRUK/01/004). *International journal of radiation oncology, biology, physics,* 87, 860.

JALAL, S., EARLEY, J.N. & TURCHI, J.J. 2011. DNA repair: from genome maintenance to biomarker and therapeutic target. *Clinical Cancer Research,* 17, 6973–84.

JAMES, N. D., HUSSAIN, S.A., HALL, E., JENKINS, P., TREMLETT, J., RAWLINGS, C., CRUNDWELL, M., SIZER, B., SREENIVASAN, T., HENDRON, C., LEWIS, R., WATERS, R., HUDDART & BC2001 Investigators. 2012. Radiotherapy with or without chemotherapy in muscle-invasive bladder cancer. *New England Journal of Medicine*, 366, 1477-88.

JAZAYERI, A., FALCK, J., LUKAS, C., BARTEK, J., SMITH, G. C. M., LUKAS, J. & JACKSON, S. P. 2006. ATM- and cell cycle-dependent regulation of ATR in response to DNA double-strand breaks. *Nature cell biology,* 8**,** 37-45.

JEGGO, P. A. 1998. Identification of genes involved in repair of DNA double-strand breaks in mammalian cells. *Radiation research,* 150**,** S80-91.

JEMAL, A., BRAY, F., CENTER, M. M., FERLAY, J., WARD, E. & FORMAN, D. 2011. Global Cancer Statistics. *Ca-a Cancer Journal for Clinicians,* 61**,** 69-90.

JENKINS, B. J., CAULFIELD, M. J., FOWLER, C. G., BADENOCH, D. F., TIPTAFT, R. C., PARIS, A. M. I., HOPESTONE, H. F., OLIVER, R. T. D. & BLANDY, J. P. 1988. Reappraisal of the Role of Radical Radiotherapy and Salvage Cystectomy in the Treatment of Invasive (T2/T3) Bladder-Cancer. *British Journal of Urology,* 62**,** 343-346.

JUN, H. J., AHN, M. J., KIM, H. S., YI, S. Y., HAN, J., LEE, S. K., AHN, Y. C., JEONG, H-S., SON, Y-I., BAEK, J-H. & PARK, K. 2008. ERCC1 expression as a predictive marker of squamous cell carcinoma of the head and neck treated with cisplatin-based concurrent chemoradiation. *British Journal of Cancer*, 99, 167–172.

KARTALOU, M. & ESSIGMAN, J. M. 2001. Recognition of cisplatin adducts by cellular proteins. *Mutation Research*, 478, 1–21.

KANOH, Y., TAMAI, K. & SHIRAHIGE, K. 2006. Different requirements for the association of ATR-ATRIP and 9-1-1 to the stalled replication forks. *Gene,* 377**,** 88-95.

KASTAN, M. B. & BARTEK, J. 2004. Cell-cycle checkpoints and cancer. *Nature,* 432**,** 316-23.

KASTAN, M. B., ONYEKWERE, O., SIDRANSKY, D., VOGELSTEIN, B. & CRAIG, R. W. 1991. Participation of p53 Protein in the Cellular Response to DNA Damage Participation of p53 Protein in the Cellular Response to DNA Damage1. *Cancer***,** 6304-6311.

KASTAN, M. B., ZHAN, Q., EL-DEIRY, W. S., CARRIER, F., JACKS, T., WALSH, W. V., PLUNKETT, B. S., VOGELSTEIN, B. & FORNACE, A. J. 1992. A mammalian cell cycle

checkpoint pathway utilizing p53 and GADD45 is defective in ataxia-telangiectasia. *Cell,* 71**,** 587-97.

KAUFMAN, D. S., SHIPLEY, W. U., GRIFFIN, P. P., HENEY, N. M., ALTHAUSEN, A. F. & EFIRD, J. T. 1993. Selective Bladder Preservation by Combination Treatment of Invasive Bladder-Cancer. *New England Journal of Medicine,* 329**,** 1377-1382.

KAUFMAN, D. S., WINTER, K. A., SHIPLEY, W. U., HENEY, N. M., WALLACE, H. J., TOONKEL, L. M., ZIETMAN, A. L., TANGUAY, S. & SANDLER, H. M. 2009. Phase I-II RTOG study (99-06) of patients with muscle-invasive bladder cancer undergoing transurethral surgery, paclitaxel, cisplatin, and twice-daily radiotherapy followed by selective bladder preservation or radical cystectomy and adjuvant chemotherapy. *Urology,* 73**,** 833-7.

KAWASHIMA, A., NAKAYAMA, M., KAKUTA, Y., ABE, T., HATANO, K., MUKAI, M., NAGAHARA, A., NAKAI, Y., OKA, D., TAKAYAMA, H., YOSHIOKA, T., HOSHIDA, Y., ITATANI, H., NISHIMURA, K. & NONOMURA, N. 2011. Excision repair cross-complementing group 1 may predict the efficacy of chemoradiation therapy for muscle-invasive bladder cancer. *Clinical cancer research : an official journal of the American Association for Cancer Research,* 17**,** 2561-9.

KELLAND, L. 2007. The resurgence of platinum-based cancer chemotherapy. *Nature Reviews Cancer*, 7, 573–584.

KHANNA, K. K. & JACKSON, S. P. 2001. DNA double-strand breaks: signaling, repair and the cancer connection. *Nature genetics,* 27**,** 247-54.

KIESEWETTER, H., KOSCIELNY, J., KALUS, U., VIX, J. M., PEIL, H., PETRINI, O., VAN TOOR, B. S. & DE MEY, C. 2000. Efficacy of orally administered extract of red vine leaf AS 195 (folia vitis viniferae) in chronic venous insufficiency (stages I-II). A randomized, double-blind, placebo-controlled trial. *Arzneimittel-Forschung,* 50**,** 109-17.

KIM, E., KIM, S. H., KIM, S. & KIM, T. S. 2006. The novel cytokine p43 induces IL-12 production in macrophages via NF-kappaB activation, leading to enhanced IFN-gamma production in CD4+ T cells. *Journal of immunology (Baltimore, Md. : 1950),* 176**,** 256-64.

KIM, J. Y., KANG, Y.-S., LEE, J.-W., KIM, H. J., AHN, Y. H., PARK, H., KO, Y.-G. & KIM, S. 2002. p38 is essential for the assembly and stability of macromolecular tRNA synthetase complex: implications for its physiological significance. *Proceedings of the National Academy of Sciences of the United States of America,* 99**,** 7912-6.

KIM, K.H., DO, I. G., KIM, H. S., CHANG, M. H., KIM, H. S., JUN, H. J., UHM, J., YI, S. Y., LIM, H., JI, S. H., PARK, M. J., LEE, J., PARK, S. H., KWON, G. Y. & LIM, H. Y. 2010. Excision repair cross-complementation group 1 (ERCC1) expression in advanced urothelial carcinoma patients receiving cisplatin-based chemotherapy. *Acta Pathologica Microbiologica et Immunological Scandinavica,* 118, 941-8.

KIM, K.-J., PARK, M. C., CHOI, S. J., OH, Y. S., CHOI, E.-C., CHO, H. J., KIM, M. H., KIM, S.-H., KIM, D. W., KIM, S. & KANG, B. S. 2008. Determination of three-dimensional structure and residues of the novel tumor suppressor AIMP3/p18 required for the interaction with ATM. *The Journal of biological chemistry,* 283**,** 14032-40.

KIM, M. J., PARK, B.-J., KANG, Y.-S., KIM, H. J., PARK, J.-H., KANG, J. W., LEE, S. W., HAN, J. M., LEE, H.-W. & KIM, S. 2003. Downregulation of FUSE-binding protein and c-myc by tRNA synthetase cofactor p38 is required for lung cell differentiation. *Nature genetics,* 34**,** 330-6. KIM, M. K., CHO, K-J., KWON, G. Y., PARK, S-I., KIM, Y. H., KIM, J.H., SONG, H-Y., SHIN, J. H., JUNG, H. Y., LEE, G. H, CHOI, K. D. & KIM, S. B. 2008. ERCC1 predicting chemoradiation resistance and poor outcome in oesophageal cancer. *European journal of cancer*, 44, 54–60.

KIRBY, R., PETRINI, J. & ALTER, C. 2000. Collecting and interpreting birth defects surveillance data by hispanic ethnicity: a comparative study. The Hispanic Ethnicity Birth Defects Workgroup. *Teratology,* 61**,** 21-7.

KNOBE, K. E., VILLOUTREIX, B. O., TENGBORN, L. I., PETRINI, P. & LJUNG, R. C. 2000. Factor VIII inhibitors in two families with mild haemophilia A: structural analysis of the mutations. *Haemostasis,* 30**,** 268-79.

KNUDSON, A. G. 1971. Mutation and Cancer - Statistical Study of Retinoblastoma. *Proceedings of the National Academy of Sciences of the United States of America*, 68**,** 820-&.

KO, H. S., VON COELLN, R., SRIRAM, S. R., KIM, S. W., CHUNG, K. K., PLETNIKOVA, O., TRONCOSO, J., JOHNSON, B., SAFFARY, R., GOH, E. L., SONG, H., PARK, B. J., KIM, M. J., KIM, S., DAWSON, V. L. & DAWSON, T. M. 2005. Accumulation of the authentic parkin substrate aminoacyl-tRNA synthetase cofactor, p38/JTV-1, leads to catecholaminergic cell death. *Journal of Neuroscience,* 25**,** 7968-78.

KO, Y.-G., PARK, H. & KIM, S. 2002. Novel regulatory interactions and activities of mammalian tRNA synthetases. *Proteomics,* 2**,** 1304-10.

KUMAGAI, A. & DUNPHY, W. G. 2000. Claspin, a novel protein required for the activation of Chk1 during a DNA replication checkpoint response in Xenopus egg extracts. *Molecular cell,* 6**,** 839-49.

KUMAGAI, A., LEE, J., YOO, H. Y. & DUNPHY, W. G. 2006. TopBP1 activates the ATR-ATRIP complex. *Cell,* 124**,** 943-55.

KURAOKA, I., KOBERTZ, W. R., ARIZA, R. R., BIGGERSTAFF, M., ESSIGMANN, J. M. & WOOD, R. D. 2000. Repair of an interstrand DNA cross-link initiated by ERCC1-XPF repair/recombination nuclease. *The Journal of biological chemistry*, 275, 26632–26636.

KURZ, E. U. & LEES-MILLER, S. P. 2004. DNA damage-induced activation of ATM and ATM-dependent signaling pathways. *DNA repair,* 3**,** 889-900.

LAVIN, M. F. 2008. Ataxia-telangiectasia: from a rare disorder to a paradigm for cell signalling and cancer. *Nature reviews. Molecular cell biology,* 9**,** 759-69.

LEE, J.-H. & PAULL, T. T. 2005. ATM activation by DNA double-strand breaks through the Mre11-Rad50-Nbs1 complex. *Science (New York, N.Y.),* 308**,** 551-4.

LEE, J., KUMAGAI, A. & DUNPHY, W. G. 2007. The Rad9-Hus1-Rad1 checkpoint clamp regulates interaction of TopBP1 with ATR. *The Journal of biological chemistry,* 282**,** 28036-44.

LEE, S. W., CHO, B. H., PARK, S. G. & KIM, S. 2004. Aminoacyl-tRNA synthetase complexes: beyond translation. *Journal of cell science,* 117**,** 3725-34.

LEE, S. W., KIM, G. & KIMT, S. 2008. Aminoacyl-tRNA synthetase-interacting multi-functional protein 1/p43: an emerging therapeutic protein working at systems level. *Expert Opinion on Drug Discovery,* 3**,** 945-957.

LEE, Y. S., HAN, J. M., KANG, T. H., PARK, Y. I., KIM, H. M. & KIM, S. 2006. Antitumor activity of the novel human cytokine AIMP1 in an in vivo tumor model. *Molecules and Cells,* 21**,** 213-217.

LEWIS, K.A., LILLY, K.K., REYNOLDS, E.A., SULLIVAN, W.P., KAUFMANN, S.H. & CLIBY, W.A. 2009. Ataxia telangiectasia and rad3-related kinase contributes to cell cycle arrest and survival after cisplatin but not oxaliplatin. *Molecular Cancer Therapeutics*, 8, 855–63.

LI, L., ELLEDGE, S. J., PETERSON, C. A., BALES, E. S. & LEGERSKI, R. J. 1994. Specific association between the human DNA repair proteins XPA and ERCC1. *Proceedings of the National Academy of Sciences of the United States of America*, 91, 5012–5016.

LIEBER, M. R. 2010. The mechanism of double-strand DNA break repair by the nonhomologous DNA end-joining pathway. *Annual review of biochemistry,* 79**,** 181-211.

LIM, D.-S., KIM, S.-T., XU, B. & MASER, R. S. 2000a. S-phase checkpoint pathway. *Nature,* 404**,** 613-617.

LIM, D. S., KIM, S. T., XU, B., MASER, R. S., LIN, J., PETRINI, J. H. & KASTAN, M. B. 2000b. ATM phosphorylates p95/nbs1 in an S-phase checkpoint pathway. *Nature,* 404**,** 613-7.

LINZER, D. I. H. & LEVINE, A. J. 1979. Characterization of a 54k Dalton Cellular Sv40 Tumor-Antigen Present in Sv40-Transformed Cells and Uninfected Embryonal Carcinoma-Cells. *Cell,* 17**,** 43-52.

LIU, Q., GUNTUKU, S., CUI, X. S., MATSUOKA, S., CORTEZ, D., TAMAI, K., LUO, G., CARATTINI-RIVERA, S., DEMAYO, F., BRADLEY, A., DONEHOWER, L. A. & ELLEDGE, S. J. 2000. Chk1 is an essential kinase that is regulated by Atr and required for the G(2)/M DNA damage checkpoint. *Genes & development,* 14**,** 1448-59.

LIU, S., OPIYO, S.O., MANTHEY, K., GLANZER, J.G., ASHLEY, A.K., AMERIN, C., TROKSA, S.A., SHRIVASTAV, M., NICKOLOFF, J.A. & OAKLEY, G.G. 2012. Distinct roles for DNA-PK, ATM and ATR in RPA phosphorylation and checkpoint activation in response to replication stress. *Nucleic Acids Research*, 40, 10780–94.

LJUNG, R., ARONIS-VOURNAS, S., KURNIK-AUBERGER, K., VAN DEN BERG, M., CHAMBOST, H., CLAEYSSENS, S., VAN GEET, C., GLOMSTEIN, A., HANN, I., HILL, F., KOBELT, R., KREUZ, W., MANCUSO, G., MUNTEAN, W., PETRINI, P., ROSADO, L., SCHEIBEL, E., SIIMES, M., SMITH, O. & TUSELL, J. 2000. Treatment of children with haemophilia in Europe: a survey of 20 centres in 16 countries. *Haemophilia : the official journal of the World Federation of Hemophilia,* 6**,** 619-24.

LÖBRICH, M., SHIBATA, A., BEUCHER, A., FISHER, A., ENSMINGER, M., GOODARZI, A. A., BARTON, O. & JEGGO, P. A. 2010. gammaH2AX foci analysis for monitoring DNA double-strand break repair: strengths, limitations and optimization. *Cell cycle (Georgetown, Tex.),* 9**,** 662-9.

LOPEZ-GIRONA, A., TANAKA, K., CHEN, X. B., BABER, B. A., MCGOWAN, C. H. & RUSSELL, P. 2001. Serine-345 is required for Rad3-dependent phosphorylation and function of checkpoint kinase Chk1 in fission yeast. *Proceedings of the National Academy of Sciences of the United States of America,* 98**,** 11289-94.

LOVEJOY, C. A. & CORTEZ, D. 2009. Common mechanisms of PIKK regulation. *DNA repair,* 8**,** 1004-8.

LYNCH, H. T. & DE LA CHAPELLE, A. 1999. Genetic susceptibility to non-polyposis colorectal cancer. *Journal of medical genetics,* 36**,** 801-18.

MAILAND, N., BEKKER-JENSEN, S., FAUSTRUP, H., MELANDER, F., BARTEK, J., LUKAS, C. & LUKAS, J. 2007. RNF8 ubiquitylates histones at DNA double-strand breaks and promotes assembly of repair proteins. *Cell,* 131**,** 887-900.

MALKIN, D., LI, F. P., STRONG, L. C., FRAUMENI, J. F., NELSON, C. E., KIM, D. H., KASSEL, J., GRYKA, M. A., BISCHOFF, F. Z., TAINSKY, M. A. & FRIEND, S. H. 1990. Germ Line P53 Mutations in a Familial Syndrome of Breast-Cancer, Sarcomas, and Other Neoplasms. *Science,* 250**,** 1233-1238.

MAMEGHAN, H., FISHER, R., MAMEGHAN, J. & BROOK, S. 1995. Analysis of Failure Following Definitive Radiotherapy for Invasive Transitional-Cell Carcinoma of the Bladder. *International Journal of Radiation Oncology Biology Physics,* 31**,** 247-254.

MARCANTONI, E., MASSACCESI, M., PETRINI, M., BARTOLI, G., BELLUCCI, M. C., BOSCO, M. & SAMBRI, L. 2000. A novel route to the vinyl sulfide nine-membered macrocycle moiety of Griseoviridin. *The Journal of organic chemistry,* 65**,** 4553-9.

MARSHALL, C. J., FRANKS, L. M. & CARBONELL, A. W. 1977. Markers of Neoplastic Transformation in Epithelial-Cell Lines Derived from Human Carcinomas. *Journal of the National Cancer Institute,* 58**,** 1743-1751.

MARTINELLI, G. & PETRINI, F. 2000. [The SIAARTI in comparison to other scientific societies in Italy and in Europe. A policy for continued improvement of quality]. *Minerva anestesiologica,* 66**,** 429-33.

MASTERS, J. R. W., HEPBURN, P. J., WALKER, L., UROTHELIAL, T.-T. H., LINES, C., HIGHMAN, W. J., TREJDOSIEWICZ, L. K., POVEY, S., PARKAR, M., HILL, B. T., RIDDLE, P. R. & FRANKS, L. M. 1986. Tissue Culture Model of Transitional Cell Carcinoma : Characterization of Twenty-two Human Urothelial Cell Lines Tissue Culture Model of Transitional Cell Carcinoma : Characterization of. *Population (English Edition)***,** 3630-3636.

MATSUBARA, J., NISHINA, T., YAMADA, Y., MORIWAKI, T., SHIMODA, T., KAJIWARA, T., NAKAJIMA, T. E., KATO, K., HAMAGUCHI, T., SHIMADA, Y., OKAYAMA,. Y., OKA, T. & SHIRAO, K. 2008. Impacts of excision repair cross-complementing gene 1 (ERCC1),

dihydropyrimidine dehydrogenase, and epidermal growth factor receptor on the outcomes of patients with advanced gastric cancer. *British journal of cancer,* 98, 832–839.

MATSUMOTO, H., WADA, T., FUKUNAGA, K., YOSHIHIRO, S., MATSUYAMA, H. & NAITO, K. 2004. Bax to Bcl-2 ratio and Ki-67 index are useful predictors of neoadjuvant chemoradiation therapy in bladder cancer. *Japanese journal of clinical oncology,* 34**,** 124-30.

MATSUMURA, N., NAKAMURA, Y., KOHJIMOTO, Y., INAGAKI, T., NANPO, Y., YASUOKA, H., OHASHI, Y. & HARA, I. 2011. The prognostic significance of human equilibrative nucleoside transporter 1 expression in patients with metastatic bladder cancer treated with gemcitabine-cisplatin-based combination chemotherapy. *The British`journal of urology International,* 32, 1889-94.

MCVEY, M. & LEE, S. E. 2008. MMEJ repair of double-strand breaks (director's cut): deleted sequences and alternative endings. *Trends in genetics : TIG,* 24**,** 529-38.

MELERO, J. A., STITT, D. T., MANGEL, W. F. & CARROLL, R. B. 1979. Identification of New Polypeptide Species (48-55k) Immunoprecipitable by Antiserum to Purified Large T-Antigen and Present in Sv40-Infected and Sv40-Transformed Cells. *Virology,* 93**,** 466-480.

MERCURO, G., PANZUTO, M. G., BINA, A., LEO, M., CABULA, R., PETRINI, L., PIGLIARU, F. & MARIOTTI, S. 2000a. Cardiac function, physical exercise capacity, and quality of life during long-term thyrotropin-suppressive therapy with levothyroxine: effect of individual dose tailoring. *The Journal of clinical endocrinology and metabolism,* 85**,** 159-64.

MERCURO, G., ZONCU, S., COLONNA, P., CHERCHI, P., MARIOTTI, S., PIGLIARU, F., PETRINI, L. & ILICETO, S. 2000b. Cardiac dysfunction in acromegaly: evidence by pulsed wave tissue Doppler imaging. *European journal of endocrinology / European Federation of Endocrine Societies,* 143**,** 363-9.

MICHEL, B., EHRLICH, S. D. & UZEST, M. 1997. DNA double-strand breaks caused by replication arrest. *The EMBO journal,* 16**,** 430-8.

MORTUSEWICZ, O. & LEONHARDT, H. 2007. XRCC1 and PCNA are loading platforms with distinct kinetic properties and different capacities to respond to multiple DNA lesions. *BMC molecular biology,* 8**,** 81.

MULLER, C., CHRISTODOULOPOULOS, G., SALLES, B. & PANASCI, L. 1998. DNA-Dependent protein kinase activity correlates with clinical and in vitro sensitivity of chronic lymphocytic leukemia lymphocytes to nitrogen mustards. *Blood,* 92**,** 2213-9.

MUNRO, A. J., LAIN, S. & LANE, D. P. 2005. P53 abnormalities and outcomes in colorectal cancer: a systematic review. *British journal of cancer,* 92**,** 434-44.

MYERS, J. S. & CORTEZ, D. 2006. Rapid activation of ATR by ionizing radiation requires ATM and Mre11. *The Journal of biological chemistry,* 281**,** 9346-50.

NANNI COSTA, A., PUGLIESE, M. R., VENTUROLI, N., DEGLI ESPOSTI, D., MAZZETTI, P., GHIRARDINI, A., PETRINI, F., VENTURI, S., RIDOLFI, L., MARTINELLI, G. & MANYALICH, M. 2000. [The transplant coordinator]. *Annali dell'Istituto superiore di sanita,* 36**,** 247-51.

NEGRUTSKII, B. S., SHALAK, V. F., KERJAN, P., EL, A. V. & MIRANDE, M. 1999. Functional Interaction of Mammalian Valyl-tRNA Synthetase with Elongation Factor EF-1 ⎵ in the Complex with EF-1H *. *Biochemistry,* 274**,** 4545-4550.

NGUEWA, P. A., FUERTES, M. A., ALONSO C. & PEREZ, J. M. 2003. Pharmacological modulation of Poly (ADP-ribose) polymerase-mediated cell death: exploitation in cancer chemotherapy. *Molecular Pharmacology*, 64, 1007–1014.

NIEDERNHOFER, L. J., ODIJK, H., BUDZOWSKA, M., VAN DRUNEN, E., MAAS, A., THIEL, A. F., DE WIT, J., JASPERS, N. G. J., BEVERLOO, H. B., HOEIJMAKERS, J. H. J. & KANAAR, R. 2004. The structure-specific endonuclease Ercc1-Xpf is required to resolve DNA interstrand cross-link-induced double-strand breaks. *Molecular and cellular biology,* 24, 5776–5787.

NORCUM, M. T. & WARRINGTON, J. A. 1998. Structural analysis of the multienzyme aminoacyl-tRNA synthetase complex: a three-domain model based on reversible chemical crosslinking. *Protein science : a publication of the Protein Society,* 7**,** 79-87.

NORCUM, M. T. & WARRINGTON, J. A. 2000. The cytokine portion of p43 occupies a central position within the eukaryotic multisynthetase complex. *The Journal of biological chemistry,* 275**,** 17921-4.

O'DRISCOLL, M., RUIZ-PEREZ, V. L., WOODS, C. G., JEGGO, P. A. & GOODSHIP, J. A. 2003. A splicing mutation affecting expression of ataxia-telangiectasia and Rad3-related protein (ATR) results in Seckel syndrome. *Nature genetics,* 33**,** 497-501.

OLAUSSEN, K. A., DUNANT, A., FOURET, P., BRAMBILLA, E., ANDRE, F., HADDAD, V., TARANCHON, E., FILIPITS, M., PIRKER, R., POPPER, H. H., STAHEL, R., SABATIER, L., PIGNON, J., TURSZ, T., LE CHEVALIER, T., SORIA, J. C. & INVESTIGATORS, I. B.

2006. DNA repair by ERCC1 in non-small-cell lung cancer and cisplatin-based adjuvant chemotherapy. *New England Journal of Medicine,* 355**,** 983-991.

OLIVIER, M., EELES, R., HOLLSTEIN, M., KHAN, M. A., HARRIS, C. C. & HAINAUT, P. 2002. The IARC TP53 database: New Online mutation analysis and recommendations to users. *Human Mutation,* 19**,** 607-614.

OZCAN, M. F., DIZDAR, O., DINCER, N., BALCI, S., GULER, G., GOK, B., PEKTAS, G., SEKER, M. M., AKSOY, S., ARSLAN, C., YALCIN, S. & BALBAY, M. D. 2013. Low ERCC1 expression is associated with prolonged survival in patients with bladder cancer receiving platinum-based neoadjuvant chemotherapy. *Urologic oncology,* 1, 403-10.

PAINTER, R. B. & YOUNG, B. R. 1980. Radiosensitivity in ataxia-telangiectasia: a new explanation. *Proceedings of the National Academy of Sciences of the United States of America,* 77**,** 7315-7.

PANDITA, T. K. & RICHARDSON, C. 2009. Chromatin remodeling finds its place in the DNA double-strand break response. *Nucleic acids research,* 37**,** 1363-77.

PARK, B.-J., KANG, J. W., LEE, S. W., CHOI, S.-J., SHIN, Y. K., AHN, Y. H., CHOI, Y. H., CHOI, D., LEE, K. S. & KIM, S. 2005a. The haploinsufficient tumor suppressor p18 upregulates p53 via interactions with ATM/ATR. *Cell,* 120**,** 209-21.

PARK, B.-J., OH, Y. S., PARK, S. Y., CHOI, S. J., RUDOLPH, C., SCHLEGELBERGER, B. & KIM, S. 2006a. AIMP3 haploinsufficiency disrupts oncogene-induced p53 activation and genomic stability. *Cancer research,* 66**,** 6913-8.

PARK, S. G., CHOI, E. C. & KIM, S. 2010. Aminoacyl-tRNA Synthetase-Interacting Multifunctional Proteins (AIMPs): A Triad for Cellular Homeostasis. *Iubmb Life,* 62**,** 296-302.

PARK, S. G., KANG, Y. S., KIM, J. Y., LEE, C. S., KO, Y. G., LEE, W. J., LEE, K.-U., YEOM, Y. I. & KIM, S. 2006b. Hormonal activity of AIMP1/p43 for glucose homeostasis. *Proceedings of the National Academy of Sciences of the United States of America,* 103**,** 14913-8.

PARK, S. G., SHIN, H., SHIN, Y. K., LEE, Y., CHOI, E.-C., PARK, B.-J. & KIM, S. 2005b. The novel cytokine p43 stimulates dermal fibroblast proliferation and wound repair. *The American journal of pathology,* 166**,** 387-98.

PARKER, R. J., GILL, I., TARONE, R., VIONNET, J. A., GRUNBERG, S., MUGGIA, F.M. & REED, E. 1991. Platinum-DNA damage in leukocyte DNA of patients receiving carboplatin and cisplatin chemotherapy, measured by atomic absorption spectrometry. *Carcinogenesis*, 12, 1253–1258.

PARRILLA-CASTELLAR, E. R., ARLANDER, S. J. H. & KARNITZ, L. 2004. Dial 9-1-1 for DNA damage: the Rad9-Hus1-Rad1 (9-1-1) clamp complex. *DNA repair,* 3**,** 1009-14.

PARTY, M. R. C. A. B. C. W., GRP, E. G. U., GRP, A. B. C. S., GRP, N. C. I. C. C. T., FINNBLADDER & GRP, N. B. C. S. 1999. Neoadjuvant cisplatin, methotrexate, and vinblastine chemotherapy for muscle-invasive bladder cancer: a randomised controlled trial. *Lancet,* 354**,** 533-540.

PAULL, T. T. & GELLERT, M. 1999. unwinding and endonuclease cleavage by the Mre11 / Rad50 complex. *Genes & Development***,** 1276-1288.

PETRINI, B. 2000a. [BCG vaccination--controversy and compromise]. *Lakartidningen,* 97**,** 5618-20.

PETRINI, C. 2000b. [Bioethics principles and prevention of environmental risks: possible interpretations]. *Annali dell'Istituto superiore di sanita,* 36**,** 117-30.

PETRINI, C. 2000c. [Considerations on the health technician's code of conduct in medical radiology]. *La Radiologia medica,* 99**,** 135-7.

PETRINI, J. H. 2000d. The Mre11 complex and ATM: collaborating to navigate S phase. *Current opinion in cell biology,* 12**,** 293-6.

PETRINI, J. H. 2000e. S-phase functions of the Mre11 complex. *Cold Spring Harbor Symposia on Quantitative Biology,* 65**,** 405-11.

PETRINI, J. H. 2000f. When more is better. *Nature genetics,* 26**,** 257-8.

PETRINI, P., TANZI, M. C., VISAI, L., CASOLINI, F. & SPEZIALE, P. 2000. Novel poly(urethane-aminoamides): an in vitro study of the interaction with heparin. *Journal of biomaterials science. Polymer edition,* 11**,** 353-65.

PETZOLDT, J. L., LEIGH, I. M., DUFFY, P. G., SEXTON, C. & MASTERS, J. R. 1995. Immortalisation of human urothelial cells. *Urological research,* 23**,** 377-80.

PICHIERRI, P., ROSSELLI, F. & FRANCHITTO, A. 2003. Werner's syndrome protein is phosphorylated in an ATR/ATM-dependent manner following replication arrest and DNA damage induced during the S phase of the cell cycle. *Oncogene,* 22**,** 1491-500.

POEHLMANN, A. & ROESSNER, A. 2010. Importance of DNA damage checkpoints in the pathogenesis of human cancers. *Pathology - Research and Practice,* 206**,** 591-601.

POETA, M. L., MANOLA, J., GOLDWASSER, M. A., FORASTIERE, A., BENOIT, N., CALIFANO, J. A., RIDGE, J. A., GOODWIN, J., KENADY, D., SAUNDERS, J.,

WESTRA, W., SIDRANSKY, D. & KOCH, W. M. 2007. TP53 mutations and survival in squamous-cell carcinoma of the head and neck. *New England Journal of Medicine,* 357**,** 2552-2561.

POETA, M. L., MANOLA, J., GOLDWASSER, M. A., SC, D., FORASTIERE, A., BENOIT, N., CALIFANO, J. A., RIDGE, J. A., GOODWIN, J., KENADY, D., SAUNDERS, J., WESTRA, W., SIDRANSKY, D. & KOCH, W. M. 2008. NIH Public Access. *English Journal,* 357**,** 2552-2561.

PROUT, G. R., SHIPLEY, W. U., KAUFMAN, D. S., HENEY, N. M., GRIFFIN, P. P., ALTHAUSEN, A. F., BASSIL, B., NOCKS, B. N., PARKHURST, E. C. & YOUNG, H. H. 1990. Preliminary-Results in Invasive Bladder-Cancer with Transurethral Resection, Neoadjuvant Chemotherapy and Combined Pelvic Irradiation Plus Cisplatin Chemotherapy. *Journal of Urology,* 144**,** 1128-1136.

QUEVILLON, S. & MIRANDE, M. 1996. The p18 component of the multisynthetase complex shares a protein motif with the beta and gamma subunits of eukaryotic elongation factor 1. *FEBS letters,* 395**,** 63-7.

QUEVILLON, S., ROBINSON, J. C., BERTHONNEAU, E., SIATECKA, M. & MIRANDE, M. 1999. Macromolecular assemblage of aminoacyl-tRNA synthetases: identification of protein-protein interactions and characterization of a core protein. *Journal of molecular biology,* 285**,** 183-95.

RENE, N. J., CURY, F. B. & SOUHAMI, L. 2009. Conservative treatment of invasive bladder cancer. *Current oncology (Toronto, Ont.),* 16**,** 36-47.

RIBALLO, E., KÜHNE, M., RIEF, N., DOHERTY, A., SMITH, G. C. M., RECIO, M.-J., REIS, C., DAHM, K., FRICKE, A., KREMPLER, A., PARKER, A. R., JACKSON, S. P., GENNERY, A., JEGGO, P. A. & LÖBRICH, M. 2004. A pathway of double-strand break rejoining dependent upon ATM, Artemis, and proteins locating to gamma-H2AX foci. *Molecular cell,* 16**,** 715-24.

RIBEIRO, J. C. C., BARNETSON, A. R., FISHER, R. J., MAMEGHAN, H. & RUSSELL, P. J. 1997. Relationship between radiation response and p53 status in human bladder cancer cells. *International Journal of Radiation Biology,* 72**,** 11-20.

ROBERTS, J. J. & PASCOE, J. M. 1972. Cross-linking of complementary strands of DNA in mammalian cells by antitumour platinum compounds. *Nature,* 235, 282–4.

ROBINSON, J. C., KERJAN, P. & MIRANDE, M. 2000. Macromolecular assemblage of aminoacyl-tRNA synthetases: quantitative analysis of protein-protein interactions and mechanism of complex assembly. *Journal of molecular biology,* 304**,** 983-94.

ROCHE, K. C., ROCHA, S., BRACKEN, C. P. & PERKINS, N. D. 2007. Regulation of ATR-dependent pathways by the FHA domain containing protein SNIP1. *Oncogene,* 26**,** 4523-30.

ROCO, A. CAYUN, J, CONTRERAS, S., STOJANOVA, J. & QUINONES, L. 2014. Can pharmacogenetics explain efficacy and safety of cisplatin pharmacotherapy? *Frontiers in genetics*, 5, 391.

RODEL, C. 2002. Combined-Modality Treatment and Selective Organ Preservation in Invasive Bladder Cancer: Long-Term Results. *Journal of Clinical Oncology,* 20**,** 3061-3071.

ROGAKOU, E. P., PILCH, D. R., ORR, A. H., IVANOVA, V. S. & BONNER, W. M. 1998. DNA double-stranded breaks induce histone H2AX phosphorylation on serine 139. *The Journal of biological chemistry,* 273**,** 5858-68.

ROSENBERG, B. 1973. Platinum coordination complexes in cancer chemotherapy. *Naturwissenschaften*, 60, 399–406.

ROTHKAMM, K., KRU, I., THOMPSON, L. H. & LO, M. 2003. Pathways of DNA Double-Strand Break Repair during the Mammalian Cell Cycle. *Society,* 23**,** 5706-5715.

RØTTERUD, R., SKOMEDAL, H., BERNER, A., DANIELSEN, H. E., SKOVLUND, E. & FOSSÅ, S. D. 2001. TP53 and p21WAF1/CIP1 behave differently in euploid versus aneuploid bladder tumours treated with radiotherapy. *Acta oncologica (Stockholm, Sweden),* 40**,** 644-52.

SAEB-PARSY, K., VEERAKUMARASIVAM, A., WALLARD, M. J., THORNE, N., KAWANO, Y., MURPHY, G., NEAL, D. E., MILLS, I. G. & KELLY, J. D. 2008. MT1-MMP regulates urothelial cell invasion via transcriptional regulation of Dickkopf-3. *British journal of cancer,* 99**,** 663-9.

SAK, S. C., HARNDEN, P., JOHNSTON, C. F., PAUL, A. B. & KILTIE, A. E. 2005. APE1 and XRCC1 protein expression levels predict cancer-specific survival following radical radiotherapy in bladder cancer. *Clinical cancer research : an official journal of the American Association for Cancer Research,* 11**,** 6205-11.

SAKANO, S. OGAWA, S., YAMAMOTO, Y., NISHIJIMA, J., MIYACHIKA, Y., MATSUMOTO, H., HARA, T. & MATSUYAMA, H. 2013. ERCC1 and XRCC1 expression predicts survival

in bladder cancer patients receiving combined trimodality therapy. *Molecular and clinical oncology*, 1, 403-10.

SAMANTA, D. & DATTA, P. K. 2012. Alterations in the Smad pathway in human cancers. *Frontiers in Bioscience-Landmark,* 17**,** 1281-1293.

SANCHEZ, Y., WONG, C., THOMA, R. S., RICHMAN, R., WU, Z., PIWNICA-WORMS, H. & ELLEDGE, S. J. 1997. Conservation of the Chk1 checkpoint pathway in mammals: linkage of DNA damage to Cdk regulation through Cdc25. *Science (New York, N.Y.),* 277**,** 1497-501.

SANGSTER-GUITY, N., CONRAD, B.H., PAPADOPOULOS, N. & BUNZ, F. 2011. ATR mediates cisplatin resistance in a p53 genotype-specific manner. *Oncogene,* 30, 2526–33.

SARTORI, A. A., LUKAS, C., COATES, J., MISTRIK, M., FU, S., BARTEK, J., BAER, R., LUKAS, J. & JACKSON, S. P. 2007. Human CtIP promotes DNA end resection. *Nature,* 450**,** 509-U6.

SAVITSKY, K., BARSHIRA, A., GILAD, S., ROTMAN, G., ZIV, Y., VANAGAITE, L., TAGLE, D. A., SMITH, S., UZIEL, T., SFEZ, S., ASHKENAZI, M., PECKER, I., FRYDMAN, M., HARNIK, R., PATANJALI, S. R., SIMMONS, A., CLINES, G. A., SARTIEL, A., GATTI, R. A., CHESSA, L., SANAL, O., LAVIN, M. F., JASPERS, N. G. J., MALCOLM, A., TAYLOR, R., ARLETT, C. F., MIKI, T., WEISSMAN, S. M., LOVETT, M., COLLINS, F. S. & SHILOH, Y. 1995. A Single Ataxia-Telangiectasia Gene with a Product Similar to Pi-3 Kinase. *Science,* 268**,** 1749-1753.

SCACCHIA, M., LELLI, R., PETRINI, A., PRENCIPE, V., CALISTRI, P. & GIOVANNINI, A. 2000. Use of innovative methods in the eradication of bovine tuberculosis. *Journal of veterinary medicine. B, Infectious diseases and veterinary public health,* 47**,** 321-7.

SCHIMMEL, P. R. & SOLL, D. 1979. Aminoacyl-tRNA synthetases: general features and recognition of transfer RNAs. *Annual review of biochemistry,* 48**,** 601-48.

SHARIAT S.F., BOLENZ, C., KARAKIEWICZ, P.I., FRADET, Y., ASHFAQ, R., BASTIAN, P.J., NIELSEN, M.E., CAPITANIO, U., JELDRES, C., RIGAUD, J., MULLER, S.C., LERNER, S.P., MONTORSI, F., SAGALOWSKI, A.I., COTE R.J. & LOTAN, Y. 2010. p53 expression in patients with advanced urothelial cancer of the urinary bladder. *British journal of urology International,* 105, 489-95.

SHARIAT, S.F., LOTAN, Y., KARAKIEWICZ, P.I., ASHFAQ, R., IASBARN, H., FRADET, Y., BASTIAN, P.J., NIELSEN, M.E., CAPATINO, U., JELDRES, C., MONTORSI, F., MULLER, S.C., KARAM, J.A., HEUKAMP, L.C., NETTO, G., LERNER S.P.,

SAGALOWSKY, A.I. & COTE, R.J. 2009. P53 predictive value for pT1-2 N0 disease at radical cystectomy. *Journal of urology,* 182:907-13.

SHAW, R. J. & CANTLEY, L. C. 2006. Ras, PI(3)K and mTOR signalling controls tumour cell growth. *Nature,* 441**,** 424-30.

SHELLEY, M., BARBER, J., WILT, T. & MASON, M. 2008. Surgery versus radiotherapy for muscle invasive bladder cancer (Review). *Internal Medicine*.

SHIEH, S.-Y., AHN, J., TAMAI, K., TAYA, Y. & PRIVES, C. 2000. The human homologs of checkpoint phosphorylate p53 at multiple DNA damage-inducible sites. *Genes & Development,* 1**,** 289-300.

SHILKRUT, M., WU, A., THOMAS, D.G. & HAMSTRA, D.A. 2014. Expression of ribonucleoside reductase subunit M1, but not excision repair cross-complementation group 1, is predictive in muscle-invasive bladder cancer treated with chemotherapy and radiation. *Molecular and clinical oncology*, 2, 479-87.

SHILOH, Y. 1997. Ataxia-telangiectasia and the Nijmegen breakage syndrome: related disorders but genes apart. *Annual review of genetics,* 31**,** 635-62.

SHILOH, Y. 2003. ATM and related protein kinases: safeguarding genome integrity. *Nature reviews. Cancer,* 3**,** 155-68.

SHILOH, Y. 2006. The ATM-mediated DNA-damage response: taking shape. *Trends in biochemical sciences,* 31**,** 402-10.

SHINOHARA, A., SAKANO, S., HONODA, Y., NISHIJIMA, J., KAWAI, Y., MISUMI, T., NAGAO, K., HARA, T. & MATSUYAMA, H. 2009. Association of TP53 and MDM2 polymorphisms with survival in bladder cancer patients treated with chemoradiotherapy. *Cancer Science,* 100, 2376-82.

SHIPLEY, B. W. U., WINTER, K. A., KAUFMAN, D. S., LEE, W. R., HENEY, N. M., TESTER, W. R., DONNELLY, B. J., VENNER, P. M., PEREZ, C. A., MURRAY, K. J., DOGGETT, R. S. & TRUE, L. D. 1999. Phase III trial of neoadjuvant chemotherapy in patients with invasive bladder cancer treated with selective bladder preservation by combined radiation therapy and chemotherapy: initial results of radiation therapy oncology group 89-03. *The Journal of urology,* 162**,** 623-4.

SHIPLEY, W. U., KAUFMAN, D. S., TESTER, W. J., PILEPICH, M. V. & SANDLER, H. M. 2003. Overview of bladder cancer trials in the Radiation Therapy Oncology Group. *Cancer,* 97**,** 2115-9.

SHIPLEY, W. U., KAUFMAN, D. S., ZEHR, E., HENEY, N. M., LANE, S. C., THAKRAL, H. K., ALTHAUSEN, A. F. & ZIETMAN, A. L. 2002. Selective bladder preservation by combined modality protocol treatment: Long-term outcomes of 190 patients with invasive bladder cancer. *Urology,* 60**,** 62-67.

SHIPLEY, W. U., WINTER, K. A., KAUFMAN, D. S., LEE, W. R., HENEY, N. M., TESTER, W. R., DONNELLY, B. J., VENNER, P. M., PEREZ, C. A., MURRAY, K. J., DOGGETT, R. S. & TRUE, L. D. 1998. Phase III trial of neoadjuvant chemotherapy in patients with invasive bladder cancer treated with selective bladder preservation by combined radiation therapy and chemotherapy: Initial results of Radiation Therapy Oncology Group 89-03. *Journal of Clinical Oncology,* 16**,** 3576-3583.

SHIRATA, N., KUDOH, A., DAIKOKU, T., TATSUMI, Y., FUJITA, M., KIYONO, T., SUGAYA, Y., ISOMURA, H., ISHIZAKI, K. & TSURUMI, T. 2005. Activation of ataxia telangiectasia-mutated DNA damage checkpoint signal transduction elicited by herpes simplex virus infection. *The Journal of biological chemistry,* 280**,** 30336-41.

SHIROTA, Y., STOEHLMACHER, J., BRABENDER, J., XIONG, Y.P., UETAKE, H., DANENBERG, K. D., GROSHEN, S., TSAO-WEI, D. D., DANENBERG, P. V. & LENZ, H. J. 2001. ERCC1 and thymidylate synthase mRNA levels predict survival for colorectal cancer patients receiving combination oxaliplatin and fluorouracil chemotherapy. *The journal of clinical oncology*, 19, 4298–4304.

SIDDIK, Z.H. 2003. Cisplatin: mode of cytotoxic action and molecular basis of resistence. *Oncogene*, 22, 7265–79.

SIMON, G. R., SHARMA, S., CANTOR, A., SMITH, P. & BEPLER, G. 2005. ERCC1 expression is a predictor of survival in resected patients with non-small cell lung cancer. *Chest*, 127, 978–983.

SIVASUBRAMANIAM, S., SUN, X., PAN, Y.-R., WANG, S. & LEE, E. Y. P. 2008. Cep164 is a mediator protein required for the maintenance of genomic stability through modulation of MDC1 , RPA , and CHK1. *Genes & Development,* 2**,** 587-600.

SMITH, G. C. M. & JACKSON, S. P. 1999. The DNA-dependent protein kinase The DNA-dependent protein kinase. *Genes & Development***,** 916-934.

SMITS, V. A. J., REAPER, P. M. & JACKSON, S. P. 2006. Rapid PIKK-dependent release of Chk1 from chromatin promotes the DNA-damage checkpoint response. *Current biology : CB,* 16**,** 150-9.

SONG, L., RITCHIE, A-M., MCNEIL, E. M., LI, W. & MELTON, D. W. 2011. Identification of DNA repair gene Ercc1 as a novel target in melanoma. *Pigment cell and melanoma research,* 24, 966–971.

SQUARZONI, S., SABATELLI, P., CAPANNI, C., PETRINI, S., OGNIBENE, A., TONIOLO, D., COBIANCHI, F., ZAULI, G., BASSINI, A., BARACCA, A., GUARNIERI, C., MERLINI, L. & MARALDI, N. M. 2000. Emerin presence in platelets. *Acta neuropathologica,* 100**,** 291-8.

SRIVASTAVA, S., ZOU, Z. Q., PIROLLO, K., BLATTNER, W. & CHANG, E. H. 1990. Germ-Line Transmission of a Mutated P53 Gene in a Cancer-Prone Family with Li-Fraumeni Syndrome. *Nature,* 348**,** 747-749.

STEHELIN, D., VARMUS, H. E., BISHOP, J. M. & VOGT, P. K. 1976. DNA Related to Transforming Gene(S) of Avian-Sarcoma Viruses Is Present in Normal Avian DNA. *Nature,* 260**,** 170-173.

STEIN, J. P., LIESKOVSKY, G., COTE, R., GROSHEN, S., FENG, A. C., BOYD, S., SKINNER, E., BOCHNER, B., THANGATHURAI, D., MIKHAIL, M., RAGHAVAN, D. & SKINNER, D. G. 2001. Radical cystectomy in the treatment of invasive bladder cancer: long-term results in 1,054 patients. *Journal of clinical oncology : official journal of the American Society of Clinical Oncology,* 19**,** 666-75.

STEIN, J. P. & SKINNER, D. G. 2006. Radical cystectomy for invasive bladder cancer: long-term results of a standard procedure. *World journal of urology,* 24**,** 296-304.

STENZL, A., COWAN, N. C., DE SANTIS, M., JAKSE, G., KUCZYK, M. A., MERSEBURGER, A. S., RIBAL, M. J., SHERIF, A. & WITJES, J. A. 2009. The updated EAU guidelines on muscle-invasive and metastatic bladder cancer. *European urology,* 55**,** 815-25.

STEWART, G. S., MASER, R. S., STANKOVIC, T., BRESSAN, D. A., KAPLAN, M. I., JASPERS, N. G., RAAMS, A., BYRD, P. J., PETRINI, J. H. & TAYLOR, A. M. 1999. The DNA double-strand break repair gene hMRE11 is mutated in individuals with an ataxia-telangiectasia-like disorder. *Cell,* 99**,** 577-87.

STRACKER, T. H., CARSON, C. T. & WEITZMAN, M. D. 2002. Adenovirus oncoproteins inactivate the Mre11 – Rad50 – NBS1 DNA repair complex. *Nature,* 418.

STRIPPOLI, P., LENZI, L., PETRINI, M., CARINCI, P. & ZANNOTTI, M. 2000a. A new gene family including DSCR1 (Down Syndrome Candidate Region 1) and ZAKI-4: characterization from yeast to human and identification of DSCR1-like 2, a novel human member (DSCR1L2). *Genomics,* 64**,** 252-63.

STRIPPOLI, P., PETRINI, M., LENZI, L., CARINCI, P. & ZANNOTTI, M. 2000b. The murine DSCR1-like (Down syndrome candidate region 1) gene family: conserved synteny with the human orthologous genes. *Gene,* 257**,** 223-32.

SU, T. T. 2006. Cellular responses to DNA damage: one signal, multiple choices. *Annual review of genetics,* 40**,** 187-208.

SUN, H., TRECO, D., SCHULTES, N. P. & SZOSTAK, J. W. 1989. Double-Strand Breaks at an Initiation Site for Meiotic Gene Conversion. *Nature,* 338**,** 87-90.

SUN, J. M., SUNG, J. Y., PARK, S. H., KWON, G. Y., JEONG, B. C., SEO, S. I., JEON, S. S., LEE, H. M., JO, J., CHOI, H. Y. & LIM, H. Y. 2012. ERCC1 as a biomarker for bladder **cancer** patients likely to benefit from adjuvant chemotherapy. *BMC Cancer,* 12, 187.

SUNDMAN, K., CHRYSSANTHOU, E. & PETRINI, B. 2000. Mycobacterium shimoidei, an easily misdiagnosed non-tuberculous pulmonary mycobacterium. *Scandinavian journal of infectious diseases,* 32**,** 450-1.

TANZI, M. C., FARE, S. & PETRINI, P. 2000. In vitro stability of polyether and polycarbonate urethanes. *Journal of biomaterials applications,* 14**,** 325-48.

TESTER, W., PORTER, A., ASBELL, S., COUGHLIN, C., HEANEY, J., KRALL, J., MARTZ, K., VENNER, P. & HAMMOND, E. 1993. Combined Modality Program with Possible Organ Preservation for Invasive Bladder-Carcinoma - Results of Rtog Protocol 85-12. *International Journal of Radiation Oncology Biology Physics,* 25**,** 783-790.

TIBBETTS, R. S., BRUMBAUGH, K. M., WILLIAMS, J. M., SARKARIA, J. N., CLIBY, W. A., SHIEH, S.-Y., TAYA, Y., PRIVES, C. & ABRAHAM, R. T. 1999. A role for ATR in the DNA phosphorylation of p53. *Genes & Development***,** 152-157.

TIBBETTS, R. S., CORTEZ, D., BRUMBAUGH, K. M., SCULLY, R., LIVINGSTON, D., ELLEDGE, S. J. & ABRAHAM, R. T. 2000. Functional interactions between BRCA1 and the checkpoint kinase ATR during genotoxic stress. *Genes & Development***,** 2989-3002.

TOMIMATSU, N., MUKHERJEE, B. & BURMA, S. 2009. Distinct roles of ATR and DNA-PKcs in triggering DNA damage responses in ATM-deficient cells. *EMBO reports,* 10**,** 629-35.

TRIPSIANES, K., FOLKERS, G., AB, E., DAS, D., ODIJK, H., JASPERS, N. G. J., HOEIJMAKERS, J. H. J., KAPTEIN, R. & BOELENS, R. 2005. The structure of the human ERCC1/XPF interaction domains reveals a complementary role for the two proteins in nucleotide excision repair. Structure,13, 1849–1858.

TSODIKOV, O. V., ENZLIN, J. H., SCHARER, O. D. & ELLENBERGER, T. 2005. Crystal structure and DNA binding functions of ERCC1, a subunit of the DNA structure-specific endonuclease XPF-ERCC1. The proceedings of the national academy of sciences of the United States of America, 102, 11236–11241.

USANOVA, S. PIEE-STAFFA, A., SIED, U., THOMALE, J., SCHNEIDER, A., KAINA, B. & KOBERLE, B. 2010. Cisplatin sensitivity of testis tumour cells is due to deficiency in interstrand-crosslink repair and low ERCC1-XPF expression. Molecular cancer, 9, 248.

VAN DEN BOSCH, M., BREE, R. T. & LOWNDES, N. F. 2003. The MRN complex: coordinating and mediating the response to broken chromosomes. *EMBO reports,* 4**,** 844-9.

VAN GENT, D. C., HOEIJMAKERS, J. H. & KANAAR, R. 2001. Chromosomal stability and the DNA double-stranded break connection. *Nature reviews. Genetics,* 2**,** 196-206.

VEERAKUMARASIVAM, A., GOLDSTEIN, L. D., SAEB-PARSY, K., SCOTT, H. E., WARREN, A., THORNE, N. P., MILLS, I. G., VENKITARAMAN, A., NEAL, D. E. & KELLY, J. D. 2008a. AURKA overexpression accompanies dysregulation of DNA-damage response genes in invasive urothelial cell carcinoma. *Cell Cycle,* 7**,** 3525-33.

VEERAKUMARASIVAM, A., SCOTT, H. E., CHIN, S. F., WARREN, A., WALLARD, M. J., GRIMMER, D., ICHIMURA, K., CALDAS, C., COLLINS, V. P., NEAL, D. E. & KELLY, J. D. 2008b. High-resolution array-based comparative genomic hybridization of bladder cancers identifies mouse double minute 4 (MDM4) as an amplification target exclusive of MDM2 and TP53. *Clinical cancer research : an official journal of the American Association for Cancer Research,* 14**,** 2527-34.

VENTUROLI, N., COSTA, A. N., RIDOLFI, L., PUGLIESE, M. R., TADDEI, S., PETRINI, F., BOLONDI, L. & MARTINELLI, G. 2000a. Reliability of ultrasound screening of liver and kidney donors: a retrospective study. *Progress in transplantation,* 10**,** 182-5.

VENTUROLI, N., VENTURI, S., TADDEI, S., RIDOLFI, L., PUGLIESE, M. R., PETRINI, F., MONTI, M., COSTA, A. N. & MARTINELLI, G. 2000b. Organ donation and transplantation as health programs in Italy. *Progress in transplantation,* 10**,** 60-4.

VIDAL, A. E., BOITEUX, S., HICKSON, I. D. & RADICELLA, J. P. 2001. XRCC1 coordinates the initial and late stages of DNA abasic site repair through protein-protein interactions. *The EMBO journal,* 20**,** 6530-9.

WALTES, R., KALB, R., GATEI, M., KIJAS, A. W., STUMM, M., SOBECK, A., WIELAND, B., VARON, R., LERENTHAL, Y., LAVIN, M. F., SCHINDLER, D. & DÖRK, T. 2009. Human RAD50 deficiency in a Nijmegen breakage syndrome-like disorder. *American journal of human genetics,* 84**,** 605-16.

WANG, D. and LIPPARD, S.J. 2005. Cellular processing of platinum anticancer drugs. *Nature Reviews,* 4, 307–19.

WARD, J. F. 1988. DNA Damage Produced by Ionizing-Radiation in Mammalian-Cells - Identities, Mechanisms of Formation, and Reparability. *Progress in Nucleic Acid Research and Molecular Biology,* 35**,** 95-125.

WARENIUS, H. M., JONES, M., GORMAN, T., MCLEISH, R., SEABRA, L., BARRACLOUGH, R. & RUDLAND, P. 2000. Combined RAF1 protein expression and p53 mutational status provides a strong predictor of cellular radiosensitivity. *British journal of cancer,* 83**,** 1084-95.

WEISS, C., ENGEHAUSEN, D. G., KRAUSE, F. S., PAPADOPOULOS, T., DUNST, J., SAUER, R. & RÖDEL, C. 2007. Radiochemotherapy with cisplatin and 5-fluorouracil after transurethral surgery in patients with bladder cancer. *International journal of radiation oncology, biology, physics,* 68**,** 1072-80.

WESNES, K. A., WARD, T., MCGINTY, A. & PETRINI, O. 2000. The memory enhancing effects of a Ginkgo biloba/Panax ginseng combination in healthy middle-aged volunteers. *Psychopharmacology,* 152**,** 353-61.

WIJKSTROM, H., NORMING, U., LAGERKVIST, M., NILSSON, B., NASLUND, I. & WIKLUND, P. 1998. Evaluation of clinical staging before cystectomy in transitional cell bladder carcinoma: a long-term follow-up of 276 consecutive patients. *British Journal of Urology,* 81**,** 686-691.

WILLIAMS, G. J., LEES-MILLER, S. P. & TAINER, J. A. 2010. Mre11-Rad50-Nbs1 conformations and the control of sensing, signaling, and effector responses at DNA double-strand breaks. *DNA repair,* 9**,** 1299-306.

WILLIAMS, R. S., MONCALIAN, G., WILLIAMS, J. S., YAMADA, Y., LIMBO, O., SHIN, D. S., GROOCOCK, L. M., CAHILL, D., HITOMI, C., GUENTHER, G., MOIANI, D., CARNEY,

J. P., RUSSELL, P. & TAINER, J. A. 2008. Mre11 dimers coordinate DNA end bridging and nuclease processing in double-strand-break repair. *Cell,* 135**,** 97-109.

WOOD, C. G. & MULDERS, P. 2009. Vitespen: a preclinical and clinical review. *Future oncology,* 5**,** 763-74.

WOZNIAK, K. & BLASIAK, J. 2002. Recognition and repair of DNA–cisplatin adducts. *Acta Biochimia Polonika*, 49, 583–596.

WU, X., PETRINI, J. H., HEINE, W. F., WEAVER, D. T., LIVINGSTON, D. M. & CHEN, J. 2000. Independence of R/M/N focus formation and the presence of intact BRCA1. *Science,* 289**,** 11.

WU, X., SHELL, S. M., LIU, Y. & ZOU, Y. 2007. ATR-dependent checkpoint modulates XPA nuclear import in response to UV irradiation. *Oncogene,* 26**,** 757-764.

WULLSCHLEGER, S., LOEWITH, R. & HALL, M. N. 2006. TOR signaling in growth and metabolism. *Cell,* 124**,** 471-84.

XU, B., DONNELL, A. H. O., KIM, S.-T., CHECKPOINT, A.-M. S.-P., IRRADIATION, I. & KASTAN, M. B. 2002. Phosphorylation of Serine 1387 in Brca1 Is Specifically Required for the Atm-mediated S-Phase Checkpoint after Ionizing Irradiation Advances in Brief. *Cancer***,** 4588-4591.

XU, B. O., KIM, S.-T. & KASTAN, M. B. 2001. Involvement of Brca1 in S-Phase and G 2 -Phase Checkpoints after Ionizing Irradiation. *Society,* 21**,** 3445-3450.

XU, Y., ASHLEY, T., BRAINERD, E. E., BRONSON, R. T., MEYN, M. S. & BALTIMORE, D. 1996. Targeted disruption of ATM leads to growth retardation, chromosomal fragmentation during meiosis, immune defects, and thymic lymphoma. *Genes & Development,* 10**,** 2411-2422.

XU, Y. & BALTIMORE, D. 1996. Dual roles of ATM in the cellular response to radiation and in cell growth control. *Genes & Development,* 10**,** 2401-2410.

YAMASHITA, A., OHNISHI, T., KASHIMA, I., TAYA, Y. & OHNO, S. 2001. Human SMG-1, a novel phosphatidylinositol 3-kinase-related protein kinase, associates with components of the mRNA surveillance complex and is involved in the regulation of nonsense-mediated mRNA decay. *Genes & development,* 15**,** 2215-28.

YANG, S., KUO, C., BISI, J. E. & KIM, M. K. 2002. PML-dependent apoptosis after DNA damage is regulated by the checkpoint kinase hCds1/Chk2. *Nature cell biology,* 4**,** 865-70.

YOO, H. Y., KUMAGAI, A., SHEVCHENKO, A., SHEVCHENKO, A. & DUNPHY, W. G. 2007. Ataxia-telangiectasia mutated (ATM)-dependent activation of ATR occurs through phosphorylation of TopBP1 by ATM. *The Journal of biological chemistry,* 282**,** 17501-6.

YUN, M. H. & HIOM, K. 2009. CtIP-BRCA1 modulates the choice of DNA double-strand-break repair pathway throughout the cell cycle. *Nature,* 459**,** 460-3.

ZHOU, B.-B. S. & ELLEDGE, S. J. 2000. checkpoints in perspective. *Nature,* 408**,** 433-439.

ZHOU, W., GURUBHAGAVATULA, S., LIU, G., PARK, S., NEUBERG, D. S., WAIN, J. C., LYNCH, T. J., SU, L. & CHRISTIANI, D.C. 2004. Excision repair cross-complementation group 1 polymorphism predicts overall survival in advanced non-small cell lung cancer patients treated with platinum-based chemotherapy. *Clinical cancer research,* 10, 4939–4943.

ZHU, X. D., KUSTER, B., MANN, M., PETRINI, J. H. & DE LANGE, T. 2000. Cell-cycle-regulated association of RAD50/MRE11/NBS1 with TRF2 and human telomeres. *Nature genetics,* 25**,** 347-52.

ZIETMAN, A. L., GROCELA, J., ZEHR, E., KAUFMAN, D. S., YOUNG, R. H., ALTHAUSEN, A. F., HENEY, N. M. & SHIPLEY, W. U. 2001. Selective bladder conservation using transurethral resection, chemotherapy, and radiation: Management and consequences of Ta, T1, and Tis recurrence within the retained bladder. *Urology,* 58**,** 380-385.

ZIETMAN, A. L., SACCO, D., SKOWRONSKI, U., GOMERY, P., KAUFMAN, D. S., CLARK, J. A., TALCOTT, J. A. & SHIPLEY, W. U. 2003. Organ conservation in invasive bladder cancer by transurethral resection, chemotherapy and radiation: results of a urodynamic and quality of life study on long-term survivors. *The Journal of urology,* 170**,** 1772-6.

Appendix A

Sample maps of the TMAs

11.1 Appendix A (i) - BCON TMA Map

BCON ARRAY SLIDE 4

liver	9008	9008	9008	9008	9009	9009	9009	9009	9010	9010	9010	9010	9011	9011	9011	9011	9011
	9016	9016	9016	9016	9015	9015	9015	9015	9014	9014	9014	9014	9013	9013	9013	9013	9013
	9017	9017	9017	9017	9018	9018	9018	9018	9019	9019	9019	9019	9020	9020	9020	9020	9020
	9024	9024	9024	9024	9023	9023	9023	9023	9022	9022	9022	9022	9021	9021	9021	9021	9021
lung	9025	9025	9025	9025	11002	11002	11002	11002	11004	11004	11004	11004	11005	11005	11005	11005	11005
	11009	11009	11009	11009	11008	11008	11008	11008	11007	11007	11007	11007	11006	11006	11006	11006	11006
	11010	11010	11010	11010	11011	11011	11011	11011	11013	11013	11013	11013	11014	11014	11014	11014	11014
lung	14002	14002	14002	14002	12005	12005	12005	12005	12002	12002	12002	12002	12001	12001	12001	12001	12001
	14003	14003	14003	14003	16004	16004	16004	16004	14005	14005	14005	14005	14016	14016	14016	14016	14016
	16007	16007	16007	16007	16003	16003	16003	16003	16002	16002	16002	16002	14017	14017	14017	14017	14017
	16008	16008	16008	16008	17001	17001	17001	17001	17003	17003	17003	17003	17006	17006	17006	17006	17006
	17014	17014	17014	17014	17012	17012	17012	17012	17008	17008	17008	17008	17007	17007	17007	17007	17007
	17015	17015	17015	17015	17017	17017	17017	17017	17019	17019	17019	17019	17022	17022	17022	17022	17022
	17026	17026	17026	17026	17025	17025	17025	17025	17024	17024	17024	17024	17023	17023	17023	17023	17023

9012 inadequate
11001 inadequate
11012 inadequate
11014 thin
12005 too small
14011 prostate
16006 inadequate
16008 inadequate
17002 no tumour
17010 inadequate
17016 inadequate
17018 inadequate
17020 inadequate

11.2 Appendix A (ii) – Radical Cystectomy TMA Map

11.3 Appendix A (iii) – Neoadjuvant TMA Map

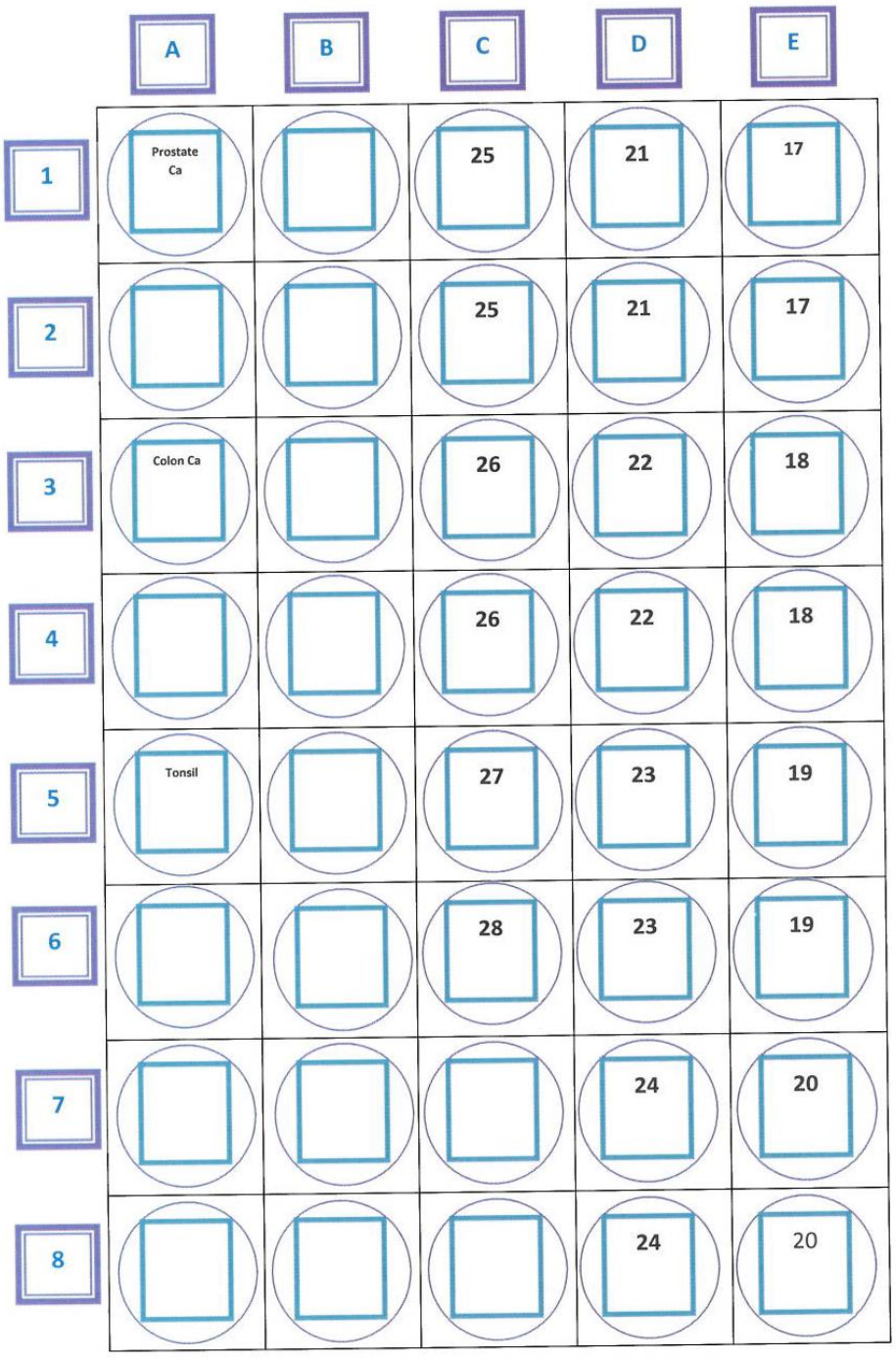

11.4 Appendix A (iv) – LaMB TMA Map

	4	6	8	10	12	14	16	18	20	22	24	
18	05 H005173 A5 Bladder control	05 H005173 A5 Bladder control	05 H005173 A5 Bladder control	05 H005173 A5 Bladder control	6415/83 Bladder control	5212/83 Bladder Control	5212/83 Bladder Control	5212/83 Bladder Control	5212/83 Bladder Control	7827/82 Bladder control	7827/82 Bladder control	18
16	gap	gap	S003	S003	S004	S004	S007	S007	S007	S024	05H005974 A8 Kidney control	16
14	gap	S024	S025	S025	S038	S038	S057	S057	S061	S061	05H005974 A8 Kidney control	14
12	gap	S091	S091	S066	S066	S067	S067	S079	S079	S061	05H005974 A8 Kidney control	12
10	04 H012187 A1 Appendix control	S093	S093	S101	S101	S104	S104	S109	S109	S111	05H005974 A8 Kidney control	10
8	04 H012187 A1 Appendix control	S111	S113	S113	S119	S119	S120	S120	S121	S121	04H013223 B16 Kidney control	8
6	04 H012187 A1 Appendix control	S122	S122	S124	S124	S131	S131	S134	S134	S136	04H013223 B16 Kidney control	6
4	04 H012187 A1 Appendix control	7827/82 Bladder control	7827/82 Bladder control	7827/82 Bladder control	641/83 Bladder control	gap	gap	gap	gap	S136	04H013223 B16 Kidney control	4
	4	6	8	10	12	14	16	18	20	22	24	

11.5 Appendix A (v) – Control TMA Map

Control TMA schema

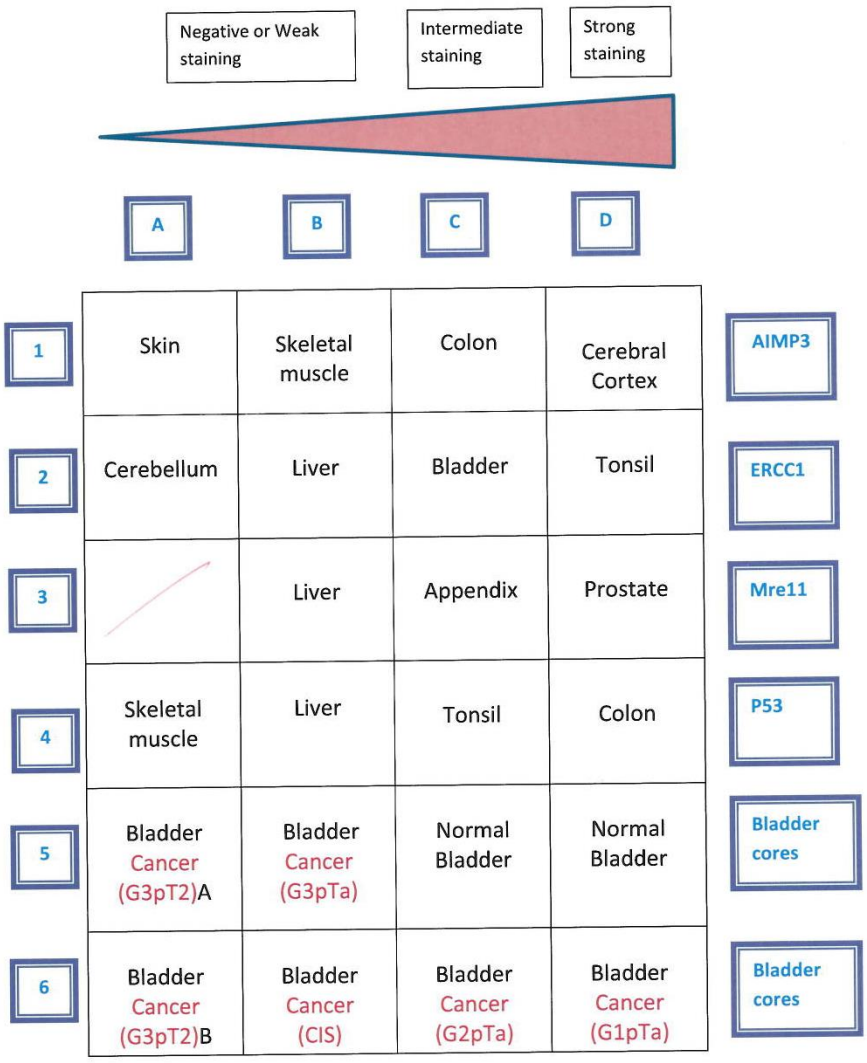

Appendix B

Ethics approval for the Neoadjuvant study

University College London Hospitals NHS
NHS Foundation Trust

UCL/UCLH Biobank for Studying Health and Disease

(based at Pathology-Rockefeller building and UCL-Cancer Institute)

21st October 2011,

Professor John D Kelly,

Translational Uro-oncology Group,

Division of Surgery & Interventional Science,

4th Floor, 74 Huntley Street, UCL, WC1E 6AU

Project Reference number and Title: EC06.11 - Predicting response of neo-adjuvant chemotherapy prior to radical therapy in patients with muscle-invasive bladder cancer.

Dear Professor Kelly,

I am writing to inform you that your application to B-ERC as detailed above has been approved by the Committee on 21st October 2011, with the following conditions:

- **The project and costs for access to archive material must be approved and signed off by the Clinical Lead in Histopathology.**
- **The tissue blocks must not be removed from Histopathology. It is required that blocks are cut in the Histopathology Department either by your own technician or by a technician/BMS from Histopathology, unless specifically negotiated. Details of this should be agreed with the Clinicial Lead.**
- **A protocol for how samples will be pseudo-anonymised and entered on Freezerworks must be provided, and agreed by Adrienne Flanagan and Nadege Presneau.**
- **Appropriate consent must be obtained from any current patients who will from now on be providing samples that will be made accessable through the diagnostic archive. Obtaining consent with the biobank not only give you access to the pathology material but also consent to access the clinical notes and imaging of the patients.**
- **Please note that if you are requesting to collect new samples at Tissue Collection Centres outside UCLH you will need to comply with the Research Governance requirements stated in the ethical approval letter included. In particular you will need to have a supply agreement with the TCC and to send a copy of this ethical approval letter to the R&D Department at the TCC.**
- **Ensure that you have appropriate R&D research permission for your project at sites where research is being carried out.**

All researchers must complete and comply with the regulatory and governance requirements and information requested on the Biobank application form. Further information is available on the UCL biobank website (http://www.ucl.ac.uk/biobank/), or on the UCL-CI WICI (http://www.ucl.ac.uk/wici/labcomp/biobank/ethics_application/index.htm)

Please find enclosed a copy of the ethics approval letter for the Biobank for your records. The current duration of the ethical approval is until 5th August 2015 in line with the duration of the Research Tissue Bank approval. This approval may be renewed for a further period in the future. We will be asking you to complete an annual return giving information on the number of patients consented and samples taken. We may at any time request to audit your project to ensure compliance with the necessary regulatory and governance requirements.

Thank you for your application to the Biobank and if you have any questions, please do not hesitate to contact Nadege Presneau (n.presneau@ucl.ac.uk) or Kirstin Goldring (k.goldring@ucl.ac.uk).

Yours Sincerely

Amanda Gibbon, **Chair, B-ERC**

cc Dr Alan Ramsay, Clinical Lead of Histopathology

Gary Brown, Head Biomedical Scientist/Service Manager - Histopathology

Appendix C

Supplementary RTPCR data

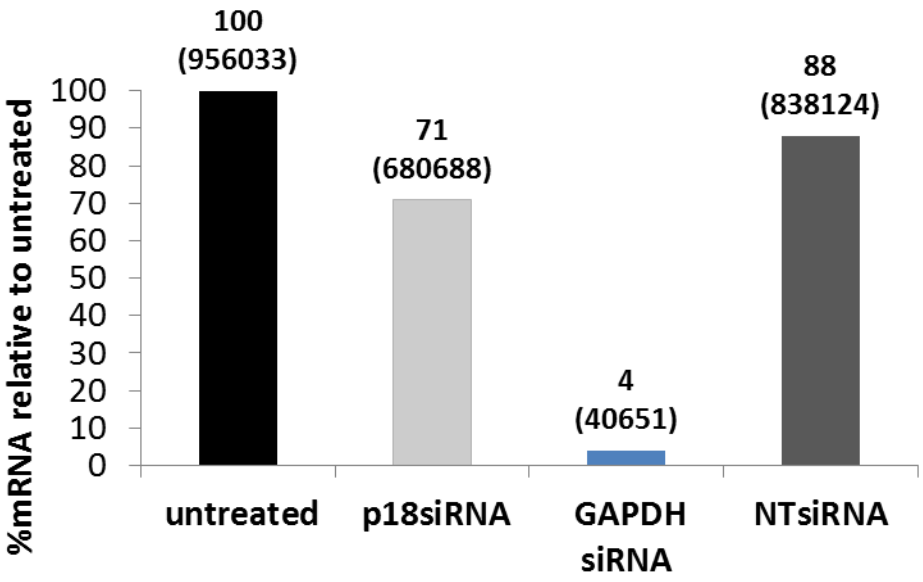

Supplementary Figure A: Relative mRNA expression of *GAPDH* in T24 cells 24 hours following siRNA transfection. Lane 1 represents *GAPDH* expression in untreated cells (negative control). Lane 2 represents cells with AIMP3 (p18) siRNA knockdown (positive control). Lane 3 represents cells with GAPDH siRNA knockdown (treatment/test group). Lane 4 represents cells with non-targeting (NT), scrambled siRNA transfection (negative control). *GAPDH* mRNA levels in Lanes 2, 3 and 4 are calculated relative to the negative control (Lane 1). Relative to Lane 1 (100%), there is a 29% reduction in *GAPDH* mRNA level (Lane 2) following AIMP3 (p18) siRNA knockdown representing off-target effects of siRNA transfection. Relative to Lane 1, there is a 96% reduction in *GAPDH* demonstrating significant downregulation of *GAPDH* expression following siRNA transfection. Relative to Lane 1, there is a 22% reduction in *GAPDH* expression in Lane 4 (non-targeting, scrambled siRNA) representing off-target effects of siRNA transfection. The numbers in brackets above each bar represent the mRNA copy numbers.

(This RTPCR work was conducted with the help of Dr Patricia de Winter)

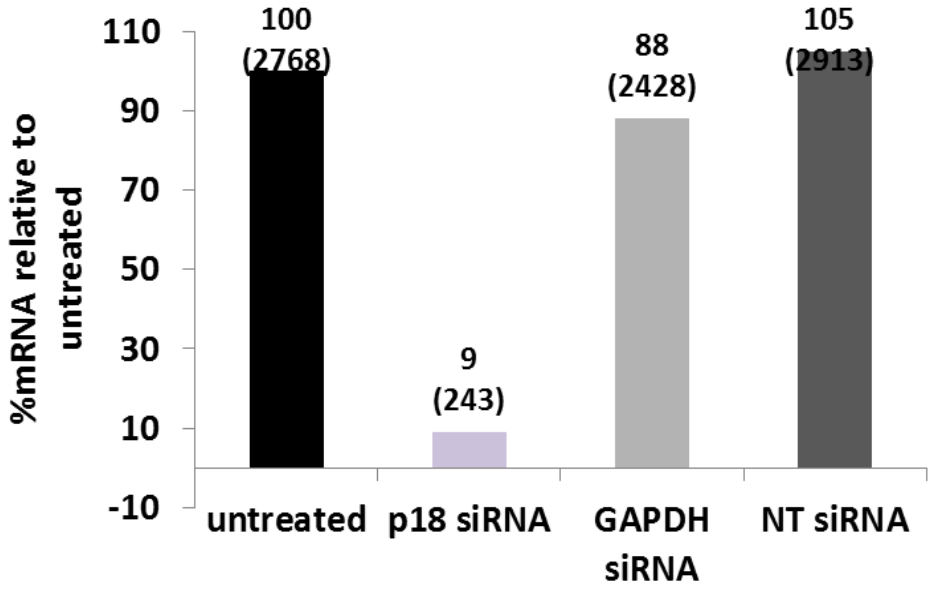

Supplementary Figure B: Relative mRNA expression of *AIMP3* in T24 cells 24 hours following siRNA transfection. Lane 1 represents *AIMP3* expression in untreated cells (negative control). Lane 2 represents cells with AIMP3 (p18) siRNA knockdown (treatment/test group). Lane 3 represents cells with GAPDH siRNA knockdown (positive). Lane 4 represents cells with non-targeting (NT), scrambled siRNA transfection (negative control). *AIMP3* mRNA levels in Lanes 2, 3 and 4 are calculated relative to the negative control (Lane 1). Relative to Lane 1 (100%), there is a 12% reduction in *GAPDH* mRNA level (Lane 3) following GAPDH siRNA knockdown representing off-target effects of siRNA transfection. Relative to Lane 1, there is a 5% increase in *AIMP3* expression in Lane 4 (non-targeting, scrambled siRNA) representing either a non-significant change or an off-target effects of siRNA transfection. The numbers in brackets above each bar represent the mRNA copy numbers.

(This RTPCR work was conducted with the help of Dr Patricia de Winter)